ANALYSIS AND DESIGN OF

STIRLING ENGINES FOR WASTE-HEAT RECOVERY

by

RAHMATALLAH SHOURESHI

B.S., Tehran University of Technology
(1976)

S.M., Massachusetts Institute of Technology
(1978)

SUBMITTED IN PARTIAL FULFILLMENT
OF THE REQUIREMENTS FOR THE DEGREE OF

DOCTOR OF PHILOSOPHY

at the

MASSACHUSETTS INSTITUTE OF TECHNOLOGY

June, 1981

Signature of Author _____
Department of Mechanical Engineering

Certified by _____
Thesis Co-supervisor

_____
Thesis Co-supervisor

Accepted by _____
Chairman, Department Committee on Graduate Students

Archives
MASSACHUSETTS INSTITUTE
OF TECHNOLOGY
OCT 29 1981
LIBRARIES

ANALYSIS AND DESIGN OF STIRLING ENGINES FOR WASTE-HEAT RECOVERY

by

Rahmatallah Shoureshi

Submitted to the Department of Mechanical Engineering on June 8, 1981 in partial fulfillment of the requirement for the degree of Docotor of Philosophy

ABSTRACT

Most of the available waste-heat sources have effective temperatures less than 700 F. In order to utilize these heat sources a low temperature and low temperature-ratio analysis is required to investigate the best alternative for waste-heat recovery among the present existing engines.

A low temperature-ratio preliminary, comparative analysis of superheated Rankine, non-ideal Stirling, and ideal Brayton engine is presented. This analysis shows the first two have comparable efficiencies at low temperature-ratios and have superiority over the ideal Brayton engine. Since the Rankine engine has been well investigated for low temperature, and low temperature-ratio duties, then a need exists for similar analysis on the Stirling engine because its open literature deals largely with high temperature applications.

A new and complete model for a Stirling engine has been established. This computerized model predicts the behavior of existing engines reasonably accurately for cases where a quantitative comparison is available. Moreover, where the information reported is incomplete, the model still offers at least qualitative explanations for the observed effects.

In order to obtain a closed form solution suitable for design optimization a simplified model for practical Stirling engines has been derived. This new model has sufficient accuracy for prediction of the behavior of real engines and its results are quite close to the complete model predictions.

A general method of Stirling design optimization is presented. This method, which is based on the simplified model, separately optimizes each component of the engine. Correlations are presented to determine optimum geometry for each of the heat-exchangers, based on Mach number, Reynolds number, operating temperature-ratio, and heat-exchanger dead volume. This optimization method utilizes derived results for optimum swept-volume ratio, phase angle difference between the cylinder displacements, bore-stroke ratio, and engine speed.

Results of the optimum designed Stirling engine have been compared with available data on Rankine waste-heat engines to determine which one performs more efficiently at low temperatures and low temperature-ratios. This comparison shows that in temperature-ratio range 1.25 to 1.6 a Rankine

engine operates more efficiently, while for higher temperature ratios a Stirling engine is the better alternative. Also it is indicated that a low power-level, waste-heat, Rankine engine has vanishing efficiency at temperature-ratio of 1.2 or less; whereas, an optimized Stirling engine would appear to be capable of operation at temperature-ratios of 1.1 or more.In the latter case, the optimum regenerator has vanishing length, i.e. the Stirling engine has practically no regenerator.

Thesis Supervisors: Professor Henry M. Paynter
Professor Joseph L. Smith Jr.,
Thesis Committee Members:
Professor Thomas P. Bligh
Professor Borivoje Mikic
Professor David Gordon Wilson

TABLE OF CONTENTS

Page

ABSTRACT ii

LIST OF TABLES vii

LIST OF FIGURES ix

ACKNOWLEGEMENTS xii

MOMENCLATURE xiv

CHAPTER I:

1.1- Introduction 1

1.2- Applications of Stirling Engines Involving Low Temperature Ratios 4

1.3- Review of Low Temperature & Low-Temperature-Ratio Efforts 7

a)- Rankine Cycle Systems 7

b)- Stirling Cycle Systems 11

1.4- Objectives and Outline of the Present Study Information Diagram of Thesis 13

CHAPTER II:

2.1- Steady State Behavior of Different Engines 16

2.1.1- Rankine Engine 16

2.1.2- Brayton Engine 19

2.1.3- Stirling Engine 22

2.1.4- Comparison of Engines 24

2.2-Ideal Stirling Engine Analysis 25

2.2.1- Ideal Stirling Cycle, Schmidt Equations 25

2.2.2- Effect of Imperfect Regenerator and Dead Volume on Ideal Engine 30

2.3- Evaluation of Different Types of Losses 33

2.3.1- Pressure-Volume Flow Domain Losses 34

2.3.2- Temperature-Entropy Domain Losses 38

2.3.2.1- Temperature-Drop Losses in Heater and Cooler 38

2.3.2.2- Imperfect Heat Transfer in Regenerator41

2.3.2.3- Axial Conduction Heat Loss 42

2.3.2.4- Shuttle Heat Transfer Loss 43

2.3.2.5- Heat Leakage 44

2.3.2.6- Transient Heat Transfer Loss in the Cylinder 46

2.3.2.7- Heat Pumping Loss Inside the Piston and Cylinder Gap 52

2.3.3- Force-Displacement Domain Loss 52

2.4- Analysis and Modelling of Practical Stirling Engines 54

2.4.1- Perfect Engine Model 55

2.4.1.1- Solution of System State Equations ...61

2.4.2- Real Engine Model 62

2.5- Results of Complete Model and Comparison with Available Data 66

2.5.1- Complete Model 66

2.5.2- Available Data and Comparison with Complete Model Results 68

a)- Philips Engine 69

b)- Allison Engine 70

c)- GPU-3 Engine 72

CHAPTER III:

3.1- Need for Simplified Stirling Engine Models ... 75

3.1.1- Basic Heat Input and Work Output Derivation76

3.1.2- Derivation of Mass Flow Rates Inside the Stirling Engine 80

3.1.3- Losses Calculations by Simplified Model ...86

3.1.3.1- Pressure Drop Losses 86

3.1.3.2- Temperature Drop Losses Inside Heat-Exchangers 88

3.2- Comparison of Complete and Simplified Models . 90

CHAPTER IV:

Procedure and Derivation of Optimization Method for Designing Stirling Engine 91

4.1- Optimum Design Model for Stirling Engine 93

4.1.1- Regenerator Optimization 98

4.1.2- Cold Heat-Exchanger Optimization 105

4.1.3- Hot Heat-Exchanger Optimization 110

4.1.4- Cylinders Optimization 112

4.2- Working Fluid for Stirling Engine 117

4.3- Derivation of Optimum Speed and Phase Angle(N&ϕ)121

4.3.2- Optimum Phase Angle 121

4.3.1- Optimum Speed 123

4.4- Derivation of Aspect Ratio for the Cylinders (B/S) 127

4.5- Comparison of Optimum Design Model Results with Available Data 130

CHAPTER V:

5.1- Stirling Engine with and without Regenerator ..133

5.2- Low Temperature Rankine Engines 136

5.3- Comparison of Stirling and Rankine Engines at Low Temperature and Low Temperature-Ratio 140

CHATER VI:

6.1- Significant Contributions of Present Investigation..... 143

6.2- Conclusion 145

6.3- Suggestions for Future Work 149

TABLES 152

FIGURES 170

REFERENCES 226

APPENDICES:

A- Survey of Stirling Engine Technology 229

B- Stirling Engine for Automative Application 200

C- Steady State Analysis of Practical Rankine Engine 236

D- Ideal Engine Analysis (Schmidt Solution) 244

E- Ideal Engine with Dead Volume 250

F- Stress Analysis for Cylinder Thickness 252

G-Calculation of Power Loss Due to Transient Non-Uniform Temperature Distribution in Cylinders.... 253

H- Derivation of State-Equations for Stirling Engine with Perfect Components..... 260

I- Computer Program of Complete Model 268

J- Derivation of Mass Flow Rate in Heat-Exchanger 274

K- Pressure Losses Derivation by Simplified Model 277

L- Optimization Formulation 287

M- Derivation of Optimum Phase Angle & Speed 306

N- Optimum Bore/Stroke Ratio 316

p- Regenerator Heat Transfer Area Derivation 320

Q- Computer Program of Optimum Model 322

LIST OF TABLES

1- Performance of Rankine Engine 152

2- Performance of Brayton Engine 153

3- Performance of Stirling Engine 154

4- Effect of Regenerator Effectiveness on Stirling Engine Efficiency 155

5- Variation of Stirling Engine Output with Dead Volume 157

6- Comparison of Philips Engine Results and Complete Model Predictions 158

7- Comparison of Allison Engine Performance with Complete Model Predictions (ϕ=118) 159

8- Comparison of Allison Engine Performance with Complete Model Predictions (ϕ=112) 160

9- Comparison of GPU-3 Performance with Complete Model Predictions (H2) 161

10- Comparison of GPU-3 Performance with Complete Model Predictions (He2) 162

11- Comparison of Simplified and Complete Model Predictions 163

12- Optimum Stirling Engine Model Results for Different Temperature-Ratios (Qin=2000 Watts) 164

13A Philips Optimum Design Model Results 165

13B Philips & G.E Optimum Design Results (Helium as Working Fluid) 165

14- Performance of Stirling Engine without Regenerator (Helium as Working Fluid) 166

15- Barber-Nichols Model Results for Rankine Engine 167

16- Thermo-Electron Results for Low Temperature-Ratio Rankine Engine 167

17- Optimum Stirling Engine Model Results for Different Temperature-Ratios (Qin=4000 Watts, Helium) 168

18- Optimum Model Results for Isothermal Stirling Engine (Qin=2000 Watts, Hydrogen) 169

LIST OF FIGURES

1- Original Single-Cylinder and Piston Stirling Engine 170

2- First Double-Acting Cylinders Stirling Engine 171

3- Schematic Diagram of OTEC Power Cycle 172

4- Cutaway View of TRW OTEC Plant Model 173

5- Allied Chemical Corp., 500 KW Sulfuric Acid Waste heat Recovery, Rankine Cycle 174

6- DOE and MTI Binary Rankine Cycle Waste-Heate Recovery 175

7- Variation of Efficiency with Heater Temperature G.M. Benson, Thermal Oscillators,..... 176

8- Philips Low Power Level Engine, Computer Results 177

9- General Electric Stirling-Engine-Powered Heat-Activated Heat Pump Results 178

10- Information Diagram of Thesis 15

11- Comparison of Steady State Performance of Real Rankine and Stirling Engines with Perfect Component and Ideal Brayton Engine 179

12- Effect of Dead Volume on Stirling Engine Performance Walker's Results 180

13- Effect of Swept-Volume Ratio on Cycle Power Walker's Results 181

14- Effect of Phase Angle (ϕ) on Cycle Power Walker's Results 182

15- Schematic Diagram of a Real Stirling Engine with Corresponding Bond Graph 183

16- Effect of Regenerator Effectiveness on Stirling Engine Efficiency 184

17- Variation of Stirling Engine Output with Dead Volume 185

18- Schematic Diagram and Energy Flow of Stirling Engine with Perfect Components and Corresponding Bond Graph 186

19- Bond Graph of a Cylinder 187

20- Energy Flow of a Real Stirling Engine with Different loss Domain 188

21- Analysis of a Real Engine, Chapter II 189

22- Variation of Mechanical Friction Mean Effective Pressure (Fmep) with Engine Speed 190

23- Thermal Conductivity of Helium and Assigned Correlation 191

24- Thermal Conductivity and Prandlt Number for Hydrogen and Assigned Correlations 192

25- Comparison of Philips Engine Output Power with Complete Model Prediction 193

26- Computed Input Heat Versus Measured Fuel Mass Flow Rate for Philips Engine 194

27- Comparison of Allison Engine Output Power with Complete Model Predictions (ϕ=112) 195

28- Comparison of Allison Engine Efficiency with Complete Model Predictions (ϕ=112) 196

29- Comparison of Allison Engine Output Power with Complete Model Predictions (ϕ=118) 197

30- Comparison of Allison Engine Efficiency with Complete Model Predictions (ϕ=118) 198

31- Comparison of LeRC Model and Complete Model Predictions for GPU-3 (He) 199

32- Comparison of LeRC Model and Complete Model Predictions for GPU-3 (H2) 200

33- Variation of Error between Schmidt and Complete Model Outputs with Temperature-Ratio 201

34- Variation of Error between Schmidt and Complete Model Outputs with Phase Angle 202

35- Dead Volume Correction Factor for Schmidt Equation (TH/TC<1.5) 203

36- Dead Volume Correction Factor for Schmidt Equation (TH/TC>1.5) 204

37- General Configuration of a Real Stirling Engine ..205

38- Temperature Correction Factors for Mass Flow Rates in Heater, Cooler, and Regenerator 206

39- Phase Angle Correction Factors for Mass Rates in Heater, Cooler, and Regenerator 207

40- Dead Volume Correction Factor for Mass Flow Rate in Heater 208

41- Dead Volume Correction Factor for Mass Flow Rate in Cooler Simplified Model 209

42- Dead Volume Correction Factor for Mass Flow Rate in Regenerator 210

43- Comparison of Simplified and Complete Models Predictions 211

44- Comparison of Working Fluids by Philips Laboratories 212

45- Comparison of Stirling Engine Output Power with Different Working Fluids and Different Processes, Qin=2000 Watt, Pm=500 Psia 213

46- Comparison of Stirling Engine Efficiency with Different Working Fluids and Different Processes, Qin=2000 Watt, pm=500 Psia 214

47- Variation of Optimum Speed and Phase Angle with Temperature-Ratio 215

48- Block Diagram of Synthesis System 216

49- Comparison of Optimum Model Results, Philips Optimum Design Model Results, and Philips & G.E. Experiment, Hydrogen as Working Fluid 217

50- Comparison of Optimum Model Results with Philips and G.E. Experiment 218

51- Comparison of Optimum Designed Stirling Engine Performance and Thermo-Electron Rankine Engine Performance 219

52- Comparison of Optimum Designed Stirling Engine Performance and Barber-Nichols Rankine Engine Performance 220

53- Stirling Engine Power Loss Due to Regenerator Pressure Drop 221

54- Stirling Engine Heat Loss Due to Regenerator Imperfection and Axial Conduction 222

55- Variation of Regenerator Optimum Length with Temperature Ratio 223

56- Variation of Net Output Power, Power Losses, and Heat Losses with Temperature-Ratio 224

57- Tension Actuators Acting like a Double-Acting Cylinder and Piston 225

ACKNOWLEDGEMENTS

I am deeply grateful to my thesis supervisors, Professor Henry M. Paynter, a source of never ending knowledge, for his stimulating guidance, patient, and counsel; and Professor Joseph L. Smith Jr., Whose never-fading enthusiasm helped keep me on the track during the course of this thesis. I sincerely appreciate them. I would like to appreciate the other thesis committee members, Professors Borivoje Mikic, David Gordon Wilson, and Thomas P. Bligh for their assistance, advices, and guidances throughout and were always willing to serve as sounding board for new ideas.

I would like to thank Mr. Francis A. DiBella, Project Engineer at Thermo-Electron Corp., for providing the Rankine engine data which made it possible to have a reasonalble comparison of the two Stirling and Rankine engines.

I appreciate Dr. Kangpil Lee, senior engineer at Foster-Miller Associates, Inc. for all of his time and effort on clarifying some of the power losses in a Stirling engine.

I am grateful to Helen Doyle for her assistance during the five years of my working with Prof. Paynter.

Most of all, I would like to express my appreciation to my wife, Azar, for her love, encouragement, patient, and supports throughout this thesis.

NOMENCLATURE

Ac	heat transfer area of compression space
Ae	heat transfer area of expansion space
AFRC	cooler free flow area
AFRH	heater free flow area
AFRR	regenerator free flow area
AH	heat transfer area
B	bore of a cylinder
Cp	specific heat of working fluid at constant pressure
Cv	specific heat of working fluid at constant volume
d	diameter of wire or sphere particles in the regenerator
D	hydraulic diameter (section 4.1) normalized dead volume D=(VDR+VDC+VDH)/VC (section 3.1.1)
DC	I.D. of cooler tubes (section 4.1.2) normalized dead volume for cooler VDC/VC (Section 4.1)
DH	I.D. of heater tubes (section 4.1.3) normalized dead volume for heater VDH/VC (section 4.1)
DRR	diameter of regenerator cross-sectional area
f	average friction factor (section 2.3.1) correction factor (section 3.2)
F	Correction factor
Fe	enhancement factor for expansion space
Fc	enhancement factor for compression space
fx	friction factor at position x
Fcc	mass flow rate correction factor in cooler
Fch	mass flow rate correction factor in heater
Fcr	mass flow rate correction factor in regenerator

H	enthalpy (section 2.2) coefficient of heat transfer (Appendix L)
hi	inner coefficient of heat transfer
h	outer coefficient of heat transfer
k	ratio of constant pressure to constant volume specific heat (Cp/Cv)
Kg	thermal conductivity of gas
Km	thermal conductivity of material
l	cylinder-piston gap size
L	length of the component
Lp	displacer length
M	mass, Mach number
$\bar{\dot{m}}$	average mass flow rate
$\dot{m}x$	mass flow rate at position x
N	engine speed
Nc	number of tubes in cooler
NH	number of tubes in heater
P	pressure
P_1	amplitude of pressure variation from its mean value
Pr	Prandlt number
ΔP	pressure drop
Qin	input heat
R	ideal gas constant (section (2.1.1)) cylinder radius (Appendix G)
Re	Reynolds number
S	stroke
t	thickness
T	temperature
TC	cold temperature

TH	hot temperature
Tr	temperature ratio (TC/TH)
TR	regenerator mean temperature
ΔT	temperature drop
V	volume
VD	dead volume
VDC	dead volume in cooler
VDH	dead volume in heater
VDR	dead volume in regenerator
Vr	volume ratio (VC/VH)
X	dead volume ratio
Xm	amplitude of piston displacement
W	work
Wout	output work (power)

Greek letters:

α	aspect-ratio
β	inverse of Mach number
γ	ratio of Re/M^2
δ	temperature ratio
ξ	dead volume ratio
λ	swept volume ratio
ω	(θt), rotational speed
ρ	density
μ	viscousity
ϕ	phase angle difference between the two cylinder displacements.
ϕp	Phase angle difference between pressure wave and expansion volume displacement.
t	time constant

Subscripts:

am	ambient
c	compressor, cooler
C	cooler, cold
D	for dead volume
e	expansion space
EQ	equivalent
h	heater
H	Heater, hot
in	input
m	mean value
min	minimum
max	maximum
out	output
R	regenerator
T	for temperature
φ	for phase angle

"TO MY WIFE AZAR AND OUR SON PEZHMAN"

CHAPTER I

1.1- Introduction

Robert Stirling, a minister of the Church of Scotland and originator of the regenerative heat exchanger, invented the closed-cycle regenerative engine in 1816, and shortly thereafter a patent on the invention was issued in his name. The engine originally used hot air as a working fluid and was, therefore, called a hot-air engine. At the time, this engine satisfied a demand for a small power plant, since the steam engine had become impractical in the low-power range because of excessive heat losses.

In modern usage, Stirling engine is a device which operates on a closed regenerative thermodynamic cycle, with cyclic compression and expansion of the working fluid at different temperature levels, and where the flow is controlled by volume changes, so that there is a net conversion of heat to work.

Engines exist which operate on an open regenerative cycle, where the flow of working fluid is controlled by valves. For convenience, these may be called Ericsoon-cycle machines , but, in practice, the distinction is not widely established and the name Stirling engine is frequently indiscriminately applied to all types of regenerative machine. The generalized definition covers machines capable of operating as prime movers, heat pumps, refrigerating engines, or pressure generators.

Figures (1) and (2) show the original single-/and double-cylinder Stirling engines. Although a number of modifications were made to the original cycle, inadequate understanding of the regeneration process and how practical regenerator design affected the performance of the cycle prevented the Stirling engine from competing with first the steam engine and later with the internal-combustion engine. Therefore, the hot-air engine, because of inferior efficiency, low mean effective pressure and low specific power seemed destined for oblivion.

Yet throughout the nineteenth century thousands of hot-air engines were made and used in a wide variety of sizes and shapes in Britain, Europe, U.S.A., and other parts of the world. They were reliable and reasonably efficient, readily permitting the use of low grade fuels. More importantly, they were safe compared with contemporary reciprocating steam engine installations and their associated boilers, which exploded with depressing regularity, due to high working stresses, poor materials and imperfect joining techniques.

About the middle of the nineteenth century, the invention of the internal-combustion engine, in the form of the gas engine, and its subsequent development as a gasoline-and oil-fueled engine, along with the invention of the electric motor, caused the use of Stirling engines to fade rapidly until, by 1914, they were no longer available commercially in any quantity.

In the late 1930s, rebirth of the Stirling engine was started at the Philips Research Laboratories in Holland. Initially

this work was directed to the development of small thermal-power electric generators for radios and similar equipment, for use in remote areas, where storage batteries were not readily available. Studies by Philips and others embraced the experimental development of engines of various sizes up to 450 h.p. as is discussed in some detail in Appendix(B).

Over the past several years, interest in the application of Stirling engines to serve a variety of power-producing needs has increased considerably. As it is shown in Appendices(A)and(B), this type of engine have been developed for serving as thermoelectric generators, motor vehicles, heat pumps in cryogenic industry, replace for electric motor in air conditioning systems, blood pumps and many other services. Since most of these applications involve with high temperatures and/or high temperature ratios, consequently in some cases such as automative applications they have ended up with two essential problems: finding materials for high temperature components and sealing problems due to the high pressure inside the system. Therefore, it has generally been concluded that the Stirling engine is not presently economical for high temperature applications.

The object of this thesis is an analysis and design of the Stirling engine following a radically different concept from most of the previous attempts. Basic concerns are: low temperatures and low temperature ratios (TH/TC<2), waste heat as the heat source, and low output power level design. As shown in next section, there has not been adequate research along these lines; in fact it is hard to find any effort of this sort.

1.2- Applications of Stirling Engines Involving Low Temperatures & Low Temperature Ratios

In the past, major industries have foregone the most efficient use of excess process heat and instead purchased supplemental power and fuel which used to be the lower-cost alternative. Much process heat above 200 F was (and still is) rejected to cooling streams. But as power and fuel costs rise, attitudes are changing. Diminishing world supplies of fossil fuels have focused attention on the development of more efficient energy-conversion systems and on the concomitant search for alternative energy sources. Efficient use of all energy resources is becoming more important, on both sociological and economic grounds.

One approach to better energy utilization is embodied in the available energy of a given system. For example, in parallel with chemical-processing plants, or for diesel-engine coolants, one might establish a sub-system for converting a fraction of the waste heat to useful power. It is obvious that the temperature ratio (to ambient) of such a waste-heat source is lower than the required temperature ratios for operation of present liquid-fuel engines.

A common and feasible waste-heat source is the exhaust of any type of internal combustion engine or open cycle gas turbine which employs the chemical energy released at high temperature by fossil fuel combustion. A significant fraction of this energy is rejected as the sensible heat of the exhaust gases, at a temperature level at which it might still be utilized as the

heat source for an appropriate thermal engine.

Therefore, it is important to find the most efficient and reliable engine to utilize the available energy of such heat sources. Since air-conditioners and refrigerators are heat pumps working at low temperature ratios, then their reversed cycles might be assumed as alternatives for low-temperature-ratio heat engines. But these cycles can not be simply reversed to generate positive power because the expansion valve must now be replaced by a pump or compressor, and it is clear that the original isenthalpic throttling process is always easier to realize than reversed isentropic compression; therefore, in the practical reversed cycle there might not be enough expansion work to supply the required compression work. The only cycle in this category which might have some hope is the Rankine cycle; the following sections (6·1·1) outlines efforts for using this cycle for waste-heat recovery or for similar use at low temperature ratios.

Since the temperature-ratios (to ambient) of most of the available waste-heat sources are substantially less than 2 and the accumulated literature of the Stirling cycle furnishes no indication of effort at low-temperature-ratio operation, then it would appear to be valuable to perform a complete research and analysis based on Stirling engines operating at temperature ratios less than 2, thus to determine how close to unity this ratio might become before the engine could no longer generate net output power.

This thesis presents the analysis and design of Stirling

engines for low-temperature-ratio applications,and compares the performance of optimized Stirling engines with the performance of Rankine engines operating under the same conditions. A significant result is the determination of the lower-temperature-ratio boundary beyond which no practical engine could generate positive shaft power.

Since waste-heat recovery is a relatively new area, then next section presents a summary of the few low-temperature-ratio efforts which have been done recently.

1.3- Review of Low Temperature & Low-Temperature-Ratio Efforts

The efficiency of both Stirling and Rankine engines increases with increasing heat source temperatures and with decreasing heat sink temperatures. But high temperatures require the use of heat resistant materials, which are relatively expensive. There are other applications, however, where high efficiencies can be traded off for lower cost, i.e. where the heat source itself is at lower temperature, and thus use of conventional or less expensive "hot side" materials is possible. A typical application in the later category is the conversion of solar energy which has the effective temperature (temperature of collected energy by flat plate or parabolic reflectors) in the 200C to 500C range

There have been some research efforts directed at using a Rankine cycle at a low temperature-ratio, and there are also a few indirect low temperature-ratio research investigations on Stirling engines as outlined below.

a)- Rankine Cycle systems:

Early attempts to use a Rankine cycle for waste-heat recovery were the initial Ocean Thermal Energy Conversion (OTEC) efforts. OTEC systems involve a process for producing energy from the difference in temperature between surface and deep sea water and such systems were first promulgated more than 150 years ago. Almost a century ago, the principle was related specifically to the use of sea water as a power source, and full-scale demonstration power plants have been built within the last 50 years [17]. Jacques d°Arsonval in 1881, suggested opera-

ting a closed system in which a working fluid would be vaporized by the warm water (30C) of the spring at Grenelle French, then condensed by colder river water (15C), the resulting pressure difference across the system provides a constant source of power. The basic operating principles of OTEC power-plants have remained to this day basically unchanged since d°Arsonval initially proposed them. As it is shown in Fig. (3) the warm water(25 C) is pumped through an evaporator containing a working fluid in a closed Rankine-cycle system. The vaporized working fluid then drives a gas turbine which provides the plant power. Then the exhaust fluid is condensed by water drawn up from deep in the ocean. Figure (4) shows an OTEC baseline system configuration. The scale of this figure may be estimated from 24-meter diameter of the evaporator and condenser faces.

The heat exchangers are probably the single most important component of OTEC systems, especially their materials of construction. Choices for material range from titanium at perhaps $\$150/m^2$ with an indefinitely long life-time to aluminum at $\$50/m^2$ bearing perhaps a five-year life and even down to a plastic at $\$10/m^2$ with a completely unknown lifetime. An obvious solution to reducing the exchanger capital cost is to increase the velocity of either or both working fluids, but this would quickly increase the parasitic pumping losses, especially on the sea-water side. Another problem is biological fouling of the heat transfer surface on the sea-water side.

The basic requirements for the ideal working fluid for

OTEC are the pressure-temperature relation of the equilibrium two-phase mixture, the latent heat of vaporization, the liquid thermal conductivity, chemical stability, low corrosiveness towards the materials of construction, safety, and cost [17]. Alternative working fluids are ammonia, propane, isobutane, and several of the Freons. Most of the studies to date have strongly favored ammonia as the working fluid of choice and indicate a very severe economic disadvantage in using any of the other candidate fluids.

Eventhough the OTEC environmental work schedule calls for a demonstration of this system by 1981, this now appears to be unrealistic. The important point about OTEC systems is that the absolute temperature ratio is about 1.07, raising the essential question: is it possible to get any net output power given a 1.07 temperature-ratio? During the course of this thesis we will look at the capabilities of Stirling and Rankine engines operating at such low-temperature-ratios.

Allied Chemical Corporation and Ishikawajima-Harima Heavy industries Company [12] have jointly pursued the installation and operation of a nominal 500 KW sulfuric acid, waste-heat recovery, Rankine cycle power plant. Fig. (5) shows a schematic of the cycle showing the waste heat source and the pertinent cycle parameters. The waste heat stream is the sulfuric acid leaving the strong acid absorber tower. The plan is to use a portion of this hot acid for the heat recovery system. The working fluid for the Rankine cycle was chosen to be Genetron

133 A, a fluorocarbon with the formula C2H2C1F3. The vapor portion of the saturation dome for G133A, in the temperature range from 100 F to 200 F, is essentially parallel to the constant entropy lines which permits very little superheating and no need for an auxiliary regenerative heat exchanger before the condenser.

Their system is under development regarding its performance. Since their temperature ratio is high enough to overcome the present losses, their system is capable of producing net power, but it may not achieve a practical efficiency.

The Department of Energy (DOE) and Mechanical Technology Incorporated (MTI) have developed a binary Rankine cycle waste-heat recovery system for diesel generating systems [21]. The demonstration site is located at a power plant in the village of Rockville center, New York. Fig. (6) shows a schematic diagram of this binary system. The system employs two common fluids, steam and Freon, and is projected to recover 500 KW. The steam topping cycle buffers the Freon bottoming cycle so that the system can be applied overy a wide range of gas temperatures and not be limited by the stability limits of organic coolants. The temperature-ratio of this system is close to 2; therefore this system is expected to have a reasonable efficiency.

There are other efforts for waste-heat recovery by applying Rankine cycles. In section (6.2), when the Stirling and Rankine engines are compared, the results and a quantitative summary of those efforts will be discussed.

b)- Stirling Cycle Systems:

In spite the fact that there have been numerous developments, employing a Rankine-cycle at low-temperature ratio, there are only a few research efforts in that area based on the Stirling cycle.

G. M. Benson [5] in his research on Thermal Oscillators, which are resonant-free-piston, valveless, closed-cycle thermal machines based on the Stirling and/or Ericson cycles, has explored some low temperature engines. Fig. (7) shows his results for variation of efficiency as a function of heater temperature. This figure indicates that when the hot temperature goes below 300 F efficiency would be close to zero or, by considering his cold source temperature, if the temperature-ratio is lower than 1.27 there would be no significant net power.

In 1976 Philips Laboratories started some studies on Stirling engine to determine its efficiency as a function of operating temperatures [15]. The engine which has been used is the I-98 Philips engine. For every combination of temperatures and working fluids and at a number of speeds, the pressure and dimensions were determined such that maximum efficiency was obtained. Fig. (8) shows the results of their analysis and experiments. These results indicate their minimum temperature-ratio is about 1.27, and in almost all of the cases there is about 5% reduction in efficiency of the engine when the shaft friction is introduced. Although they have concluded that the best working fluid for Stirling engines is hydrogen, yet if we

look at the results of the low temperature-ratios (TH/TC<2.0) we see there is not that much difference between helium and hydrogen results. This follows because flow losses no longer play a large role and the gas density is no longer so significant. Finally, at low heater temperatures, the use of a working fluid with a high density relative to that of hydrogen, results in low specific power outputs.

There have been, recently, some efforts on using Stirling and Rankine cycles jointly. General Electric has developed a Stirling-engine-powered heat-activated heat pump. This 3-ton heat pump employs a natural gas-fired Stirling engine to drive the vapor compressor. The concept of a heat-activated heat pump has the potential of reducing the amount of gas required for space heating. The Stirling engine/Rankine cycle refrigeration loop concept being developed would consume about one-half the gas required by conventional space heating equipment. Fig. (9) shows computed characteristic for this system [1].

1.4- Objectives and Outline of the Present Study

Since all of the above confirms that there presently exists no clear analysis of Stirling engines operating at low-temperature-ratio (close to unity), it is the purpose of this thesis to present and evaluate an analysis which will be of more general application to the Stirling engines operating at low temperature ratios than are the existing analyses. An information diagram for this study is shown as Fig. (10).

In order to justify the choice of a Stirling engine for waste-heat-recovery applications, Chapter II begins with the comparison of steady state performances of different engines and continues with ideal cycle analyses (i.e, the Schmidt equations) which includes its predictions for optimum design characters. The last part of this chapter is involved with modelling practical Stirling engines, evaluation of different types of losses and comparison of the complete model with available data. In order for the analysis to be useful for design purposes, where a large number of alternatives must be compared, it must not require extensive computations. All of the present, practical Stirling cycle models require a good portion of computer time which make them expensive; therefore, Chapter III represents a simplified Stirling engine model and compares its evaluations with the complete model of Chapter II. Chapter IV deals with the derivation of optimum speed and phase angle difference between the hot and cold spaces. Chapter V shows the special behavior of the engine at low temperatures and low temperature-

ratios. Chapter VI compares low-temperature Stirling and Rankine engines.

Fig.(10):

INFORMATION DIAGRAM OF THESIS

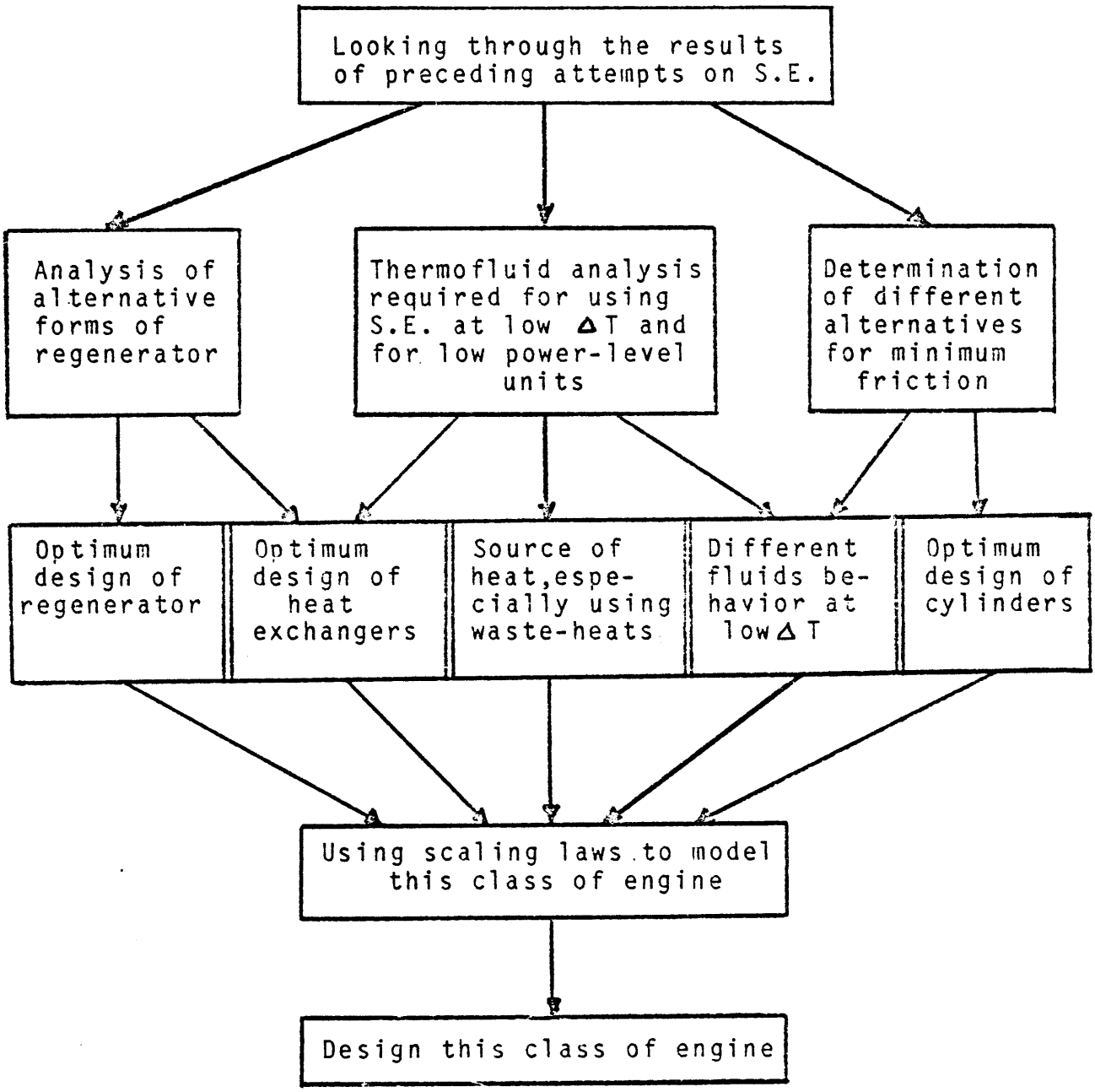

CHAPTER II

2.1- Steady State Behavior of Different Engines

Utilization of waste-heat sources require the proper type of engines. Following Martini [13] a first order (steady state) analysis would be a simple and quick way of comparing different engine performance. Since Rankine, Brayton and Stirling cycles are present possible alternatives, in this section we will evalutate and compare the performance of each, at low temperatures and at low-temperature-ratios.

2.1.1- Rankine Engine:

In order to make this comparison closer to reality, the engine should be more practical and not taken as the ideal case. As is shown in the following figure, the ideal Rankine cycle, having isentropic expansion and compression, is identical to Carnot cycle in operation and efficiency. At two states, the entrance to the pump and at exit from the expander, the flow

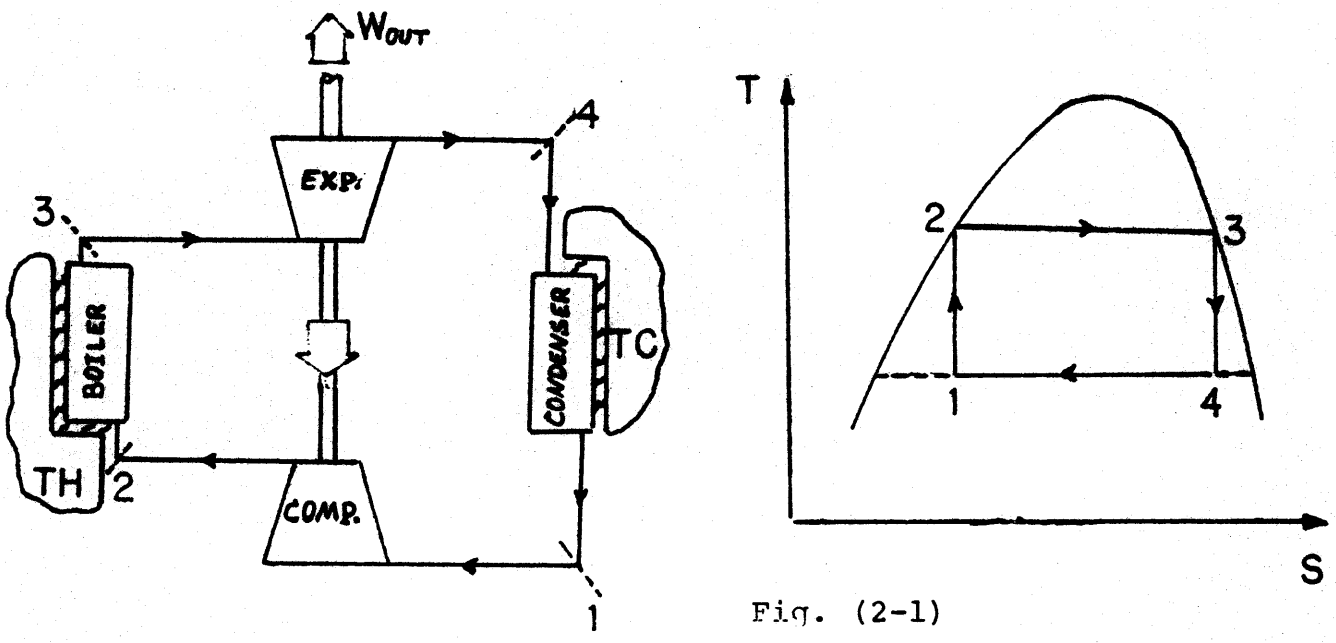

Fig. (2-1)

is a mixture of liquid and vapor and would create some design problems. For example, great difficulties would be encountered in building a pump that will handle the mixture of liquid and vapor at 1 and deliver saturated liquid at 2. Therefore, this cycle is not generally practical.

In a practical Rankine engine, the vapor is completely condensed and liquid is delivered to the pump 1-1′-2. In order to increase the efficiency and have vapor phase in most parts of expander, vapor is superheated at constant pressure 3-3′. In the Carnot engine all the heat transfer is at constant temperature, and therefore the vapor is superheated in process 3-3′. During this process the pressure is dropping, which means that heat must be tranferred to the vapor as it undergoes an expansion process in which work is done. This also is very difficult to achieve in practice. Therefore the following cycle which has a super heat-reheat process would represent a more practical Rankine engine. Since this engine is used for low temperatures then the expansion and compression processes are assumed isentropic.

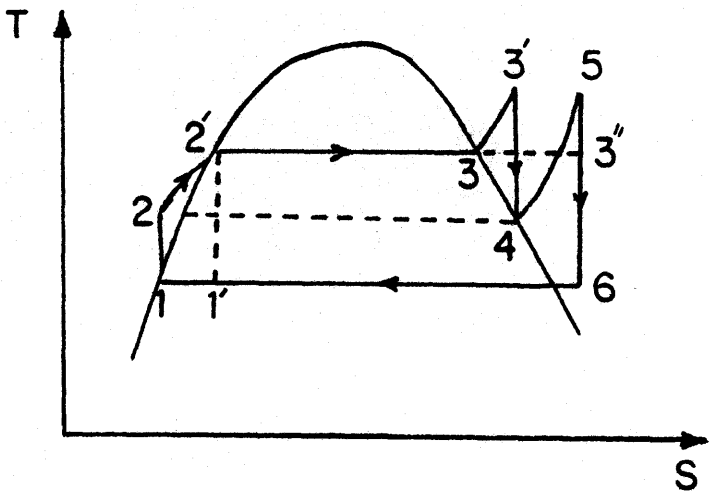

Fig.(2-2)

For the absolute temperature-ratio ranging from 1.0 to 2.0 with the maximum engine pressure less than 500 psia a proper working fluid would be difluoro-monochloro-ethane ($C_2H_3F_2Cl$). Following states are a sample for calculation of engine performance at TH/TC = 1.4 . Appendix (C) has these states for various temperature ratios.

$TC = T_1 = 55^\circ F$

$TH = T_3' = 260^\circ F$ $\Longrightarrow$ TH/TC=1.4

State 1:

T	= 55° F	
P	= 33.23	Psia
H	= 21.86	Btu/lb
S	= .0477	Btu/lb R
V	= 1/71.24	Ft^3 /lb

State 2:

S	= .0477	Btu/lb R
P	= 413.8	Psia
H	= 22.85	Btu/lb

State 3':

P	= 413.8	Psia
T	= 260 F	
H	= 133	Btu/lb
S	= .22	Btu/lb R

State 4:

P	= 120	Psia
H	= 122.5	Btu/lb
S	= .22	Btu/lb R

State 5:

P = 120 Psia
H = 151 Btu/lb
S = .264 Btu/lb R

State 6:

P = 33.23 Psia
H = 135 Btu/lb
S = .264 Btu/lb R

The intermediate pressure, which is the 120 Psia the pressure of reheat process, is calculated by $P=\sqrt{P_{min} * P_{max}}$

Thus the overall performance measures bocome:

$Wout = Wexp - Wcomp. = (H_3 - H_4)+(H_5 - H_6)-(H_2 - H_1)=25.51$ Btu/lb

$Qin = (H_3 - H_2) + (H_5 - H_4) = 138.65$ Btu/lb

$$\text{Efficiency} = \frac{Wout}{Qin} = 18.4\%$$

Table (1) has the comparable results for Rankine engines operating at different temperature-ratios.

2.1.2- Brayton Engine:

The air standard cycle or Brayton cycle is the normal closed cycle model for the gas turbine plant. It consist of two adiabatic work transfer processes (in ideal case they are isentropic) and two constant pressure heat transfer processes. The performance of this engine is very sensitive to the compressor and turbine efficiency. With compressor and turbine efficiencies of 85%, the maximum power is only 49% of the power which could be obtained with perfect components.

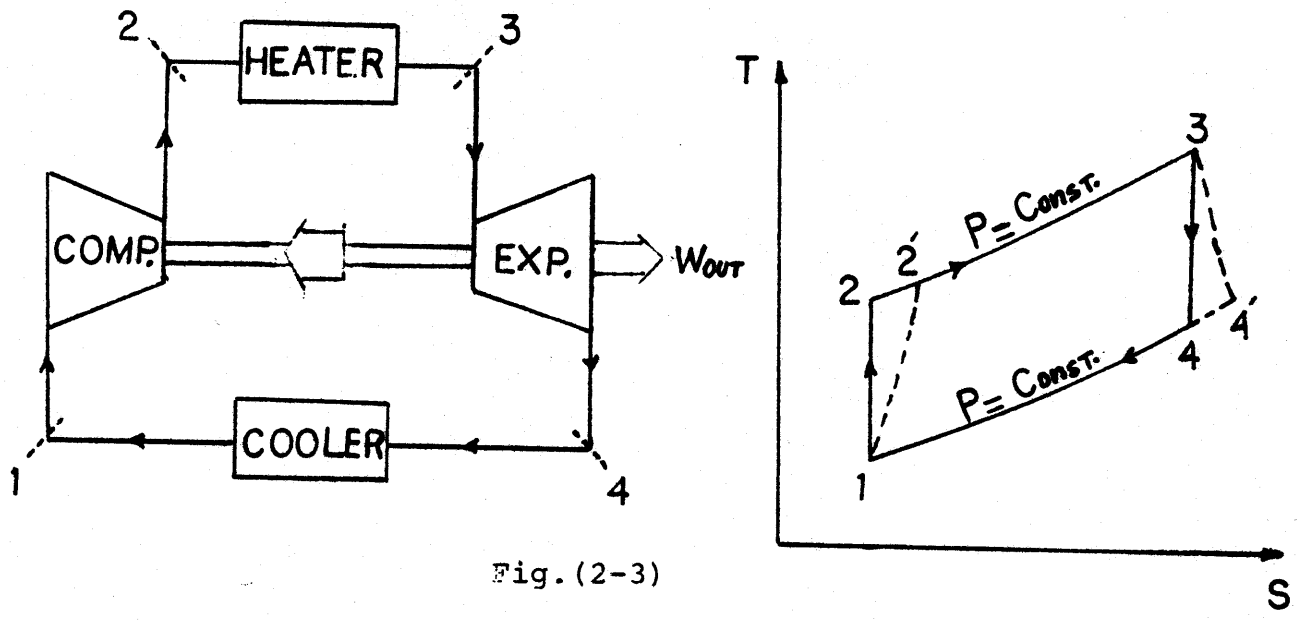

Fig.(2-3)

$$W_{net} = W_{exp} - W_{comp} = C_p(T_3 - T_4) - C_p(T_2 - T_1)$$

$$Q_{in} = C_p(T_3 - T_2)$$

$$\text{Efficiency} = \frac{W_{net}}{Q_{in}} = \frac{(T_3 - T_4)-(T_2 - T_1)}{T_3 - T_2} = 1 - \frac{T_4 - T_1}{T_3 - T_2} =$$

$$1 - \frac{T_1 (T_4/T_1 - 1)}{T_2 (T_3/T_2 - 1)}$$

From isentropic expansion and compression:

$$\Longrightarrow \quad T_4 / T_3 = (P_4/P_3)^{\frac{k-1}{k}} \quad , \qquad T_2 / T_1 = (P_2/P_1)^{\frac{k-1}{k}}$$

or $\quad T_4 / T_3 = T_1 / T_2$

Therefore:

$$\text{Efficiency} = 1 - T_1 / T_2 = 1 - (P_2/P_1)^{1-k/k}$$

For the following performance calculations the isentropic assumption is used, as it was for Rankine engine. In order to increase the engine efficiency a regenerative heat exchanger can be used between compressor and heater.

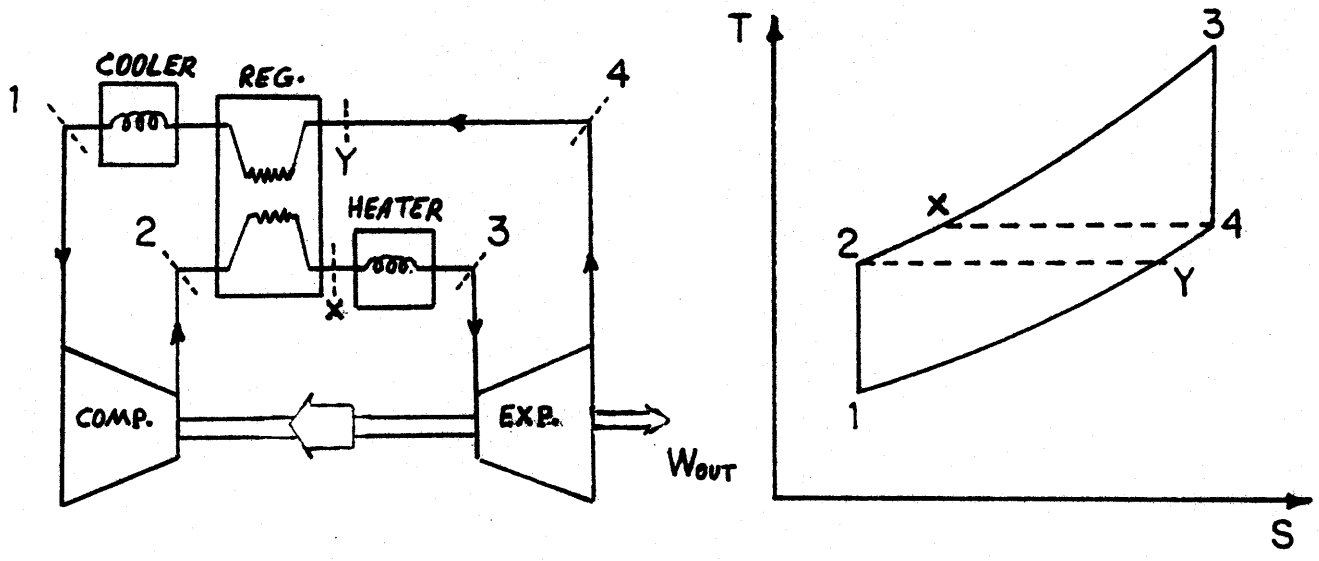

Fig.(2-4)

It can be shown that for ideal regeneration($T_4 = T_x$, $T_2 = T_y$) the efficiency is:

$$\text{Efficiency} = 1 - (T_1 / T_3)(P_2 / P_1)^{\frac{1-k}{k}} = 1 - T_2 / T_3$$

$$Q_{in} = C_p(T_3 - T_x) = C_p(T_3 - T_4) = C_p T_1((T_3 / T_1) - (T_4 / T_1)) =$$

$$= C_p T_1 (T_3 / T_1 - T_3 / T_2) = C_p T_3 (1 - T_1 / T_2)$$

$$W_{out} = C_p(T_3 - T_4) - C_p(T_2 - T_1) = C_p T_1((T_3 / T_1) - (T_4 / T_1 + T_2 / T_1) + 1)$$

Helium is used as working fluid, because it has high k = 1.66, and pressure ratio is of order of 2.0. Table (2) shows the results for different temperature-ratios.

2.1.3- Stirling Engine:

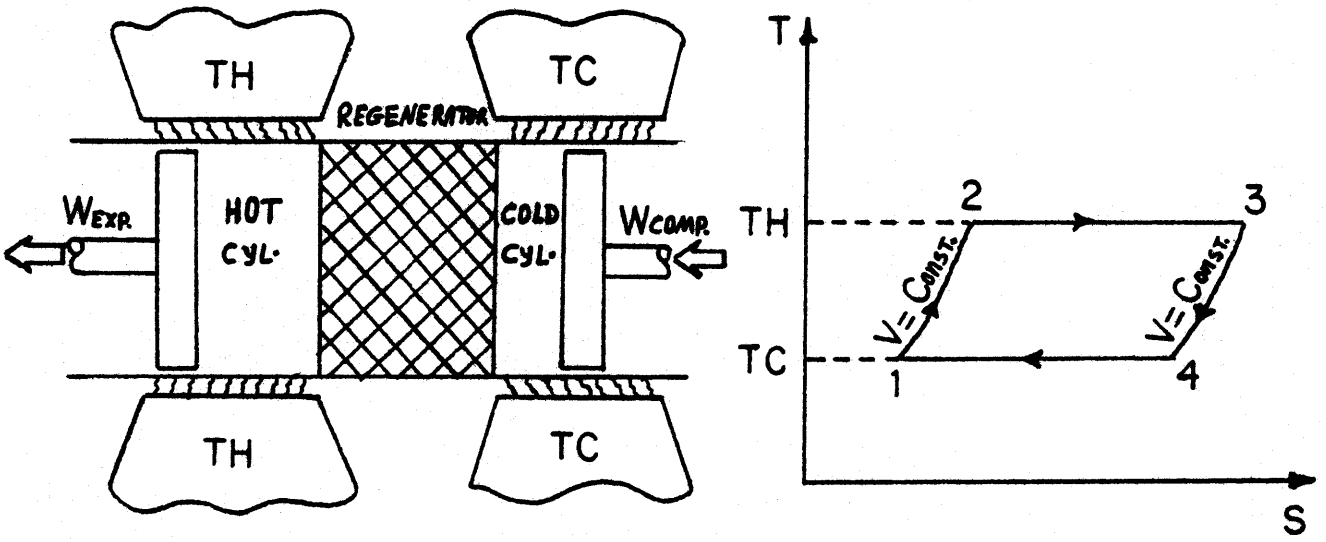

Fig.(2-5)

In the ideal case a Stirling engine consists of two isothermal expansion and compression processes and two constant volume heating and cooling processes. This ideal cycle might be achieved if there would be no pressure drop in the components of the engine and if an infinitesimal difference occured between the two streams in the regenerator. In this case, by applying first and second law of thermodynamics we obtain the following results

1st Law: $Q_H - Q_C = W_{out}$

2nd Law: $Q_H/T_H - Q_C/T_C = 0$

==> Efficiency = $W_{out}/Q_{in} = 1 - Q_C/Q_H = 1 - T_C/T_H$

Thus the Stirling engine again achieves the Carnot efficiency in this ideal case.

However the piston motion is continuous, not step-wise, and there are thermal resistances in every heat exchange process.

As a result, the assumed constant volume heating and cooling processes and instantaneous heat transfer, in isothermal processes, are not practical. Therefore, a more practical Stirling cycle consists of two adiabatic expansion and compression processes having non-uniform temperature distribution inside the hot and cold spaces. In order to make a more practical Stirling engine comparable to the practical Rankine one, those losses which seem most important and push the engine farther from ideal case (Carnot efficiency) must be taken into account. These include heat-transfer losses due to the imperfect regenerator, and work losses due to the non-uniform temperature distribution inside the cylinders.

If the regenerator effectiveness is defined as:

$$E = \frac{TR - TC}{TH - TC}$$

where $TR = (TH - TC)/(\ln TH/TC)$, then it can be shown that for isothermal expansion and compression:

$$\text{Efficiency} = \frac{1 - TC/TH}{1 + (1-E)(1-TC/TH)/((k-1)*(\ln P_2/P_1))}$$

It is estimated that the work loss due to the non-uniform temperature distribution is about 20% of the output work, then:

$$Wout = R * (TH-TC) * \ln P_2 / P_1 * 0.80$$

$$Qin = R * TH * \ln P_2 / P_1 + C_v * (TH-TR)$$

$$Qin = R * [TH * \ln P_2 / P_1 + (TH-TC)(1-E)/(k-1)]$$

As is shown in the following sections, hydrogen generally is the most efficient working fluid for Stirling engine. Based on the use of hydrogen, the Stirling engine performance is calculated. Table (3) shows the results.

2.1.4- Comparison of Engines:

Comparison of the results of these three engines shows that Stirling and Rankine engines are more efficient than Brayton engine (efficiency of ideal Brayton engine is less than the practical Stirling and Rankine engines). Comparison of Stirling and Rankine engines at low temperature-ratios shows that under practical conditions comparable Stirling and Rankine engines work almost at the same efficiency level and a more detailed analysis is required to discriminate between them. On the other hand, at temperature ratios close to unity a Stirling engine with zero regenerator effectiveness has a comparable efficiency to both the Rankine and highly regenerative Stirling engines. Therefore, as is shown in chapter V it would be interesting to determine at low temperature ratios the precise efficiency of the Stirling engine is with and without a regenerator.

Fig. (11) shows the steady state performances of the above three engines. Since Stirling engine shows a better result, then it would be one more reason why this thesis has concentrated on Stirling engine for waste-heat recovery.

2.2- Ideal Stirling Engine Analysis

Analysis of the Stirling cycle is complicated by the fact that not all elements of the working fluid pursue the same thermodynamic cycle. Since the ideal cycle analyses have been presented in closed form solutions, then they are useful for preliminary design and first order calculations. In this section the first order analysis (Schmidt equations) are presented and the optimum design characteristics are derived. In Chapter IV the practical optimum results are compared with the optimum predictions of this section.

2.2.1- Ideal Stirling Cycle, Schmidt Equations:

The ideal Stirling cycle, as discussed in the previous section, consists of two isotherms connected by two isochores. These processes may be produced by interconnecting two suitably varying volumes through a regenerator. The cycle starts with isothermal compression in the cold space at cold temperature,TC, process (4-1). Then the gas flows through the regenerator and gains enough heat to reach the hot temperature, TH. This heating is such that the same volume of gas which enters to the regenerator from cold space should discharge from regenerator to hot space, i.e. the volume variations of hot and cold spaces must be appropriately related. This constraint is necessary to satisfy the isochoric heating process (1-2). Then, as gas expands isothermally in hot space (hot cylinder) at TH, requiring heat to be added to gas to maintain it at TH, process (2-3).

Then the gas returns through the regenerator where heat is removed from the working fluid and stored for its subsequent return, process (3-4), see Fig.(2-5) of previous section.

As we see, so defined is very idealized and impractical engine. A more realistic cycle and corresponding analysis was devised by Gustav Schmidt in 1871. This analysis which has a sinusoidal volume variation has now become the classical analysis of the cycle and is generally believed to give a more reasonable approximation of actual engine performance. Nevertheless, the analysis still remains very highly idealized, so that in practice the indicated performance of an engine will likely be no better than 60% of the predicted Schmidt cycle performance. Principal assumptions of the Schmidt cycle are [25]:

1- The regenerative process is perfect.

2- The instantaneous pressure is the same throughout the system.

3- The working fluid obeys the charcteristic gas equation, $PV = RT$.

4- There is no leakage, and the mass of working fluid remains constant.

5- The volume variations in the working space occur sinusoidally;(this will be used throughout the thesis).

6- There are no temperature gradients in the heat exchangers.

7- The cylinder-wall and piston temperatures are constant.

8- There is perfect mixing of the cylinder contents.

9- The temperature of the working fluid in the dead volumes is constant.

10- The speed of the machine is constant.

11- Steady state flow conditions are established.

As it is shown in Appendix (D) by applying the above assumptions and using $Vh = 1/2VH(1+\cos\omega t)$ for volume of expansion space and $Vc = 1/2VC[1+\cos(\omega t-\varphi)]$ for volume of compression space, followings are resulted:

Instantaneous Pressure = $Pmax(1-A)/[1+A\cos(\omega t-\theta)]$ (D-14)

pressure Ratio = $Pmax/Pmin = (1+A)/(1-A)$

Mean Pressure = $Pm = Pmax * \sqrt{(1-A)/(1+A)}$

Where

X = (Dead Volume)/VH

$A = \sqrt{B}\ /[TC/TH+VC/VH+4X*TC/(TC+TH)]$

$B = (TC/TH)^2 + (VC/VH)^2 + 2TC*VC*\cos\varphi/(TH*VH)$

$\tan(\theta) = [VC/VH*\sin\varphi]/(TC/TH+VC/VH*\cos\varphi)$

Since the expansion and compression processes take place isothermally from the first law the heat transferred Q is equal to the work done W. As shown in Appendix (D), followings are resulted.

==> Expansion Work = $\pi\ Pm*VH*A*\sin\theta/(1+\sqrt{1-A^2})$ (D-21)

==> Compression Work = $\pi\ Pm*VC*A*\sin(\varphi-\theta)/(1+\sqrt{1-A^2})$ (D-22)

Efficiency = $(QE-QC)/QE = 1-QC/QE = \underline{1-TC/TH}$ = Carnot Efficiency

$Wout = \pi * Pm*A*VH*\sin\theta*(1-TC/TH)/(1+\sqrt{1-A^2})$ (D-23)

Instantaneous mass:

Hot Space:

$MH = 1/2VH*Pm*(1-A^2)^{1/2}*(1+\cos\omega t)/[R*TH*(1+A\cos(\omega t-\theta)]$

Cold Space:

$MC = 1/2VC*Pm*(1-A^2)^{1/2}*(1+\cos(\omega t-\varphi)]/[R*TC*(1+A\cos(\omega t-\theta)]$

DEAD SPACE:

$$MD = X*VH*Pm(1-A^2)^{1/2}/[R*TD(1+ACOS(\omega t-\theta)]$$

Total Mass:

$$MT = \frac{VH*Pm(1-A^2)^{1/2}}{R*TC(1+A*COS\theta)}[TC/TH+2X*TC/(TC+TH)+VC(1+COS\varphi)/(2VH)]$$

The normalized output power is:

$$W \triangleq Wout/(Pm*VT) = \pi/(1+VC/VH)*A*SIN\theta/(1+\sqrt{1-A^2})*(1-TC/TH)$$

This equation indicates that output power is a function of temperature-ratio (TH/TC), volume ratios (VH/VC,VD/VH), and phase angle difference between the two spaces (φ).

Appendix (D) shows the derivation of the optimum parameters. To get the optimum dead volume ratio (X = VD/VH) the derivative results is:

$$\frac{\partial W}{\partial X} = -\frac{4\pi A*Tr*SIN\theta*Tr*(1-Tr)}{(1+Tr)(1+Vr)*\sqrt{1-A^2}[1+\sqrt{1-A^2}]*[Tr+Vr+4XTr/(1+Tr)]} \quad (D-33)$$

This means that output has a negative slope with respect to X and it decreases continuously by increasing X. Therefore, there is no optimum dead volume ratio and it should be made small as much as possible in practice. Fig. (12) shows the same conclusion which Walker [25] has come to by doing significant amount of calculations.

In order to find the optimum swept-volume (Vr = VC/VH) based on Schmidt analysis Appendix (D) shows that derivative of output respect to Vr yields following quadratic equation:

$$Vr^2(1-A^2-A^2\sqrt{1-A^2})-Vr(A^2+A^2*Tr+4XA^2*Tr/(1+Tr)+2A^2\sqrt{1-A^2}*Tr+$$
$$8A^2\sqrt{1-A^2}X*Tr/(1+Tr)-1)-(A^2*Tr+4XTrA^2/(1+Tr)+A^2\sqrt{1-A^2}*Tr^2+$$
$$16[AXTr/(1+Tr)]^2\sqrt{1-A^2}+8A^2X\sqrt{1-A^2}*Tr^2/(1+Tr)) = 0 \quad (D-38)$$

For Tr = .5 , X = 1 , $\varphi = 90^{\circ}$ ==> Vr = 1.07

For Tr = .25 , X = 1 , $\varphi = 90^{\circ}$ ==> Vr = .84

By plotting output versus Vr Walker [25] has come to the same results, Fig.(13) shows his curves.

To get the optimum phase angle difference φ, as it shown in Appendix (D), derivative of normalized output has taken respect to φ . The results are summarized in the following quadratic equation:

$$Vr*Tr[1/\sqrt{1-A^2}-1/A^2]\cos^2\varphi+[Tr^2+Vr^2+4X*Tr/(1+Tr)]^2\cos\varphi+$$
$$Vr*Tr[1/A^2-1/\sqrt{1-A^2}]=0 \qquad (D\text{-}42)$$

This equation shows how the optimum φ is related to temperature ratio and swept-volume ratio. Walker [25] has found the optimum phase angle difference by plotting the output versus φ. Fig. (14) shows his results for two different temperature ratios. The above equation would give the same results directly and quickly.

As the temperature ratio (TH/TC) increases the output would increase and the slope of output power with respect to temperature-ratio is always positive and non-zero.

The result of this section shows the basic equations for design and optimization of Stirling engine for an ideal case. Chapter IV will show the validity of these results for practical engines.

2.2.2- Effect of Imperfect Regenerator and Dead Volume on Ideal Engine:

Practical regenerators are not perfect which means the amount of heat gained by the gas from regenerator material is less than the heat which was extracted from the gas by the regenerator during the first part of the cycle. Therefore, on the way to the hot space, the gas leaves the regenerator with a temperature less than the hot temperature of the cycle (TH) and that is the reason for having the heater between regenerator and hot space in real engines. Fig. (15) shows a schematic diagram of a real engine, for this engine based on hot and cold temperatures we can define a log-mean temperature for the regenerator as follows.

$$TR = (TH-TC)/(\ln TH/TC)$$

$$\text{Regenerator Effectiveness} = E \triangleq (TR-TC)/(TH-TC)$$

$$\Longrightarrow TH - TR = (1-E)(TH-TC)$$

$$Qin = Cv\,(TH-TR) + R\,TH \ln P_2/P_1 = Cv\,(1-E)(TH-TC) + R\,TH \ln P_2/P_1$$

$$Wout = R\,TH \ln P_2/P_1 - R\,TC \ln P_2/P_1$$

$$\text{Efficiency} = \frac{1 - TC/TH}{1+Cv/R^*(1-E)(1-TC/TH)/(\ln P_2/P_1)}$$

$$\frac{\text{Efficiency}}{\text{Ideal Eff.}} = \frac{1}{1+(1-E)/(k-1)(1-TC/TH)/(\ln P_2/P_1)} \qquad \text{(E-16A)}$$

Fig. (16) and table (4) show how the efficiency varies with regenerator effectiveness for different temperature ratios. As the results show, at low temperature ratios (about 1.2) the real engine (i.e, engine with imperfect regenerator) is close to ideal cycle (Carnot efficiency), even at E = 0 the engine

efficiency is about 60% of the ideal engine.

Due to the introduction and addition of heater and cooler to the system and because of imperfect regenerator, there are some additional dead volumes (void volume) present in the system. These dead volumes would push the engine farther from ideal case. An inefficient regenerator backed up by an adequate gas heater and gas cooler will not change the work realized per cycle but will definitely increase the heat required per cycle. But addition of dead volume, which must be present in any real engine, decreases the work available per cycle.

Appendix (E) shows the net output of the engine for case of having dead volume as:

$$\frac{W_{out}}{W_{out}\big|_{\substack{\text{Zero}\\\text{Dead}\\\text{Volume}}}} = \frac{T_H/T_C \ln\left[\left(\frac{1-X}{1+\bar{A}}\cdot\frac{\bar{A}}{T_H}+X/T_R\right)\Big/\left(\frac{1-X}{1+\bar{A}}\cdot\frac{1}{T_H}+X/T_R\right)\right]-\ln\left[\left(\frac{1-X}{1+\bar{A}}\cdot\frac{\bar{A}}{T_C}+X/T_R\right)\Big/\left(\frac{1-X}{1+\bar{A}}\cdot\frac{1}{T_C}+X/T_R\right)\right]}{(T_H/T_C-1)\cdot\ln\bar{A}} \qquad \text{(E-16B)}$$

Where: $T_R/T_H = (1-T_C/T_H)/(\ln T_H/T_C)$, $\bar{A} = P_1/P_2 = \frac{V_{H2}}{V_{H1}}$

$T_R/T_C = (T_H/T_C-1)/(\ln T_H/T_C)$

Fig. (17) and table (5) show the variation of output with increasing dead volume of the system for case A=2 and different temperature ratios. From the above equation we see if TH/TC gets large Wout becomes very small. But in the temperature-ratio range 1.0 to 2.0 the variation of output work with respect to dead volume is almost independent of temperature-rato.

Although the above calculations regarding the imperfect regenerator and the presence of dead volume are for steady state cases and are only first order, nevertheless they show how the

real engine trends farther and farther from ideal case. Also they indicate that at low-temperature-ratios dissipation terms and entropy generations are lower.

2.3- Evaluation of Different Types of Losses

Analysis of the Stirling engine is complicated by the fact that not all elements of the working fluid pass through the same thermodynamic cycle. The first order analysis and some of the conventional techniques of considering a fixed mass of working fluid passing through a unique cycle can not be used. It is necessary instead to examine individual volume elements and take into account the movement of working fluid into and out of each one. Since the volume in the heat exchangers (dead volume) is a significant portion of the total volume in an engine, an important fraction of the working fluid is utilized to pressurize this space instead of being actually moved from one variable volume to another to contribute effectively to the net output work. In the ideal cycle, where pressurization and depressurization of this volume takes place reversiblly, both effects will cancel out so that no work is required.

However, in a practical engine the hot and cold spaces (cylinders) are nearly adiabatic, and an irreversibility does exist when gas moves from a cylinder into the adjacent heat exchanger at a temperature different from the heat-exchanger wall temperature, and this can produce a significant loss.

In general, the losses due to imperfect components can be divided into three types: those which are in the pressure-volume flow domain, those in the force-velocity domain, and those which are in the temperature-entropy domain. Pressure drop in the heat-exchangers, which produces power loss, belongs to the first

group, while axial conduction and the effect of piston motion are in the third group, and coulumb friction is in second group. In this section different types of losses, which have been realized up to this time, are evaluated based on the most recent analytical techniques.

2.3.1- Pressure-Volume Flow Domain Losses

Although there are some differences in design configurations of Stirling engine, but for analysis all of them can be simplified as shown in Fig. (15). There are five major components: cold space, hot space, cooler, regenerator, and heater. In the ideal cycle there are only three components, i.e. there is no heater and cooler in the system. In fact, the hot and cold spaces are surrounded by hot and cold temperature sources.

Considering the general configuration of a real engine, free flow areas in the three heat-exchangers are relatively small which result a significant pressure loss in the system. Power loss due to the pressure drop has been evaluated in a similar fashion in all of the previous analysis. References [18], [22], [13] have shown the complete derivation. There follows a summary of the basic principles and equations.

The existing pressure gradient is a function of time and position. Since the free flow area inside the hot and cold spaces (cylinders) are generally large relative to the other components, then the pressure drop inside these spaces are negligible. Therefore, this gradient is calculated only for heat-exchangers.

Let x denote the distance along any heat-exchange component and let L denote the length of this component. The pressure drop at a point x may be expressed in terms of the friction factor fx as

$$d(\Delta P) = 1/2*fx*(L/d)\rho x*Vx*|Vx|*d(x/L)$$

where d is the hydraulic diameter, Vx is the velocity and ρx is the density at point x and time t. It will be assumed at this point that the hydraulic diameter d and the free flow area AFR of the components do not vary with x for each component. If one of the heat-exchange components does have a change in these variables, it may simply be treated as several components of different hydraulic diameters and free flow areas.

$$\dot{m}x = \rho x*AFR*Vx$$

$$\Longrightarrow |d(\Delta P)| = 1/2*fx*(L/d)*(\dot{m}x)^2/(\rho x*AFR*AFR)*d(x/L)$$

$$\rho x = Px/(R*Tx)$$

$$|d(\Delta P)| = 1/2*fx*(L/d)*(\dot{m}x^2*R*Tx)/(AFR*AFR*Px)*d(x/L)$$

$$|\Delta P| = 1/2\int_0^1 fx(L/d)*(\dot{m}x^2*R*Tx)/(AFR*AFR*Px)*d(x/L)$$

For Cooler:

$$|\Delta P| = 1/2(L/d)_C*(R*TC)/(AFRC*AFRC)\int_0^1 fx*\dot{m}x^2/Px*d(x/LC) \qquad (2\text{-}1)$$

For Heater:

$$|\Delta P| = 1/2(L/d)_H*(R*TH)/(AFRH*AFRH)\int_0^1 fx*\dot{m}x^2/Px*d(x/LH) \qquad (2\text{-}2)$$

For Regenerator:

$$|\Delta P| = 1/2(L/d)_R*(R*TR)/(AFRR*AFRR)\int_0^1 fx*\dot{m}x^2/Px*d(x/LR) \qquad (2\text{-}3)$$

Based on the given geometry, the free flow area (AFR) and other dimensions are specified. As the above equations show, mass flow rates are required to calculate pressure drops, fx which is the

coefficient of friction depends on Reynolds number which itself depends on mass flow rate.

$$fx = a/(Re)^{**}b$$

$$Rex = (\rho x*Vx*d)/\mu = (\dot{m}x*d)/(AFR*\mu)$$

Therefore, it is important to calculate mass flow rate of each component. In order to simplify the whole calculation process, a time averaged mass flow rate can be used for each heat-exchanger. Therefore, equations (2-1) through (2-3) are rewritten as:

For Cooler:

$$|\Delta P| = 1/2(L/d)_C * (R*TC)/(AFRC*AFRC) * \bar{f}C * \bar{\dot{m}}C/PC \qquad (2\text{-}4)$$

For Heater:

$$|\Delta P| = 1/2(L/d)_H * (R*TH)/(AFRH*AFRH) * \bar{f}H * \bar{\dot{m}}H/PH \qquad (2\text{-}5)$$

For Regenerator:

$$|\Delta P| = 1/2(L/d)_R * (R*TR)/(AFRR*AFRR) * \bar{f}R * \bar{\dot{m}}R/PR \qquad (2\text{-}6)$$

Where PC, PH, and PR are the mean pressures inside the cooler, the heater, and the regenerator, respectively.

Now, supposing the pressure drops have been calculated, how they can be related to the power loss is important, yet not quite clear. Proper allocation of the losses and determination of where the entropy generation is occuring both significantly affect the engine performance. Engines which have been presumed to have high efficiencies often in practice do not perform as well. This is most often due to the improper allocation of the losses in the system.

In the design of a steady-flow cycle the inlet and discharge

conditions of the compressor are usually fixed first for the design. Then the performance is calculated for the system assuming perfect components. This first approximation yields information which may then be used to calculate the performance with real components, but maintaining the same compressor inlet and outlet conditions.

This approach can be used here, i.e. the effect of the pressure drop in the heat-exchangers may be ascertained by maintaining the warm-end (hot cylinder) conditions at the same values but the cold-end (cold cylinder) conditions would change. This means that most entropy generations and system dissipations are located at the cold-end of the engine. Therefore, at the hot space pressure and mass variations are unchanged by introduction of pressure drops. For the cold-end we get:

Cold Space Volume:

$$VC = VC + \Delta VC$$

with ΔP

Cold Space Pressure:

$$PC = PH + \Delta P$$

Work at Cold Space:

$$WC = \oint PC * d(VC) = \oint (PH + \Delta P) d(VC + \Delta VC)$$

By neglecting the second order terms we get:

$$WC = \underbrace{\oint PH * d(VC)}_{1} + \underbrace{\oint \Delta P * d * VC}_{2}$$

The first term is the compression work for case of having no pressure loss, and the second term is the power loss due to the pressure gradient. Because the compression work has increased

by the second term this extra work has to be subtracted from the output work of the engine.

$$Wloss = \oint \Delta P * d(VC)$$

This integration can be done either by computer or by some averaging process as shown in chapter III.

2.3.2- Temperature-Entropy Domain Losses

Events which decrease the effective hot temperature of the hot space and increase the effective cold temperature in the cold space would push the engine farther from the ideal case and generate entropy inside the system. Those losses which are in this category and which have been considered by investigators up to this time are: temperature drop losses in heater and cooler, regenerator imperfection from heat transfer view point, axial conduction heat transfer loss, piston-motion or shuttle heat transfer loss, heat leakage from the system, transient heat transfer loss due to the non-uniform temperature distribution, and heat pumping loss inside the gap between cylinder and piston. In this section derivation of each of these losses is presented.

2.3.2.1- Temperature-Drop Losses in Heater and Cooler

A temperature difference is necessary in order to transfer heat between the working fluid and the heat-exchanger walls. This means that the temperature of the gas entering the hot and cold spaces (cylinders) and the regenerator will not be the same as heat exchanger wall temperature but a slightly different temperature.

In a Stirling engine, especially when the temperature ratio is high (TH/TC>2.0), the heat transferred in moving the gas through the regenerator is large compared to the heat transferred in moving the gas from the cylinder to the regenerator. In other words, the work transfer in the cylinders is smaller than the heat which is transferred to the gas from the heat-exchangers.

That quantity which is of interest in order to evaluate the effect of the imperfect heat exchange on the over-all performance of the engine is the average temperature of the gas entering the hot or cold space (cylinder). A simple approach to find the effective temperatures is to consider that a heat transfer equal to the work done by the gas in the adjacent space (cylinder) must take place in every cycle.

Consider the following figure, the basic work delivered by one piston = $\int_0^{2\pi} \dot{m}*Cp*T*dt$ at the face of the heat exchanger.

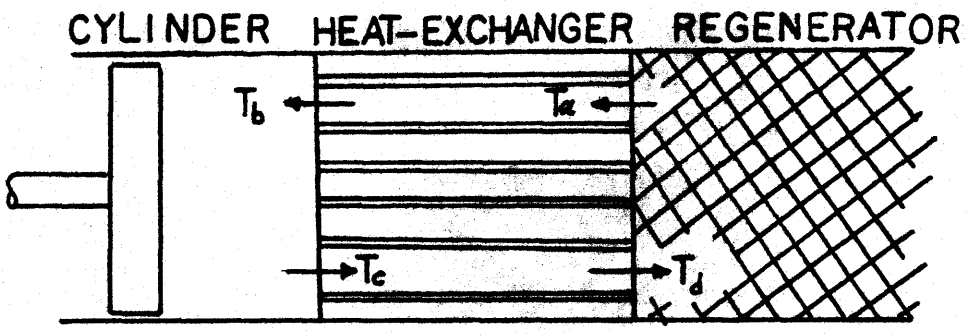

then $m*C_p*\Delta T_{EQ}$ = Work or ΔT_{EQ} = work/$m*C_p$

The gas enters the heat-exchanger from the regenerator with a temperature Ta; at the exit of the heat-exchanger, the temperature is Tb. When the gas enters the heat-exchanger from the cylinder side, its temperature is Tc; at the entrance of the

regenerator the temperature is Td. For a perfect regenerator Ta = Td, furthermore ΔT_{EQ} = Tc - Tb. The temperature of the heat-exchanger is assumed to remain constant at T_s throughout the cycle. Then it follows from heat-exchanger theory [23] that:

$$(Ts - Ta)*EXP(-NTU) = Ts - Tb$$

$$(Ts - Tc)*EXP(-NTU) = Ts - Ta$$

By combining the above equations:

$$\Delta T \triangleq Ts - Tb = (\Delta T_{EQ})/[EXP(2*NTU)-1] =$$

$$\Delta T = Work/[m*Cp*(EXP(2*NTU)-1)] \qquad (2-7)$$

Equation (2-7) shows the difference between temperatures of the gas entering the cylinder and the heat-exchanger surface temperature, or the source temperature.

Effective Temperature in Cold Space:

$$\overline{TC} = TC * [1-Wc*(k-1)/(mc*R*TC*k)/[EXP(2*NTUc)-1]] \qquad (2-8)$$

Effective Temperature in Hot Space:

$$\overline{TH} = TH * [1-Wh*(k-1)/(mh*R*TH*k)/[EXP(2*NTUh)-1]] \qquad (2-9)$$

These effective temperatures which are different from the source temperatures, TC & TH, would represent temperature drop in heater and temperature increase in cooler. The consequent entropy generation in these heat-exchangers results in a power loss which is taken out in the compressor. This means that the compression work would be increased by a factor $(\overline{TC}/TC)*(TH/\overline{TH})$. Then by using equations (2-8) and (2-9) the following are resulted.

$$\frac{Wc,real}{Wc,ideal} = \left[1 - \frac{Wc*(k-1)}{mc*R*TC*k}*\frac{1}{e^{2NTUc}-1}\right] \Big/ \left[1 - \frac{Wc*(k-1)}{mh*R*TH*k}*\frac{1}{e^{2NTUh}-1}\right]$$

$$\approx 1 - \frac{Wc*(k-1)}{mc*R*TC*k}\frac{1}{e^{2NTUc}-1} + \frac{Wc*(k-1)}{mh*R*TH*k}*\frac{1}{e^{2NTUh}-1}$$

Which means:

power loss due to the temperature drop in heater=

$$Wh*Wc*(k-1)/(mh*R*TH*k)/[EXP(2*NTUh)-1] \quad (2-10)$$

power loss due to the temperature drop in cooler=

$$Wc*Wc*(k-1)/(mc*R*TC*k)/[EXP(2*NTUc)-1] \quad (2-11)$$

2.3.2.2- Imperfect Heat Transfer in Regenerator

In the ideal (perfect) regenerator, when gas flows through the regenerator, coming from the warm-end of the engine at hot temperature TH, it releases heat such that by the time that the flow leaves the regenerator it reaches the cold temperature TC and the regenerator gains all of the heat. Then similarly, when gas flows back from the cold-end at TC temperature and back through the regenerator it should be reheated by the regenerator such that when the flow leaves the regenerator it should have temperature TH. This happens only in ideal case,i.e. having instantaneous heat transfer with no thermal resistances. Therefore, we can define a regenerator effectiveness as the ratio of the actual heat which is transferred to the gas, by the regenerator, to that transferred ideally.

$$E = QR/[m*Cp(TH-TC)] \quad (2-12)$$

If the effectiveness can be calculated then QR and consequently [m*Cp(TH-TC)-QR] which the heat loss due to the imperfect regenerator can be evaluated. Qvale and Smith [20] have derived on approximate closed form solution for the enthalpy flow through the regenerator. This solution was derived for sinusoidal pressure and flow variations. Rios [22] derived a more general

solution for this enthalpy flow calculation but it requires computer simulations. His derivation is in fact used for the analysis in the next section. In Chapter III a closed form solution is used which results in the same amount that the Rios [22] computer method calculates. This solution is

$$QR = ft * \dot{m}_R * Cv(TH-TC) * \underbrace{[2/(NTUv+2)]}_{\text{Reg. Ineffectiveness}} \qquad (2\text{-}13)$$

Where $NTUv = H*(AH)/(\dot{m}_R*Cv)$

2.3.2.3- Axial Conduction Heat Loss

All materials conduct heat to a greater or lesser extent. Metals are generally good conductors. Since there is a temperature gradient between the two ends of the Stirling engine, then one might expect a significant amount of heat conduction from the warm side of the system (heater) to the cold side (cooler). The intermedia which conduct this heat are regenerator internal solid material and also the gas inside the void volume of the regenerator. Therefore this conduction depends on the porosity of the regenerator. Usually the regenerator of a Stirling engine is made of many layers of fine screen lightly sintered together. The degree of sintering would have a big bearing on the thermal conductivity of the screen stack since the controlling resistance is now the contact between adjacent wires. Since the wires are somewhat like uniformly sized cylinders then the formula which is given by Gorring [13] can be used for thermal conductivity of the combination of gas and material of the combination

of gas and material of the regenerator.

$$Kmg = Kg \left[\left(\frac{1+Km/Kg}{1-Km/Kg} - 1 + SIG \right) / \left(\frac{1+Km/Kg}{1-Km/Kg} + 1 - SIG \right) \right] \qquad (2\text{-}14)$$

Where SIG is the regenerator porosity, Kg is the gas conductivity and Km is the metal conductivity. Therefore, the conducted heat would be

$$Qc = Kmg * AR * (TH-TC)/LR \qquad (2\text{-}15)$$

Where LR is the regenerator length and AR is the cross-sectional area of the regenerator.

2.3.2.4- Shuttle Heat Transfer Loss

Shuttle loss is one of the important thermal effects found in Stirling engines. This effect comes from the reciprocating action of the displacer (piston) in the cylinder. There is a temperature difference along the walls of the cylinder and the displacer (piston), from the hot end to the cold end.

At Top Dead Center:

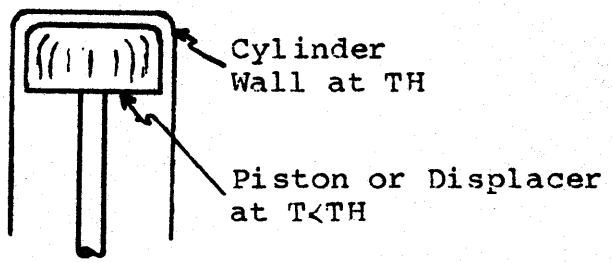

At Bottom Dead Center:

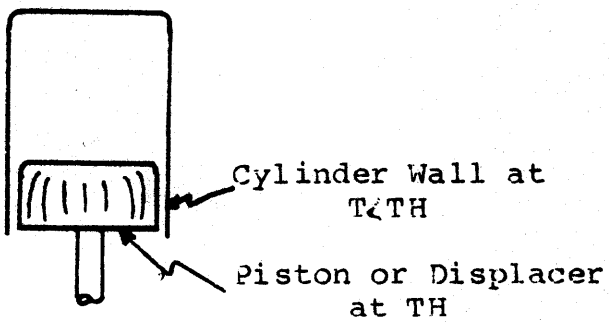

When the displacer (piston) moves toward the top dead center position its temperature is less than TH and it is entering to a region with TH temperature; therefore there is a heat conduction from the cylinder walls to the displacer (piston). The reverse conduction occurs when the displacer (piston) is at bottom dead center. This conduction occurs through each reciprocation. Rios [22] has presented a nice derivation for this heat conduction.

$$Q = \pi/8*Kg*S*(TH-TC)*(B/\ell)*(S/L)*(BET) \qquad (2\text{-}16)$$

$$BET = (2C^2 - C)/(2C^2 - 1)$$

$$C = Kp/Kg * \ell * \sqrt{\omega/(2*\alpha p)}$$

Where B and S are the bore and stroke of the hot cylinder, Kp and αp are thermal conductivity and thermal diffusivity of the displacer (piston), ℓ is the gap between piston and cylinder, L is the piston length and ω is the frequency of the engine.

2.3.2.5- Heat Leakage

Since the warm-end of the system operates at a temperature greater than the ambient temperature, then heat conduction and radiation effects are present. Depending on the hot temperature if TH is high enough i.e. of the order of 1000° F then radiation heat transfer would be significant otherwise, conduction would be the primary mechanism for significant heat leakage from the system. Because the present work deals with the temperature ratios less than 2.0, then only conduction heat transfer is assumed.

Appendix (F) shows the stress analysis for the calculation of the cylinder thickness. The result is:

$$t = (Pm*R)/5000 \qquad (2\text{-}17)$$

Where t is the cylinder thickness, Pm is the mean pressure, and R is the cylinder radius.

Inside the cylinder, there is forced convection mechanism and outside of it there is a free convection heat transfer.

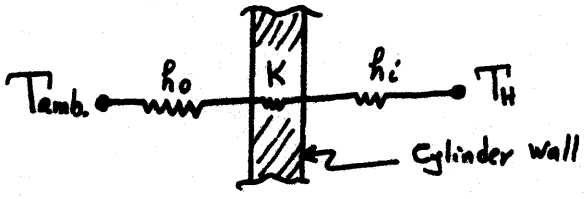

$$QL = \frac{2\pi(TH - Tam)}{1/(L*R*hi)+\ln((R+t)/R)/(L*K)+1/[L*(R+t)*ho} \qquad (2\text{-}18)$$

For forced convection inside the cylinder we take $hi*D/Kg = 6$

$$\Rightarrow \quad hi = 3*Kg/R$$

For free convection outside, especially because the outside fluid is air, we assume ho = 3.5 Btu/ft^2 hr ^{0}R. Also for length L one-half of the stroke is chosen. This is due to the fact that gas has almost a sinusoid motion the amplitude of that which is half of the stroke would be a suitable characteristic of length. Therefore, by substituting all of these in equation (2-18) we get:

$$QL = \frac{\pi(TH - Tam)}{1/(3S*Kg)+\ln((R+t)/R)/(S*K)+1/(3.5S*(R+t))} \qquad (2\text{-}19)$$

Where Kg and K are thermal conductivities of the gas inside the cylinder and the wall material, respectively, S is the stroke and R is one-half of the bore.

If the radiation heat transfer is significant then a similar analysis with radiation heat transfer equation can be used. Although the temperature inside the cylinder has a sinusoidal variation with a mean value, i.e. it is a combination of a constant and an alternatory temperatures, but because of low amplitude of the alternatory part, less than 10% of the constant value, the mean (or constant) value can be used in equation (2-19) for heat leakage calculation.

2.3.2.6- Transient Heat Transfer Loss in the Cylinders

One of the important characteristics of an ideal Stirling engine is the assumed uniform temperature distribution of the gas inside the cylinders. However, in a real engine the temperature is not uniformly distributed at any time inside the cylinders. The resultant temperature gradient between the layers of the gas in the center and near the wall of the cylinder produces a heat flow from the wall to the center and vice-versa, which Smith and co-writer have called the instantaneous or transient heat transfer. Various formulae have been proposed to estimate this heat rate inside the cylinder of internal combustion engines [28] and compressors [30]. Although some of these formulae can predict heat transfer rates reasonably close to test data for particular applications, they can not be readily applied to Stirling engines because of the unique pressure, temperature and flow patterns in the latter case. Since there are no internal valves, Stirling engines have nearly sinusoidal pressure and local temperature variations. In 1980, for the first time

Kangpil Lee, Joseph Smith, and Henry Faulkner [10] presented a closed form solution for derivation of this heat transfer loss. Their solution is used for the present work in the next section. It can be summarized as

$$Qloss = \frac{30\sqrt{(k-1/k)^3/\pi N}*P_1\left[TC/TH*\sqrt{Kgh*TH}*Fe*Ae+\sqrt{Kgc*TC}*Fc*Ac\right]*B}{Pm*\sqrt{Pm}*VC(1+\lambda*TC/TH+V)} \qquad (2\text{-}20)$$

Where P_1 = Amplitude of pressure variation = (Pmax-Pmin)/2

$B = [(SIN\varphi_p+COS\varphi_p)(\lambda+COS\varphi)+SIN\varphi(SIN\varphi-COS\varphi_p)]$

Pm = mean pressure

φ_p = Pressure wave phase angle with respect to expansion space volume displacement

φ = Phase angle between the cold and hot spaces

Ae, Ac = Heat transfer areas of hot and cold spaces

N = Angular speed [RPM]

λ = VH/VC

V = VCD/VC + VHD/VC* TC/TH + VRD/VC * TC/TR

VCD, VHD, VRD = dead volumes of cooler, heater, and regenerator there are two unknown coefficients Fe and Fc which are called "heat transfer enhancement factors". In the cited reference [10] it is said that these coefficients are functions of Reynolds and Prandlt numbers, bore-stroke ratio, and relative clearance volume. There now exist correlations for these coefficients based on the data from experiments as part of Foster-Miller Associates proprietary information. However for some cases used of the present work appropriate coefficients have been obtained.

An alternative for calculating this loss would use experimental data from internal combustion engine testing for determining non-uniform temperature distribution inside the cylinder; this technique seems to give good estimates. Taylor [24] has given the following correlation for calculation of heat transfer coefficient between the gas inside the cylinder and the walls.

$$h*D/Kg = C*(GL/\mu)^{n}*(Cp\ \mu/Kg)^{m}$$

Where h is the coefficient of heat transfer which a function of Reynolds and Prandlt number. C, n, and m are dimensionless numbers which depend on the geometry of the flow system and on the regime of the flow. For a good number of experiments Taylor has obtained the following result.

$$h*D/Kg = .023*(Rey)^{.8}*(Pr)^{.4} \qquad (2\text{-}21)$$

In order to avoid the use of the empirical correlation factors (enhancement factors) in equation (2-20) for non-uniform temperature loss, the above correlation (2-21) can be used. To do that, a form for temperature distribution inside the thermal boundary layer is required. Appendix (G) shows how the temperature distribution which is calculated in [10] is converted to the following form.

$$\Delta T/Tm = (k-1/k)*Pl/Pm*(1-e^{-1})SIN(\omega t-\phi p) \qquad (2\text{-}22)$$

Where Tm and Pm are mean values for the flow temperature and pressure respectively, Pl is the amplitude of the pressure variation, and ϕp is the phase difference between pressure wave and expansion space volume displacement.

Since convection heat transfer is the dominant mechanism for heat transfer between the gas and the cylinder wall, then by combining the general convection heat equation and equations (2-21) and (2-22) the following solution is resulted, see Appendix (G).

$$Q(t)=.01454\pi*Kg*Tm*(Re)^{.8}(Pr)^{.4}*(k-1)/k*Pl/Pm*Xm(1+SIN\omega t)*$$
$$SIN(\omega t-\phi p) \qquad (2\text{-}23)$$

This equation can be integrated over a cycle to find the average heat transfer between the gas and cylinder wall. The result becomes:

$$Q= .052\ (Re)^{.8}(Pr)^{.4}*(k-1)/k*Pl/Pm*COS(\phi P)*Kg*Tm*Xm \qquad (2\text{-}24)$$

Where Xm is the amplitude of the piston displacement which equals to one-half of the stroke.

A third approach to this problem involves a lumped element modelling of the thermal diffusion problem. As discussed in the next section for a practical engine the cylinder processes are assumed adiabatic for each cylinder there is an enthalpy flow from the system into it. Thus the gas inside behaves like infinite number of thermal capacitances with thermal resistances in between. Therefore, each cylinder can be modelled as parallel capacitances with resistances in series with them. Appendix (G) shows circuit graph and bond graph of such a gas cylinder. The simplest model is a two-lump model which assumes part of the gas inside a sub-layer close to wall is at temperature equal to the cylinder wall temperature and the rest of the gas is at a core temperature different from the wall temperature.

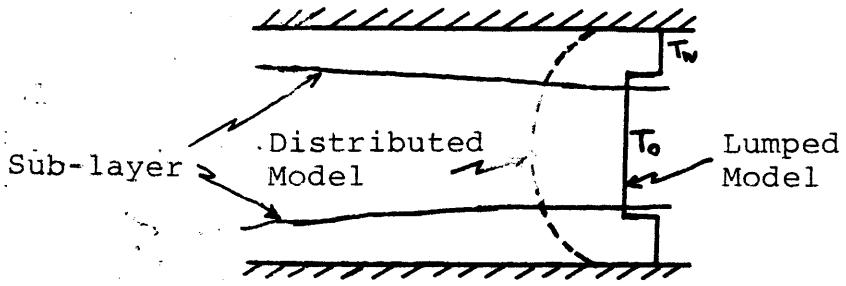

As derived in Appendix (G), for this two-lump model the governing transfer function is:

$$T0/Tm=(1+\tau_1 S)/(1+\tau_2 S) \quad ,$$

$$Tw/Tm=1/(1+\tau_b S)$$

Substitution of $i\omega$ for S shows that $T0/Tm=(1+\tau_1 * i\omega)/(1+\tau_2 * i\omega)$ contains the first order approximation for $e^{i\omega\tau}$. It is clear that by increasing the number of lumps we get closer to the exact solution. If we use N-lumps then it can be shown that the governing transfer function would approximate well the form $TN/T0=((1+\tau_1 S)/(1+\tau_a S))^N$. Although the N-lump solution is more accurate for higher values of N, yet if the time constants (τ_a, τ_b) are selected properly then the result of the N=1 model can follow a similar behavior as higher order models. Appendix (G) shows a sample of t_1, tvderivations and calculations.

Since the system can be either temperature or pressure forcing, then a similar result can be derived for the instantaneous pressure. For a reversible adiabatic process we have:

$$P.(T)^{k/1-k}=Const. \qquad (2-25)$$

By taking the logarithmic derivative of equation (2-25) respectively we get:

$$\Delta P/P = k/(k-1) * \Delta T/T$$

This means that for instantaneous pressure we have the following equation, based on the previous result for instantaneous temperature.

$$\Delta P/Pm = k/(k-1) * (1+\tau_i S)/(1+\tau_o S) \qquad (2-26)$$

This lumped modelling which results in estimated transient response of the pressure and temperature can be used as part of the basic thermodynamic equations for the Stirling engine analysis. By using Euler's integration method, equation (2-26) can be rewritten as

$$dP = 1/\tau_o * [k/(k-1) * Pm - P] + \tau_i/\tau_o * dPm \qquad (2-27)$$

Addition of this equation to each of the four sets of equations given in the next section, equations (2-35) through (2-42) which calculate the basic heat input and the output work, would introduce the change in instantaneous pressure to the basic equations. This means that in this way the transient heat transfer loss can be automatically inserted into the Stirling engine analysis.

This formulation has been treated as applied to heat transfer in the radial direction, but it can be used for axial direction as well. The same region, i.e., sub-layer which exists on the cylinder wall is present on the piston face too. The longer stroke produces a thicker boundary layer which results to a higher temperature gradient and, consequently, additional heat transfer losses in the axial direction. The same thing happens with a larger bore but now in the radial direction. Therefore, there would appear to be an optimum bore-stroke ratio based on

minimization of this loss.

In order to include the axial direction heat transient loss, we must increase the total heat transfer area of the first two methods, or else add a new set of thermal capacitances and resistances following the third approach.

2.3.2.7- Heat Pumping Loss Inside the Piston and Cylinder Gap:

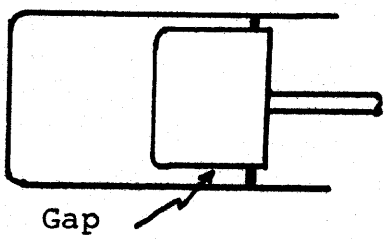

There is a radial gap between the inner diameter (ID) of the engine cylinder and the outer diameter (OD) of the piston (displacer). This gap is ring-sealed at the cold end. As the engine is pressurized and depressurized, gas flows into and out of this gap. Since the closed end of the gap is cold, extra heat must be added to the gas as it comes back from this gap. Leo [13] has derived the following semi-empirical equation for the amount of heat loss by this mechanism

$$2\dot{w}/3\pi * [\omega * B * Cp/(2Kg)]^{.6} * [(Pmax-Pmin) * \ell/(R*TR)]^{1.6} * Cp(TH-TC) * L * Lp \qquad (2\text{-}38)$$

Where B is the bore, ℓ is the gap size, Lp is the length of the displacer (piston) and ω is the frequency.

2.3.3- Force-Displacement Domain Loss

The only utilized loss in this category is mechanical friction loss. In the literature of Stirling engine there is no equation or correlation or even any data for this type of

loss. Martini [13] has arbitrarily used 20% of the basic output power as mechanical friction. For the present analysis, the data for internal combustion engines has been used to estimate this loss. Fig.(22) shows the basic correlation which is derived from reference [27] . This figure shows mechanical friction loss for the piston in terms of the friction-mean-effective-pressure (fmep). Since it approximates a linear relationship between fmep and engine speed, then the following correlation has been used.

$$fmep=.002N+1 \qquad (2\text{-}29)$$

Where N[RPM] and fmep[psi].

Then the power loss due to this friction effect, based on the mean effective pressure definition, is:

$$P=fmep*V*N*n/531$$

Where n is the number of cylinders, and V is the displacement volume.

$$P_{loss}=2N*(.002N+1)*(VH+VC)/531 \qquad (2\text{-}30)$$

N[RPM], VH,VC[in^3] , and P_{loss}[Watts].

Although equation (2-33) is based on IC engines and here is used for Stirling engine nevertheless, as is shown in the following sections, it matches reasonably well the only data published by Philips Laboratories [15] concerning this loss.

2.4- Analysis and Modelling of Practical Stirling Engines

Analysis of the Stirling engine can be divided into three groups or so called "orders" [13] . First order analysis includes the basic thermodynamics of the engine on a stepwise model which is usually called the Schmidt analysis. In order to make this analysis comparable with real engine performance it should be combined with some critical experience factors. Second order analysis starts with the Schmidt analysis or something similar. Various power losses are calculated and deducted from the Schmidt power. Various heat losses are calculated and added to the Schmidt heat input. All these engine processes are assumed to proceed in parallel and independently of each other. Finally, the third order analysis divides the engine into a number of nodes and solves the basic differential equations that govern this engine by numerical methods. Third order methods are much more laborous, but since fewer assumptions are made, prediction of engine performance is expected to be more accurate.

In this section the method of analysis which is used for this thesis is presented. This method is more accurate than the second order analysis and it is essentially based on the Rios [22] second order model. Similarity of this model and the second order methods is because calculation of the losses is independent of the basic engine thermodynamics calculations. Otherwise, it makes no use of the Schmidt model, as being too idealized.

As a first approximation to the Stirling cycle, consider a system with five perfect components as shown in Fig (18). By perfect it is meant that there is no pressure drop and no gas-to-wall temperature difference in the heat-exchange components, no axial conduction nor heat transfer to the environment, and no irreversibility due to friction in the cylinders or in any other components. It is also presumed that the cylinders are perfectly adiabatic and the temperature inside them has a uniform distribution.

2.4.1- Perfect Engine Model

The differential equations governing the behavior of the Stirling engine with perfect components are derived in appendix (H). The assumptions made in this derivation are as follows :

a- The cylinders are adiabatic. In the early analyses of the Stirling engine the cylinders were considered to be isothermal. This was due more to the ease of analyzing a constant-temperature cylinder than to the existence of isothermal conditions even in the slow machines of the nineteenth century. Stirling engines which have been designed recently operate at relatively high speeds. This makes the heat transferred per cycle in a cylinder negligible when compared to the work transfer per cycle. Attempts have been made to obtain isothermal compression and expansion by increasing the piston and cylinder areas, but up to the present time they have not been of practical importance.

b- Perfect heat-exchange components. This assumption is

made for the first approximation only and will be removed by subsequent corrections.

c- The gas density at any point in a heat-exchange component is a function of pressure only, and, therefore, the mass of gas in a component is a function of pressure only. Since the working gas is exchanging heat with a constant-temperature medium in the heat exchangers, it follows that for efficient heat-exchangers the variation in the temperature of the gas in the heat exchanger must be small when compared to the absolute temperature. Therefore, the mass contained in a heat exchanger may be considered to vary with pressure only. This is true even for the regenerator because gas is exchanging heat with a solid matrix material which has a heat capacity higher than the gas heat capacity by several orders of magnitude. Then for a relatively efficient regenerator the temperature variation at a point must be small when compared to the absolute temperature.

d- The temperature is uniform throughout any plane perpendicular to the direction of flow; therefore, the problem may be treated as one dimensional in space.

e- The gas in each cylinder is perfectly mixed. The amount of mixing in the cylinder will depend on the way in which the gas enters the cylinder from the heat exchanger. Generally, the free flow area of the heat exchanger will be less than that of the cylinder, and there will be relatively effective mixing when the jet of gas enters from the heat exchanger into the slower-moving gas in the cylinder.

As it is discussed in the previous section the above two assumptions (e,f) will be removed later on by calculation of transient heat loss inside the cylinders.

f- The working fluid is a perfect gas. As shown later, helium and hydrogen are the best gases to use as working fluids because of their heat transfer and viscous properties. These two gases behave as perfect gases in the operating temperature range of the Stirling engine.

The above assumptions yield the additional constraints that the mass contained in the dead spaces may vary only with pressure, and the effect of the dead volumes on overall performance may be lumped.

The differential equations for pressure, mass, and work transfer are derived in Appendix (H). There are four sets of equations because each cylinder obeys a different equation when gas is moving into or out of it, so that four combinations may be formed with two cylinders. In order to determine which equation applies at a given time it becomes necessary to keep track of the signs of the mass flows at all times.

The equations have been derived in terms of the following dimensionless parameters and variables. The basic geometry parameters are:

$$vd \equiv (mD)*R*TH\ /(P*VH) \qquad (2\text{-}31)$$

$$r_{vt} \equiv (VC*TH)/(VH*TC) \qquad (2\text{-}32)$$

$$vc \equiv VC/VC \qquad (2\text{-}33)$$

$$vh \equiv Vh/VH \qquad (2\text{-}34)$$

Where Vd is the normalized mass in the dead volumes, r_{vt} is the

ratio of maximum masses in hot and cold cylinders, vc is the ratio of the instantaneous cold cylinder volume and maximum cold cylinder volume, and vh is the same as vc but for the hot cylinder.

The mass in a cylinder, mc or mh, may be scaled in terms of the mass contained in one half the corresponding cylinder displacement assumed held at the maximum cycle pressure Pmax and at the temperature of the adjacent heat-exchanger. This norming process leads to:

$M_c \equiv (mc*R(TC)/(Pmax*VC)$ (Cold Cylinder)

$M_h \equiv (m_h*R*TH)/(Pmax*VH)$ (Hot Cylinder)

The pressure can be scaled as a fraction of the maximum pressure $P=p/P_{max}$

In terms of these variables the differential equations for the momentary pressure may then be written as:

$$dP = \left[-k*P*(r_{vt}*dV_c + dV_h)\right] / (r_{vt}*V_c + V_h + k*V_d) \qquad (2\text{-}35)$$

$$dM_c > 0 \quad , \quad dM_h > 0$$

$$dP = \frac{-k*P*(r_{vt}*M_c*dV_c/V_c + M_h*V_h/dV_h)}{r_{vt}*M_c + M_h + k*V_d*P} \qquad (2\text{-}36)$$

$$dM_c < 0 \quad , \quad dM_h < 0$$

$$dP = \frac{-k*(P*dV_h + r_{vt}*M_c*dV_c/V_c)}{V_h + r_{vt}*M_c/P + k*V_d} \qquad (2\text{-}37)$$

$$dM_c < 0 \quad , \quad dM_h > 0$$

$$dP = \frac{-k*(r_{vt}*P*dV_c + M_h*dV_h/V_h)}{r_{vt}*V_c + M_h/P + k*V_d} \qquad (2\text{-}38)$$

$$dM_c > 0 \quad , \quad dM_h < 0$$

The differential equations for the mass are:

$$dM_c = P * dv_c + v_c * dP/k \qquad dM_c > 0 \qquad (2\text{-}39)$$

$$dM_c = M_c * (dv_c/v_c + 1/k * dP/P) \qquad dM_c < 0 \qquad (2\text{-}40)$$

$$dM_h = P * dv_h + v_h * dP/k \qquad dM_h > 0 \qquad (2\text{-}41)$$

$$dM_h = M_h * (dv_h/v_h + 1/k * dP/P) \qquad dM_h < 0 \qquad (2\text{-}42)$$

A simple and understandable method to derive these differential equations is through the modelling of the engine as a whole system. In every component of the system we encounter momentum of the gas (inertia-I), elastic and thermal capacitance of gas and solids (C), and fluid and thermal resistances (R). Then by using bond-graph techniques [31] the whole system can be modelled with these I, R, and C elements; transformers (TF) or gyrators (GY) relate the different power domains. Fig. (19) shows the bond-graph of a cylinder. This particuler model is taken for the case assuming a given form of the volume variation; such as a sinusoidal form. The power of this technique is that one can pass from a first order analysis to higher orders very easily simply by adding more bonds and elements for more

detailed analysis of the system. In the first bond graph of Fig. (19), the motion of the piston is converted to the volume flow of the gas,i.e. going from the force-velocity domain to the pressure-volume flow domain. Then a viscous resistance and fluid inertance is used for the gas motion inside the cylinder. There is a free bond from the 1-junction identifying the gas flow in the cylinder with the gas flow of the adjacent heat-exchanger. A modulated transformer is used for converting the pressure-flow domain to the temperature-entropy domain,i.e. the thermal side of the model. This conversion is accomplished through the gas state equation such as the ideal gas law (P*V=MRT). Besides thermal capacitance and resistance, there is a free bond which shows the coupling of temperature and entropy of the cylinder with the temperature and entropy of the adjacent heat-exchanger, i.e. the rest of the system.

In this model there is only one independent energy storage element, therefore it is, in a differential equation sense, a first order system. The second bond graph in Fig.(19) shows a more detailed model of the cylinder. This model includes the piston inertia, thermal resistance due to the shuttle loss and the number of RC units to take into account the non-uniform temperature distribution loss(i.e.the previously discussed transient heat transfer loss).

By using the above techniques the state equations of the system or equations (2-38) through (2-45) can be routinely derived.

2.4.1.1- Solution of System State Equations:

It is clear from the system state equations, equations (2-38) through (2-45), that there would not be analytical solutions to them, therefore a discrete and approximate method should be used. In most cases computer would be very helpful. For the present work, where the forcing function is the volume variation given by crank-connecting-rod mechanism, the solution is obtained by the computer progarms in Appendix (I). This program is in FORTRAN language and it has its own integration subroutine. The integration has been done by Runge-Kutta method; whole there are many other methods, such as Runge-Kutta forth order, with more accuracy, they would generally increase the computation time and consequently the cost of running the program. The details of the solution are explained in Appendix (I) and only its limitations will be discussed here.

The solution to the differential equations is carried out by selecting an initial condition for the complete system and emulating the system through its transient behavior until an over-all steady state is reached. This solution has been set up to utilize the fact that when a piston is at its top dead center position the mass in the corresponding cylinder is zero. This provides knowledge of the mass at one point in the cycle for each cylinder. Any error in the mass computation may be corrected at this point. In addition, the lack of gas in the cylinder at one point in the cycle accelerates the convergence to the over-all steady state.

2.4.2-Real Engine Model:

In the previous section a model for an engine with perfect components and the corresponding computer program were discussed. Now, the combination of the losses, which were discussed in section 2.3, with the perfect engine analysis furnishes a model of the real engine.

Fig.(18) shows both energy flow, and bond-graph of an ideal Stirling engine. The thickness of the arrow indicates the engine efficiency. When all of the losses are introduced then that energy flow of the engine is augmented as shown in Fig.(19). This figure shows the different domain losses, entropy generations, and mechanical dissipations. As the thickness of the arrows show, the output of real Stirling engine is less than a half of that of the ideal Stirling engine (Fig. (15) describes this phenomenon through a bond-graph of a real engine). There are two sources of temperature, TH^* & TC^*, these are connected to series of thermal resistances which generate entropy and add through the thermal feed-backs to the other internal entropy generations. In addition to the thermal mechanisms for entropy generation, there are viscous dissipations which generate more entropy. This is shown in the bond graph by a feed-back from the pressure-flow domain to the temperature entropy domain. The important factors for generating power from the engine are the effective hot and cold temperatures; as is shown in section (2.2) smaller TC and larger TH produce more output. Because of the various dissipations and irreversibilities the hot temperature TH^* decreases to TH and the

cold temperature TC^* increases to TC (see Fig.(15)). Consequently, the output of the system would drop by nearly the factor $\left[(TH/TC)/(TH^*/TC^*)\right]$.

In order to calculate the real engine performance, the losses should be calcuated and added to basic heat input and subtracted from basic output which are computed through the computer program of the engine with perfect components.

The perfect component engine calculation is done by increasing steps the rotational angle, ($\theta=\omega t$). The whole length of the three heat exchangers is divided to N-sublengths. For each of these N sections the following quantities are calculated in a non-dimensional form.

$$DMRE = \frac{1}{2\pi}\oint\left|\frac{\partial m}{\partial(\omega t)}\right| * d(\omega t) \tag{2-43}$$

$$INTEGRAL = \oint \frac{1}{P}\left|\frac{\partial m_K}{\partial(\omega t)}\right| * \frac{\partial m_K}{\partial(\omega t)} * \frac{\partial V_C}{\partial(\omega t)} * d(\omega t) \tag{2-44}$$

$$XI1 = -\oint \frac{\partial P}{\partial(\omega t)}\left|\frac{\partial(m/M)}{\partial(\omega t)}\right|^{-n} * \frac{\partial(m/M)}{\partial(\omega t)} * d(\omega t) \tag{2-45}$$

$$XI2 = \oint \left|\frac{\partial(m/M)}{\partial(\omega t)}\right|^{2-n} * d(\omega t) \tag{2-46}$$

$$XI3 = XI1/XI2 \tag{2-47}$$

Where n is the exponent for Reynolds number in the correlation for convective-heat-transfer coefficient, which is about 0.405.

These quantities are used for calculation of losses due to the pressure drops and temperature drops inside the three heat-exchangers. For example DMRE, equation (2-43), produces an average mass flow rate which can be used for calculating the Reynolds number and,consequently, the friction factor in each component.

In the Rios model [22]one needs to know the details concerning these quantities and even with his computer results there still remain a significant amount of real time calculations and graphical reductions in order to obtain the final real engine performance. But in the complete model of the present work all of these calculations are done by the supplementary modelling steps which have been added to the program itself and the previously required graphics are done automatically in such a way that by giving the necessay input data to the model, with no extra calculations, the engine performance will be presented as the output of the program.

There are some special points about this complete model which make it more general and decrease the amount of the required input data. These features are discussed in the next section.

Equations (2-43) through (2-46), which depend on the history of the basic calculations, are used only for the pressure and temperature drop losses in the heat-exchangers. The other types of the losses are calculated independently by using the closed form solutions which are given in the previous section (section 2.3).

When all of the loss calculations are completed they will be added to the required heat input and subtracted from the output power as shown in Fig.(20). In this way, the overall performance of a real engine is determined.

2.5- Results of Complete Model and Comparison with Available Data

2.5.1- Complete Model:

The basis for analysis of a real engine performance was discussed in the previous section. Fig.(21) gives a summary of this procedure. The whole analysis has been written in FORTRAN language (see the attached computer program)and is called the Complete Model. The input data for this model are: temperatures of the hot and cold sources, mean pressure inside the system, working fluid, speed of the engine, cold and hot space volumes, dead volumes, phase angle difference between hot and cold spaces volume displacements, and if the heat-exchngers geometries are not given then the total rate of heat input to the engine should be given in order to calculate the required heat transfer areas for meeting the duty.

When all of the engine geometries are calculated and completed then the analysis of the engine with perfect component begins. By the time that this analysis is completed, both those losses which depend on the results of this analysis as well as those which can be calculated by closed form solutions independently have been computed. The summation of the above computation results produce a first-pass analysis of a real engine. The results determine the amount of heat transfer in each heat-exchanger; therefore, by a subsequent feed-back of these results the geometry computation is corrected and the other steps are repeated. Usually the second iteration is sufficient and any

further iteration will not change the overall performance significantly.

A sample of the complete model output is attached. This output, which repeats the intput data, shows the pressure drop in each component together with the corresponding power loss as well as the power loss due to the temperature drops, axial conduction, transient heat transfer, heat leakage, shuttle heat transfer, pumping loss, and dry friction. Finally, the output includes the total heat transfer in heater/and cooler, the total power in hot and cold spaces, the net output and efficiency, the brake-mean-effective-pressure, the torque, and the total loss due to the entropy generation inside the engine.

In the process of calculating the various losses we need to know the viscosity, thermal conductivity, and Prandlt number for the working fluid and the construction material of the engine. Also we need to know the relationship between friction factor and Reynolds number. On the other hand, we wish to make the model as general as possible, which means requiring minimum input data. In order to achieve this, the fluid and thermal properties of the three working fluids(hydrogen, helium, and air) are represented by empirical correlations in particular for viscosity the following correlations are used [13].

For H2: $\mu=(30.13+T/9+.0013*Pm)*2.4191/10^4$

For He2: $\mu=(60.188+T/3.88-.00064*Pm)*2.4191/10^4$

For Air: $\mu=(24.812+T/3.36+.0084*Pm)*2.4191/10^4$

Where μ[lbm/hr/ft] , T[^oR] , Pm[psi.]

For friction factor:

In heater and cooler-

$Re<2000 \quad F=16/Re$

$Re>2000 \quad F=.0457/Re^{.2}$

In regenerator-

$Re\leq 60 \quad F=53.7/Re^{.93}$

$60<Re<1000 \quad F=5.176/Re^{.365}$

$Re\geq 1000 \quad F=1.035/Re^{.125}$

Figures (23) and (24) show the data for thermal conductivity and Prandtl number with their assigned correlations.

These correlations case the computations and minimize the required input data.

Finally, the complete model has two switches for activating the coulumb friction calculations and consequently obtaining shaft output and efficiency instead of indicated ones; and for adding or eliminating the regenerator from the Stirling engine, as discussed in Chapter V.

2.5.2- Available Data and Comparison with Complete Model Results:

The complete model can be used for any operational temperature ratio and mean pressure. Since the low temperature-ratio results are to be compared with the available data in the following chapters, then in this section we use the certain high

temperature measured data on Stirling engines to compare with the complete model predictions. In this way, we might better test the accuracy of this model over a wide operating range for temperature and temperature-ratio.

Many different types of Stirling engines have been designed and built. However, only a few of them have published specifications wherein sufficient details have been given in the literature. For the comparison purposes of this section, the following engines are considered and discussed.

a)- Philips Engine:

Design details of this engine is given in [25] . The operating characteristics of this small engine were never published by Philips or any of the recipients. In early 1970s the operating characteristics of the engine were carefully measured by Ward (1972) at the University of Bath. This was done as part of a program of development for small Stirling engines for navigation signal beacons, encouraged by the Trinity House Light house Service, London, England, and by Atomic Energy of Canada Ltd. The engine used by Ward was removed from a Philips Type 102 C motor generator set and modified to operate with water cooling and liquid petroleum gas (LPG) as heat source. This engine has:

Cylinder bore	:2.2 in
Stroke of piston	:1.1 in
Hot space swept volume	:3.9 in^3
Cold space swept volume	:4.1 in^3
Dead volume	:4.8 in^3

Since the geometry of the heat-exchangers have not been specified, the optimum design model of Chapter IV has been used to find the optimum dimensions based on the given operating conditions.

Table (6) and Fig. (25) show the Ward performance data and the complete model predictions. There is a small difference between the experimental data and the model results. This error would appear to come from two sources: (1) the first one results from having no access to the real geometry of heat-exchangers for the experimental engine; (2) the second reason is that the cold temperature of the engine is not specified so that 70 F (530R) has been used for TC. Since the experimental data does not give the amount of input heat, then in Fig. (26) the calculated input heat is plotted versus the measured fuel mass flow rate. As shown, this plot is a straight line which means its slope is the heat value of the fuel.

b)- Allison Engine:

The investigation conducted by the Allison Division of General Motors Corporation [18] has been the only test reported in which all conditions were described in sufficient detail to give a reliable verification of the overall model. The development of this engine was part of a space-power program and several engine designs were built and tested as part of the project. The recorded performance data of two of the designs are compared to the results of the complete model. Tables (7) and (8) and Figs.(27) through (30) show this comparison. The two designs differ in only one respect. The first one runs with

a phase shift of 112° between the cold and hot space displacement. In the second one, this phase difference has been changed to 118°. In Figs(28) and (30) the Carnot efficiency (corresponding to the ideal Stirling cycle efficiency) is plotted to indicate how far the performance of a real engine is from the ideal engine. Comparison of the experimental data and the predictions of complete model shows that the model represent a great improvement in performance predictions over the ideal cycle. Furthermore, the performance level, the decrease in output per cycle with increased speed, and the change in performance with phase angle difference of the hot and the cold volumes are all predicted to a relatively high degree of precision.

Specifications of the Allison engine are as follow:

Engine speed	=3000 RPM
Mean pressure	=1544 Psia
Working fluid	=He2
Expansion volume amplitude	=2.475 in^3
Compression volume amplitude	=2.33 in^3
Dead volume of cold heat-exchanger	=1.5 in^3
Ducting and clearance volume in cooler	=1.215 in^3
Regenerator dead volume	=3.35 in^3
Regenerator clearance volumes at both ends	=1.038 in^3
Dead volume of hot heat-exchanger	=1.3 in^3
Ducting and clearance volume in heater	=1.29 in^3

TH=1680° R

TC= 628° R

Cold Heat-exchanger:

Number of tubes =152

I.D. of tubes =.04 in

Length of tubes =2.6 in

Hot heat-exchanger:

Number of tubes =76

I.D. of tubes =.06 in

Length of tubes =6. in

Regenerator:

Matrix: screen stack

Wire diameter =.0016 in

Mesh =250 in

Porosity =0.69

Length =.8 in

c- GPU-3 Engine:

General Motors Research conducted a program for the U.S. Army to produce a silent electric power source in 1960s. This Ground Power Unit (GPU) development went through three different models. Two of the last model GPU-3 were preserved and are now being used by NASA Lewis Research Center to obtain reliable measurements of a more or less modern type of Stirling engine. Some of specifications of this type of engine is given in [13] which are listed below.

Engine speed =3000 RPM

Mean pressure =1000 Psia

Bore =2.75 in

Stroke =1.208 in

TH=1860° R

TC=560° R

Displacement volume=2.175 in^3

Working fluid =H2

Cold heat-exchanger:

Tube length =1.76 in

I.D. of tubes =.04 in

O.D. of tubes =.06 in

Number of tubes =312

Hot heat-exchanger:

Tube length =9.539 in

Tube I.D. =.119 in

Tube O.D. =.19 in

Number of tubes =40

Regenerator:

Length =.89 in

Diameter =.89 in

Wire diameter =.0016 in

Mesh =213 in

Porosity =.714

Although Martini [13] has given the engine specifications, nevertheless there is no experimental data available. However, Lewis Research Center (LeRC) has used a third order analysis and presented a series of test points with computed performances. Therefore, the results of LeRC are compared with the complete model results in Tables (9) and (10), and Figs.(31) and (32). This comparison shows that LeRC model is more optimistic than

the present complete model from the output power view point. On the other hand, their heat input is more than what the complete model is predicting. This is due to the fact that the complete model has been run with incomplete specifications of the engine, such as dead volumes inside the system; and that is the reason for having higher efficiences from the complete model than LeRC results. Finally, the LeRC performance is assuming the mechanical dry friction losses to be 20% of the basic output power, which has no reason to be a good approximation.

CHAPTER III

3.1- Need for Simplified Stirling Engine Models

Due to the difficulties involved in the use of elaborate computerized models of Stirling engines people still use the idealized Schmidt equations for preliminary design and for determination of optimum design parameters for the system. This follows because the Schmidt model is in a closed form solution, which is easy to work with and easy to differentiate for optimization purposes. However, Schmidt solutions don't predict real engine behavior accurately; people have tried to introduce some power "experience factors" to the Schmidt solution [13] . In spite of many efforts for determination of these power factors, so far there have been no definite recommended values for these correction factors which have been determined on a rational basis. Those which have been introduced typically are estimated numbers taken independent of the physics of the system and its operating conditions. Perhaps that is why these approaches have been unable to predict real engine performance.

In this chapter a new method of improving the basic Schmidt equations is introduced and a simplified model for a Stirling engine is derived. This new simplified model has sufficient accuracy for prediction of the behavior of real engines and its results are very close to the second order model results, even surprisingly close to the results of

the complete model which was discussed in Chapter II. Yet, it supplies a closed form solution which is easy to work with; some of its applicaions for optimization purposes are shown in the following chapters.

3.1.1- Basic Heat Input & Work Output Derivation:

An approach similar to that taken for derivation of the complete model will be again followed here; which is to calculate basic heat input and work output first for an engine with perfect component; then the losses are calculated and introduced into the basic calculations.

The Schmidt model assumes isothermal expansion and compression processes inside the cylinders, but the real engine works nearly adiabatically. Therefore, by adding some correction factors to the Schmidt basic work output equation (see section 2.2), it can be modified for determining real engine output in the form:

$$W_{OUT} = \pi * N * P_m * A * VH * SIN\theta * (1 - TC/TH)/(1 + \sqrt{1 - A^2}) \qquad (3\text{-}1)$$

In order to determine appropriate correction factors to apply to this expression one needs to find the important parameters which influence the output of the engine. In equation (3-1) Pm, VH, ϕ, and TC/TH are the terms which determine the output Wout. Based on the physics and thermodynamics of the system we can see Pm and VH are linearly related to the output work, but temperature ratio, phase difference between the two cylinders (ϕ), and dead volumes have non linear effects on

the output. Therefore, three essential correction factors have to be added to equation (3-1), $F_T(T)$, $F_D(D)$, $F_\phi(\phi)$, which means the new equation would become:

$$W_{OUT} = \pi * N * P_m * A * VH * SIN\theta * (1-TC/TH)/(1+\sqrt{1-A^2}) * F_T(T) * F_\phi(\phi) * F_D(D) \quad (3-2)$$

To determine the factor $F_T(T)$, the phase angle (ϕ) and geometry of the heat-exchangers are(VD)kept constant and only the temperature-ratio (TC/TH) is changed. For different values of (TC/TH) the complete model has been run where helium as the working fluid and TC held constant at 530°R, the results were then compared with the values calcuated by equation (3-1). Assuming the output work of the complete model to be the exact solution, the error between that solution and the Schmidt equation was determined and has been plotted versus temperature ratio as shown in Fig.(33). Different empirical correlations can be fitted to the data of Fig.(33). A simple one is determined as:

$$Y=542*EXP(-8.56*x)+1.36 \quad (3-3)$$

Where $Y \equiv (W-W_{real})*100/W_{real}$

and $x=1-TC/TH$

Since F(T), as defined by equation (3-2), is the ratio of the real output and Schmidt model output, then by using equation (3-3) we get:

$$F_T(T)=1/[1.0136+.00104*EXP(8.56\ TC/TH)] \quad (3-4)$$

In order to determine $F_\phi(\phi)$, the above correlation for F(T) is substituted in equation (3-2) and for a constant temperature ratio, the value of ϕ has been changed in the range of 80° to 130°.

The results of the complete model for different ϕ is calculated and compared with the results of equation (3-2) and the error is calculated and plotted versus (ϕ) as shown in Fig.(34). It seems that the error is a linear function of ϕ, and a simple correlation fitted to the data is taken as:

$$Y=.36167x-87.4476 \qquad (3\text{-}5)$$

Where $$Y=\frac{W-W_{real}}{W_{real}}*100$$

and $$x=360+\phi$$

Since in the Stirling engine the cold space volume is lagging the hot space volume, then ϕ is a negative angle. In order to eliminate the negative sign, both in the complete model and in the correction factor(3-5) a 360 is added to the angle. Therefore, $F_\phi(\phi)$ would be written as:

$$F_\phi(\phi)=1/\left[1.4275-3.6167*10^{-3}*\phi\right] \qquad (3\text{-}6)$$

In equation (3-6) the $360^\bullet$ has already been added so that the absolute value of ϕ should be substituted.

Finally the dead volume correction factor, $F_D(D)$, should be determined for this purpose, taking constant phase angle(ϕ) and temperature ratio (TC/TH), the heat-exchanger geometries have been varied, this has been done for different sets of constant (ϕ)and (TC/TH) and Figs.(35) and (36) show the results of $F_D(D)$ versus the total dead volume in the system. These two figures are the conclusion of many different runs and comparisons of the complete model with equation (3-1). Their concentration onto curves indicates that no other terms than $F_T(T)$, $F_\phi(\phi)$,and

$F_D(D)$ would appear to have any significant effect.

Different correlations can be fitted to the results of Figs.(35) and (36), however, simplest one is the better one. Following are linear correlations which has been used for $F_D(D)$.

$$\text{For } TH/TC<1.5 \quad F_D(D)=\begin{cases}(.58D-.13)(.803\ TH/TC); & \text{if } D\leq 2.\\ (.303D+.418)(TC/TH)^{1/3}*1.076; & \text{if } D>2.\end{cases} \tag{3-7A}$$

$$\text{For } TH/TC>1.5 \quad F_D(D)=\begin{cases}.1143D+.72\ ; & \text{if} \quad D\leq 3\\ .02D+1.02\ ; & \text{if} \quad 3<D\leq 6\\ .004D+1.12; & \text{if} \quad D>6\end{cases} \tag{3-7B}$$

Where D=(VDR+VDC+VDH)/VC

VDR=Dead volume inside the regenerator (including ducting and clearances)

VDC=Dead volume inside the cooler (including ducting and clearances)

VDH=Dead volume inside the heater (including ducting and clearances)

By substituting equations (3-7), (3-6), and (3-4) into equation (3-2), we get the basic output for a real engine very accurately.

An easy way to calculate the basic heat input to a real engine is by using the output work and a thermal efficiency term. Since the output work is already given by equation (3-2), then we need only to determine an efficiency term. Through the results for various cases performed by the complete model it has been estimated that for a real engine efficiency is about 10% less than the corresponding Carnot efficiency. Therefore, if the temperature-ratio is given then the efficiency term and, consequently, the basic heat input are as follow.

$$\text{Efficiency} = (1 - TC/TH) - .10 = .90 - TC/TH \qquad (3\text{-}8)$$

$$Q_{in} = \frac{W_{OUT}}{Eff.} = \pi \cdot N \cdot P_m \cdot A \cdot V_H \cdot \sin\theta \cdot \frac{(1 - TC/TH) \cdot F_T(T) \cdot F_\varphi(\varphi) \cdot F_D(D)}{(.9 - TC/TH)\left(1 + \sqrt{1 - A^2}\right)} \qquad (3\text{-}9)$$

Performance calculations can be done by using equations (3-2) and (3-9). If, at the end, the calculated efficiency is significantly different from that calculated by equation (3-8) then the new efficiency can be used and the calculations should be repeated again. Usually, this has not been the case and equation (3-8) gives reasonable values for efficiencies.

3.1.2- Derivation of Mass Flow Rates Inside the Stirling Engine:

As discussed in Chapter II, one of the important tasks of modelling a Stirling engine is to present a model which is able to represent the dynamics involved in all essential processes of the engine. Determination of an accurate average mass flow rate, over a cycle, inside each component of the system is very important, because these values determine the Reynold's number, pressure drop, and temperature drop-inside the corresponding components. This constitutes one more reason why most over-simplified closed form solutions which have been previously presented do not predict the behavior of a real Stirling engine accurately. In this section a method for calculating the mass flow rates is shown.

Fig.(37) shows a general configuration of a Stirling engine. Since it is assumed the total mass of the working fluid is constant and there is essentially no mass leakage, then it means what ever mass flows into the three heat-

exchangers in the first half of the cycle should come out of them during the second half of the cycle. The assumption of sinusoidal volume variations inside the hot and cold spaces usually helps to provide simpler mass-flow results. The derivatives of the two volume variations give the net volume flow rate to the three heat-exchangers. This is shown in Appendix (J) which yields the following results:

$$V_H = V_H * (1 - SIN(\omega t))/2 \qquad (3\text{-}10)$$

$$V_C = V_C * [1 - SIN(\omega t - \varphi)]/2 \qquad (3\text{-}11)$$

$$Q_{NET} = \frac{V_C * \omega * SIN\varphi}{2\,COS\alpha} * SIN(\omega t + \alpha) \qquad (3\text{-}12)$$

Where $TAN(\alpha) = (V_H/V_C + COS\varphi)/SIN(\varphi)$

Equation (3-10) shows the instantaneous volume flow rate through the three heat-exchangers. It has a sinusoidal form which means over half of the cycle it is positive, representing flow into the heat-exchangers, and for the next half it would be negative, corresponding to flow out of the heat exchnanger. Fig(37) shows this variation. The maximum volume flow rate, Q_{max}, and the half period, $t_{H.P.}$, have the following relationship, as shown in Appendix (J).

$$t_{H.P.} * Q_{max} * \frac{2}{\pi} = \text{occupied volume} \qquad (3\text{-}13)$$

Where

$$Q_{max} = V_C * \omega * SIN\varphi / (2 * COS\alpha)$$

Equation (3-12) is true for an ideal case, i.e. the maximum flow rate and half period can show the occupied volume during the period. In a real engine because of the presence of the dead volumes, it would be better to use effective volume which is a proper fraction of the occupied volume. This suggests that the volume flow rate in each of the heat-exchanger can be written as:

$$\overline{Q}_{net} = VC * \omega * SIN\varphi * F_C * SIN(\omega t + \alpha)/(2\cos\alpha) \qquad (3\text{-}14)$$

Where F_C is a correction factor (less than unity) for calculating the effective volume.

In order to calculate the mass flow rate, we need to find an average density for the working fluid inside of each heat exchanger. This can be done by assigning a pressure and a temperature to each of the components. As shown in Appendix (J), the following pairs of properties have been assigned.

For Hot Heat-Exchanger:

$$P = P_m(1 + A/\sqrt{1-A^2}) \ , \ T = TH$$

For Cold Heat-exchanger:

$$P = P_m(1 - A/\sqrt{1-A^2}) \ , \ T = TC$$

For Regenerator:

$$P = P_m \ , \ T = TR = (TH - TC)/[\ln(TH/TC)]$$

These pressures and temperatures would result in the following mass flow rates.

Heater:

$$\dot{m}_H = P_m * (1 + A/\sqrt{1-A^2}) * VC * \omega * SIN\varphi/(2 * R * TH * \cos\alpha) * F_{CR} \qquad (3\text{-}15)$$

Cooler:

$$\dot{m}_C = P_m * (1 - A/\sqrt{1-A^2}) * VC * \omega * SIN\varphi / (2 * R * TC * \cos\alpha) * F_{cc} \quad (3\text{-}16)$$

Regenerator:

$$\dot{m}_R = P_m * VC * \omega * SIN\varphi / (2 * R * TR * \cos\alpha) * F_{cr} \quad (3\text{-}17)$$

Where F_{ch}, F_{cc}, and F_{cr} are the correction factors, which have to be determined. As might be expected, they are very close to unity. In order to determine specific numerical values, we have to find which terms would affect them. The same consideration used for basic output power correction factors can once again be applied here. This means that each of these correction factors F_{cc}, F_{ch}, F_{cr} are functions of temperature ratio (TH/TC), phase angle difference ϕ, and dead volume ratio. Therefore, each of them can be taken as a multiplication of three factors.

$$F_{cc} = f_{c_T}(T) * f_{c_\varphi}(\phi) * f_{c_D}(D) \quad (3\text{-}18)$$

$$F_{cr} = f_{r_T}(T) * f_{r_\varphi}(\phi) * f_{r_D}(D) \quad (3\text{-}19)$$

$$F_{ch} = f_{h_T}(T) * f_{h_\varphi}(\phi) * f_{h_D}(D) \quad (3\text{-}20)$$

To calculate each of the nine factors (three sub-factors for each of the three basic correction factors), first the geometry and the phase angle are kept constant and with the ratio of the mass flow rate determined from the complete model as the results of equations (3-15) through (3-17), the subfactors $f_{h_T}(T)$, $f_{c_T}(T)$, and $f_{r_T}(T)$ are calculated for different values of the temperature-ratio. Fig.(38) shows the result of this calculation, where the values of f(T)'s lie in the range 0.9 to 1.2 as was mentioned before. The same

procedure has been done for phase angle correction factors. However, this time the temperature-ratio is kept constant and ϕ has been changed. Fig.(39) shows the results for $f_{c\varphi}(\phi)$, $f_{h\varphi}(\phi)$, and $f_{r\varphi}(\phi)$. Then finally, by keeping temperature-ratio and phase angle (ϕ) constant, in different set, and varying the heat-exchanger geometries in a random order then the correction factors based on the dead volumes of heat-exchangers are calculated and plotted in Fig.(40) through (42).

Now, the important task is to determine the corresponding correlations for each of the figures. In pursuing this, an attempt has been made to find the simplest possible correlations, even by using different zones in a graph. The following are the resultant correlations.

For temperature-ratio (TH/TC):

Heater-

$$f_{h_T}(T) = \begin{cases} -.024\,(TH/TC)^2 + .187\,(TH/TC) + .8455 & ;\ TH/TC \geq 1.5 \\ .205\,(TH/TC) + 0.7645 & ;\ TH/TC < 1.5 \end{cases} \quad (3\text{-}21)$$

Cooler-

$$f_{c_T}(T) = \begin{cases} .01962\,(TH/TC)^2 - .2088\,(TH/TC) + 1.3102 & ;\ TH/TC \geq 1.5 \\ -.178\,(TH/TC) + 1.309 & ;\ TH/TC < 1.5 \end{cases} \quad (3\text{-}22)$$

Regenerator-

$$f_{r_T}(T) = \begin{cases} 1.052 & ;\ TH/TC > 2 \\ -.0194\,(TH/TC)^2 + .0923\,TH/TC + .943 & ;\ TH/TC \leq 2 \end{cases} \quad (3\text{-}23)$$

For the phase angle difference (ϕ):

Heater- $f_{h\phi}(\phi)=1.463667*10^{-4}\phi^2-1.5516*10^{-2}\phi+.798$ (3-24)

Cooler- $f_{c\phi}(\phi)=7.04762*10^{-5}\phi^2-1.504764*10^{-3}\phi+.201$ (3-25)

Regenerator- $f_{r\phi}(\phi)=8.0381*10^{-5}\phi^2-1.60382*10^{-3}\phi+.08$ (3-26)

Note: The absolute value of ϕ should be used for above equations.

For the dead volumes:

$$\text{Heater- } f_{hD}(DH)=\begin{cases}.1373*DH+.8864; & DH\leq 2\\ .0408*DH+1.08; & DH>2\end{cases} \quad (3\text{-}27)$$

$$\text{Cooler- } f_{cD}(DC)=\begin{cases}-.333*DC+1.293; & DC\leq .6\\ -.111*DC+1.163; & DC>.6\end{cases} \quad 3\text{-}28)$$

$$\text{Regenerator-} f_{rD}(DR)\begin{cases}1.06; & TH<1000^{\circ}R\\ 1.06; & DR<1.17\\ 1/30*DR+1.072; & DR>1.17\ \&\ TH>1000^{\circ}R\end{cases} \quad (3\text{-}29)$$

Where:

DH=VDH/VC

DC=VDC/VC

DR=VDR/VC

Substitution of equations (3-21) through (3-29) into equations (3-18) through (3-20) would give the correlations for F_{cc}, F_{cr}, F_{ch}. Having these correction factors and equations (3-15) through (3-17), the mass flow rates inside the three heat exchangers can be calculated. While, the correlations for these correction factors might seem complicated, nevertheless, all of the results are in order of unity (in the range .8 to 1.2).

3.1.3- Loss Calculations by the Simplified Model:

In Chapter II the derivation of losses in different domain was discussed. The difficulties encountered in their detailed calcualtion arose through integrations which were not possible to perform analytically so that a computer was needed. For the simplified model, because mass flow rates occured in a closed form, the corresponding integrations and loss calculations could be done by hand so that no computer was required for either part of the calculations.

3.1.3.1- Pressure Drop Losses:

Appendix(K) shows the derivation of power loss due to the pressure drop in each heat-exchanger, the result follows in a closed form solution.

$$W_{loss}=\frac{f}{8\pi}*\frac{L}{RH}*\frac{\rho}{(AFR)^2}*\frac{VC^3*\omega^3*SIN^2\varphi}{Cos^2\alpha}*F_c^2*\left[SIN\varphi+\frac{1}{6}SIN(2\alpha-\varphi)+\frac{1}{2}SIN(2\alpha+\varphi)\right]$$

(3-30)

Where f is the friction factor, A is the flow path area, L is the length of the heat-exchanger and

RH = AFR*L/(AHT)

AHT is the total heat transfer area.

Equation (3-30) can be rewritten for each of the heat-exchangers, based on their geometries, as follows.

For Heater:

$$RH=\frac{1}{4}*DH \quad , \quad \rho=\frac{P_m}{RTH}*\left(1+A/\sqrt{1-A^2}\right)$$

$$W_{Loss} = \frac{8}{\pi^3} * (fH) * \frac{LH}{DH} * \frac{Vc^3 * \omega^3 * P_m (1 + A/\sqrt{1-A^2})}{NH^2 * DH^4 * R * TH} * F_{ch}^2 * \frac{SIN^2\varphi}{Cos^2\alpha} * \left[SIN\varphi + \frac{1}{6} SIN(2\alpha - \varphi) + \frac{1}{2} SIN(2\alpha + \varphi) \right] \quad (3\text{-}31)$$

Where DH is the heater tube diameter, NH is the number of tubes, LH is the tube length, and fH is the friction factor in the heat, Appendix(K) shows how it can be calculated.

For Cooler:

$$W_{Loss} = \frac{8}{\pi^3} * (fC) * \frac{LC}{DC} * \frac{Vc^3 * \omega^3 * P_m (1 - A/\sqrt{1-A^2})}{NC^2 * DC^4 * R * TC} * F_{cc}^2 * \frac{SIN^2\varphi}{Cos^2\alpha} * \left[SIN\varphi + \frac{1}{6} SIN(2\alpha - \varphi) + \frac{1}{2} SIN(2\alpha + \varphi) \right] \quad (3\text{-}32)$$

Friction factor fc is given in Appendix(K).

For Regenerator:

From Appendix(K), we get:

$$(L/D)_R = \frac{1-\sigma}{\sigma} * \frac{LR}{dw} \qquad \text{(for wire filling)}$$

$$\Rightarrow \quad RH = \frac{1}{4} * \frac{\sigma}{1-\sigma} * dw \qquad (3\text{-}33A)$$

$$(L/D)_R = \frac{3}{2} \frac{1-\sigma}{\sigma} * \frac{LR}{dS} \qquad \text{(for sphere filling)}$$

$$\Rightarrow \quad RH = \frac{1}{6} * \frac{\sigma}{1-\sigma} * dS \qquad (3\text{-}33B)$$

AFR=VDR/LR

$$W_{Loss} = \frac{(fR)}{16\pi} * \frac{LR}{RH} * \frac{P_m}{(VDR/LR)^2} * \frac{Vc^3 * \omega^3 * SIN^2\varphi}{Cos^2\alpha * R * TR} * F_{cr}^2 * \left[SIN\varphi + \frac{1}{6} SIN(2\alpha - \varphi) + \frac{1}{2} SIN(2\alpha + \varphi) \right] \quad (3\text{-}33)$$

Equations (3-31) through (3-33) give the power loss due to the pressure drops inside the three heat-exchangers.

3.1.3.2- Temperature Drop Losses Inside Heat-Exchangers:

In section (2.3.2.1), the power loss due to the temperature drop inside the heat-exchangers is derived and the results are given by equations (2-10) and (2-11).

Power loss due to heater $\Delta T = \frac{We * W_c}{\dot{m}_H * R * TH} * \frac{k-1}{k} * \frac{1}{e^{2NTU_H} - 1}$ (2-10)

Power loss due to cooler $\Delta T = \frac{We^2}{\dot{m}c * R * Tc} * \frac{k-1}{k} * \frac{1}{e^{2NTUc} - 1}$ (2-11)

Based on the simplified model, We a Wc can be written as:

We=1/2(Wout+Qin)

Wc=1/2(Qin+Wout)

Wout is given by equation (3-2) and Qin is given by (3-9), mH and mC are given by equations (3-15) and (3-16).

$$NTUc = 4 * (L/D)_c * (.023 * Re_c^{-.2} * Pr^{-.6})$$

$$NTU_H = 4 * (L/D)_H * (.023 * Re_H^{-.2} * Pr^{-.6})$$

Where Pr is the Prandlt number and ReC and ReH are Reynold's numbers which are defined in Appendix(K).

For the regenerator Martini [13] has shown that its ineffectiveness can be written as:

Ineffectiveness=2/(NTUV+2) (3-34)

Therefore, the heat loss due to the regenerator imperfection can be written as:

$$Q_R = 1/3 * \dot{m}R * CV * (TH - TC) * \frac{2}{NTUV+2} \quad (3\text{-}35)$$

Where $\dot{m}R$ is given by equation (3-17).

NTUV=H*AHT/mR*Cv (3-36)

In reference [13] a correlation for the heat transfer coefficient, H, is given as:

$$H = .7413 * \frac{\dot{m}_R * C_V}{AFR} * P_r^{-2/3} * (Re_R)^{-.410}$$

Therefore,

$$NTUV = 4\frac{1-\sigma}{\sigma} * \frac{L_R}{d_W} * .7413 * P_r^{-2/3} * (Re_R)^{-.410} \qquad (3-37)$$

Substitution of equations (3-17) and (3-37) into (3-35) would then give the heat loss in the regenerator.

As shown in Chapter II, all those losses other than the just-derived ones above exist in closed form expressions. Therefore, the same equations which are shown in Chapter II can again be used here for the simplified model.

As shown in these two sections, all of the calculations for performance of the Stirling engine are written and derived as closed form solutions so that there is no need for a computer for any part of the process. In the next section the simplified model and complete model results will be compared.

3.2- Comparison of Complete and Simplified Models:

Appendix(K) shows a sample of calculating Stirling engine performance via the simplified model. This sample shows how the calculations should be carried out and it also demonstrates the accuracy of the simplified model in comparison with the simulated complete model of Chapter II. In similar fashion, the accuracy of the simplified model has been checked over the temperature-ratio range of 1 to 2.0; the results are shown in table (11) and Fig.(43).

CHAPTER IV

Procedure and Derivation of Optimization Method for Designing Stirling Engine

An important goal of this thesis is to find the temperature-ratio boundary beyond which no engine can produce positive shaft power. In order to determine that boundary, the engine should be designed in such a way that all losses be at their minimum levels. Therefore, there is a real need for an optimization method for Stirling engines. Yet in the published Stirling engine literature, there appears to be no general method of optimization for practical Stirling engines. There are a few cases for ideal engines based on the Schmidt solution in reference [25]. However, they do not cover the whole range of operating conditions for Stirling engines; furthermore, they are useful only for preliminary design purposes, not for detailed engine design.

In this chapter, a new method of optimization will be derived which covers the whole range of operating conditions for practical Stirling engines. This method is based on the closed form solutions of Chapter III (simplified model) and optimizes each component of the system separately. However, this doesn't mean that the optimization of different components is totally independent, partly because the ducting and clearance volumes which connect various components are included in the optimization parameters. On the other hand,

because regenerator and cylinder losses are the dominant losses in the system, sub-optimization of these particular components is nearly equivalent to optimization of the entire engine.

The first question is what quantity is going to be optimized? In the method used here for each component, one aims to find an optimum geometry ratio such that the ratio of the total loss in that component to the output power of the system is minimized. That geometric ratio, which might be called an "aspect ratio", is taken as the ratio of heat transfer length to hydraulic diameter for the three heat exchangers; and as the swept-volume ratio for the hot and cold space volumes.

4.1- Optimum Design Model for Stirling Engine

Through the next four sections of this chapter, it will be shown how to optimize each component of the engine, how to calculate the optimum swept-volume ratio, how to find the optimum phase angle and speed of the engine, and finally what should be the bore-stroke ratio for minimizing the cylinder losses. This section shows how the results of the following sections should be put together for derivation of an optimum design model for a Stirling engine. The optimum design procedure of this chapter can be applied to any type of Stirling engine over the whole range of operating conditions. It is a general method of optimization filling the need for an optimum design procedure for many applications of Stirling engine in the published literature. In section 4.6 the results of this optimum design method will be compared with some available data to indicate its accuracy.

Based on the application of the Stirling engine, especially for waste-heat recovery, it is almost always the case, that there are two temperature sources and with a certain available heat flow from the hot source and the question is: what should be the design of a Stirling engine in order to exploit these available sources and get the maximum output power? And how much is that output power?

Based on the above logic, the optimum model of this section has been made with the following data as the basic input for this model.

Inputs:

TH=hot source temperature

TC=cold source temperature

Pm=mean pressure of the system (given based on the engine material)

Qin=available rate of input heat

VD=percentage of the dead volum (based on the available space)

Performance of the optimum designed engine will be calculated by either complete or simplified models. Both of them require the complete data about the engine geometry. Determination of this geometry data is the optimization task which will be shown in this chapter and is summarized as follows.

a)- By using equation (3-9) the required cold volume (cold cylinder volume) can be calculated.

$$Q_{in} = \pi * N * P_m * A * VH * SIN\theta * \frac{(1-TC/TH) * F_T(T) * F_\theta(\varphi) * F_D(D)}{(.9-TC/TH)(1+\sqrt{1-A^2})} \qquad (3\text{-}9)$$

For the first round calculation, it can be assumed that swept volume ratio is unity, $F_D(D)$ is equal to one, and optimum speed & phase angle can be selected from Fig. (47). The reason for calculating VC instead of VH is because the major losses occur in the hot space, therefore if VC is determined then by using the optimum design method, derived from minimizing the losses, the swept volume ratio and conseqently the hot space volume can be calculated.

b)- Since in all of the analysis of Stirling engines it is assumed that the heater & cooler have constant wall temperature, therefore for the coefficient of heat transfer

between heater or cooler wall and the working fluid the following equation can be used [23].

$$Nu_d = 5.75 \qquad (4\text{-}1)$$

Since all of the input heat should be given to the working fluid via heater, then we can calculate the required number of tubes for the heater, by assigning a standard tube diameter, see Appendix (L).

$$Qin = h*A*(TH-TR) \qquad (4\text{-}2)$$

$$A = NH*\pi*DH*LH \qquad (4\text{-}3)$$

$$h = 5.75\ Kg/DH \qquad (4\text{-}4)$$

$$NH = Qin/[5.75\pi Kg*LH*(TH-TR)]$$

$$TR = (TH-TC)/[\ln TH/TC]$$

By using a ten percent safety factor, the result would be:

$$NH = (1.1*Qin)/[5.75\pi Kg*LH*(TH-TR)] \qquad (4\text{-}5)$$

Equation (4-5) has LH, the heater tube length, but this equation can be solved simultaneously with the result of the heater optimization, i.e. equation (4-37).

Similar procedure can be applied to the cooler, except that in cooler the amount of heat which is exchanged between the working fluid and coolant is not Qin, it is (1-Eff.)*Qin, Since equation (3-8) represents a good estimate of efficiency then for the number of tubes required in the cooler we get the following, see Appendix (L).

$$NC = [1.1*(0.1+TC/TH)*Qin]/[5.75\pi*Kg*LC*(TH-TC)] \qquad (4\text{-}6)$$

Because equation (4-6) has LC, cooler tube length which is unknown, then this equation should be solved simultaneously with equation (4-27) which is the result of

optimization for cooler aspect ratio.

C)- Cylinders, heater, and cooler geometries have now been calculated. The only part which is left is the regenerator. Equations (3-33A) and (3-33B) show that the hydraulic diameter for the regenerator depends only on the porosity and wire or sphere diameter of the filling material in the regenerator. Therefore, by using nominal values for porosity and particle (or wire) diameter, 70% and .0016 in, respectively regenerator hydraulic diameter can be calculated.

Equation (4-19) shows the result of optimization for the regenerator. Having that equation and the hydraulic diameter, the optimum regenerator length can be calculated. The only problem is that the diameter of the regenerator cross-sectional area (DRR) should be determined, if it is circular otherwise an equivalent circular area should be calculated. However, from the heat transfer view point, there would be a geometrical relationship for a regenerator in order to exchange the required heat with the working fluid. Appendix (P) has shown the derivation of this equation and the result is following, also see the next section for derivation of this equation.

$$LR * DRR^2 = 2/3 * \frac{P_m * \sqrt{2}}{\rho * R * TR} * \frac{CP}{(1-\sigma)CR} * \frac{SIN\varphi}{\cos\alpha} * \frac{TH - TC}{TR - TC} \qquad (4\text{-}7)$$

Where

TR= (TH-TC)/[ln TH/TC] ,

ρ=Regenerator material density

CR=Regenerator material specific heat

CP=Working fluid specific heat

σ=Porosity

Therefore, equation (4-7) and (4-14) should be solved simultaneously, in order to get the whole geometry of the regenerator.

When the optimum geometry of the engine is determined then the complete or simplified model can be used in order to find the performance of the engine. Completion of Stirling engine performance shows how much heat is required. If that heat is less than Qin, then the cold space volume (VC) will be increased by ΔVC, which is part of the input for model, and the whole geometry calculation will be repeated and a new performance will be calculated. This continues until the calculated required heat will be in the neighbourhood of the Qin. If the first time calculated required heat is greater than Qin, then VC will be decreased by ΔVC and the similar procedure will be continued. During each iteration, equations (4-54), (4-64), and (4-72) have to be used for calculating optimum phase angle, speed, and bore-stroke ratio.

At this stage the optimum design model is completed and the final geometry and engine performance will be printed out. Fig.(59) shows a block diagram of how the optimum design model works.

Appendix (Q) shows the computer program of the optimum design model based on the complete model. This design model has a switch (SW3) which can be used to indicate either the input heat or the required net output power is given.

This section indicates how the results of the following sections, namely the optimum geometry derivation, should be used in order to get the optimum designed engine and its performance.

Since for a Stirling engine, regenerator and cylinder losses are the dominant power losses, then in the following procedure the optimization of the regenerator will be performed first and, due to the similarity in derivation, optimization of cooler and heater will be followd. Finally, cylinder optimizations will be presented. However, this derivation sequence does not imply the relative importance order.

4.1.1- Regenerator Optimization:

As discussed in the last two chapters there are three major power losses associated with a regenerator: loss due to the pressure drop; axial conduction loss; and loss due to the regenerator imperfection. From fluid and heat transfer viewpoints, it can be seen that an increase in aspect ratio of the regenerator (length over hydraulic diameter) would increase the pressure drop power loss while, at the same time increasing the heat transfer area so to decrease the regenerator imperfection and decrease axial heat conduction. Therefore, this aspect ratio has opposite effects on the fluid and the thermal losses of the regenerator, and there should be an optimum value corresponding to the minimum value of the total power loss.

The analysis to follow is based on the simplified model results because they exist in closed form. Equation (3-33) expresses the power loss in the regenerator because of pressure drop.

$$W_{loss} = \frac{(PR)}{16\pi} * (L/D)_R * \frac{P_m * Vc^3 * \omega^3 * SIN^2\varphi * F_{cr}^2}{(AFRR)^2 * R * TR * COS^2\alpha} \left[SIN\varphi + \tfrac{1}{6} SIN(2\alpha - \varphi) + \tfrac{1}{2} SIN(2\alpha + \varphi) \right]$$

By using equation (3-2) which gives the output power we get the following equation, see Appendix (L).

$$\frac{W_{loss}}{W_{OUT}} = C_1 * \frac{(PR)}{8\pi} * (L/D)_R * \frac{Vc^2 * \omega^2}{R * TR * (AFRR)^2} * \bar{F}_\varphi(\varphi) * \left(\frac{Vc}{VH}\right) * \frac{1 + \sqrt{1 - A^2}}{A\,(1 - TC/TH)\, F_r(r) * F_D(D)} \tag{4-8}$$

Where $$C_1 = \left(SIN^2\varphi / COS^2\alpha\right) * F_{cr}^2 * \left[SIN\varphi + \tfrac{1}{6} SIN(2\alpha - \varphi) + \tfrac{1}{2} SIN(2\alpha + \varphi) \right]$$

Since the optimum phase angle (φ) will be calculated for overall processes of the engine in the next section, then those terms which depend on φ are grouped together as the single fuction $C_1 \bar{F}_\varphi(\varphi)$ for equation (4-8). Also there are some additional corrections for the final optimum result which will take into account these minor points.

For a given temperature-ratio and mean pressure the regenerator has to have enough thermal capacity to handle the resultant heat transfer between the working fluid and the regenerator filling material. Appendix (P) shows how by applying an averaged energy equation we can get the following relationship between the length (LR) and cross-sectional

diameter (DRR) of a regenerator.

$$LR * DRR^2 = 2/3 * \frac{C_p}{(1-\sigma)C_R} * \frac{P_m * \sqrt{C}}{\rho_R * R * TR} * \ln\frac{TH}{TC} * \frac{SIN\varphi}{COS\alpha} \qquad (4\text{-}9)$$

This equation indicates that for a given P_m and TH/TC the regenerator dead volume ($VDR = \frac{\Pi}{4} * LR * DRR^2 * \sigma$) is frozen, i.e. the dead volume is independent of regenerator length (LR).

Equation (4-8) has AFRR term which is the regenerator free path area, i.e. $AFRR = \frac{\Pi}{4} * \sigma * DRR^2$, then by using equation (4-9) equation (4-8) can be written in non-dimensional form as (see Appendix (L)):

$$\frac{W_{LOSS}}{W_{OUT}} = \left[\bar{C}_1 * Z^{1.07} * \beta^2/\gamma^2 * (\ln\delta)^{-1.07} * (L/D)_R^{2.07}\right] F_R(\varphi, D, T_r, V_r) \qquad (4\text{-}10)$$

Where:

$$\bar{C}_1 = \frac{53.7}{2\Pi}\left(\frac{3}{\Pi}\right)^{1.07} * \left(\frac{1-\sigma}{\sigma}\right)^{.14} * F_{cr}^2 * \left[SIN\varphi + \tfrac{1}{6}SIN(2\alpha-\varphi) + \tfrac{1}{2}SIN(2\alpha+\varphi)\right]$$

$$F_R(\varphi, D, T_r, V_r) = \bar{F}_\varphi(\varphi) * \frac{1}{F_D(D)} * \frac{VC}{VH} * \frac{1+\sqrt{1-A^2}}{A(1-TC/TH)\,F_T(T)}$$

$$\bar{F}_\varphi(\varphi) = 1/\left[SIN\theta * F_\varphi(\varphi)\right]$$

$$Z \triangleq \frac{C_p}{C_\rho} * \frac{\rho_R * \omega * DR^2}{\mu} \propto \text{Profos Number}$$

$$\delta \triangleq TH/TC$$

$$\beta \triangleq \left[\sqrt{R * TR} * (DR)^2 * (1-\sigma)^2\right]/\left[\omega * VC * \sigma\right]$$

$$\gamma \triangleq \left[DR^3 * P_m * (1-\sigma)^2\right]/\left[\omega * VC * \sigma * \mu\right]$$

The regenerator imperfection causes a heat transfer loss which is calculated by equation (3-35)

$$Q_R = 1/3 * \dot{m}_R * C_V * (TH - TC) * \frac{2}{NTUV + 2} \qquad (3\text{-}35)$$

Where

$$NTUV = 4 * (L/D)_R * .7413 * P_r^{-2/3} * (Re_R)^{-.41} \qquad (3\text{-}37)$$

Appendix (L) shows that equation (3-35) can be written in non-dimensional form as:

$$\frac{Q_R}{W_{OUT}} = \left[\bar{C}_2 * Z^{.41} * (\ln\delta)^{.59} * (L/D)_R^{-.59}\right] * F_R(\varphi, D, T_r, V_r) \qquad (4\text{-}11)$$

Where

$$\bar{C}_2 = \frac{SIN\varphi}{COS\alpha} * F_{cr} * \frac{P_r^{2/3}}{3 * 2.9652 (k-1)} * \left(\frac{3}{\pi}\right)^{.41} * \left(\frac{1-\sigma}{\sigma}\right)^{.82}$$

Heat transfer loss due to the axial conduction in a regenerator is expressed by equation (2-15) as:

$$Q_C = K_{mg} * (AR) * (TH - TC)/LR \qquad (2\text{-}15)$$

$$AR = \pi/4 * (DRR)^2$$

Appendix (L) shows derivation of the following non-dimensional form of equation (2-15):

$$\frac{Q_C}{W_{OUT}} = \left[\bar{C}_3 * Z^{-1} * (\ln\delta)^2 * (L/D)_R^{-2}\right] * F_R(\varphi, D, T_r, V_r) \qquad (4\text{-}12)$$

Where

$$\bar{C}_3 = \frac{2\pi}{3}\left(\frac{\sigma}{1-\sigma}\right)^2 * P_r * \frac{k}{k-1}\left[\frac{1 + K_m/K_g}{1 - K_m/K_g} + \sigma - 1\right] \Big/ \left[\frac{1 + K_m/K_g}{1 - K_m/K_g} + 1 - \sigma\right]$$

As mentioned before, the purpose of optimization is to get the minimum power loss in the regenerator. This power loss is not simply the summation of Wloss, QR, and QC equations

(4-10) through (4-12), because QR and QC are in the form of a heat transfer rate where as, Wloss is in form of mechanical power (work transfer). The following diagram shows QR and QC are the by pass heat flows from the hot temperature source to the cold temperature source.

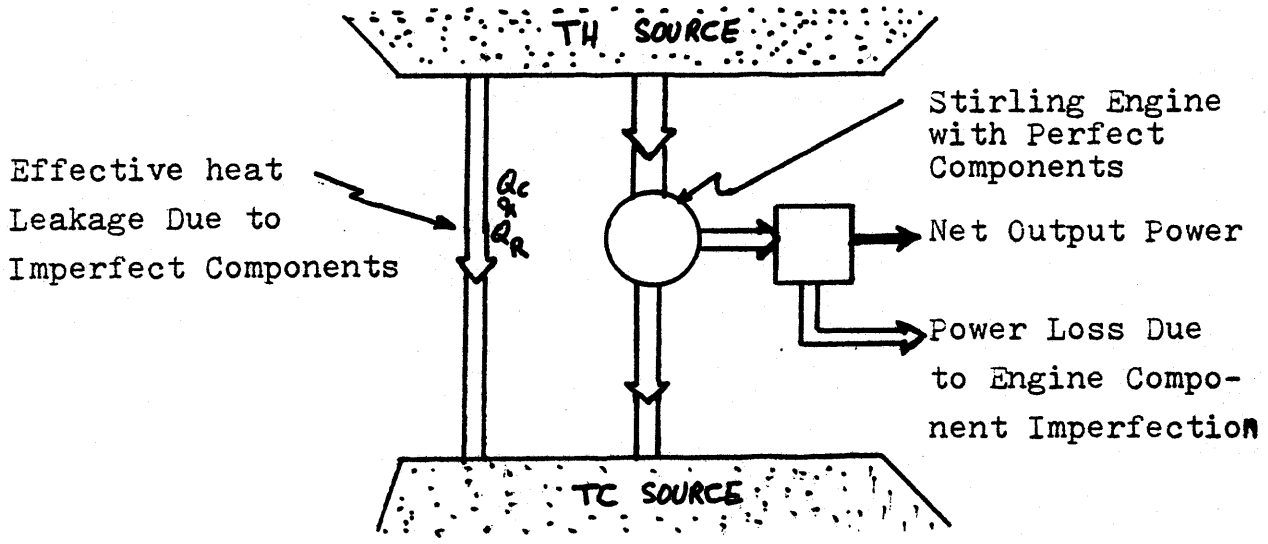

In order to see how much power loss the engine has due to the heat transfer losses and compare them with the other power losses we can put an irreversible engine in the by pass flow and convert those heat leakages to mechanical power (work transfer) losses. This idea is shown in the following diagram.

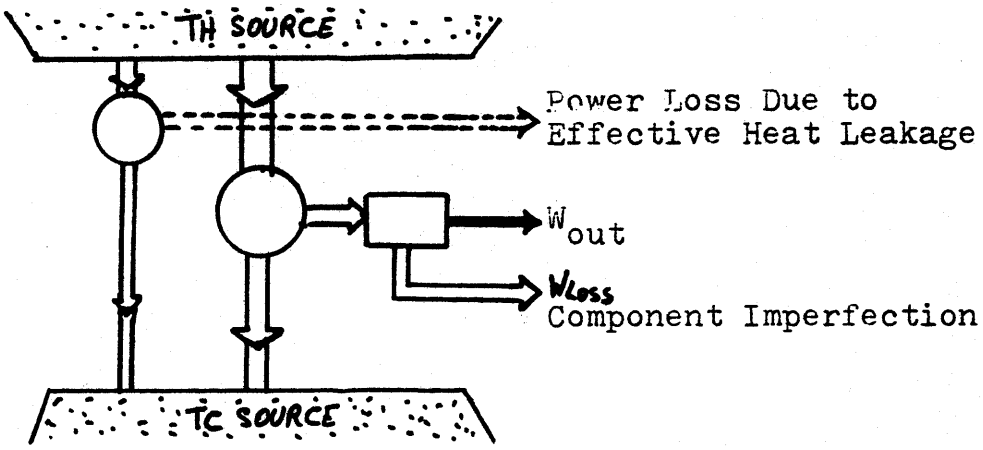

This suggests that in order to calculate the regenerator total power loss QC and QR should be first multiplied by the real Stirling engine efficiency then added to the pressure drop power loss.

$$\frac{\text{Total } W_{Loss}}{W_{OUT}} = \left\{ \bar{C}_1 \bar{z}^{1.07} \cdot (\ln\delta)^{-1.07} \cdot (L/D)_R^{2.07} + \left[\bar{C}_2 \bar{z}^{.41} \cdot (\ln\delta)^{.59} \cdot (L/D)_R^{-.59} + \bar{C}_3 \bar{z}^{-1} \cdot (\ln\delta)^{2} \cdot (L/D)_R^{-2} \right] \cdot \eta \right\} \cdot F_R \qquad (4\text{-}13)$$

For the first round calculation efficiency (η) can be approximated as:

$$\eta = \eta_c - 10\% = 0.9 - T_C/T_H = 0.9 - \delta^{-1}$$

In order to get the optimum $(L/D)_R$ we should differentiate equation (4-13). Note that the regenerator dead volume, as discussed before, is independent of $(L/D)_R$; therefore F_R is independent of $(L/D)_R$ and has no effect on differentiation.

Appendix (L) shows the result of differentiation as:

$$\left[2.07\, \bar{z}^{2.07} \cdot \frac{\beta^2}{\gamma^2}\right](L/D)_R^{4.07} - \left[.59 \frac{\bar{C}_2}{\bar{C}_1} \bar{z}^{1.41} (\ln\delta)^{1.66} (.9 - \delta^{-1})\right](L/D)_R^{1.41} - \left[2 \frac{\bar{C}_3}{\bar{C}_1} (\ln\delta)^{3.07} (.9 - \delta^{-1})\right] = 0 \qquad (4\text{-}14)$$

Equation (4-14) shows that if the temperature-ratio ( ) approaches unity, then $(L/D)_R$ approaches zero, i.e. near the unity temperature-ratio the engine does not have any regenerator.

Equation (4-14) is a non-linear equation and requires some trial and error in order to find its solution. To get a good first estimate for $(L/D)_R$ we can neglect the heat conduction term in comparison with the regenerator imperfection, good approximation for low temperature-ratios, then equation

(4-14) can be approximated as:

$$(L/D)_R = \sqrt[2.44]{.285 \frac{\bar{C}_2}{\bar{C}_1} * \bar{Z}^{-.66} * (\ln\sigma)^{1.66} * \eta * \gamma^2/\beta^2} \qquad (4\text{-}15)$$

For typical values of porosity (σ) and Prandelt number Pr i.e. 70% and .72, respectively, with the assumption of hydrogen as the working fluid the values for $\bar{C}_1$, $\bar{C}_2$, and $\bar{C}_3$ can be calculated as:

$$\frac{\bar{C}_2}{\bar{C}_1} = 47.6 * \frac{\sin\varphi}{\cos\alpha} / \left[\sin\varphi + 1/6 \sin(2\alpha-\varphi) + 1/2 \sin(2\alpha+\varphi)\right] \qquad (4\text{-}16)$$

$$\frac{\bar{C}_3}{\bar{C}_1} = 2.54 / \left[\sin\varphi + 1/6 \sin(2\alpha-\varphi) + 1/2 \sin(2\alpha+\varphi)\right] \qquad (4\text{-}17)$$

As shown in Appendix (L), there has been no simplification in deriving of equation (4-14) except that a correction factor should be added to that equation in order to take into account the effect of ducting and clearance volumes at both ends of the regenerator. In order to find that effect and check the results of the equation (4-14) the complete model of Chapter II was used. That model has been run for about one hundred different cases in various series. For example, to see the effect of temperature ratio the β, γ, and $\bar{Z}$ parameters are kept constant and σ, has been changed for a wide range of temperature-ratios. For each σ, the optimum aspect ratio is determined by trial and error. This has been done more than five times, i.e. each time the β, γ, and $\bar{Z}$ have been kept at different values and σ is changed. It is interesting to observe (after the fact) that nearly identical results could in fact be

obtained using the simplified model.

The results of equation (4-14) and complete model are very close (within ±2 units of L/D). This comparison also suggests that for effect of ducting and ends dead volumes the following correction should be added to the result of equation (4-14).

$$f_R(\xi) = 80 * \xi - 20 \qquad (4\text{-}18)$$

Where $\xi = (\text{Reg. Dead Volume} + \text{Reg. Ends Dead Volume}) / [1/2(VC+VH)]$

$$(L/D)_{R,opT} = (L/D)_R + f_R(\xi) \qquad (4\text{-}19)$$

4.1.2- Cold Heat-Exchanger Optimization:

The procedure to derive the optimum aspect ratio of the cold heat-exchanger is similar to that for the regenerator, except that for the cooler there are two types of losses: Power loss due to the pressure drop; and power loss due to the temperature drop.

The previously derived equation (3-32) gives the power loss due to the pressure drop.

$$\frac{W_{loss}}{W_{out}} = \frac{8}{\pi^3} * (fC) * (L/D)_C * \frac{VC^3 * \omega^3 * P_m (1 - A/\sqrt{1-A^2})}{(NC)^3 * (DC)^4 * R * TC} * E_{cc}^2 * \frac{SIN^2\varphi}{\cos^2\alpha} \left[SIN\varphi + \frac{1}{8} SIN(2\alpha - \varphi) + \frac{1}{2} SIN(2\alpha + \varphi) \right]$$

By normalizing this equation with respect to the output power it can be written in terms of the non-dimensional parameters. Appendix (L) shows the derivation of the following resultant equation.

$$\frac{W_{LOSS}}{W_{OUT}} = \frac{PC}{\pi} * (L/D)_c * \frac{Vc^2 * \omega^2 * C}{(AFRC)^2 * R * Tc} * \frac{(1-A/\sqrt{1-A^2})(1+\sqrt{1-A^2})}{A\,(1-Tc/Th)} * \frac{\bar{F}_\varphi(\varphi)}{F_T(T) * F_D(D)} * \frac{Vc}{Vh} \qquad (4\text{-}20)$$

Where

$$C = F_{cc}^2 * \frac{SIN^2\varphi}{\cos^2\alpha}\left[SIN\varphi + \tfrac{1}{6}\,SIN(2\alpha-\varphi) + \tfrac{1}{2}\,SIN(2\alpha+\varphi)\right] \qquad (4\text{-}21)$$

Lets define:

$$\gamma \triangleq \frac{P_m * Dc^3}{\omega * Vc * \mu_c}$$

$$\beta \triangleq \frac{\sqrt{R*Tc} * Dc^2}{\omega * Vc}$$

Then

$$\frac{\gamma}{\beta^2} = \frac{\pi}{2} * Nc * \frac{\cos\alpha}{SIN\varphi} * Rec$$

$$\frac{\gamma^2}{\beta^2} = \frac{P_m^2 * Dc^2}{R * Tc * \mu_c^2}$$

These result to the following representation of equation (4-20).

$$\frac{W_{LOSS}}{W_{OUT}} = \left[E_1 * \beta^{1.6} * \gamma^{-.2} * (L/D)_c\right] * F_c(\varphi, D, T_r, V_r) \qquad (4\text{-}22)$$

Where

$$E_1 = \frac{2^{3.8} * .0457}{\pi^{2.8} * (Nc)^{1.8}} * \left(\frac{SIN\varphi}{\cos\alpha}\right)^{1.8} * \left[SIN\varphi + \tfrac{1}{6}\,SIN(2\alpha-\varphi) + \tfrac{1}{2}\,SIN(2\alpha+\varphi)\right] * F_{cc}^{1.8}$$

$$F_c(\varphi, D, T_r, V_r) = \frac{(1-A/\sqrt{1-A^2})(1+\sqrt{1-A^2}) * \bar{F}_\varphi(\varphi)}{A\,(1-Tc/Th) * F_T(T) * F_D(D)} * \frac{Vc}{Vh}$$

As shown in Appendix (L), the number tubes for cooler can be calculated based on the given input heat (Qin) to the engine.

$$NC = (1-\eta) * Q_{in} / [5.75\,\pi * K_g * LC * (TR-TC)] * 1.1 \qquad (4\text{-}23)$$

By using a standard tube diameter for cooler and apply equation (4-23) for the number of tubes, the dead volume of the cooler would be constant and frozen for a given Qin and a given temperature-ratio.

Appendix (L) shows how the power loss due to the temperature drop in cooler can be written in the following non-dimensional form.

$$\frac{W_{Loss}}{W_{OUT}} = \left[E_2 * \delta^2 * (L/D)_c^{-1} * \dot{\gamma}^2 * \bar{\beta}^{-.4}\right] * F_c(\varphi, D, T_r, V_r) \qquad (4\text{-}24)$$

Where $$E_2 = \frac{2^{.2}}{.046\,(\pi * NC)^{.2}} * \left(\frac{\cos\alpha}{\sin\varphi}\right)^{.8} * \frac{k-1}{k} * P_r^{-.6}$$

$$\delta = TH/TC$$

Therefore, the total power loss of the cold heat-exchanger would be:

$$\frac{\text{Total } W_{Loss}}{W_{OUT}} = \left[E_1 * \bar{\beta}^{1.6} * \dot{\gamma}^{-2} * (L/D)_c + E_2 \delta^2 * \dot{\gamma}^2 * \bar{\beta}^{-.4} * (L/D)_c^{-1}\right] * F_c(\varphi, D, T_r, V_r) \qquad (4\text{-}25)$$

In equation (4-25) F_c (D, φ, T_r, V_r) is independent of $(L/D)_c$ because the volume of the cooler is frozen by equation (4-23); therefore, F_c has no effect on differentiation of equation (4-25) with respect to $(L/D)_c$.

$$\left.\frac{\partial\left(\frac{\text{Total } W_{Loss}}{W_{OUT}}\right)}{\partial (L/D)_c}\right|_{\substack{\text{const. Cooler} \\ \text{Dead Volume}}} = 0$$

$$(L/D)_c = \sqrt{\frac{E_2}{E_1}} * \delta * \dot{\gamma}^2 * \bar{\beta}^{.6} \qquad (4\text{-}26)$$

Equation (4-26) shows the optimum aspect ratio as a function of three parameters coupled together. Because of the simplifying assumptions which were made in derivation of equation (4-26), it might be improved by some correction terms, especially those due to dead volume effects, as follows:

$$(L/D)_{c,OPT} = \sqrt{\frac{G_2}{E_1}} \times \delta \times \dot{\gamma}^2 \times \beta^{.6} + f_\beta(\beta) + f_\gamma(\gamma) + f_\delta(\delta) + f_\xi(\xi) \qquad (4\text{-}27)$$

Then in order to find each of the correction terms to the right in equation (4-27), the results of the complete model and those of equation (4-26) could be compared. In fact the complete model was run for about fifty different cases, i.e. different operating conditions to determine $(L/D)_{c,\,OPT}$ by direct interpolation. In each run one of the four parameters was varied and the others were kept constant. All of the runs were divided into different sets, such as β set, used to determine f_β. This consists of more than twelve runs, in all of which β is taken as variable while the others are kept constant at different values for every four runs.

Comparison of the complete model and equation (4-26) results gives the following correlations. Appendix (L) shows an example of how the $f(\xi)$ has been derived. In deriving these correlations, an attempt was made to keep them both simple and accurate.

$$f_\beta(\beta) = -688.3 \times \beta + 47 \qquad (4\text{-}28)$$

$$f_\gamma(\gamma) = .0275 \times \gamma - 7 \qquad (4\text{-}29)$$

$$f_\delta(\delta) = -59.2 \times \delta + 146 \qquad (4\text{-}30)$$

$$f_\xi(\xi) = -19.2 \times \xi + 6 \qquad (4\text{-}31)$$

Where

VCD/[1/2(VH+VC)]=(Cooler Dead Volume + Cooler Ends Dead Volume)/[1/2(VH+VC)]

Therefore, the combination of equations (4-26) through (4-31) now represents the corrected optimum value of the cold heat-exchanger aspect ratio based on the four non-dimensional parameters.

Although the above corrections have to be add to equation (4-26), it doesn't mean there is a significant difference between equation (4-23) and (4-27). In order to see that typical values for the parameters have been used to calculate this difference as follows.

$\beta = .084 \Rightarrow f_\beta = -11$

$\gamma = 27 \Rightarrow f_\gamma = .6$

$\delta = 2.1 \Rightarrow f_\delta = 21$

$\xi = .32 \Rightarrow f_\xi = -.2$

TOTAL = 10.4

This means that equation (4-27) results to L/D=130 and equation (4-26) gives L/D=120. However, this 10 units difference has only one percent error in calculating the minimum power loss in the cooler.

4.1.3- Hot Heat-Exchanger Optimization:

The same procedure which was taken for cold heat-exchanger can be used for hot heat-exchanger too. Pressure losses for heater are given by equation (3-31). The normalized form of this equation with respect to the output power can be written as following.

$$\frac{W_{loss}}{W_{OUT}} = \frac{16}{\pi^3} * (PH) * (L/D)_H * \frac{VC^2 * \omega^2 * \bar{F}_f(q)}{R * TH * NH^2 * (DH)^4} * \frac{VC}{VH} * \frac{(1-A/\sqrt{1-A^2})(1+\sqrt{1-A^2})}{A(1-TC/TH)\,F_T(T) * F_D(0)} \tag{4-32}$$

Due to the similarities between the heater and cooler we can write the final optimization results of the heater as:

$$(L/D)_H = \sqrt{\frac{E_4}{E_3}} * \delta * \gamma_H^{.2} * \beta_H^{.6} \tag{4-33}$$

Where

$$E_4 = E_2 * \left(\frac{NC}{NH}\right)^{.2}$$

$$E_3 = E_1 * \left(\frac{NC}{NH}\right)^{1.8} * \left(\frac{F_{CR}}{F_{CC}}\right)^{1.8}$$

$$\gamma_H = \frac{P_m * (DH)^3}{\omega * VC * \mu_H} \tag{4-34}$$

$$\beta_H = \frac{\sqrt{R * TH} * (DH)^2}{\omega * VC} \tag{4-35}$$

There is a similar equation to equation (4-23) for calculation of NH, the heater tube number, as follows. This equation would freeze the dead volume of the heater.

$$NH = Q_{in} * 1.1 \Big/ \left[5.75\,\pi * K_g * LH * (TH - TR)\right] \tag{4-36}$$

Since this is not the complete form of the optimum aspect ratio and still needs some modification, equation (4-33) will be rewritten as:

$$\left(\frac{L}{D}\right)_{H,OPT} = \sqrt{\frac{E_4}{E_3}} * \delta * \gamma_H^{.2} * \beta_H^{.6} + f_{\beta H}(\beta) + f_{\delta H}(\delta) + f_{\gamma H}(\gamma) + f_{\xi H}(\xi) \qquad (4\text{-}37)$$

Where

ξ = VHD/[1/2(VH+VC)] =

=[Heater Dead Volume + Heater Ends Volume]/[1/2(VH+VC)]

For more than fifty different runs the complete model has been used in order to find these correction terms. Since the procedure is the same as that done for cold heat-exchanger, only the results are given below.

$$f_{\beta H}(\beta) = -356 * \beta_H + 100 \qquad (4\text{-}38)$$

$$f_{\delta H}(\delta) = -75.7 * \delta + 152 \qquad (4\text{-}39)$$

$$f_{\gamma H}(\gamma) = .01 * \gamma_H - 11 \qquad (4\text{-}40)$$

$$f_{\xi H}(\xi) = -16 * \xi + 3 \qquad (4\text{-}41)$$

Substitution of equations (4-38) through (4-41) into equation (4-37) would give the expression for optimum aspect ratio of the hot heat-exchanger based on four non-dimensional parameters which are related to Mach number, Reynolds number, temperature-ratio, and the dead volume percentage.

As shown for the cooler, the optimum aspect ratios for heater calculated by equations (4-33) and (4-37) would not have a significant effect on the value of minimum power loss. For the following typical values:

β=.321

ν=550

δ=1.83

ξ=.27

This difference in L/D calculation is seven units which has less than one percent error in the minimum value of the heater power loss.

4.1.4- Cylinder Optimizations:

One of the important tasks of Stirling engine optimization is to minimize the cylinder power losses. What this means is that the cylinders should be designed in such a way that the total power loss of the cylinder be at its minimum value. The first question is what dimension(s) should be taken for optimization? Upon reviewing the equations in Chapter III for the different power losses and the basic output power of the engine, it can be seen that the volume ratio (VH/VC) is the important factor both in the various cylinders losses and in the output power.

The cylinder losses are: shuttle losses; non-uniform temperature distribution loss; dry friction loss; heat leakage and pumping loss. Details and derivations of all of them are given in Chapter II. Since the first three losses are the dominant ones (as indicated in Fig.(64)), then only they will be used for optimization purpose.

In fact, an increase in the cylinder volume ratio (VH/VC) would increase the basic output of the engine, while at the same time it would increase the cylinders losses. Since the net output power increases by an increase in basic output

power and decreases by increasing cylinders losses, then there would be an optimum cylinder volume ratio corresponding to the maximum net output power. This means that the cylinder optimization should be performed based on the swept-volume ratio of the two cylinders (VH/VC).

Equation (2-16) gives the shuttle loss, although, this loss is calculated for the hot cylinder, however, when it is normalized with respect to the output power it will include the volume ratio.

Equation (2-20) calculates the power loss due to the transient non-uniform temperature distribution inside the cylinders. There is no direct cylinder volume term in this equation, rather, there are the heat transfer areas of the two cylinders (Ae, Ac). But these two areas are directly related to the two volumes.

Power loss due to the dry friction is given by equation (2-33), in this equation the volumes are directly involved, and by the time that this loss is normalized based on the output power we get the volume ratio of the cylinders.

Although, the above losses would increase by increasing the volume ratio, however, as shown in equation (3-2) the basic output power would also increase and both of them have opposite effect on the net output power. Appendix (L) shows how these significant losses in cylinders can be normalized with the output power.

The resulting equations are:

Friction: $$\frac{W_{Loss}}{W_{OUT}} = C_1 (1+1/\lambda)(1+\lambda/\delta+\xi)/(1-1/\delta) * F(\varphi) \qquad (4\text{-}42)$$

Shuttle: $$\frac{W_{Loss}}{W_{OUT}} = C_2 * \beta^{-1} * \delta * (1+\lambda/\delta+\xi) * F(\varphi) \qquad (4\text{-}43)$$

Non-Uniform Temperature:

$$\frac{W_{Loss}}{W_{OUT}} = C_3 * (\delta^{-0.5} + \lambda^{2/3} * \beta^{0.5} + C_4 \beta^{0.5}) * F(\varphi) \qquad (4\text{-}44)$$

In the above equations the minor factors and the coefficients have been put together in forms of new coefficients c_1, c_2, and c_3. In these equation, λ, δ, β, ξ, are defined as:

λ=VH/VC

δ=TH/TC

β=Reynold Number=Pm/(RTC)*ω*(VC/Ac)$^{2}/\mu_c$

Ac=Heat transfer area of cold cylinder

ξ=(VDC+VDH*TC/TH+VDR*TC/TR)/VC

By summing those losses and taking the derivative of the normalized total loss with respect to λ, the following equation would be resulted (see Appendix(L) for the derivation of the following equation).

$$\lambda = \sqrt{d_3 * \delta (1+\xi) / \left[1 + d_1 (\delta-1)\beta^{-1} + d_2 (\delta-1)\delta^{-0.5}\beta^{0.5}\right]} \qquad (4\text{-}45)$$

In order to calculate the three coefficients d_1, d_2, d_3 the complete model has been used. It has been run for two extreme cases and an intermediate case, and by trial and error the corresponding values of λ for these cases calculated as follows.

δ=1.8113
ξ=1.859 $\Rightarrow$ λ=1.6
β=8678

$\delta = 1.6226$
$\xi = 2.03 \quad \Rightarrow \quad \lambda = 1.3$
$\beta = 9140$

$\delta = 1.434$
$\xi = 2.42 \quad \Rightarrow \quad \lambda = 1.1$
$\beta = 9900$

By using these data, the following equation for optimum swept volume ratio has been derived:

$$\lambda = \sqrt{0.11(1+\xi)\delta / \left[1 + 3400(\delta-1)/\beta - .02(\delta-1)(\beta/\delta)^{.5}\right]} \qquad (4\text{-}46)$$

Since there has been some simplification in derivation of equation (4-46), then some correction terms should be added to it.

$$\lambda_{opt} = \sqrt{0.11(1+\xi)\delta / \left[1 + 3400(\delta-1)/\beta - .02(\delta-1)(\beta/\delta)^{.5}\right]} + f_\xi(\xi) + f_\beta(\beta) + f_\delta(\delta) \qquad (4\text{-}47)$$

By using different sets of the complete model runs, similar to the previous cases, the correction terms have been determined as following.

$$f_\xi(\xi) = .357 * \xi - .78 \qquad (4\text{-}48)$$

$$f_\beta(\beta) = -8.8 \times 10^{-5} \beta + .525 \qquad (4\text{-}49)$$

$$f_\delta(\delta) = .548 * \delta - .54 \qquad (4\text{-}50)$$

Substitution of equations (4-48) through (4-50) into equation (4-47) gives the final correlation for calculating optimum volume ratio of the two cylinders.

As discussed in heat-exchangers optimization, there would not be a significant difference on the maximum net output power by using the optimum swept volume ratio

calculated by equation (4-45) instead of (4-47).

Fig. (L-1) through (L-6) of Appendix (L) show the variation of optimum geometries as functions of different non-dimensional numbers.

4.2- Working Fluid for Stirling Engine:

The performance of any type of engine is highly dependent on the choice of working fluid. Sometimes the working fluid must be replaced upon changing the operating conditions, in order to get acceptable performance; this is normally true for Rankine engines where different organic fluids should be used at different operating temperatures.

In case of a Stirling engine, the properties of the working fluid used are important in two ways: (1) properties affecting heat transfer, especially in the regenerator; (2) properties affecting friction losses. Thus heat capacity and thermal conductivity are important as far as heat transfer in the cooler, heater, and regenerator is concerned while density and viscosity of the working fluid are important in relation to the flow friction losses. As shown in Chapter III, these latter losses are directly proportional to $(\rho v^2/2)$, ρ being the density and v the gas velocity.

Initially the preferred working fluids for Stirling engine were air, nitrogen, ammonia, carbon dioxide, steam vapor, helium and hydrogen [5]. The first five give substantially lower power densities and lower thermal efficiencies than helium or hydrogen for equal mean pressure, pressure ratio, engine speed and heat-exchanger cost (even when cosidering water and carbon dioxide). In addition the first five fluids cause metallurgical problems. Air and water produce scale-growth on all metals exposed at representative heater temperature which

cause problems in precision-controlled clearances in gas bearings and in reciprocating seals. Nitrogen and ammonia produce both scale-growth and nitride formations that are deleterious to thin-skinned hot heat exchangers. Carbon dioxide produces carbide formations in heat resistant alloys. Helium is an inert gas while hydrogen presently appears compatible with specific alloys not subject to hydrogen embrittlement. As a result, the choice narrows to helium and hydrogen, with choice based on engine performance, gas availability leakage and hazard.

Some years ago, Philips Laboratories [15] made a comparison between the three working fluids: helium hydrogen, and air. Fig.(44) shows their results. This comparison was made for a large engine rated at 165 KW per cylinder; that is, the three curves in that figure are all for 165 KW total output power. This figure, giving the overall efficiency as a function of specific power, shows that the speed increases and the swept volume decreases along the curves at increasing specific power output. Furthermore, superiority of hydrogen at high specific power levels is clearly indicated. However, this figure also shows that helium can be used with small penalty in efficiency or specific power in those applications where the use of hydrogen would be objectionable. Also, if low specific powers are acceptable ,e.g., in stationary applications. even air can be used as a working fluid with still tolerable efficiencies.

Using the optimum Stirling engine model of section (4.1) for temperature ratios from 1.2 to 2.2, different engine performances have been calculated for two working fluids, hydrogen and helium, under the same operating conditions(i.e. temperatures, speed, and mean pressure). The results are shown in Figs.(45) and (46). From these figures also we can see the advantage of using hydrogen over helium for Stirling engines, particularly at high temperature-ratios. Again, for low temperature-ratios the difference between fluids is noticable but not particularly significant.

Considering that the cost and availability of helium would become critical if the Stirling engine ever became widely used and also that helium gives lower performance than hydrogen and can not be generated on-site, then suggests that methods of controlling hydrogen leakage and reducing its hazards be seriously considered.

Leakage can be reduced to tolerable levels by appropriate surface coatings, and by improved joining methods, while hazards can be reduced by venting the system through a burner. Permeability into a sodium heat pipe appears controllable by using semi-permeable septums and by operating the heat pipe above the sodium-hydride dissociation temperature (1900°R), [5]. On-site hydrogen supply is state-of-the art using replaceable pressurized-cartridge electrolysis units or, alternatively, returnable metal-hybrid storage canisters.

Summarizing, hydrogen would appear to be the best choice

of working fluid especially at high temperatures and high temperature-ratios. But for the other end of the scale, i.e. at low temperatures and low temperature-ratios, either hydrogen or helium can be used with only modest differences in overall performance.

4.3- Derivation of Optimum Phase Angle and Speed via Simplified Model

4.3.1- Derivation of Optimum Phase Angle:

In Chapter II section (2.2), an equation for optimum phase angle was derived based on the Schmidt equations. Since in the ideal model (Schmidt solution) there is no loss term, then the resultant optimum phase angle of that section can not be used for a real engine. On the other hand, it is not possible to get an analytical solution for determination of optimum phase angle by using the complete model. The only reason why that complete model can be used for this purpose is through iteration which means every time the phase angle should be changed and the whole model should be run in order to find the phase angle corresponding to the maximum net output. This method is time consuming and expensive, because the complete model should be run many times. Therefore, it is clear again how helpful is the simplified model. Because of closed form solutions for basic power and different forms of losses in the simplified model, we are able to differentiate them and find the desired equation for optimum phase angle.

Equations which include the phase angle terms are: basic power output equation (3-2); power loss due to the pressure drop in heat-exchangers, equations (3-31) through (3-33); losses due to the temperature drop in heater and cooler, equations (2-10), (2-11); and power loss due to the non-uniform temperature distribution inside the cylinders, equation (2-20). Appendix(M) shows how each of these equations should be treated

before differentiation.

$$\underbrace{\text{Net Output Power}}_{W_{out}} = \underbrace{\text{Basic Power}}_{W} - \text{Total Loss}$$

Then $$\frac{\partial (W_{out})}{\partial \varphi} = \frac{\partial W}{\partial \varphi} - \frac{\partial (\text{Total Loss})}{\partial \varphi} \qquad (4\text{-}51)$$

In order to simplify the whole derivation, in all of the involved equations those terms which are independent of phase angle (ϕ) have been substituted by K's (constants). Therefore, as shown in Appendix(M), the followings have been resulted.

$$\frac{\partial W}{\partial \varphi} = \sin\theta * [K_1 \cot(\varphi) + K_2 * \sin\varphi] \qquad (4\text{-}52)$$

$$\frac{\partial (\text{Total Loss})}{\partial \varphi} = [(K_3+K_4)M^{1.8} + K_5 M^{1.07}][\cos\varphi - \tfrac{1}{6}\cos(2\alpha-\varphi) + \tfrac{1}{2}\sin(2\alpha+\varphi)] + [1.8(K_3+K_4) * M^{.8} + 1.07 K_5 M^{.07}] * \frac{\partial M}{\partial \varphi} * [\sin\varphi + \tfrac{1}{6}\sin(2\alpha-\varphi) + \tfrac{1}{2}\sin(2\alpha+\varphi)] - K_8(\sin\varphi - K_7\cos\varphi)$$

Where $$M = \frac{\sin\varphi}{\cos\alpha} = \sqrt{1 + (V_H/V_C)^2 + 2 * V_H/V_C * \cos\varphi} \qquad (4\text{-}53)$$

Substitution of equation (4-52) and (4-53) into (4-51) would result to the following equation which has been derived in Appendix(M) after a quite amount of mathematical and trigonometrical simplifications.

$$(K_9 - K_2 * K_{10})\cos^2\varphi - (K_8 - K_1 * K_{10} + K_6 * K_7)\cos\varphi + \tfrac{1}{6}K_8 + K_2 * K_{10} + .93 K_6 = 0 \qquad (4\text{-}54)$$

The equations for each of the K's are given in Appendix (M), and a sample of how equation (4-54) should be used is presented in that appendix. For that example, the optimum value of ϕ is calculated by equation (4-54) which is 107° and for the same engine, by going through the iterations, the

complete model is giving 110° . As we see, the result are close enough and the method is very simple and easy to follow. Fig.(58) shows a comparison of the results of equation (4-54) with the complete model results over the temperature-ratio range of 1.2 to 2.0. This figure also shows the accuracy of equation (4-54) and proves that simplified model can be apply to this type of derivation too.

4.3.2- Derivation of Optimum Speed:

It is important to run an engine at the proper steady state speed. This comes from the fact that for an engine, the mean effective pressure decreases with increasing the engine speed.

$$MEP = P_o - f(\omega) \approx P_o - a * \omega$$

Since torque is proportional to the mean effective pressure then:

$$\text{Torque} \approx T_o - b * \omega$$

Therefore, the engine power would be

$$\text{Power} = \text{Torque} * \omega \approx T_o\,\omega - b\omega^2$$

This means that there would be an optimum speed for the engine which delivers the maximum power.

By looking at the ideal analysis of section (2.2), it is clear that the output power is proportional to the speed, equation (3-1). The reason of having linear relationship is because this system, ideal Stirling engine, has no losses or resistances. Therefore, it is obvious that Schmidt equation is suggesting the highest possible speed in order to get

maximum power. But it isn't true for a real engine. In a practical engine there are various losses which would increase by any amount of increase in speed of the engine. Such as, mechanical friction loss which is proportional to the square of speed. Therefore, there is a trade-off between higher power and increase in losses. In fact, the optimum speed can be seen much better by looking at the efficiency of the engine, because some of the losses which depend on the speed have effects only on the heat input not the output power.

Appendix(M) shows the derivation of the optimum speed by using the simplified model. Since the ideal equations (Schmidt analysis) can not be applied to a real engine, then the only choices for determination of optimum speed are the complete model and the simplified model. The first choice doesn't give the optimum speed directly. Because the computer model should be run for many times, sufficient to get the highest output amongst the resulting performances. This method would be time consuming and needs a good amount of computer time. Therefore, we can see again how helpful is the simplified model.

As shown in Appendix(M), the basic output power and those power losses which are speed dependent can be written as follows:

$$W_{OUT} = K_1 * \omega \qquad (4\text{-}55)$$

ΔP - Heater $\qquad W_{Loss} = K_2 * \omega^{2.8} \qquad (4\text{-}56)$

ΔP - Cooler $\qquad W_{Loss} = K_3 * \omega^{2.8} \qquad (4\text{-}57)$

ΔP - Regenerator $\quad W_{Loss} = K_4 * \omega^{2.07}$ (4-58)

ΔT - Heater $\quad W_{Loss} = K_5 * \omega$ (4-59)

ΔT - Cooler $\quad W_{Loss} = K_6 * \omega$ (4-60)

Non-Uniform Temperature $\quad W_{Loss} = K_7 * \omega^{.5}$ (4-61)

Friction $\quad W_{Loss} = K_8 (.002\omega^2 + \omega)$ (4-62)

Therefore, the net output of the Stirling engine can be written as:

$$Net\ Output = K_1\omega - (K_2+K_3)\omega^{2.8} - K_4\omega^{2.07} - (K_5+K_6)\omega - K_7\omega^{.5} - K_8(.002\omega^2+\omega)$$

$$\frac{\partial(Net\ Output)}{\partial\omega} = 0 \qquad (4\text{-}63)$$

$$\Rightarrow \quad 2.8(K_2+K_3)\omega^{1.8} + (2.07K_4\omega^{.07} + .004K_8)\omega + K_5 + K_6 + K_8 - K_1 + .5K_7\omega^{-.5} = 0 \qquad (4\text{-}64)$$

Equation (4-64) presents the optimum speed for Stirling engines. In order to calculate K's, for any arbitrary speed we can calculate the engine performance, then by using equations (4-55) through (4-62) all of the K's can be determined. Then by substituting in equation (4-64) we can determine the optimum ω. Since equation (4-64) is non-linear, then it requires some trial and error. In order to get the first guess we can use the following equation which is approximate form of equation (4-64). The following equation can be derived by setting the exponents of equation (4-64) to nearest integers and taking into account that the K7 term is negligible.

$$2.8\,(K_2+K_3)\omega^2+(2.07K_4+.004K_8)\omega+K_5+K_6+K_8-K_1=0 \qquad (4\text{-}65)$$

Equation (4-65) is a quadratic equation which is easy to solve and to determine the first value for trial and error of equation (4-64).

Appendix (M) shows an example for how the K's can be determined and how results can be obtained from this derivation. As shown, the optimum value of speed which has been determined by equation (4-64) is very close to sample results obtained by iterating the complete model. Fig. (47) shows the optimum speed for the whole range of temperature ratio from 1.2 to 2.0. This figure shows the accuracy of equation (4-64) by comparison with the complete model results.

4.4- Derivation of Aspect Ratio for the Cylinders (B/S)

Part of the optimum design of Stirling engine is to determine the ratio of bore over stroke for the cylinders. This ratio can be determined by considering different power losses inside the cylinders. Consider the non-uniform temperature distribution inside the cylinders. If the cylinder has a long stroke and small bore, then the temperature gradient in the axial direction is much higher than the radial direction. Therefore, the power loss in the axial direction is more significant than the radial direction. A reverse situation happens when the cylinder has a short stroke and long bore. Therefore, by considering this single loss we can see there has to be an optimum bore over stroke ratio.

As discussed in Chapters II & III, there are two major power losses inside the cylinder which depend on the bore-stroke ratio: shuttle loss, and non-uniform temperature distribution loss. Heat leakage depends on this ratio too, but for low temperature applications this term is not significant in comparison with the two mentioned losses, see Fig.(64).

As shown in Appendix(N), equation (2-24) can be used for power loss in radial direction due to the non-uniform temperature. This appendix shows how a similar equation can be derived for power loss in axial direction. Therefore, for this type of loss we have the following equations:

$$\underset{R \leftrightarrow}{W_{Loss}} = .052 (Re)^{.8} \cdot (Pr)^{.4} \cdot \frac{k-1}{k} \cdot \frac{P_i}{P_m} \cdot K_g \cdot T_m \cdot X_m \cdot \cos(\varphi_p) \qquad (3\text{-}24)$$

$$A \updownarrow \quad W_{Loss} = .00727\,(Re)^{.8} \cdot (Pr)^{.4} \cdot B \cdot \frac{k-1}{k} \cdot K_g \cdot T_m \cdot \frac{P_1}{P_m} \cdot \cos(\varphi_p) \tag{4-66}$$

Assuming a given cylinder volume, the bore and stroke can be written as:

$$V = \frac{\pi}{4} B^2 \cdot S \qquad \beta \triangleq B/S \quad \Rightarrow$$

$$B = \sqrt[3]{\frac{4V}{\pi}}\,\beta^{1/3} \tag{4-67}$$

$$S = \sqrt[3]{\frac{4V}{\pi}}\,\beta^{-2/3} \tag{4-68}$$

Since Reynolds number for cylinder is defined as:

$$Re = \frac{\rho \cdot \omega \cdot B^2}{\mu} \tag{4-69}$$

and

$$X_m = 1/2\ S$$

Then the above equations can be written as:

$$R \longleftrightarrow \quad W_{Loss} = .026\,\left(\frac{\rho\omega}{\mu}\right)^{.8} \cdot (Pr)^{.4} \cdot \frac{k-1}{k} \cdot \frac{P_1}{P_m} \cdot K_g \cdot T_m \cdot \cos(\varphi_p) \cdot \left(\frac{4V}{\pi}\right)^{2/3} \cdot \beta^{-.4/3} \triangleq K_1 \cdot \beta^{-.4/3} \tag{4-70}$$

$$A \updownarrow \quad W_{Loss} = .00727\left(\frac{\rho\omega}{\mu}\right)^{.8} \cdot (Pr)^{.4} \cdot \frac{k-1}{k} \cdot \frac{P_1}{P_m} \cdot K_g \cdot T_m \cdot \cos(\varphi_p) \cdot \left(\frac{4V}{\pi}\right)^{2.4/3} \cdot \beta^{2.4/3} \triangleq K_2\,\beta^{2.4/3} \tag{4-71}$$

Equation (2-16) represents the shuttle loss.

$$W_{Loss} = \frac{\pi}{8} \cdot K_g \cdot S \cdot (TH - TC) \cdot \frac{B}{\ell} \cdot \frac{S}{L} \cdot (BET) \tag{2-16}$$

By using equations (4-67) & (4-68), equation (2-16) can be rewritten as:

$$W_{Loss} = \frac{\pi}{8} \cdot K_g \cdot \frac{BET}{\ell L} \cdot (TH - TC) \cdot \frac{4V}{\pi} \cdot \beta^{-1} \triangleq K_3 \cdot \beta^{-1}$$

Appendix(N) shows that by differentiating the total loss with respect to β we get the following equation for derivation of optimum bore/stroke ratio.

$$3K_3\beta^{2.6} - 2.6K_2\beta + .4K_1 = 0 \qquad (4\text{-}72)$$

Where

$$K_1 = .026\left(\frac{\rho\omega}{\mu}\right)^{.8}(P_r)^{.4} * \frac{k-1}{k} * \frac{P_1}{P_m} * K_g * T_m * \cos(\varphi_p) * \left(\frac{4V}{\pi}\right)^{\frac{2.6}{3}} \qquad (4\text{-}73)$$

$$K2 = .28\ K1 \qquad (4\text{-}74)$$

$$K_3 = \frac{\pi}{8} * \frac{K_g}{\rho L} * (TH - TC) * (BET) * \frac{4V}{\pi} \qquad (4\text{-}75)$$

There is an example in Appendix(N) to show how equation (4-73) should be used. For that example, which is for TH/TC=1.62 the optimum ratio is about 1.8.

Since solution of (4-72) requires some trial and error, then in order to start with a proper value for β it would be better to use the value which is calculated by the following equation.

$$\beta = \sqrt[3.6]{\frac{3K_3}{2.6K_2}} \qquad (4\text{-}76)$$

4.5- Comparison of Optimum Design Model Results with Available Data

This chapter introduced a new method for optimization of Stirling engine based on the operating conditions and physics of the system. The method is not restricted to low temperature or low temperature ratio applications, it can be applied for whole range of operating conditions. However, this thesis concentrates only on the low temperature-ratio duties and in this section the results of this optimum model will be compared with the only published data by Philips Laboratories [15] which has the comparable operating temperature range.

Since the operating temperatures and temperature-ratios are low, due to the use of waste-heat as input energy source ,then the output of the engines will assumed in the order of one KW.

In 1976, Philips Laboratories [15] started a study on Stirling engine efficiency as a function of operating temperatures and working fluids for low power level applications. By using the Philips Stirling engine optimization computer program, a large number of engines were calculated to determine the influence of heat and cooler temperatures on the efficiency. Followings are the characteristics of their analysis.

1)- Since the study was planned to satisfy the geometry of Philips I-98 engine, then the engine size was chosen to be equal to that, and the same stroke and piston dimensions

were taken.

2)- Three different heater tube temperatures were used, i.e. 850 C, 400 C and 250 C.

3)- Three different working fluids were used: hydrogen, helium and nitrogen.

No indication is given about their design model. Fig. (8) and Table(13) show the results of their study.

The optimum design model of this chapter has been used for temperature-ratios between 1.2 to 2.0. The mean pressure of 500 Psia and input heat rate 6850 Btu/hr or 2000 Watt have been used. As derived in previous sections the speed of the engine and phase angle difference between the two cylinders have been calculated based on the operating conditions and optimum geometry of the engine for each case. The results of this analysis are shown in Table(13) and Fig.(49).

Fig.(49) shows the comparison between the results of this thesis optimum design model and the Philips optimum design model. As shown, the results are reasonably close, yet there is a significant difference between the two models. In fact, the Philips results seems more optimistic than the results of the present study. Temperature-ratios data for this Philips model go down to 1.3, but it is interesting to see if similar agreement would hold for lower temperature-ratios, closer to unity.

Two years later, in 1978, Philips and General Electric [26] performed a low temperature and low temperature-ratio

experiment on a Stirling engine based on the 1976 Philips Laboratories study. The results of their experiments are shown in Fig.(50). They have gone to temperature-ratio down to 1.6 but not lower than that. As this figure indicates, the results of the experiment are closer to the optimum design model of this chapter than Philips' optimum model results. This shows the accuracy and validity of the present study optimum model. Even the gradient of the efficiency curve has been predicted well, by comparing with the experimental data.

CHAPTER V

5.1- Stirling Engine both with and without Regenerator

In the cursory analysis of Chapter II section (2.1), it was indicated that at low temperature and low temperature-ratio a Stirling engine with zero regenerator effectiveness has an efficiency comparable to that of a highly regenerative Stirling engine and even to that of practical Rankine engines. Since in Chapters II through IV, the Stirling engine has been studied in great detail, then it would be interesting to investigate the behavior of the optimum design engine operating at these low temperature-ratios to see if these tentative conclusions are confirmed.

The optimum model of Chapter IV is used to investigate the performance of Stirling engine, especially its regenerator geometry.

One of the major reasons that a Stirling engine reaches the Carnot efficiency in the ideal case is due to presence of a regenerator. However, it has been shown in previous chapters that the imperfect regenerator produces entropy even while it improves the engine performance. When temperature ratio becomes close to unity, then the Carnot efficiency whould itself be low and a practical engine would not be expected to work with high performance. Therefore, this consideration would suggest that a practical Stirling engine might indeed perform better without a real regenerator. This supposition is reinforced when we look at the sources

of imperfection of the regenerator, namely the regenerator losses. One would anticipate that at low temperature-ratios the pressure drop in the regenerator will be significant in comparison to indicated mean effective pressure of the engine. Since in this same situation the temperatures are not high enough to fully exploit the power-gain value of the regenerative heat-exchanger compared to the power loss due to the pressure drop in the regenerator, then it may be concluded that the presence of the regenerator might indeed lower the performance of the engine rather than improve it.

Fig. (55) shows the variation of optimum design regenerator length with temperature ratio. These are the results of the optimum design model of Chapter IV. As shown in this figure, when temperature-ratio is less than 1.3 the regenerator length is so small that it suggests to use Stirling engine without any regenerator. This means that although the regenerator is one of the distinguishing features of the Stirling engine, yet, for temperature-ratios less than 1.3 the engine evidently behaves more efficiently without a regenerator. Figs. (53) and (54) show the variation of regenerator power loss and heat loss for an optimum design Stirling engine. As shown, the optimum design model vanishes the regenerator when the temperature-ratio goes toward unity, which results in vanishing values for regenerator power loss and heat loss.

This means that although the regenerator is one of the distinguishing features of the Stirling engine, yet, for temperature-ratios less then 1.4 the engine evidently behaves more efficiently without a regenerator.

5.2- Low-Temperature Rankine Engines:

Among the published literature regarding low-temperature and low temperature-ratio Rankine engines there are some limited results indicating concern with temperature-ratios close to unity. Most of these efforts have been concentrated on the use of solar energy. However there are others which have concentrated on waste-heat recovery, especially addressed to recovering some of the energy from the exhaust gas of trucks and automobils.Thermo-Electron Corp. [16] has studied the use of an organic Rankine cycle system operating on the exhaust energy of a gas turbine. The special organic fluid which they have used is trifluoroethanol CF3CH2OH (85%) and water (15%). This working fluid performes efficiently for temperature ratios more than 2.0. Although Thermo-Electron has done much research and development on waste-heat recovery using Rankine cycle systems nevertheless, these efforts have been concentrated on waste-heat sources with temperatures more than 600°F. Yet, they have in fact made some studies for lower temperature and their results are shown on Fig.(51). While these results are largely theoretical rather than experimental, nevertheless certain experience power-factors have been used in order to bring results as close as possible to achievable Rankine engine performance. In the corresponding analysis for their results shown on Fig.(51), the following assumptions have been used; these assumptions would appear to represent reasonable practice.

a)- Turbine expander efficiency (including 75% thermal and 95% mechanical efficiencies)=71%

b)- Coolant has temperature at 70°F and temperature rise across the condensor is 20°F, i.e. the condenser temperature is 90°F (TC=90°F).

c)- Pressure drop in the condenser is about one percent (1%) of the mean pressure in the system.

d)- Boiler (vapor generator) has a 20°F temperature change across, i.e. TH is 20°F less than the heat source temperature.

e)- Pressure drop across the boiler is assumed to be five percent (5%) of the system mean pressure.

f)- Regenerator has 90% effectiveness with 2% pressure drop (1% on each side).

g)- Feed pump has a 65% efficiency.

h)- Working fluid is R-85 for $TH/TC \geq 1.4$ and R-113 for $TH/TC < 1.4$.

Table (15) and Fig.(51) show the results of their analysis for a Rankine engine operating at low temperature and low temperature-ratio. In the next section these results will be compared with the corresponding results of a Stirling engine.

For several years, Robert E. Barber, of Barber-Nichols Engineering Co., has initiated efforts for waste-heat recovery by means of Rankine engines[2]. Recently he has studied this engine for solar energy systems [3]. Part of this effort involves the efficiency and other practical considerations of

the combined collector-Rankine engine system; these studies have concluded that based on use of particular working fluids temperatures of 200 F, 300-400 F and 600 F represent optimum operating conditions for flat plate concentrators. These studies also report that the peak solar conversion efficiencies of these systems are in the range of 5 to 11 percent.

Part of the requirements for the solar application is to find the optimum efficiency of the Rankine engine under different operating conditions. Barber [3] has shown his results as a generalized curve of efficiency versus maximum cycle temperature. By generalized curve, he means a single curve which covers the performance of different working fluids at different temperature ranges. Clearly, as mentioned above and as discussed later, any optimum Rankine engine requires different working fluids depending on the operating temperatures.

In fact, refrigerant 113 most nearly follows Barber's generalized curve up to a hot temperature of 400 F, assuming a fixed cold temperature of 95°F; it should be noted that this 400°F temperature is near the critical point of R-113. Above the 400°F temperature, R-113 decomposes rapidly and is not suitable as working fluid [3]. For application above 400°F, possible working fluids are pure, fluorinated, or chlorinated toluenes or benzenes.

The results of Barber-Nichols analysis are shown in Table (16) and Fig.(52) the assumption for derivation of these results are as follow:

a)- Expander efficiency is 80%

b)- Mechanical efficiency is 95%

c)- Condenser temperature is 95°F

d)- Feed pump efficiency 50%

e)- Regenerator effectiveness is 80%

f)- Pressure losses are 5% in high pressure side, and 8% in low pressure side.

Barber-Nichols results seem to be more optimistic than Thermo-Electron results. This might be due to the fact that Thermo-Electron assumptions appear to be closer to the characeristics of a particular real Rankine engine. In the next section these results will be compared with the corresponding results for Stirling engines.

5.3- Comparison of Stirling and Rankine Engines at Low Temperature and Low Temperature-Ratio

Two sets of results for low temperature ratio Rankine engines were presented in the previous section. There are other published literature concerning Rankine engines for waste-heat recovery applications, however, most of this presents theoretical results, often too optimistic to be true of practical cases. Since the Stirling engine results which were used for comparison purposes in this section have been obtained by detailed analysis of this thesis (Chapter IV), then an attempt was made to find comparable Rankine engine results. However, this effort was not completely successful and the presumably more practical results from Thermo-Electron play a larger rule in this comparison than other results. This action may not lead to a completely fair comparison, yet it doesn't seem to be altogether unrealistic. Moreover, it suggests a need for future work, namely completion of similar open literative objective and detailed analysis for the Rankine engine at these operating conditions, showing how the two compatible detailed analyses will in fact compare.

Figs.(51) and (52) show this final comparison of Stirling and Rankine engine performances at low temperatures and low temperature-ratios. It is clear from both figures that a Rankine engine has superiority over a Stirling engine with regenerator up to about a 1.6 temperature ratio. For temperature ratios more than 1.6 (TH/TC>1.6), a Stirling engine

appears to perform better than a Rankine engine. Another observation is that at temperature-ratios close to unity the optimum design Stirling engine which has practically no tends to behave more efficiently than a Rankine engine. Finally, it appears that the temperature-ratio 1.2 is an operational limit for Rankine engine; that is, this engine produces no net power for temperature-ratios less than 1.2. On the other hand, the optimum design Stirling engine which now has vanishing regenerator can still produce output power even for temperature-ratios less than 1.2 down to a new limit at about temperature ratio of 1.1.

It is recognized that a Stirling engine is efficient at high temperatures and high temperature-ratios, due to the fact that its behavior becomes closer to the Carnot engine. That is why for temperature-ratios more than 1.6 it might be expected to perform better than a Rankine engine. On the other hand, as shown in Chapter II and III the regenerator is one of the sources of entropy generation in Stirling engine. Therefore, with entropy source eliminated from the system, more efficient behavior results in comparison with Rankine and Regenerative Stirling engines operating at temperature-engine operating at temperature-ratio less than 1.25.

A further important note about Rankine engines is that in all of the analysis, as shown in cursory analysis of Chapter II, it is assumed that the Rankine engine was mildly superheated. This process would increase the entropy

generation inside this engine. Therefore, if a wet-Rankine engine (ile. an engine with two phase flow expander) could be designed and built, then the engine efficiency will be significantly increased, because a wet cycle Rankine, as shown in section 2.1 reaches the Carnot efficiency. Therefore, this engine in a wet-cycle might be more efficient than Stirling engine at all temperature-ratios.

CHAPTER VI

6.1- Significant Contributions of Present Investigation

During the course of this thesis analysis elucidating some of the interesting features of the Stirling engine have been undertaken which have yielded important conclusions.

In Chapter II, in addition to providing a simplistic preliminary analysis of Rankine, Stirling, and Brayton engines and their comparison, a more thoroughgoing and complete computerized model for Stirling engines was established. This so-called complete model includes all of the significant losses which have been considered upto present time; moreover all of the loss derivations have been put on a firm rational basis. For some cases new derivations have been presented, such as the two additional new approaches for calculating the power loss due to the transiant non-uniform temperature distribution inside the cylinders. For calculation of mechanical friction loss in Stirling engines a rational method is presented for the first time. This method is necessary and suitable for one KW waste-heat engines which were the purpose of this thesis and for which the lower limit of temperature ratio will depend directly on the magnitude of this loss.

The complete model of Chapter II is able to predict engine performances reasonably accurately, at least within the range of uncertainty determined by the scatter in the initial design data and by other experimental errors.

Chapter III furnishes a derivation of a new so-called

"simplified model". The purpose of this model was to be able to optimize Stirling engines by analytic means in a general way. Although, there are at present various models for calculation of Stirling engine performance, nevertheless, they are unsuitable for optimization studies because they are not presented in directly differentiable algebraic form, and would require extended computer iteration. In contrast, the simplified model supplies closed form results for practical Stirling engines, yet with accuracy comparable to computerized models such as the complete model of Chapter II. Of course, this confirmation required the necessary prior establishment of the latter model.

In Chapter IV a general method of Stirling engine design optimization is presented. This method can be applied to any type of Stirling engine under the entire range of operating conditions, because it is rationally based and characterized by dimensionless groups; in particular by the Mach number, Reynolds number, temperature ratio, and percent dead volume, such a design model appears for the first time in the open literature.

Finally, the results of the optimum model of Chapter IV have led to some interesting conclusions regarding the Stirling engine when operating at low temperature-ratios. In particular, definitive conclusions have been reached concerning the behavior of this engine without the regenerator, these will be discussed in the following section.

6.2- Conclusions

By means of closed form solutions of simplified model a general method of Stirling engine design optimization was derived. This method was used for calculation of Stirling engine performance for temperature-ratio range of 1.0 to 2.0 which is the region for temperature-ratio of most available waste-heat sources. This analysis yields to following definitive conclusions:

a)- Fig. (55) shows the variation of a regenerator length with temperature-ratio. This variation shows one of the important results of the detailed analysis of Stirling engine, namely elimination of a regenerator from a Stirling engine for temperature-ratios less than 1.3. This means that although the regenerator is one of the distinguishing features of the Stirling engine, yet the engine evidently behaves more efficiently without a regenerator for temperature ratios less than 1.3.

b)- Figs.(51) and (52) compare performances of Stirling and Rankine engines. There are some interesting and important temperature-ratios in this comparison. It is indicated that in temperature-ratio range 1.25 to 1.6 a Rankine engine operates more efficiently, while for higher temperature ratios a Stirling engine is the better alternative. Also it is shown that Rankine engine has vanishing efficiency at temperature-ratio of 1.2 or less. For temperature ratios less than 1.25 Stirling engine without the regenerator appears to perform more efficiently than either Rankine engine. However, a

Stirling engine without a regenerator would have vanishing efficiency when it reaches the temperature-ratio of 1.1 or less.

c)- Table(12) and Figs.(45) and (46) show a comparison between the results of optimum designed Stirling engine with two working fluids: helium and hydrogen. It is clear that hydrogen improves the Stirling engine performance significantly. This improvement is noticeable at temperature-ratios 1.4 or more. Therefore, if the working temperature-ratio is very close to unity (1.3 or less) then there is not that much difference between hydrogen and helium performances. But for temperature-ratios higher than 1.3 hydrogen will be the number one alternative.

The complete model of Chapter II has been successfully applied to the analysis and prediction of the performance of paractical Stirling engine. This requires no "real time" calculations; merely by giving the operating conditions and engine geometry the model yields the performance of the engine with detailed values of the different losses.

In modelling of a practical engine aided by the bond graph technique it has been shown how internal effects occurring in one region of the system generate entropy, but the power losses due to those effects should be recover in another region of the system, such as temperature drops in heater and cooler which produce losses that will be taken out of the system output power in the compressor.

Simplified model of Chapter II, which expresses the Stirling engine performance in closed form solution, predicts the behavior of real engines accurately and it is well suited for optimization studies and for studies of engine performance under extreme conditions. This model allowed to derive a general optimization method.

Optimum design method of Chapter IV which includes correlations for optimum geometry of each component, for optimum phase angle and engine speed, and for optimum bore, stroke ratio, represents a general method for optimizing Stirling engine. The result of this optimum model has shown a good agreement with the available experimental data.

Comparison of Stirling and Rankine engine which is shown in Chapter V is for low output power level(1KW)engines. Since at these power levels the optimum design Stirling engine seems to perform as efficiently as a Rankine engine at temperature ratios close to unity, then it would be interesting to see if the same conclusion can be reached at higher output power levels. Namely, this thesis suggests that for Ocean Thermal Energy Conversion (OTEC) project, which undergoes a Rankine cycle and has temperature-ratio of order of 1.1, the optimum design Stirling engine should be investigated as an efficient alternative. Because a Stirling engine with no regenerator might have higher efficiency than a Rankine engine at high output power level. The optimum design model of Chapter IV enables us to investigate this comparison.

Table (18) and Figs. (45) and (46) show the behavior of Stirling engine with isothermal expansion and compression processes. The results are much closer to the Carnot engine, and engine performs more efficiently than the adiabatic case.

Stirling engine has some advantages over Rankine engine, no matter what the operating conditions are, such as working fluid. If helium or hydrogen or any other working fluid is chosen for Stirling engine, it doesn't have any operating temperature restriction, i.e. over the entire temperature range engine can work efficiently with one working fluid. But for a Rankine engine depending on the operating temperature range the working fluid should be changed in order for engine to work efficiently. Also Stirling cycle is a reversible cycle, i.e. it can go back and forth between an engine and a heat pump just by changing the direction of the process. This is not possible for Rankine cycle because the throttling process in the Rankine cycle is not a reversible process. Therefore, flexibilities of Stirling cycle in practice are more than a Rankine cycle.

As a result, for waste-heat recovery there are three alternatives, presently, which depending on the operating temperature-ratio one of them should be selected as discussed above, Stirling engine without the regenerator for temperature-ratios close to unity, Rankine engine for temperature-ratios less than 1.6 and regenerative Stirling engine for high temperature-ratios.

6.3- Suggestions for Future Work

The present analysis explores some new ideas about the Stirling and Rankine engines for low temperature and low temperature-ratio applications. However, these results should be checked in practice. Particular areas and problems of interest are:

1- An experiment should be set up to see the behavior of Stirling engine without the regenerator, because this component has been the major part of this engine and its elimination for low temperature-ratios should be investigated practically.

2- Mechanical friction loss is the important item which pushes Stirling engine to zero efficiency at 1.2 temperature-ratio. As mentioned before, the mechanism for calculating this loss, in the present analysis, was derived by using the internal combustion results. Therefore, it should be checked to indicate if this derivation is comparable with experimental observations. Otherwise a more accurate method should be presented. However, the results of present derivation are very close to the Philips mechanical power loss [15]. There is no indication of how Philips has calculated this loss.

There are some alternatives for lowering this loss, and that is the use of flexure material such as tension actuators [32] and rolling diaphragm. Fig.(57) shows how the tension actuators, which have been manufactured by some reinforced rubber material, can be set up to behave as a double acting

cylinder and piston. By a simple set up of four actuators connected to an eccentric shaft from one side and to a pressurized air tank on the other side, it was demonstrated that friction-mean-effective-pressure of these actuators is about 5 Psi which is less than half of the Fmep which is used in the present analysis by using the IC engine results. Since at low temperatures and low temperature-ratios these flexure material can have a reasonable economic life, then it might be worthwhile to investigate their applications as substitute for cylinder and piston in Stirling engine.

3- In the present analysis the effect of finite matrix heat capacity in the regenerator is not included, and it is interesting to add that to the analysis and see the behavior of the system at very low temperatures and/or high pressures.

4- The effect of finite heat transfer in the heat exchangers should be investigated, especially at low temperatures.

5- For the purpose of comparison between Stirling and Rankine engines a superheated Rankine engine was used, because it is a practical design of this engine. Due to this superheating there is an entropy generation which is very significant; therefore, if a wet-Rankine engine can be designed and constructed where the expander and compressor can handle two phase flows then that engine can behave more efficiently than Stirling engine over the whole range of waste-heat recovery application.

6- There is a need for a completion of an open literative objective and detailed analysis for a Rankine engine at low temperatures and low temperature-ratios, similar to the present study on Stirling engines.

Table (1): Performance of Rankine Engine

TH/TC	Wout Btu/lb	Dissip. Energy Btu/lb	Wcomp. Btu/lb	Qin Btu/lb	Eff. %
1.1	5.174	91.466	.94	96.64	5.35%
1.2	12.58	99.42	.417	112	11.23%
1.4	25.51	113.14	.989	138.65	18.4%
1.6	40.52	123.3	.98	163.82	24.73%
1.8	55.28	125.74	.95	181.02	30.54%
2.0	61.57	135.43	.126	197	31.25%

Table (2): Performance of Brayton Engine

TH/TC	Wout Btu/lb	Wcomp. Ideal Btu/lb	Qin Ideal Btu/lb	Wcomp. Reg. Btu/lb	Qin Reg. Btu/lb	Eff. Ideal %	Eff. Reg. %
1.1	1.5	32.25	33.75	28.	29.5	4.4%	5.1%
1.2	6.03	63.97	70.	56.17	62.2	8.6%	9.6%
1.4	22.24	121.52	143.76	113.02	135.26	15.5%	16.4%
1.6	46.5	176	222.5	163	209.5	20.9%	22.2%
1.8	77.3	225.8	303.1	213	290.3	25.5%	26.6%
2.0	113.7	273.9	387.6	262.9	376.6	29.3%	30.2%

Table (3): Performance of Stirling Engine

TH/TC	Wout Btu/lb	W Displ. Btu/lb	Dissp. Energy Btu/lb	Qin E=90% Btu/lb	Dissp. Energy Btu/lb	Qin E=0% Btu/lb	Eff. E=90%	Eff. E=0%
1.1	29.18	364.77	385.22	414.4	503.62	532.8	7.04%	5.5%
1.2	58.36	364.77	405.64	464	642.44	700.8	12.58%	8.33%
1.4	116.7	364.77	446.6	563.3	920.2	1036.9	20.72%	11.26%
1.6	175.	364.77	487.6	662.6	1198	1373	26.4%	12.75%
1.8	233.4	364.77	528.4	761.8	1475.7	1709.1	30.6%	13.7%
2.0	291.8	364.77	569.3	861.1	1753.2	2045	33.9%	14.3%

Table (4A): Effect of Regenerator Effectiveness on Stirling Engine Efficiency

TH/TC=].2						
E	0%	20%	40%	60%	80%	100%
Eff.	10.4%	11.25%	12.25%	13.43%	14.88%	16.67%
Eff./Eff idl	62.4%	67.5%	73.5%	80.6%	89.3%	]00%
TH/TC=1.6						
E	0%	20%	40%	60%	80%	100%
Eff.	15.9%	18.0%	20.7%	24.3%	29.5%	37.5%
Eff./Eff Edl	42.5%	48.0%	55.2%	64.9%	78.7%	100%

Table (4B): Effect of Regenrator Effectiveness on Stirling Engine Efficiency

TH/TC=2.0						
E	0%	20%	40%	60%	80%	100%
Eff.	17.8%	20.5%	24.0%	29.0%	36.7%	50%
Eff./Eff idl	35.7%	40.9%	48.0%	58.1%	73.5%	100%
TH/TC→∞						
E	0%	20%	40%	60%	80%	100%
Eff./Eff. idl	21.7%	25.7%	31.6%	40.7%	58.1%	100%

Table (5): Variation of Stirling Engine Output with Dead Volume

TH/TC = 1.2						
X	0%	20%	40%	60%	80%	10
Wout/ Wout ideal	100%	45.4%	20.3%	8.0%	2.2%	0.%
TH/TC = 1.6						
X	0%	20%	40%	60%	80%	100%
Wout/ Wout ideal	100%	42.5%	17.4%	6.0%	1.2%	0.%
TH/TC = 2.0						
X	0%	20%	40%	60%	80%	100%
Wout/ Wout ideal	100%	42.2%	17.3%	6.0%	1.2%	0.%

Table (6): Comparison of Philips Engine Results and Complete Model Predictions

	TH R	N RPM	Pm psi	Q Watts	m g/min	W Watts	Eff. %
Experiment	2112	1800	200	7.7		465.5	
Complete Model	2112	1800	200	1200		455	38.0%
Experiment	1752	1200	200	5.1		292	
Complete Model	1752	1200	200	800		316	39.7%
Experiment	2112	1600	200	7.7		480	
Complete Model	2112	1600	200	1200		497	41.4%
Experiment	1752	1600	200	6.1		251	
Complete Model	1752	1600	200	950		306	32.2%
Experiment	1752	1400	200	5.5		285	
Complete Model	1752	1400	200	860		308	36.0%

Table (7): Comparison of Allison Engine Performance with Complete Model Predictions(ϕ=118)

	TH	TC	N	Pm	Qin lb-ft/ cycle	Wout lb-ft/ cycle	Eff. %
Experiment	1680	628	3000	1544	292	113	39%
Complete Model	1680	628	3000	1544	275	118.2	43%
Experiment	1680	628	2500	1544	300	120	40%
Complete Model	1680	628	2500	1544	280	121.7	43.5%
Experiment	1680	628	2000	1544	302	124	41%
Complete Model	1680	628	2000	1544	277	122.5	44.2%
Experiment	1680	628	1500	1544	319	134	42%
Complete Model	1680	628	1500	1544	278.3	128	46%

Table (8): Comparison of Allison Engine Performance with Complete Model Predictions (ϕ=112)

	TH R	TC R	N RPM	Pm psi	Qin lb-ft/ cycle	Wout lb-ft/ cycle	Eff. %
Experiment	1680	628	3000	1544	259	97	37.5%
Complete Model	1680	628	3000	1544	269	108	40.2%
Experiment	1680	628	2500	1544	260	106	40.8%
Complete Model	1680	628	2500	1544	274.7	114	41.5%
Experiment	1680	628	2000	1544	271.8	112	41.2%
Complete Model	1680	628	2000	1544	274	118.4	43.2%
Experiment	1680	628	1500	1544	275.5	119	43.2%
Complete Model	1680	628	1500	1544	275	123.6	45.%

Table (9): Comparison of GPU-3 Performance with Complete Model Predictions (H2)

	TH R	N RPM	Pm psi	Qin lb-ft/ cycle	Wout lb-ft/ cycle	Eff. %
LeRC	1760	3000	300	139.6	49.2	35.3%
Complete Model	1760	3000	300	114.5	43.	37.5%
LeRC	1760	2000	300	139	50.3	36.2%
Complete Modle	1760	2000	300	125	45.5	36.3%
LeRC	1760	1500	300	129.4	48.8	37.7%
Complete Model	1760	1500	300	124	44.8	36.2%

Table (10): Comparison of GPU-3 Performance with Complete Model Predictions (He^3)

	TH R	N RPM	Pm psi	Qin lb-ft/ cycle	Wout lb-ft/ cycle	Eff. %
LeRC	1762	1500	400	178	65.2	36.6%
Complete Model	1762	1500	400	157	57.3	36.5%
LeRC	1762	1500	600	251	101	40.2%
Complete Model	1762	1500	600	247	96.3	39%
LeRC	1762	3000	400	153.1	57.2	37.8%
Complete Model	1762	3000	400	144.4	54.3	38%
LeRC	1762	3000	600	225	92	41%
Complete Model	1762	3000	600	237	88.5	39%

Table (11): Comparison of Simplified and Complete Model Predictions

Type of MOdel	TH/TC	Qin [Watt]	Wout [Watt]	Eff. %
Complete Model	1.4	3270	170	5.2%
Simplified Model	1.4	3200	173	5.4%
Complete Model	1.6	2591	355	13.7%
Simplified Model	1.6	2568	360	14%
Complete Model	1.8	3845	777	20.2%
Simplified Model	1.8	3830	781	20.4%
Complete Model	2.0	5390	1267	23.5%
Simplified Model	2.0	5373	1263	23.5%
Complete Model	2.6	19045	7600	39.9%
Simplified Model	2.6	19130	7560	39.5%

Table (12): Optimum Stirling Engine Model Results for Different Temperature-Ratios (Qin=2000 Watts)

TH/TC	Hydrogen			Helium			N RPM	ϕ Deg.
	Wout [Watt]	Ind. Eff.	Shaft Eff.	Wout [Watt]	Ind. Eff.	Shaft Eff.		
1.20	56	5.5%	2.8%	50	5.2%	2.5%	800	118
1.25	80	7.2%	4%	78	7.2%	4%	900	117
1.3	125	9.8%	6.5%	124	9.6%	6.3%	950	116
1.43	220	15.3%	11%	214	13%	10.7%	1050	113
1.62	380	20.9%	19.4%	354	19%	17.7%	1120	110
1.81	450	25.3%	22.5%	406	23%	20.3%	1210	108
2.0	530	29.2%	26.5%	466	27%	23.3%	1350	104
2.2	591	32.5%	28.8%	526	27.7%	26.3%	1500	95

Table (13A): Philips Optimum Design Model Results Ref. [15]

TH/TC	Helium		Hydrogen	
	Indicated Eff.	Shaft Eff.	Indicated Eff.	Shaft Eff.
1.33	10.8%	7.5%	11.9%	8.5%
1.4	13.7%	10%	15.6%	12%
1.54	18.5%	15%	20.4%	17%
1.66	23%	20.5%	25.5%	22.5%
1.80	26.5%	23%	29%	26%
1.9	28%	25%	30.8%	27.7%
2.0	30%	28%	32.7%	30%
2.1	33%	30%	35%	32%

Table (13B): Philips & G.E. Optimum Design Results (Helium as Working Fluid) Ref. [26]

TH/TC	1.7	1.9	2	2.1
Eff.	14%	17%	22%	24%

Table (14): Performance of Stirling Engine without Regenerator (Helium as Working Fluid)

TH/TC	Qin=2000 Watts			Qin=4000 Watts		
	Wout [Watt]	Ind. Eff.	Shaft Eff.	Wout [Watt]	Ind. Eff.	Shaft Eff.
1.1	-	-	-	-	-	-
1.15	20	3.5%	1%	80	4.%	2%
1.2	40	5%	2%	118	5%	3%
1.3	88	7.2%	4.7%	214	7%	5.5%
1.43	100	8.1%	5.5%	240	9.4%	6.%
1.62	150	9.3%	7.1%	370	11.6%	9.1%
1.81	175	10%	8.4%	456	13.3%	11.2%
2.0	186	10.5%	9.3%	490	14.2%	12.3%

Table (15): Barber-Nichols Model Results for Rankine Engine Ref. [2]

TH/TC	1.10	1.19	1.37	1.55	1.73	1.90
Eff.	5%	10.5%	17.2%	20.5%	23%	26%

Table (16): Thermo-Electron Results for Low Temperature-Ratio Rankine Engine. Ref. [7]

TH/TC	1.3	1.4	1.6	1.8	2.0
Eff.	10.2%	13%	18%	22%	23.6%
Ideal Eff.	11.6%	15%	19.5%	23%	25%

Table (17): Optimum Stirling Engine Model Results for Different Temperature-Ratios (Qin=4000 Watts, Hydrogen, pm=400 Psia)

TH/TC	Wout [Watt]	Ind. Eff.	Shaft Eff.	N RPM	ϕ Deg.
1.2	112.2	5.63%	3%	800	120
1.3	272	8.6%	6.8%	900	117
1.43	447	14.6%	11.2%	1000	115
1.62	774	21.8%	19.5%	1100	110
1.81	907	25.0%	22.7%	1200	106
2.	1089	29.8%	27.2%	1350	103
2.2	1135.6	32.2%	29.0%	1500	95

Table (18): Optimum Model Results for Isothermal Stirling Engine (Qin=2000 [Watts], Hydrogen)

TH/TC	Wout [Watt]	Ind. Eff.	Shaft Eff.
1.2	200	13%	10.%
1.3	289	18.8%	15.3%
1.43	373	23.9%	20.5%
1.62	532	30%	27%
1.81	649	34.3%	31.5%
2.	719	37%	34.4%
2.2	797	39.4%	36.9%

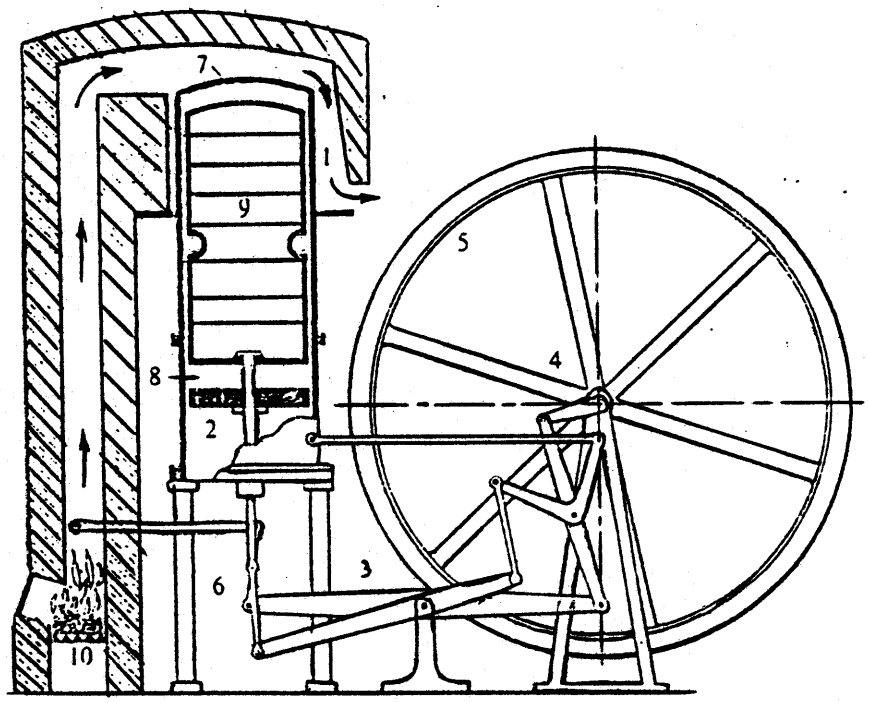

Fig. (1): Original Single-Cylinder and Piston Stirling Engine Ref.[25]

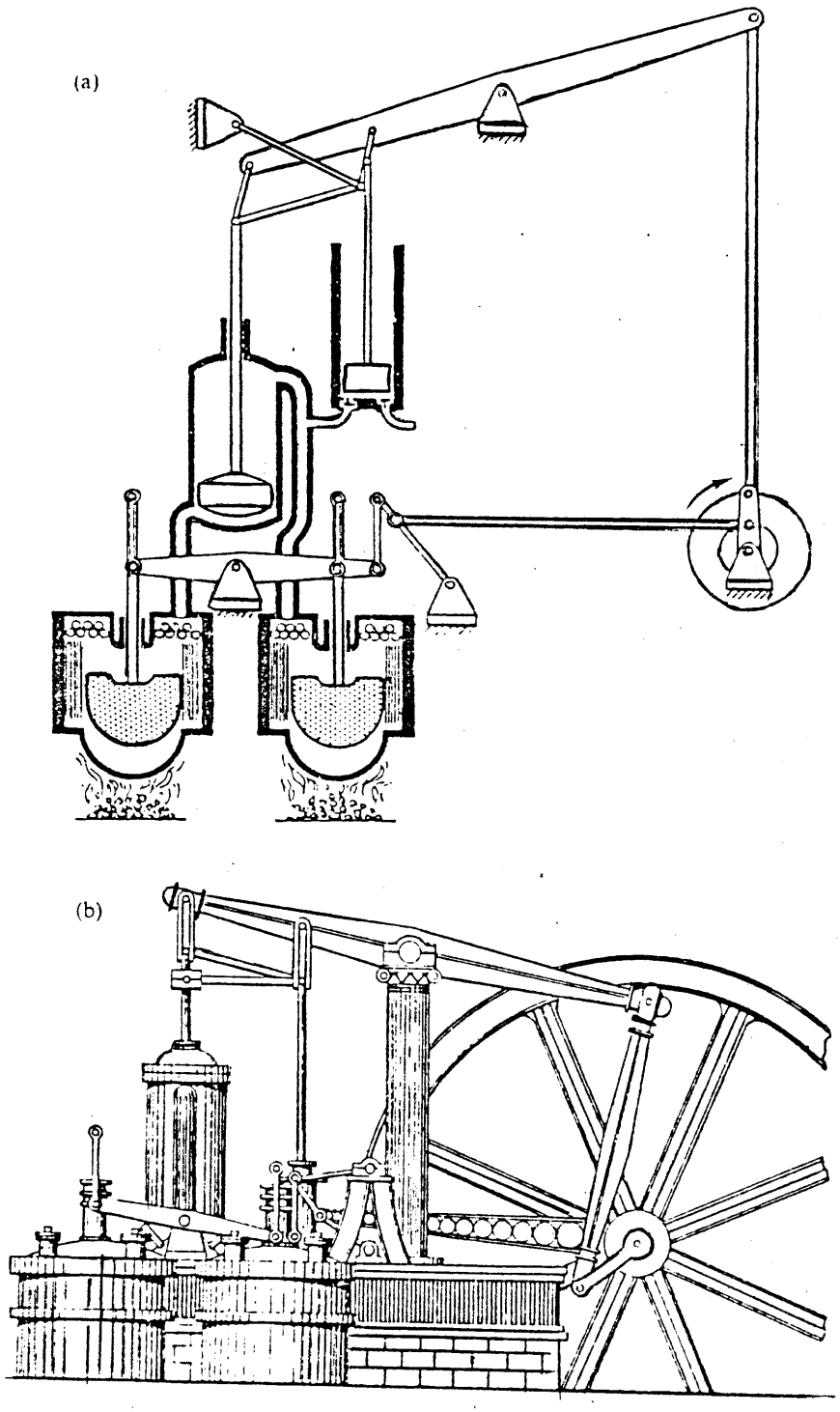

Fig.(2): First Double-Acting Cylinders Stirling Engine
Ref.[25]

Fig.(3):

SCHEMATIC DIAGRAM OF OTEC POWER CYCLE , Ref.[17]

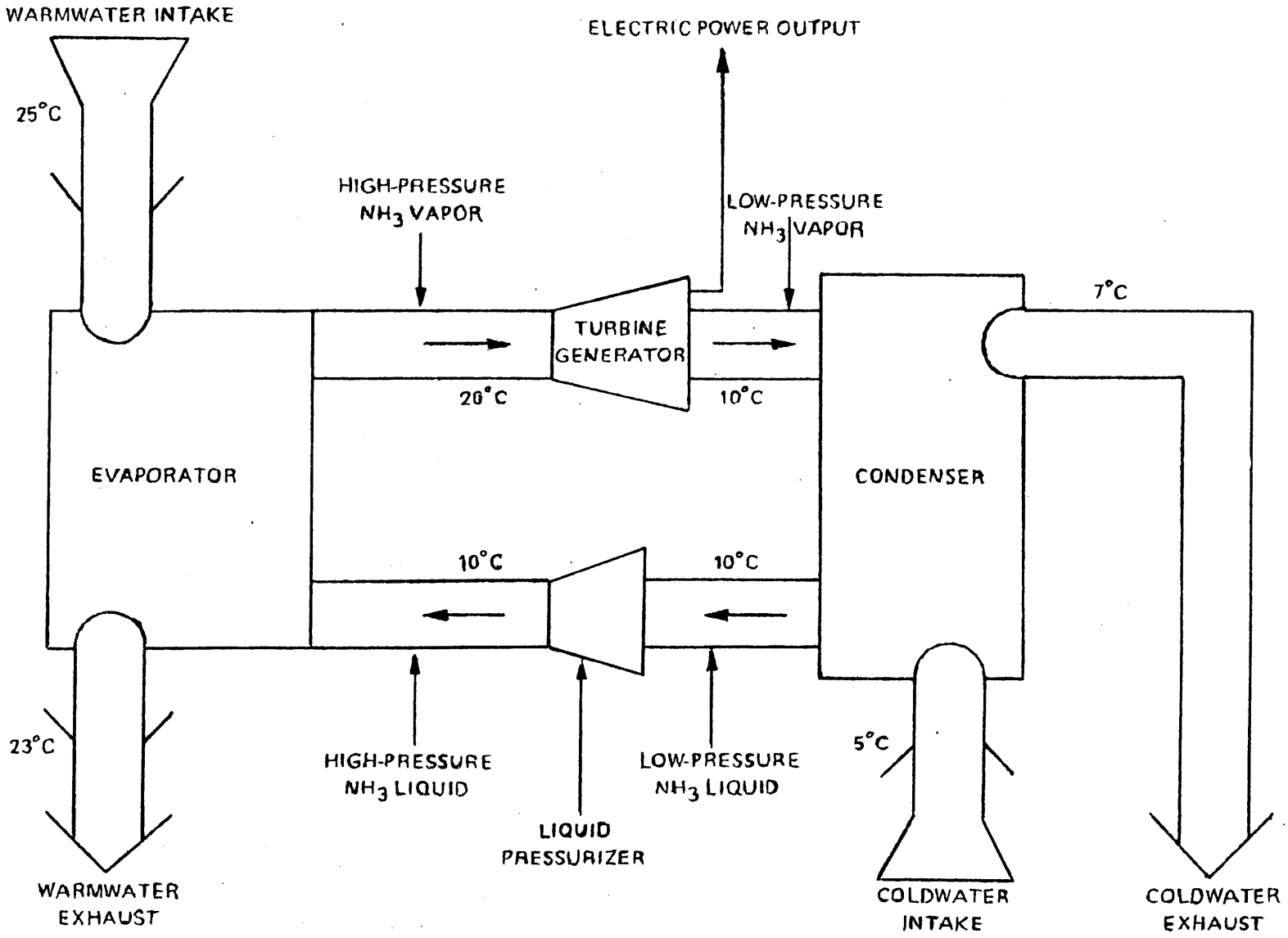

Fig.(4): CUTAWAY VIEW OF TRW OTEC PLANT MODEL
Ref.[17]

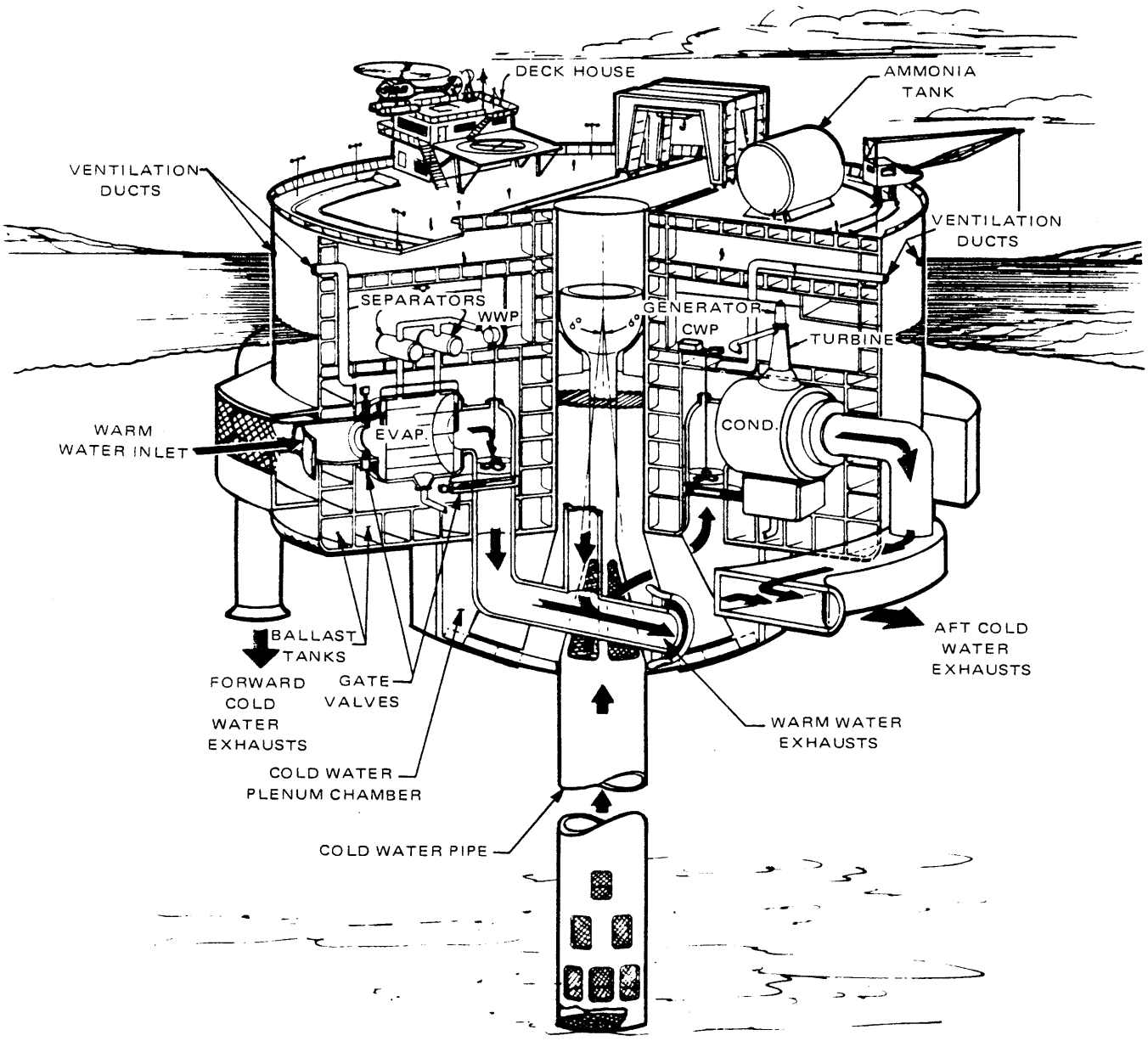

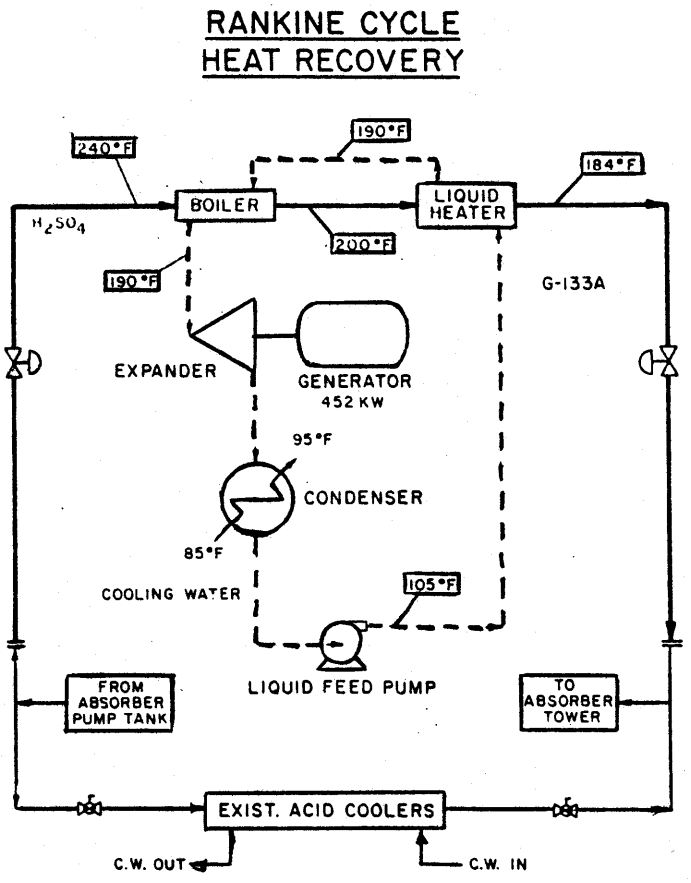

Fig.(5): Allied Chemical Corp., 500 KW Sulfuric Acid Waste-Heat Recovery, Rankine Cycle

Ref.[12]

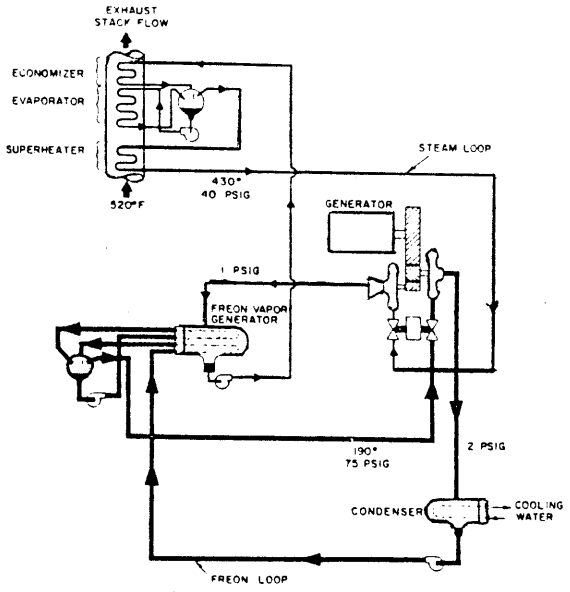

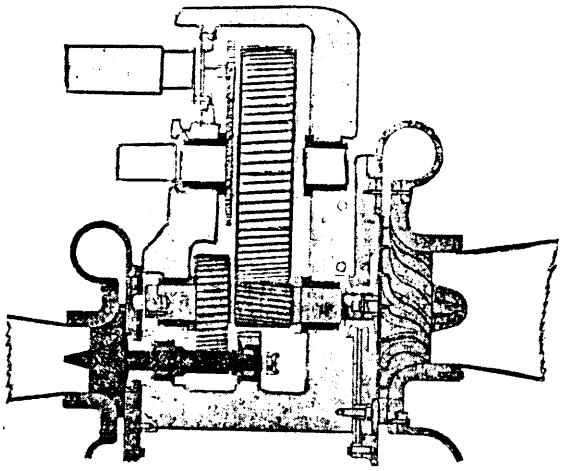

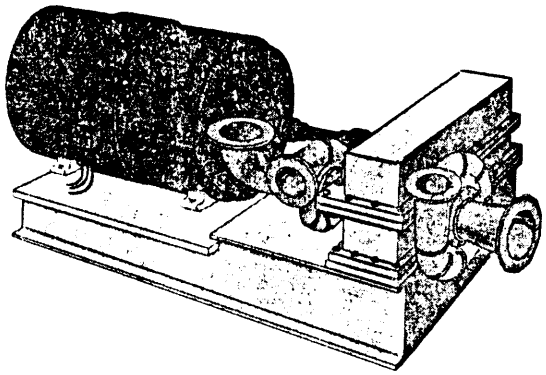

Fig.(6): DOE and MTI Binary Rankine Cycle Waste-Heat Recovery
Ref. (21)

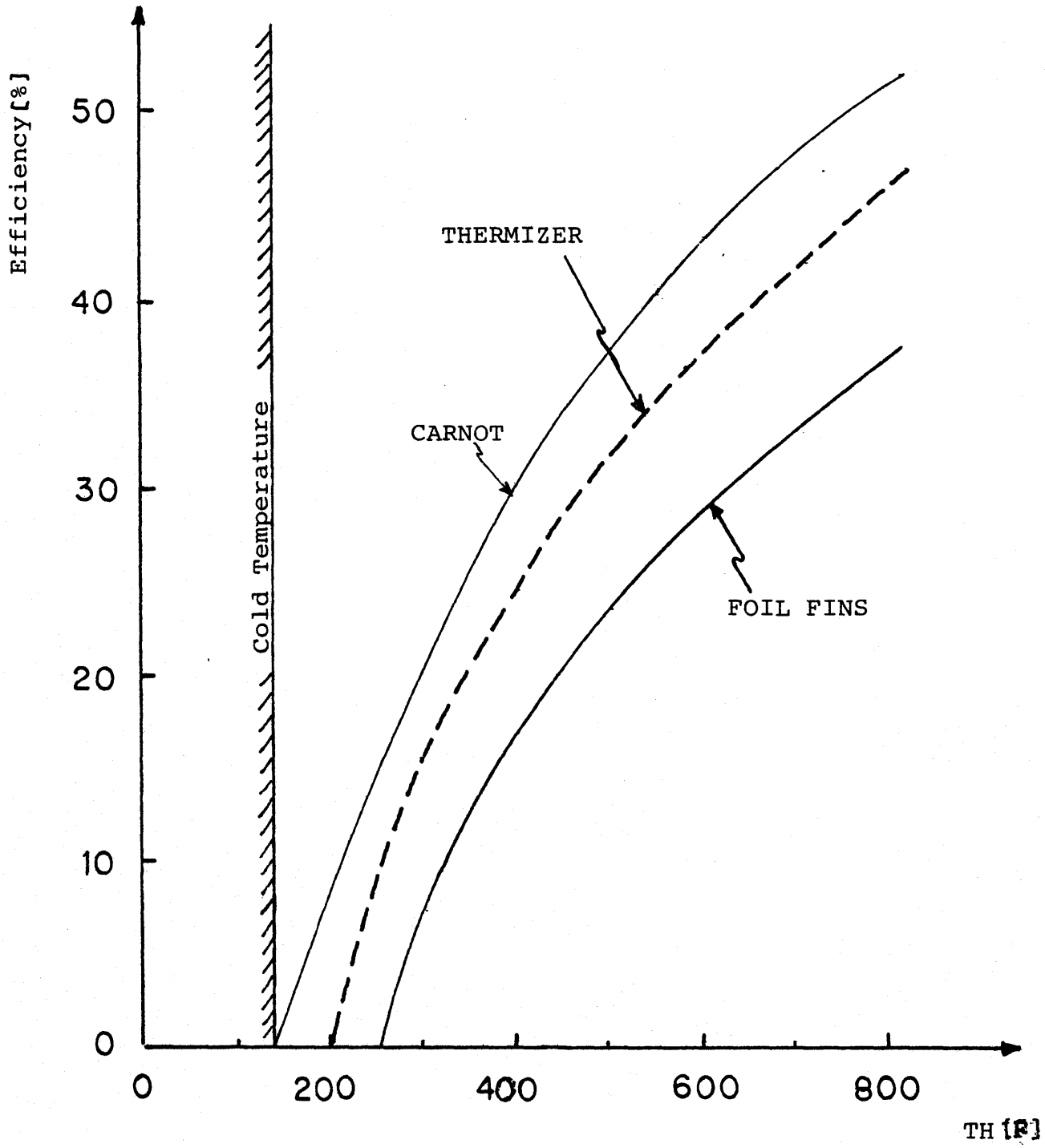

Fig.(7): Variation of Efficiency With Heater Temperature
G.M. Benson, Thermal Oscillators, Ref.[5]

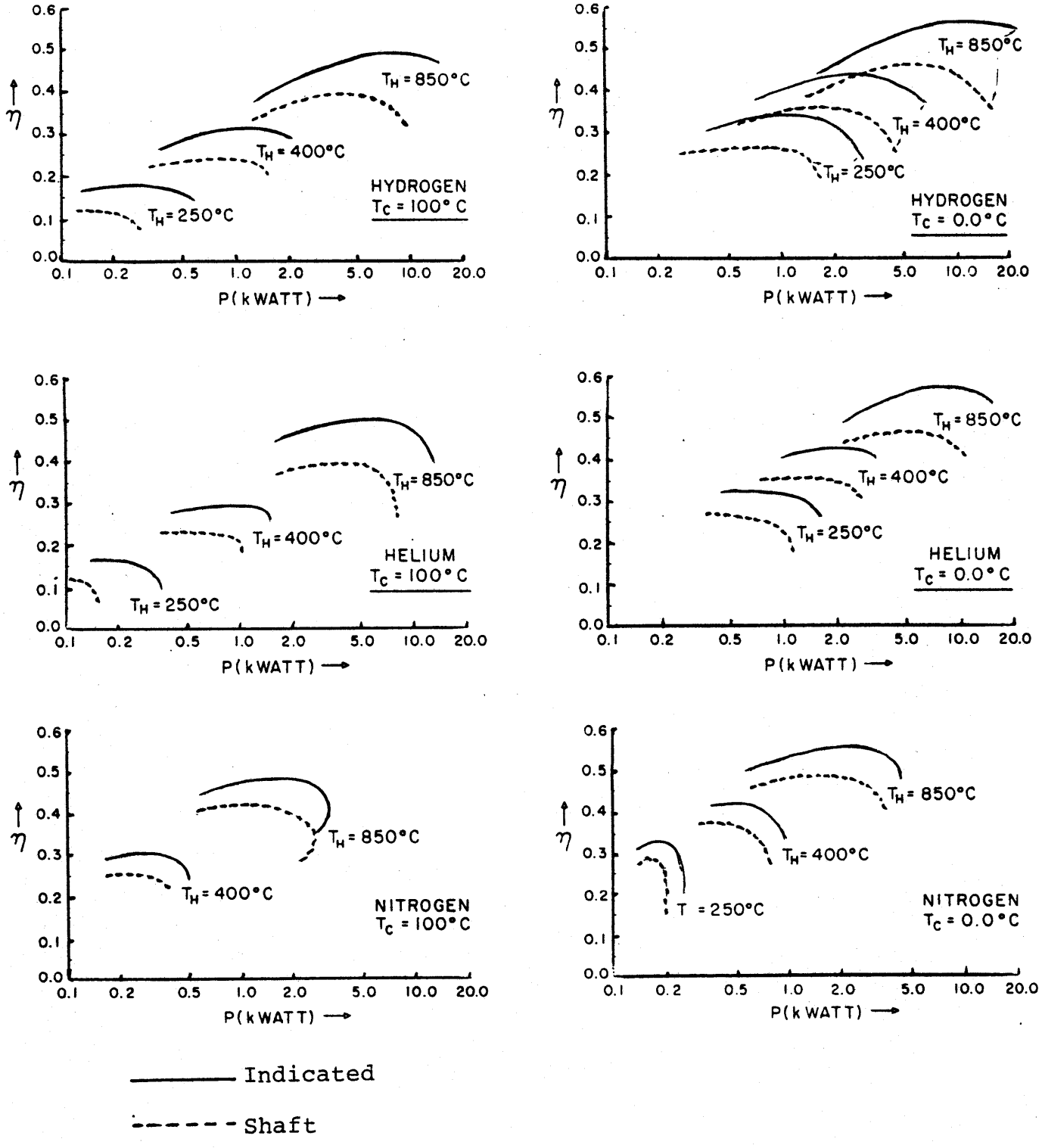

Fig.(8): Philips Low Power Level Engine, Computer Results
Ref.[15]

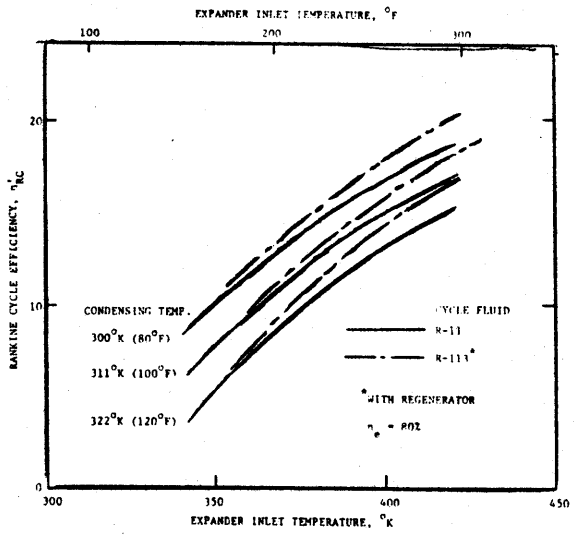

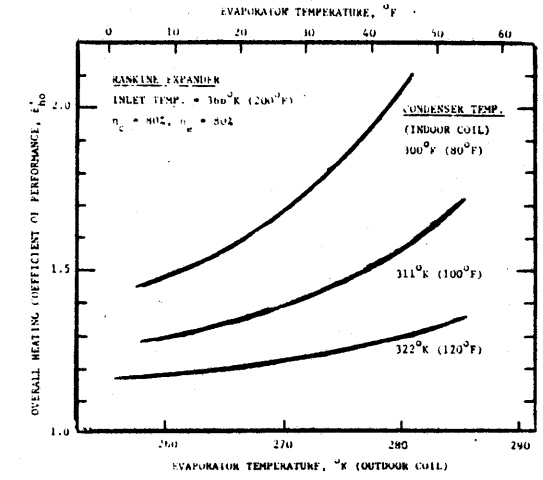

Fig.(9): General Electric Stirling-Engine-Powered Heat-Activated Heat Pump Results
Ref.[8]

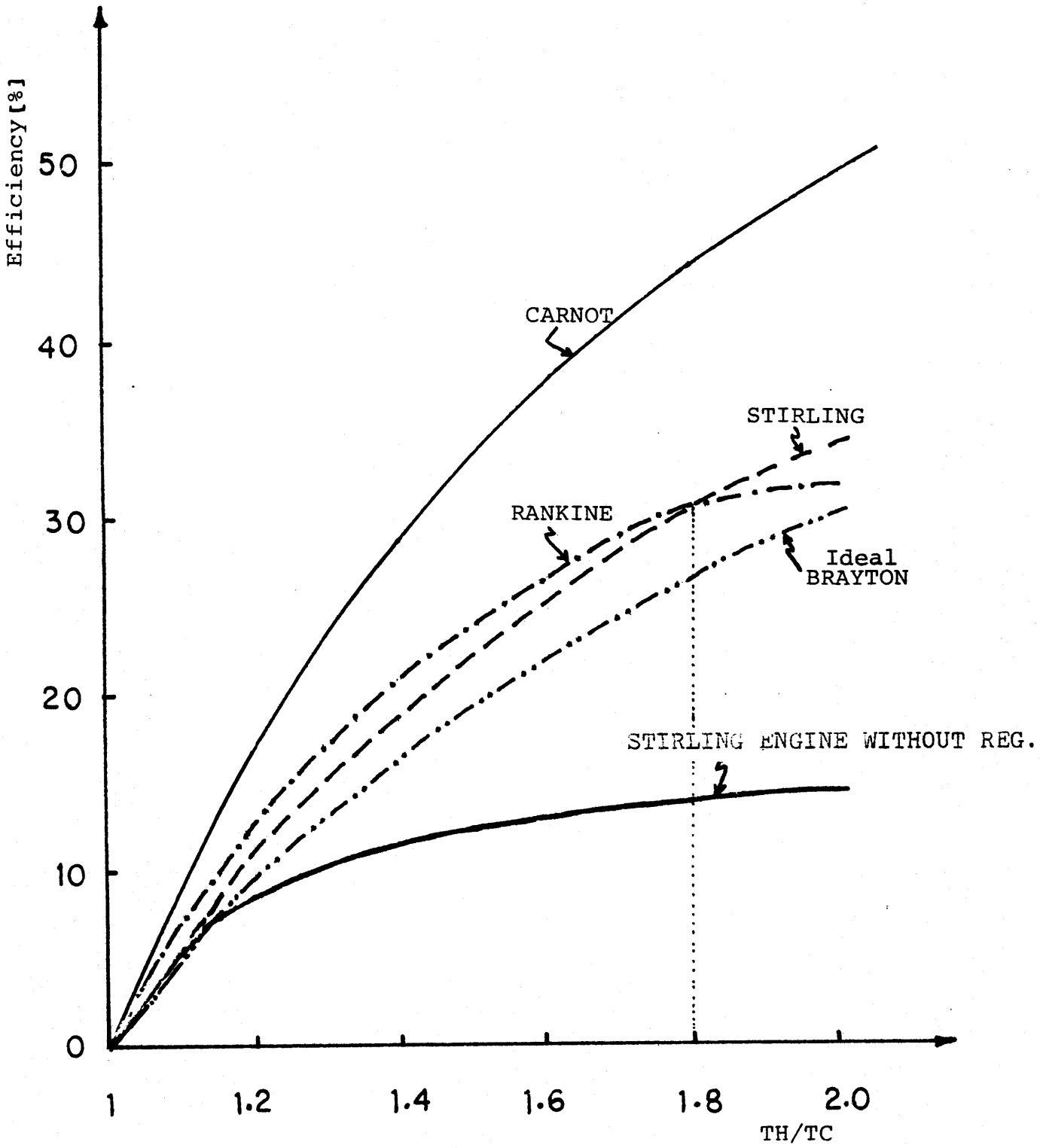

Fig.(11): Comparison of Steady State Performance of Rankine and Stirling Engines with Perfect Component and Ideal Brayton Engine. Tables (1), (2), and (3)

Note: Rankine Engine is Super-Heated; Stirling Engine Has Estimated Loss about 20% of the Ideal Output Power

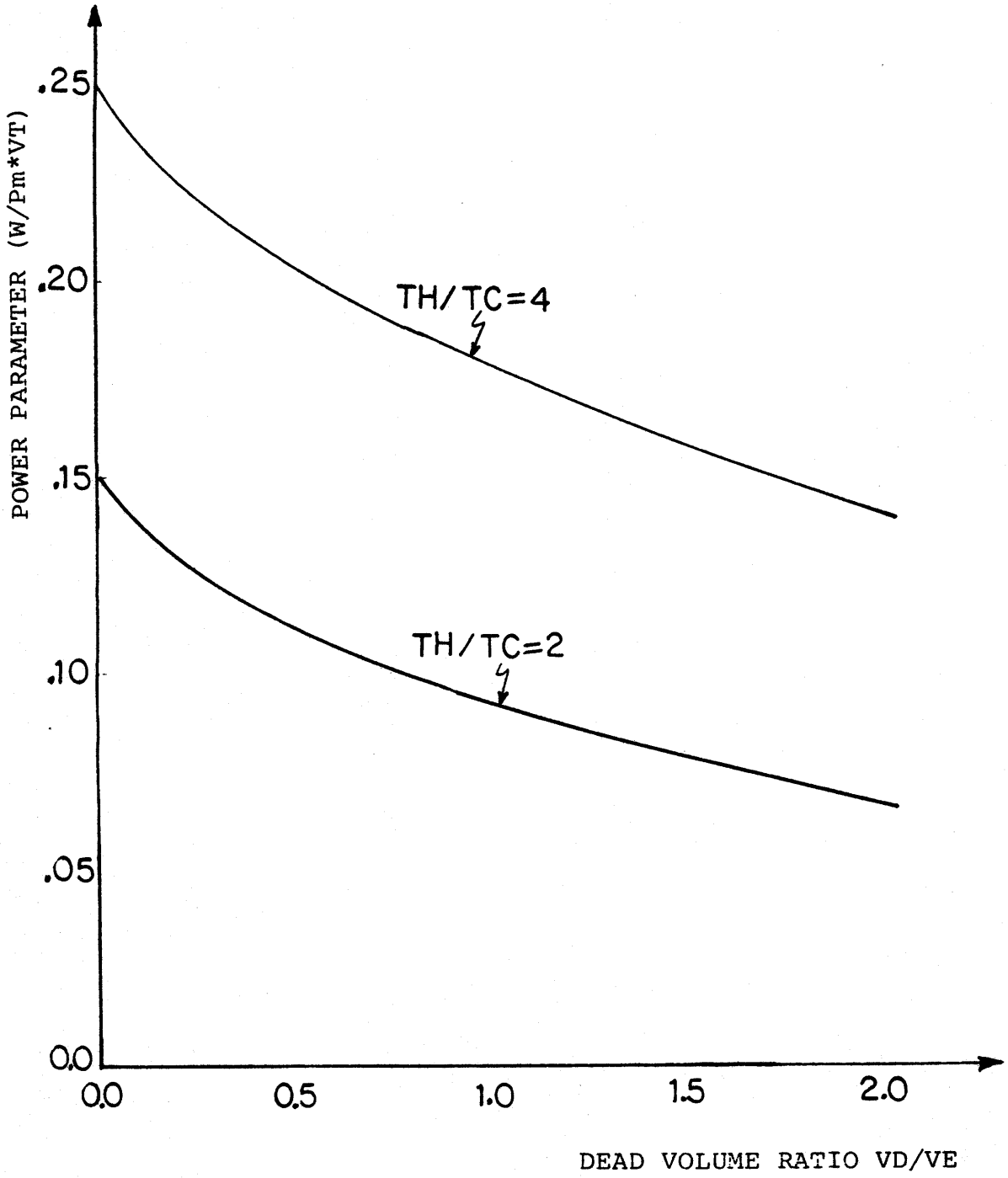

Fig.(12): Effect of Dead Volume on Stirling Engine Performance
Walker's Results Ref. [25]

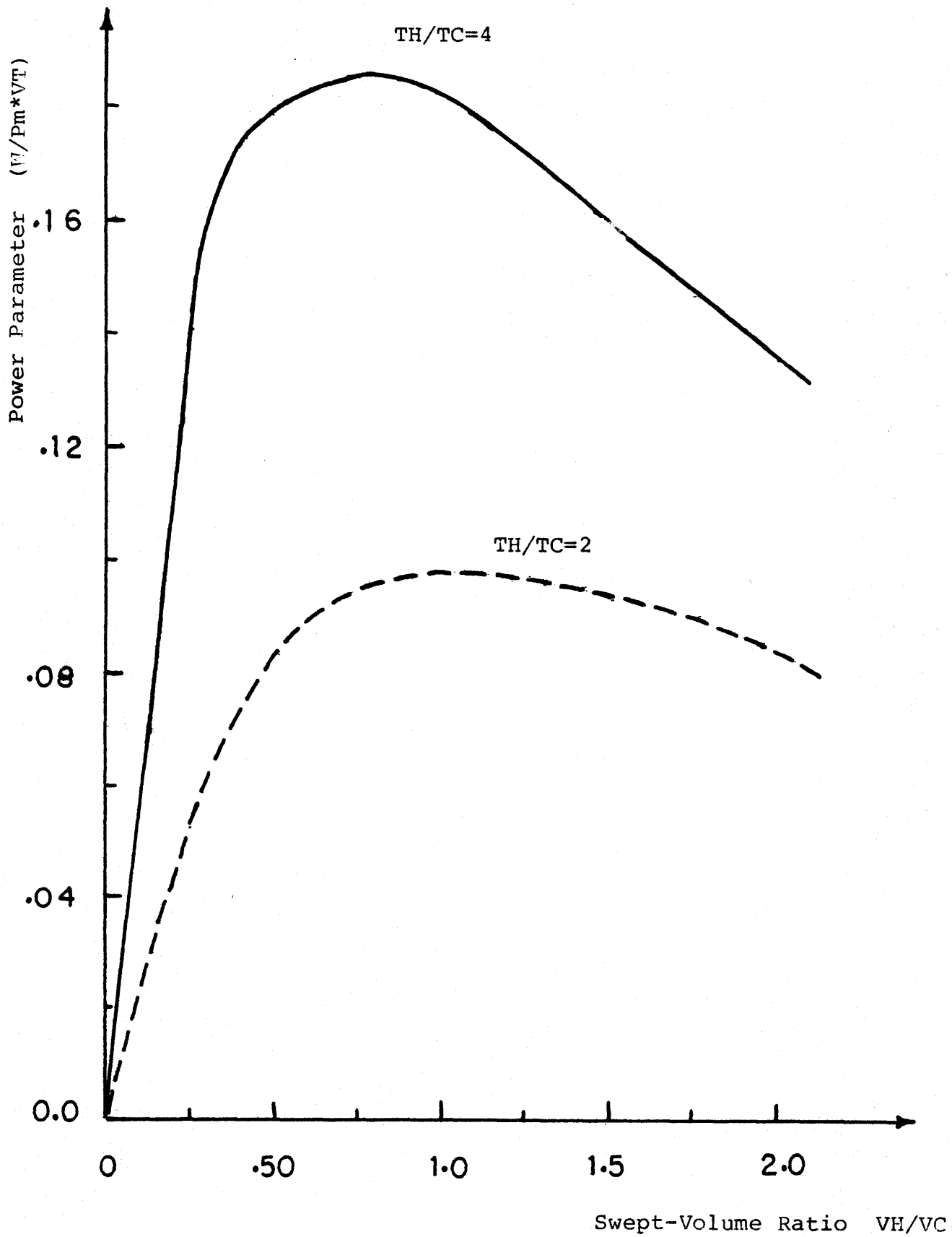

Fig.(13): Effect of Swept-Volume Ratio on Cycle Power
Walker's Results, Ref. [25]

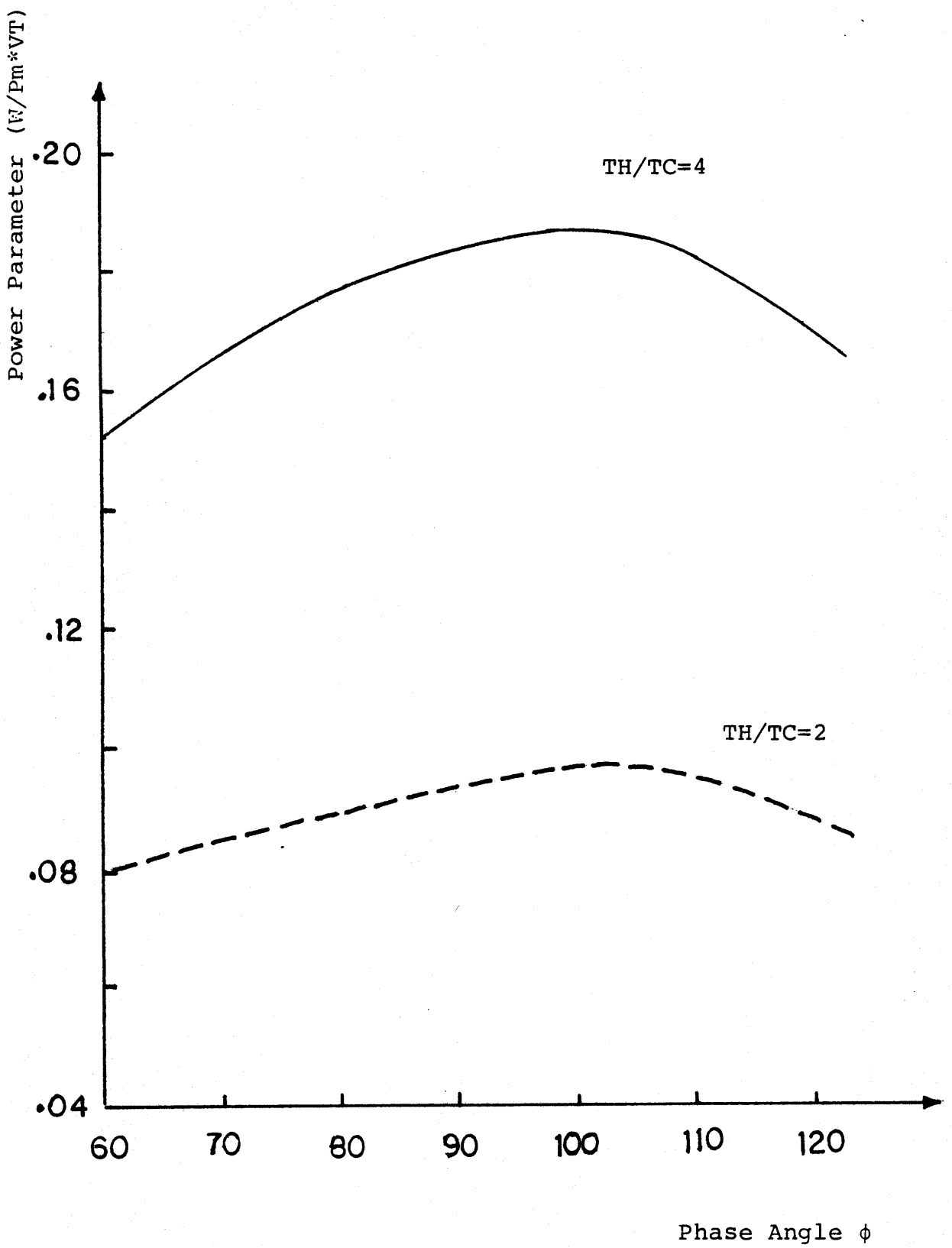

Fig.(14): Effect of Phase Angle (ϕ) on Cycle Power
Walker's Results, Ref. [25]

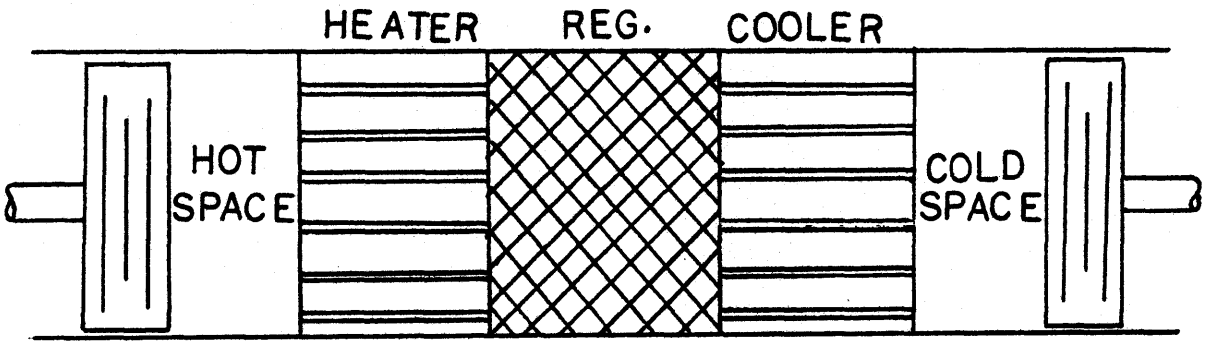

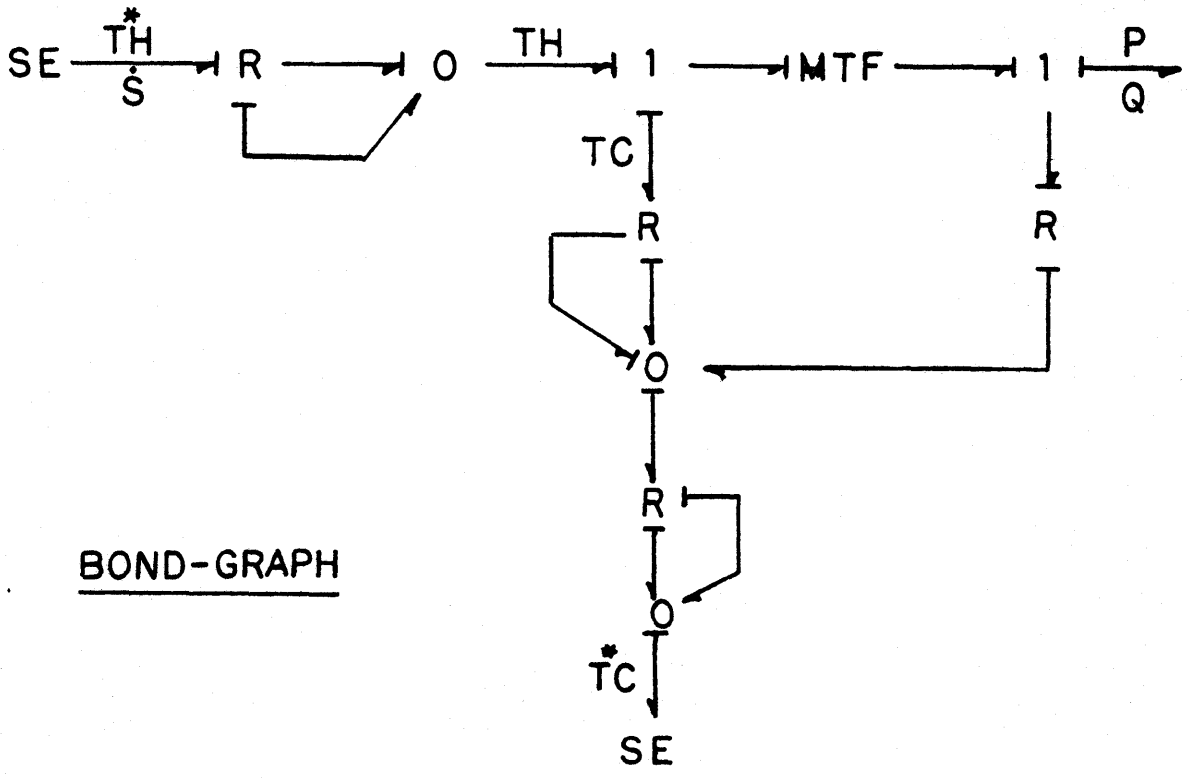

Fig.(15): Schematic Diagram of a Real Stirling Engine with Corresponding Bond Graph

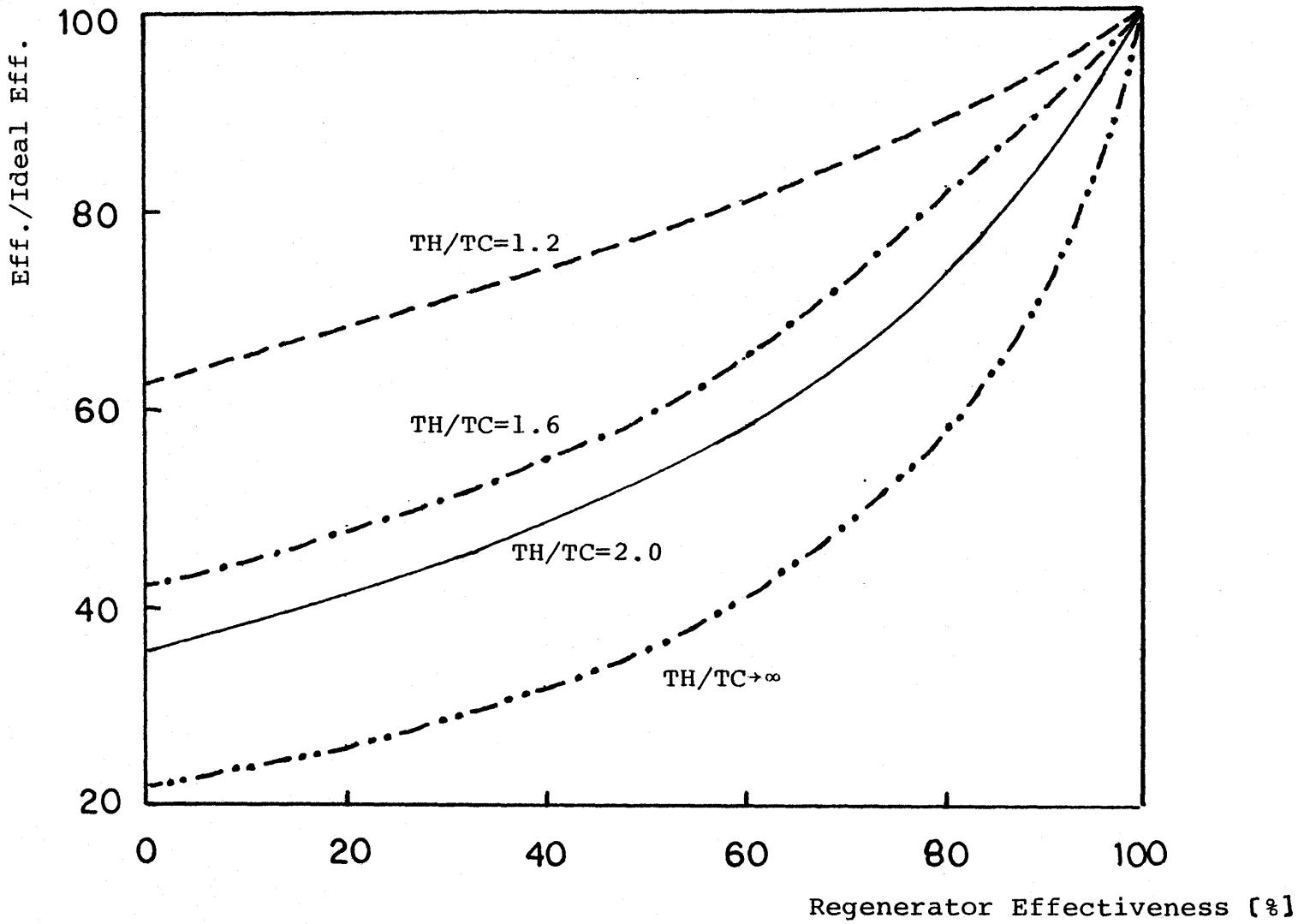

Fig.(16): Effect of Regenerator Effectiveness on Stirling Engine Efficiency, Table(4), Equation (E-16A)

Fig.(17): Variation of Stirling Engine Output with Dead Volume, Table (5), Equation (E-16b)

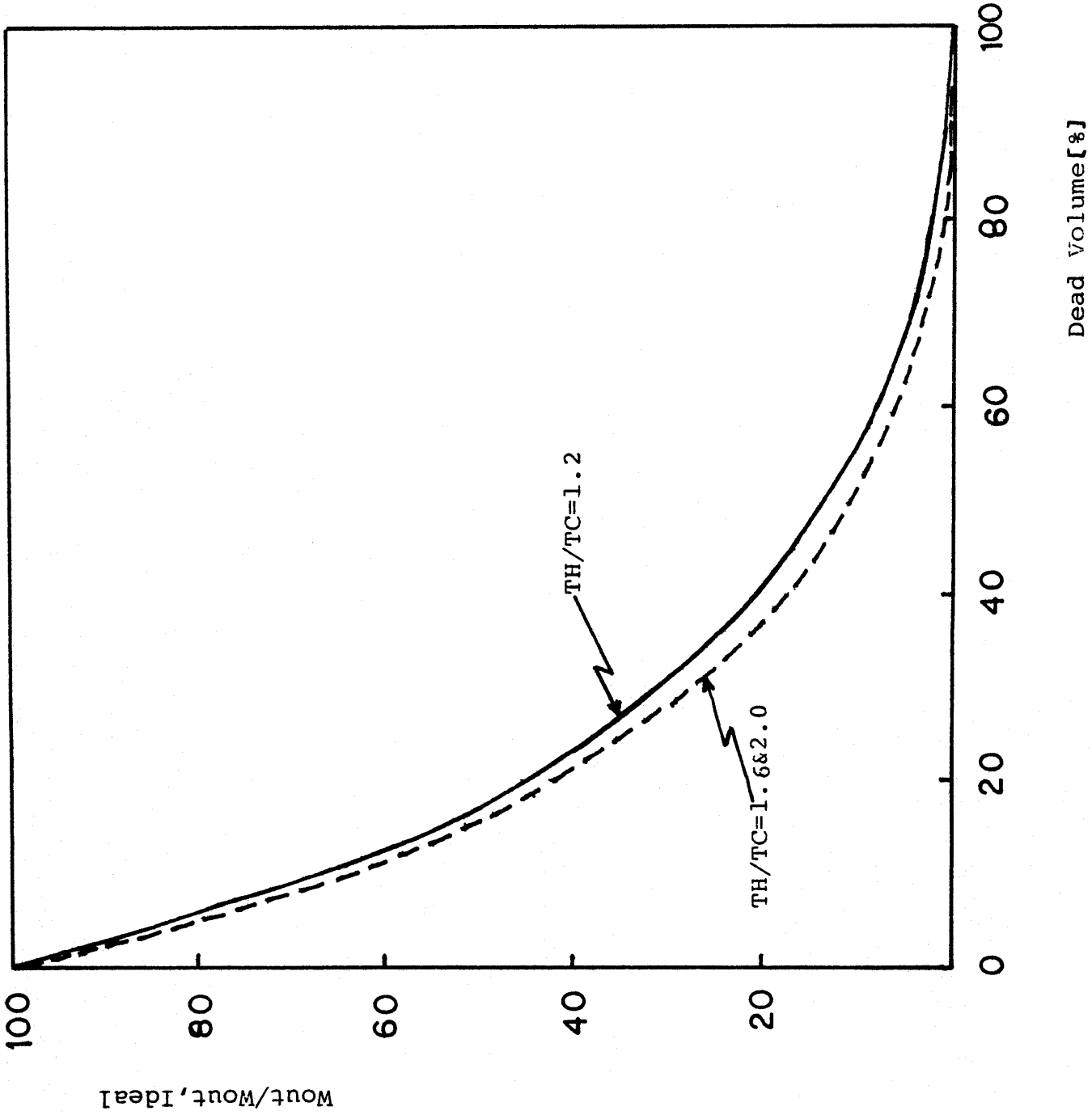

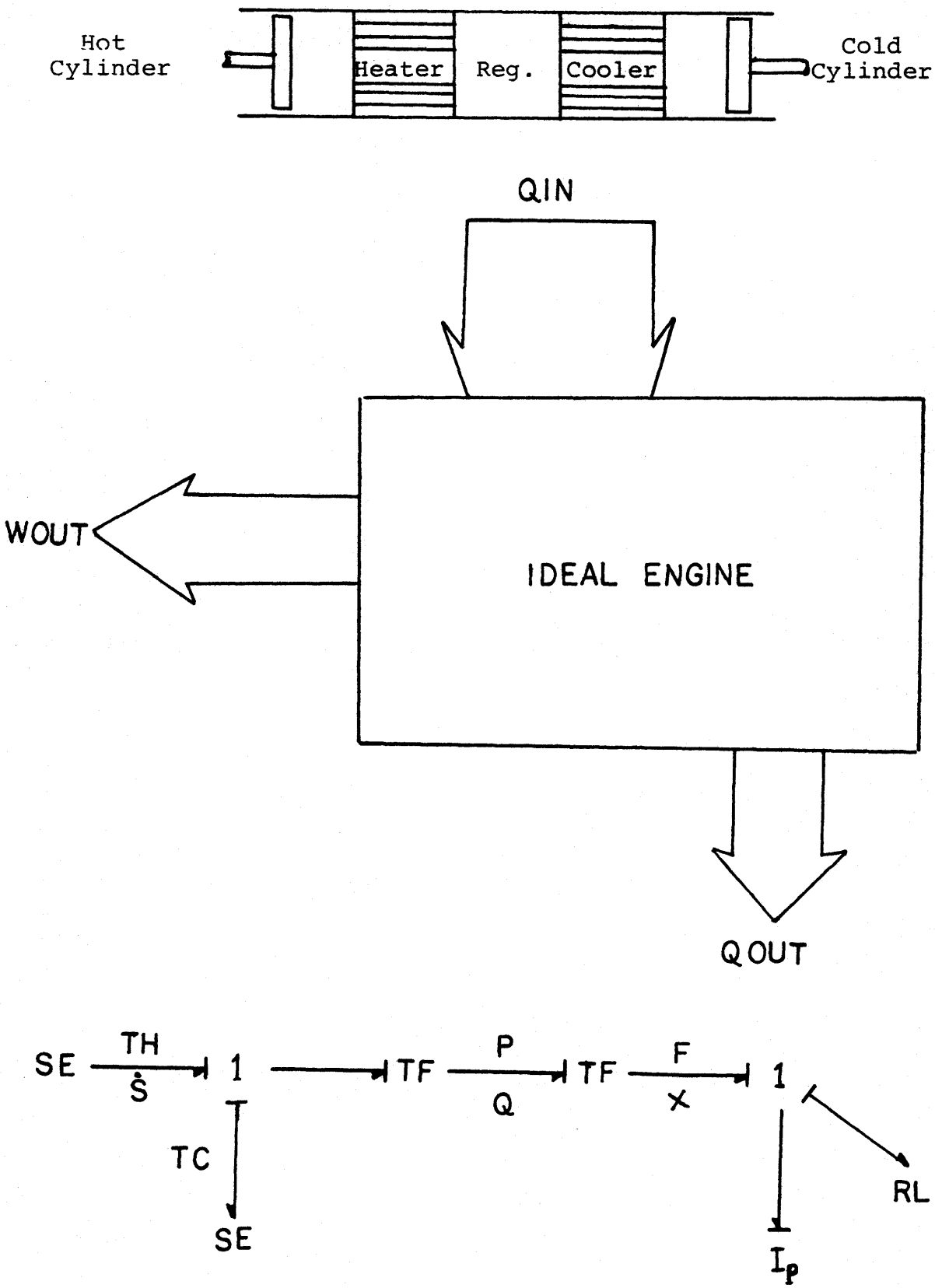

Fig.(18): Schematic Diagram and Energy Flow of Stirling Engine with Perfect Components and Corresponding Bond Graph.

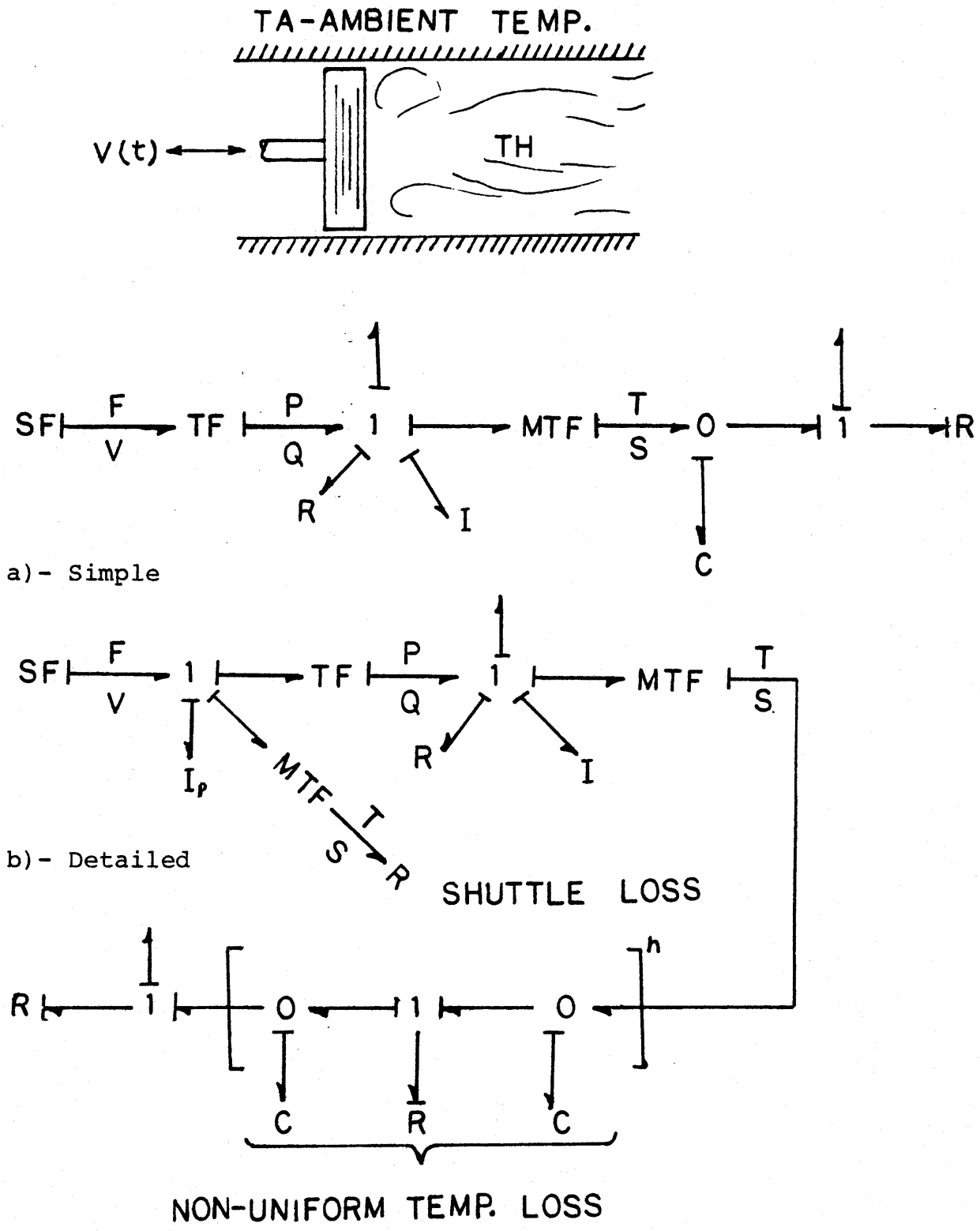

Fig.(19): Bond Graph of a Cylinder

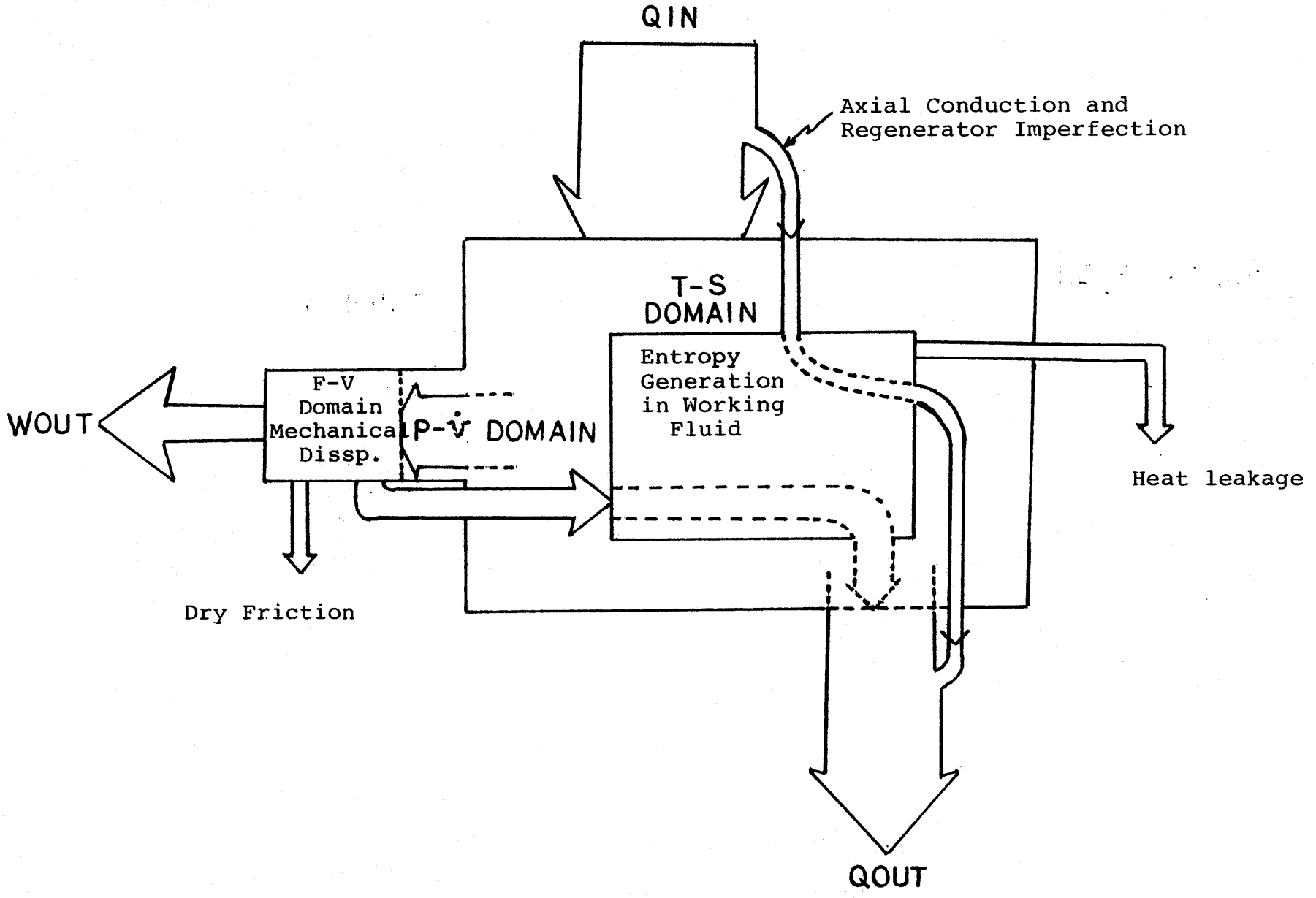

Fig.(20): Energy Flow of a Real Stirling Engine with Different Loss-Domain

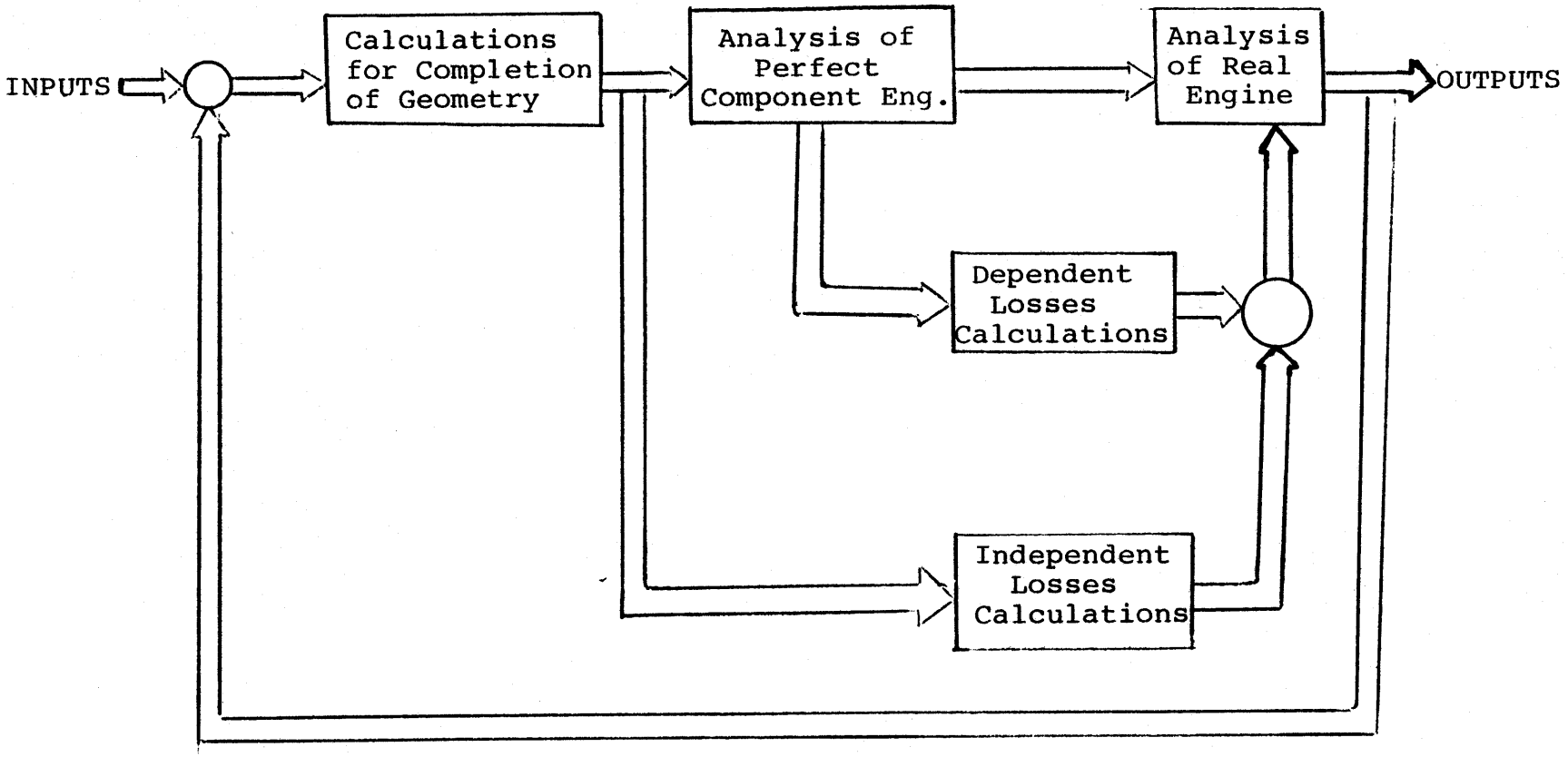

Fig.(21): Analysis of a Real Engine , Chapter II

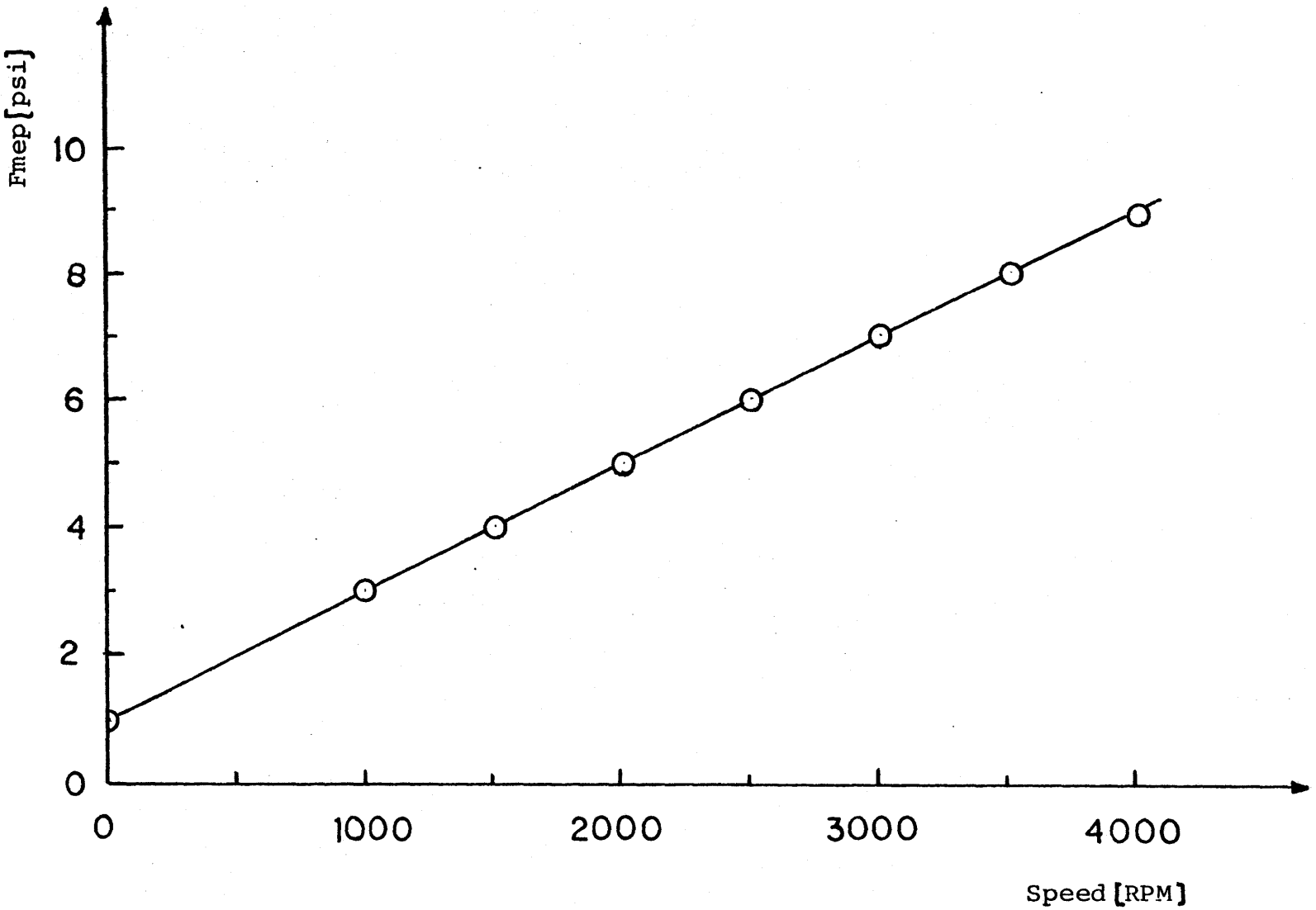

Fig.(22): Variation of Mechanical Friction Mean Effective Pressure (Fmep) with Engine Speed, Ref.[27]

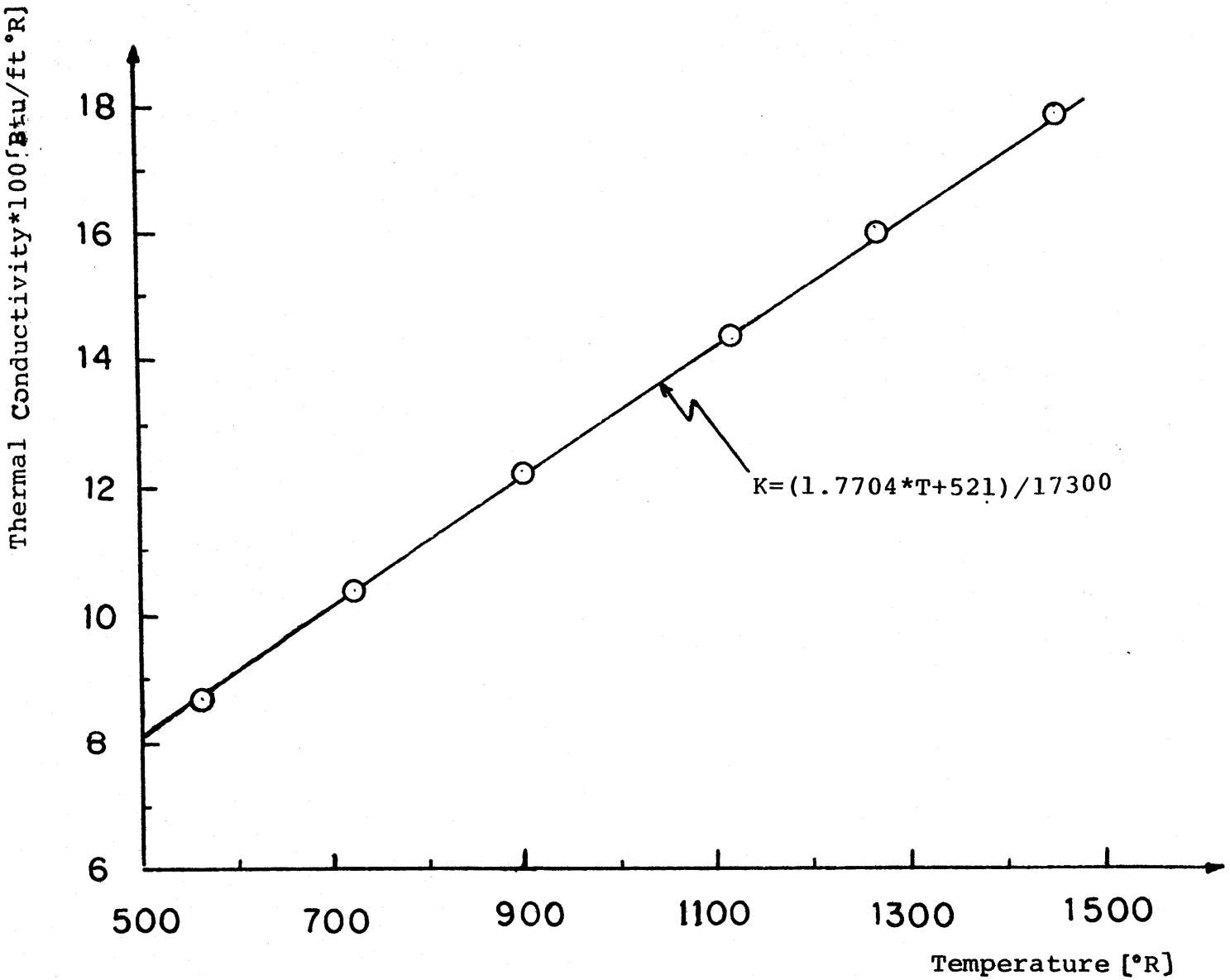

Fig.(23): Thermal Conductivity of Helium and Assigned Correlation Ref.[13]

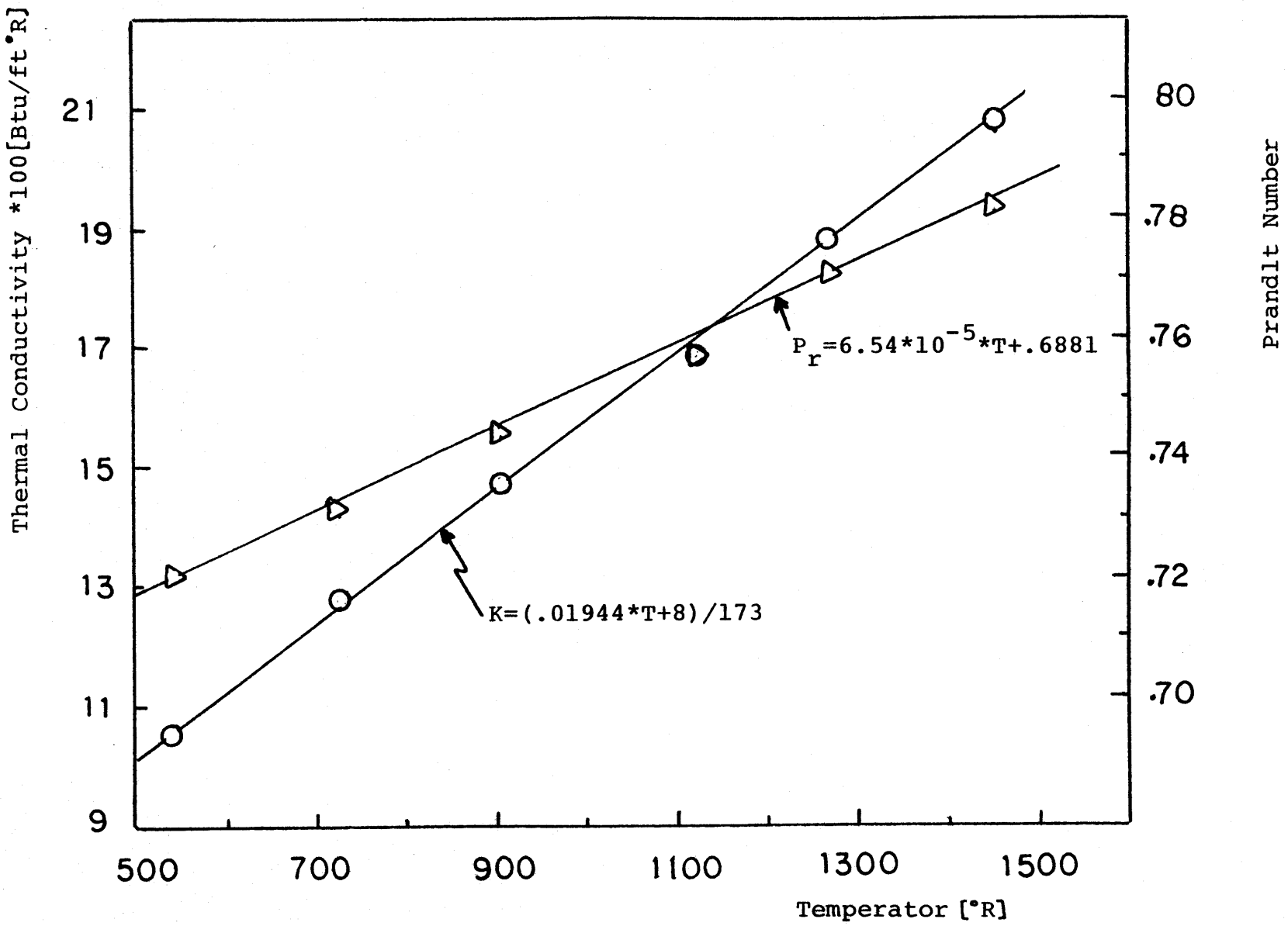

Fig.(24): Thermal Conductivity and Prandtl Number for Hydrogen and Assigned Correlations
Ref.[13]

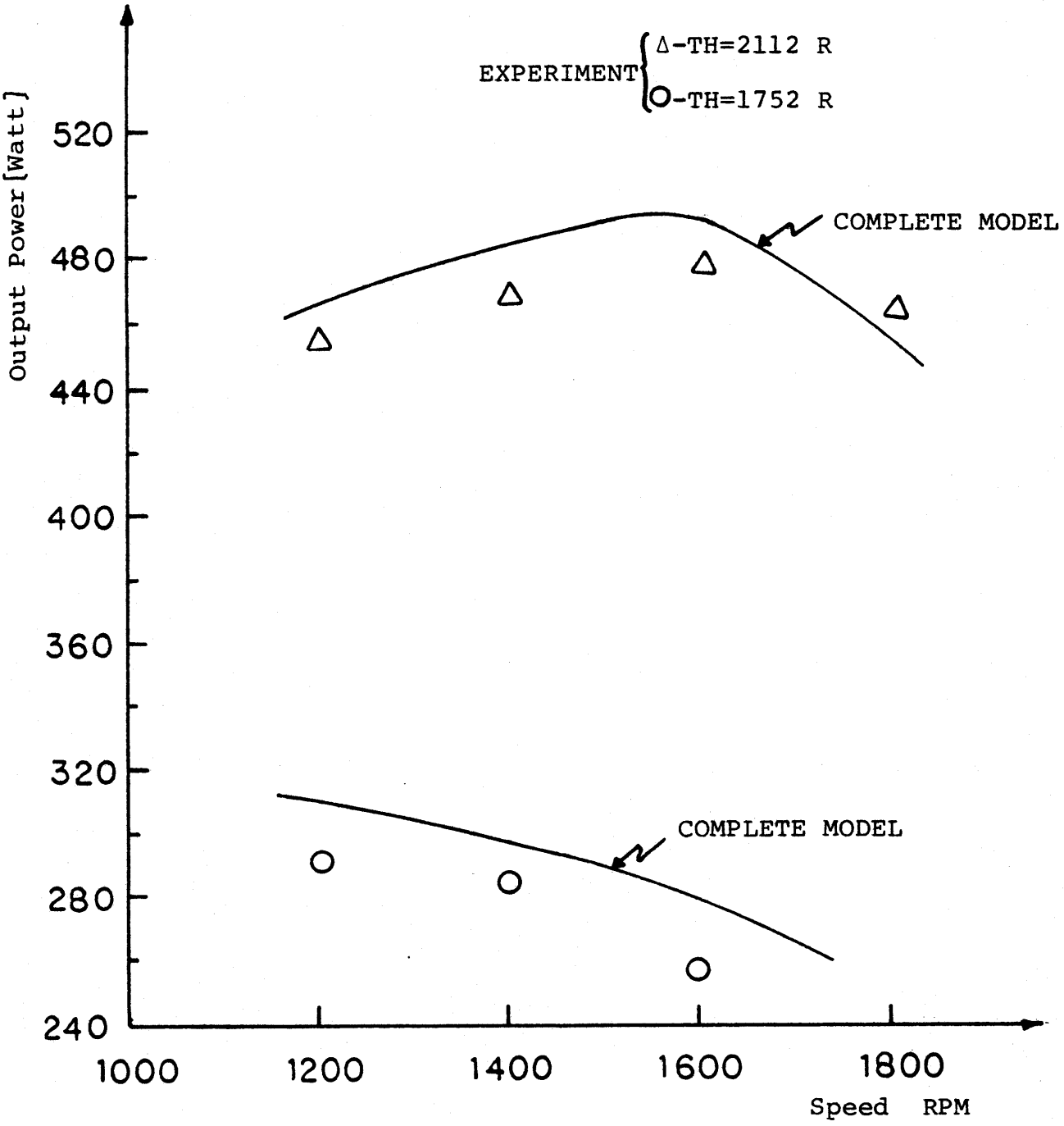

Fig.(25): Comparison of Philips Engine Output Power with Complete Model Predictions, Ref.[25] Table(6)

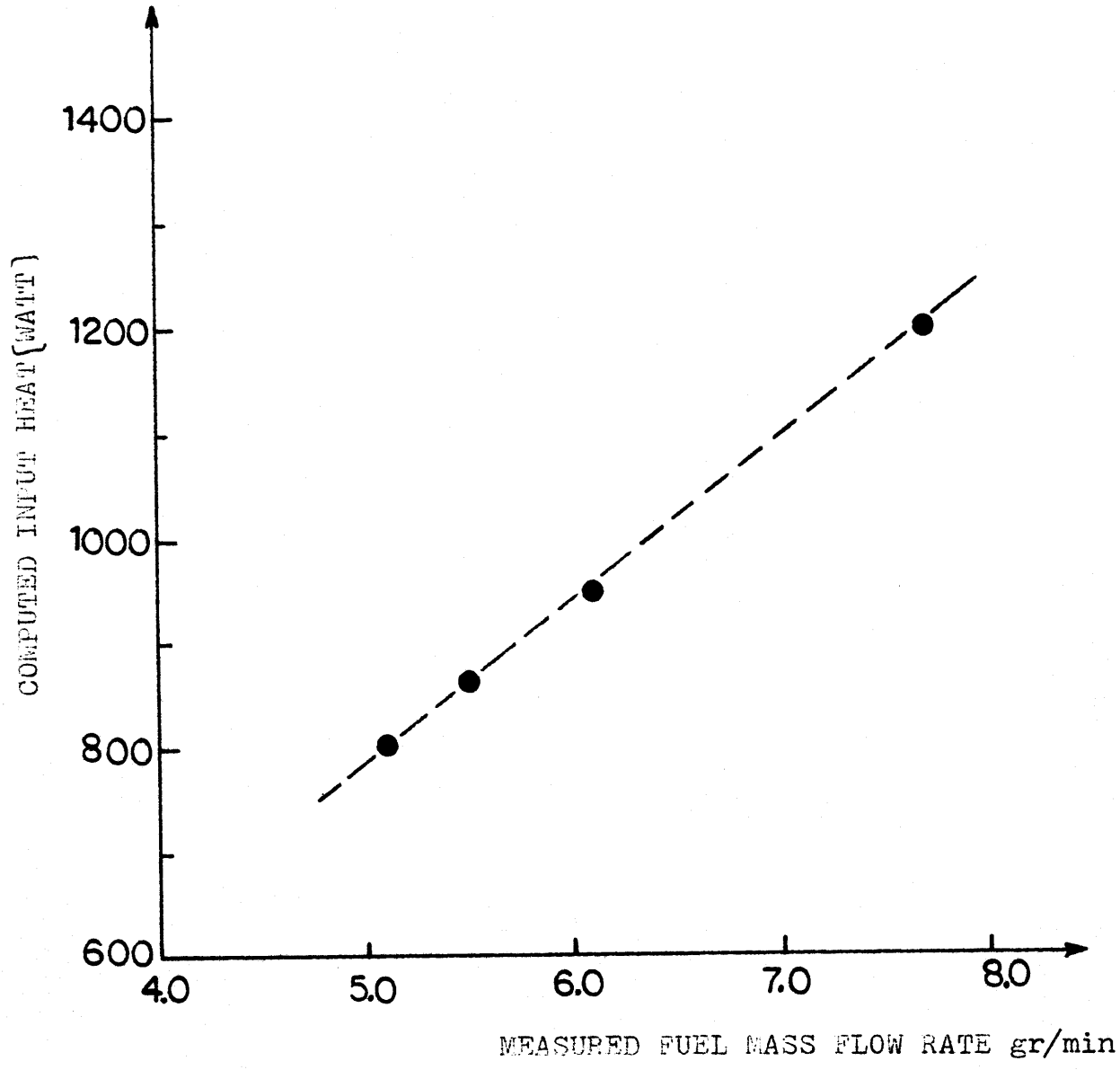

Fig. (26): Computed Input Heat by Complete Model Versus Measured Fuel Mass Flow Rate for Philips Engine. Ref.[25] , Table (6)

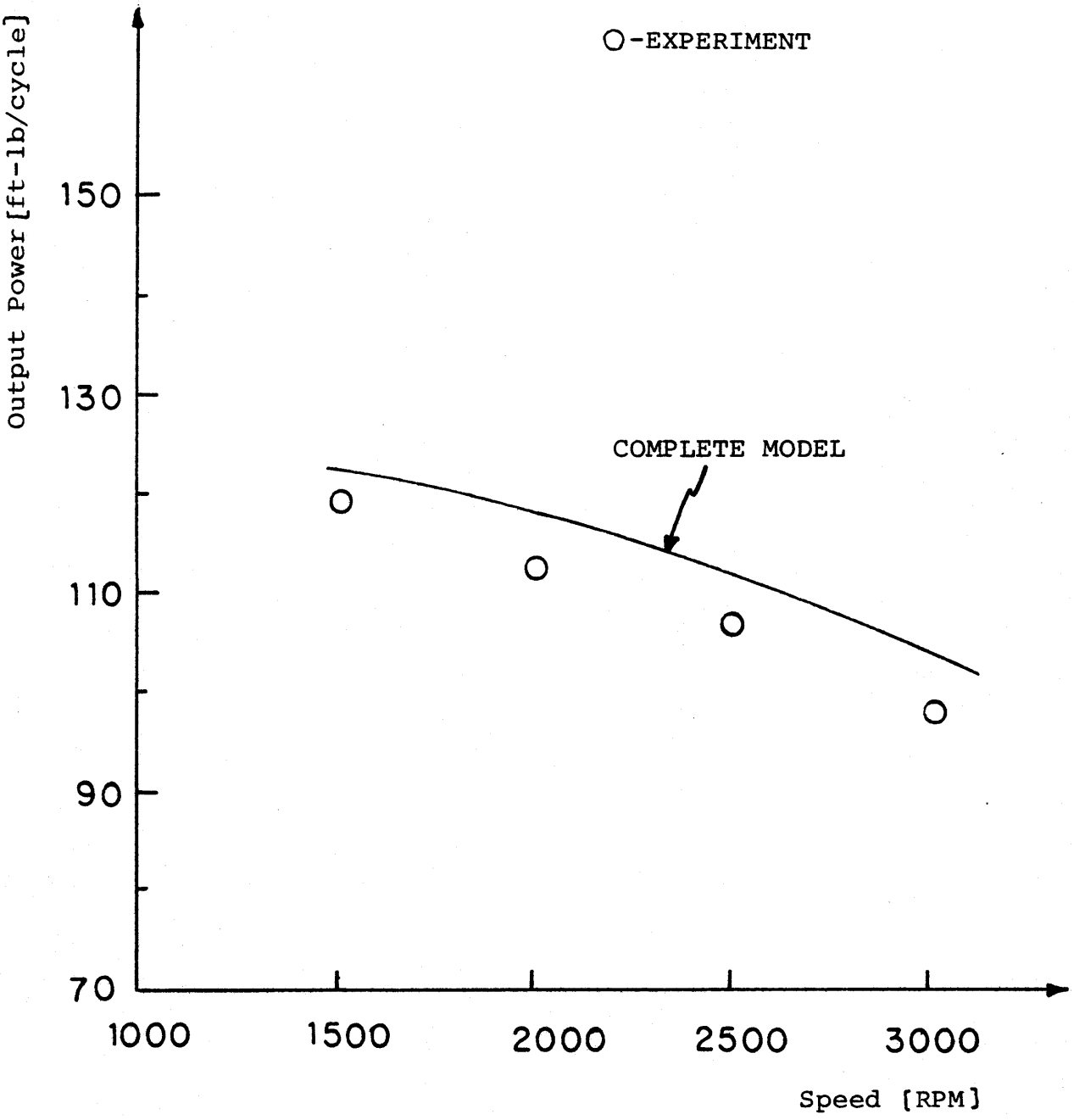

Fig.(27): Comparison of Allison Engine Output Power with Complete Model Predictions (ϕ=112), Ref.[18], Table (8)

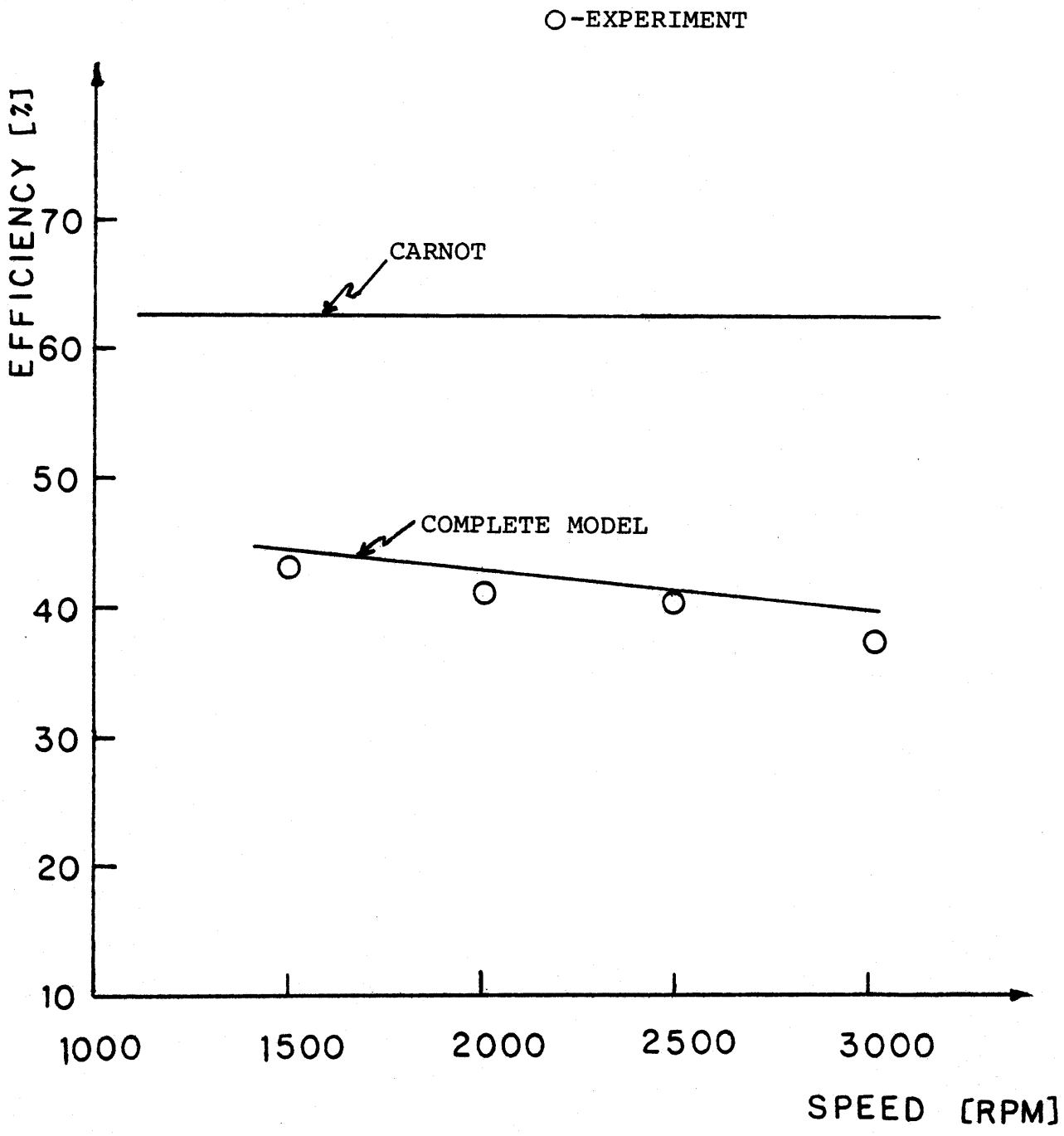

Fig.(28): Comparison of Allison Engine Efficiency with Complete Model Predictions (ϕ=112), Ref.[18], Table (8)

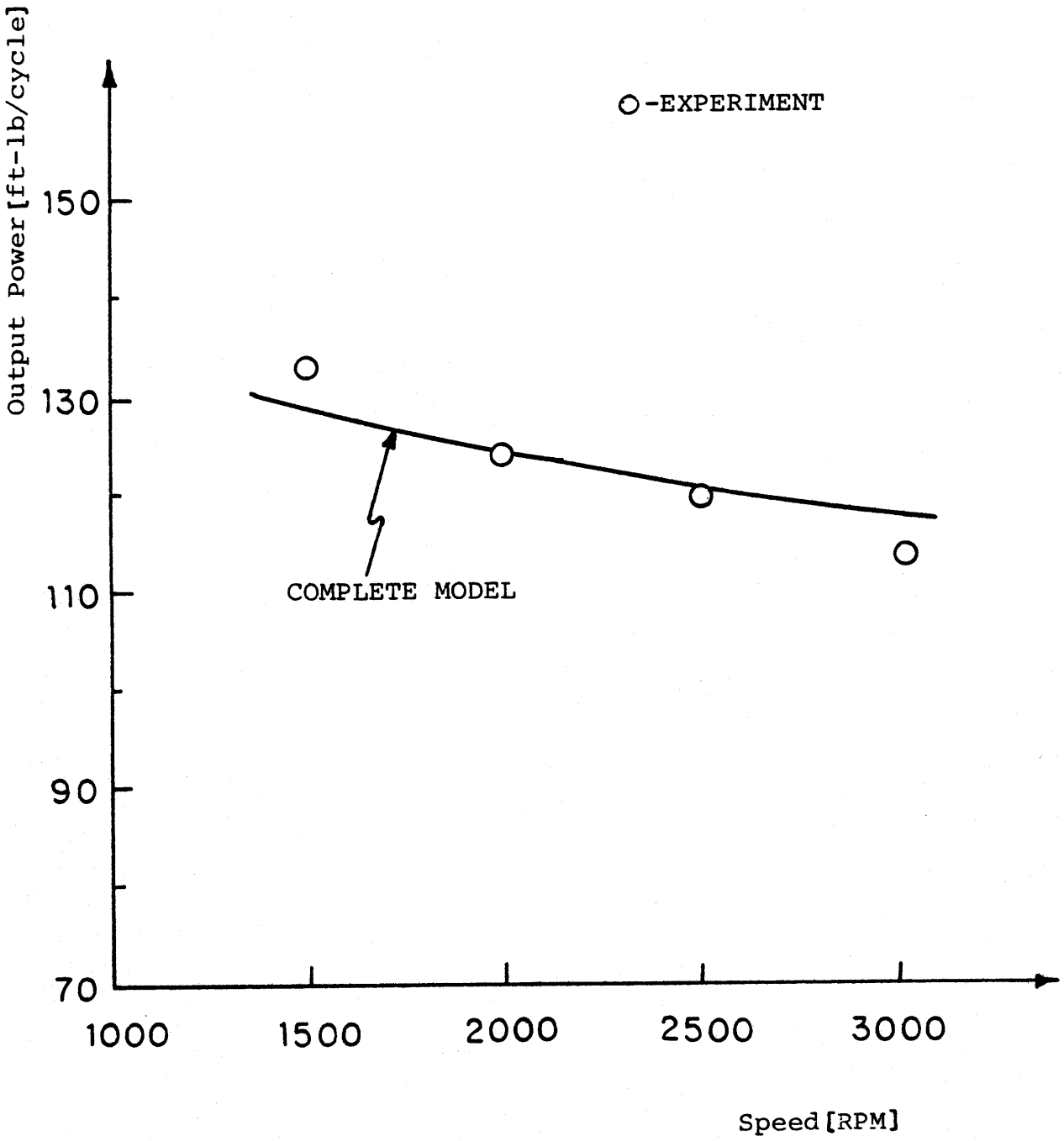

Fig.(29): Comparison of Allison Engine Output Power with Complete Model Predictions (ϕ=118), Ref.[18] Table (7)

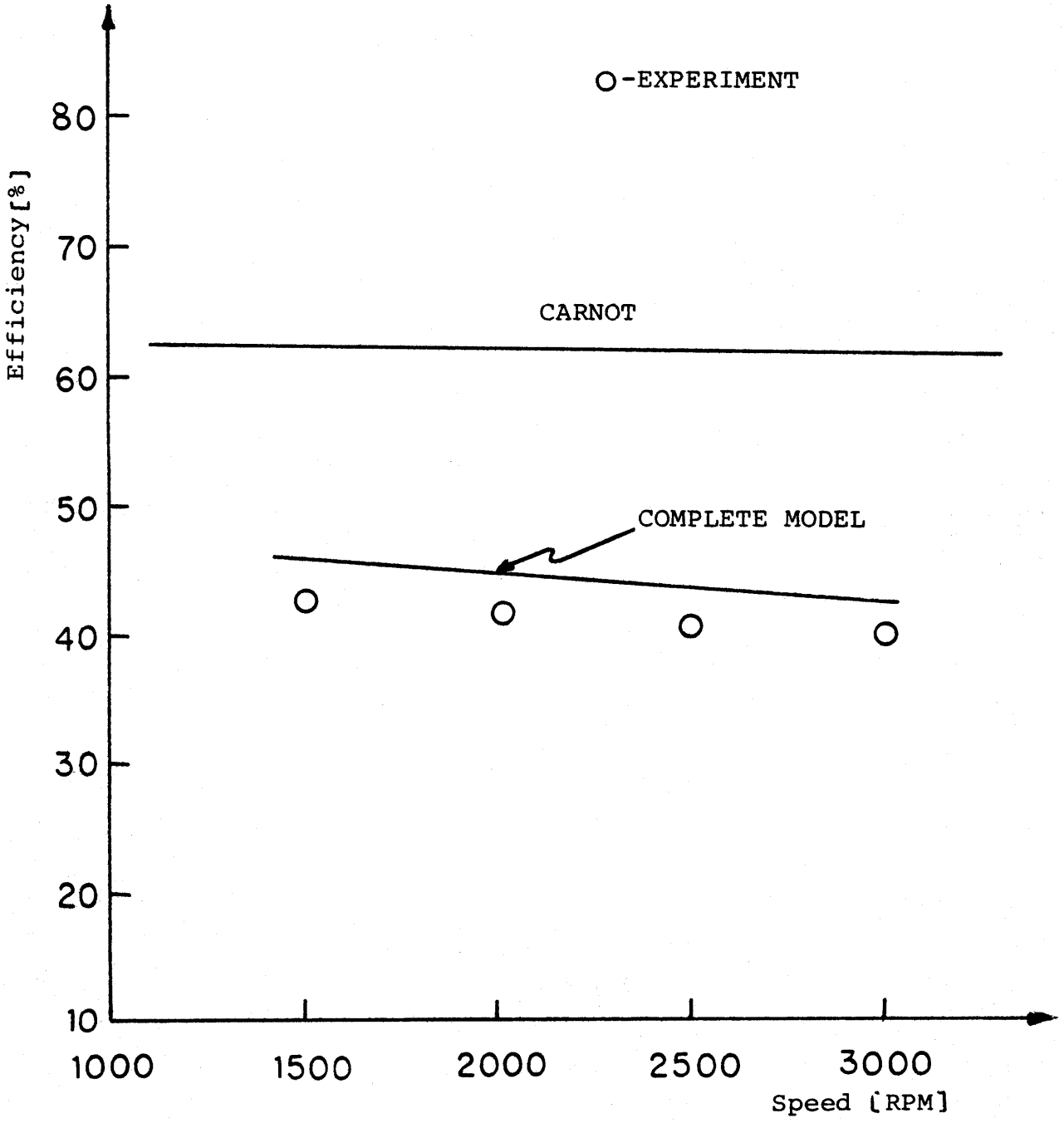

Fig.(30): Comparison of Allison Engine Efficiency with Complete Model Predictions (ϕ=118), Ref.[18], Table (7)

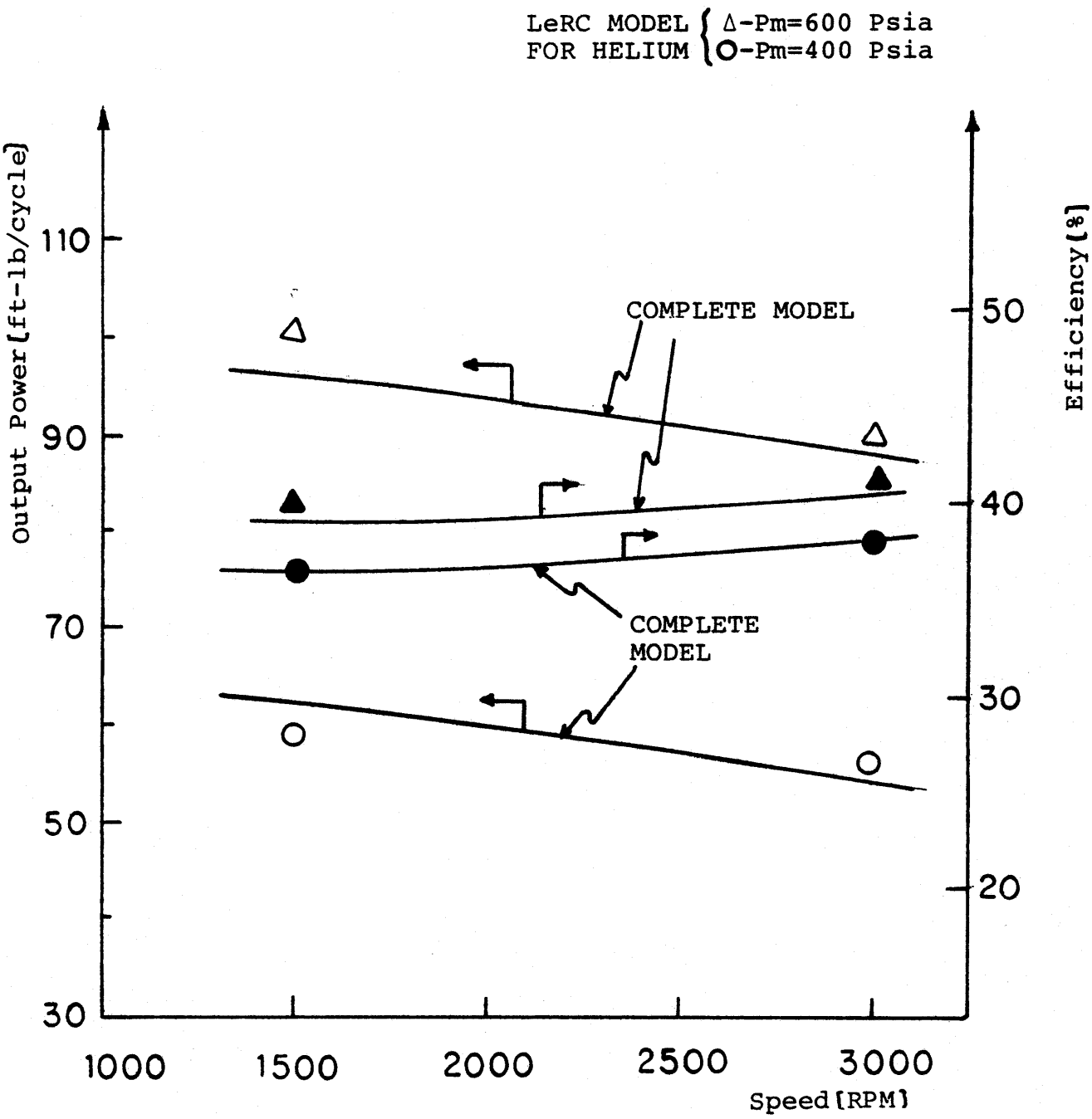

Fig.(31): Comparison of LeRC Model and Complete Model Predictions for GPU-3(He) Ref.(3), Table (10)

Note: Different Points Have Different Engine Geometries

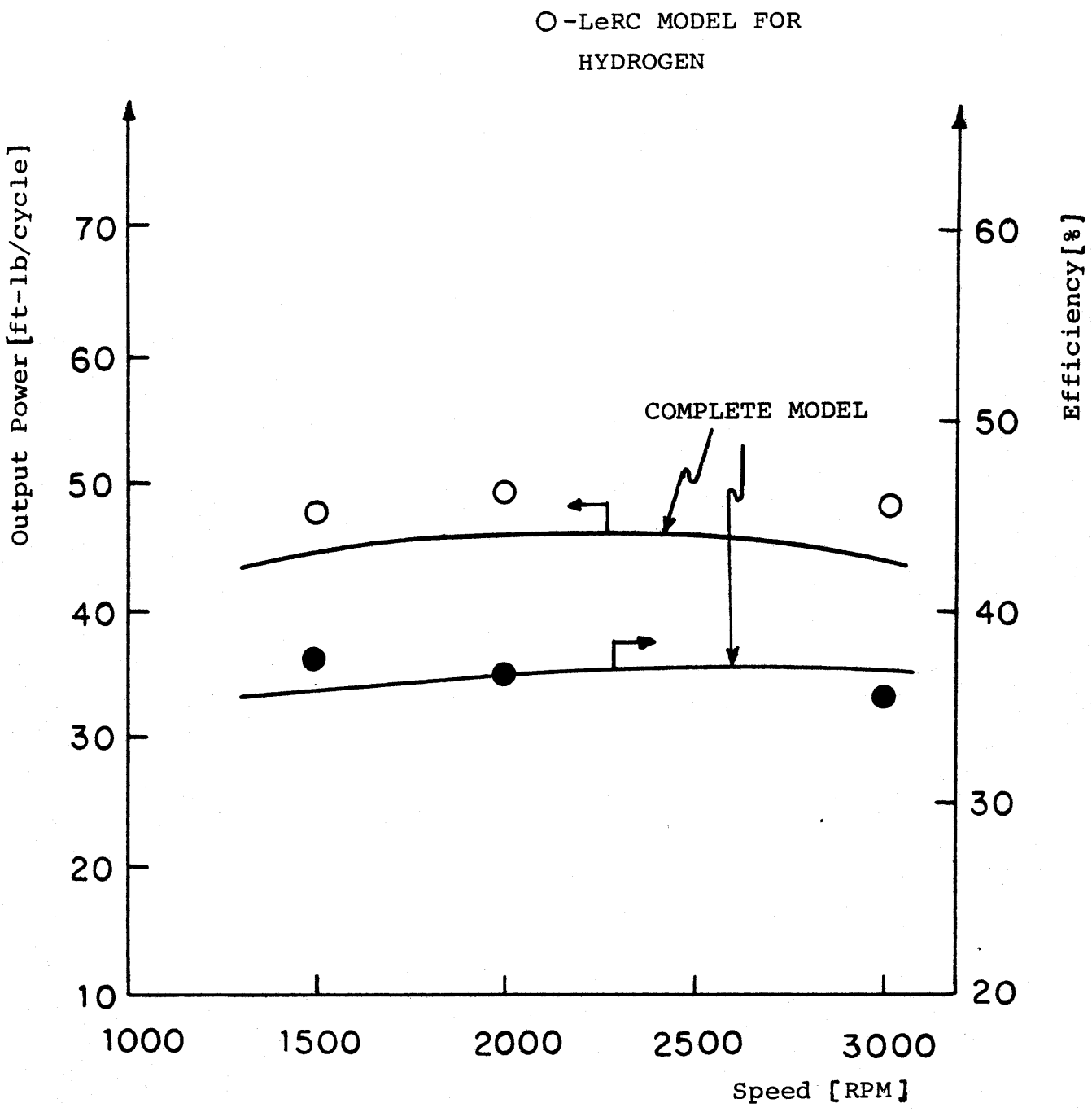

Fig.(32): Comparison of LeRC Model and Complete Model Predictions for GPU-3 (H_2), Ref.[13], Table (9)

Note: Different Points Have Different Engine Geometries

Fig.(33): Variation of Error between Schmidt & Complete Model Outputs with Temperature-Ratio Simplified Model, Equation (3-4)

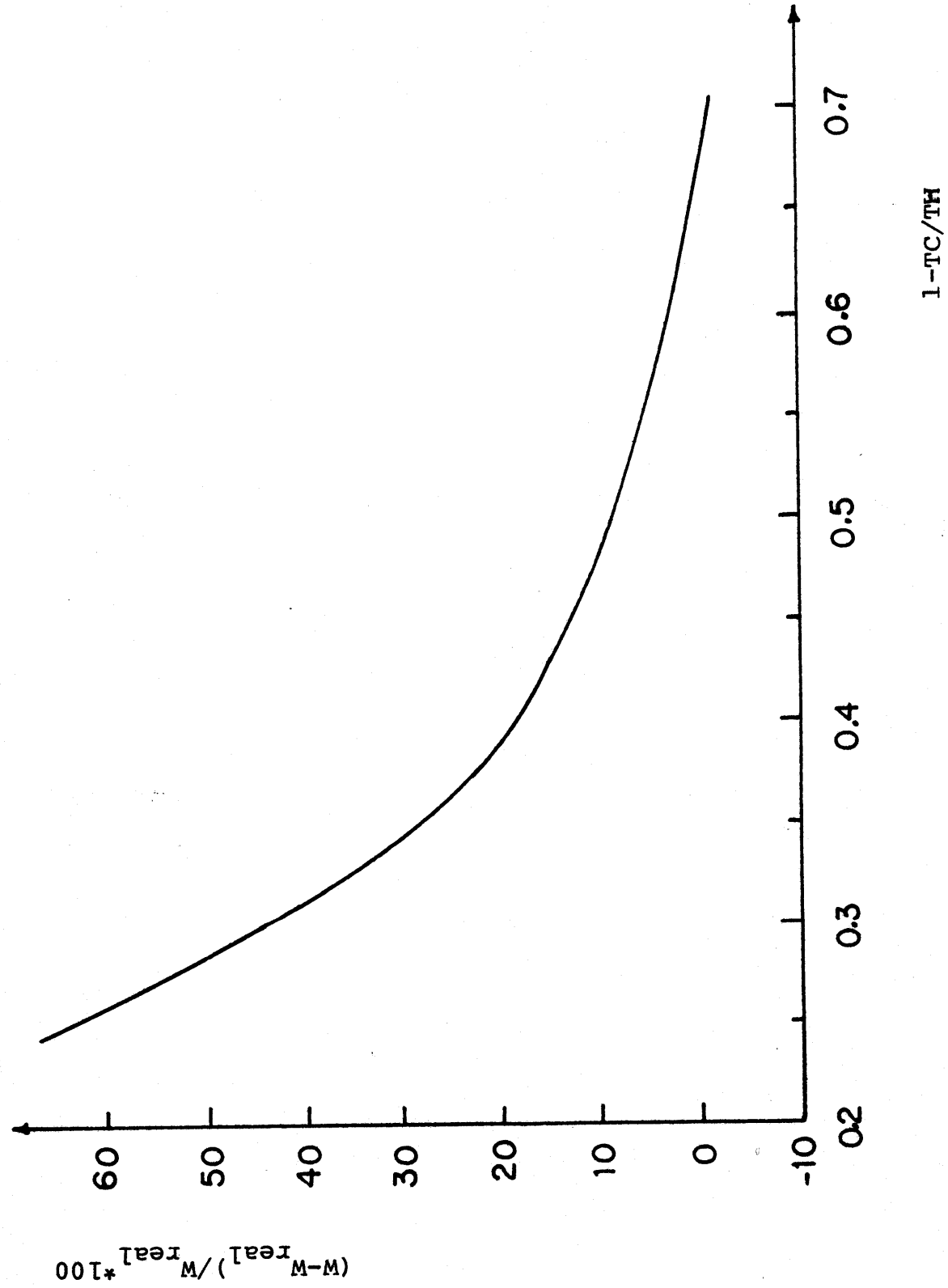

Fig.(34): Variation of Error between Schmidt and Complete Model Outputs with Phase Angle
Simplified Model, Equation (3-6)

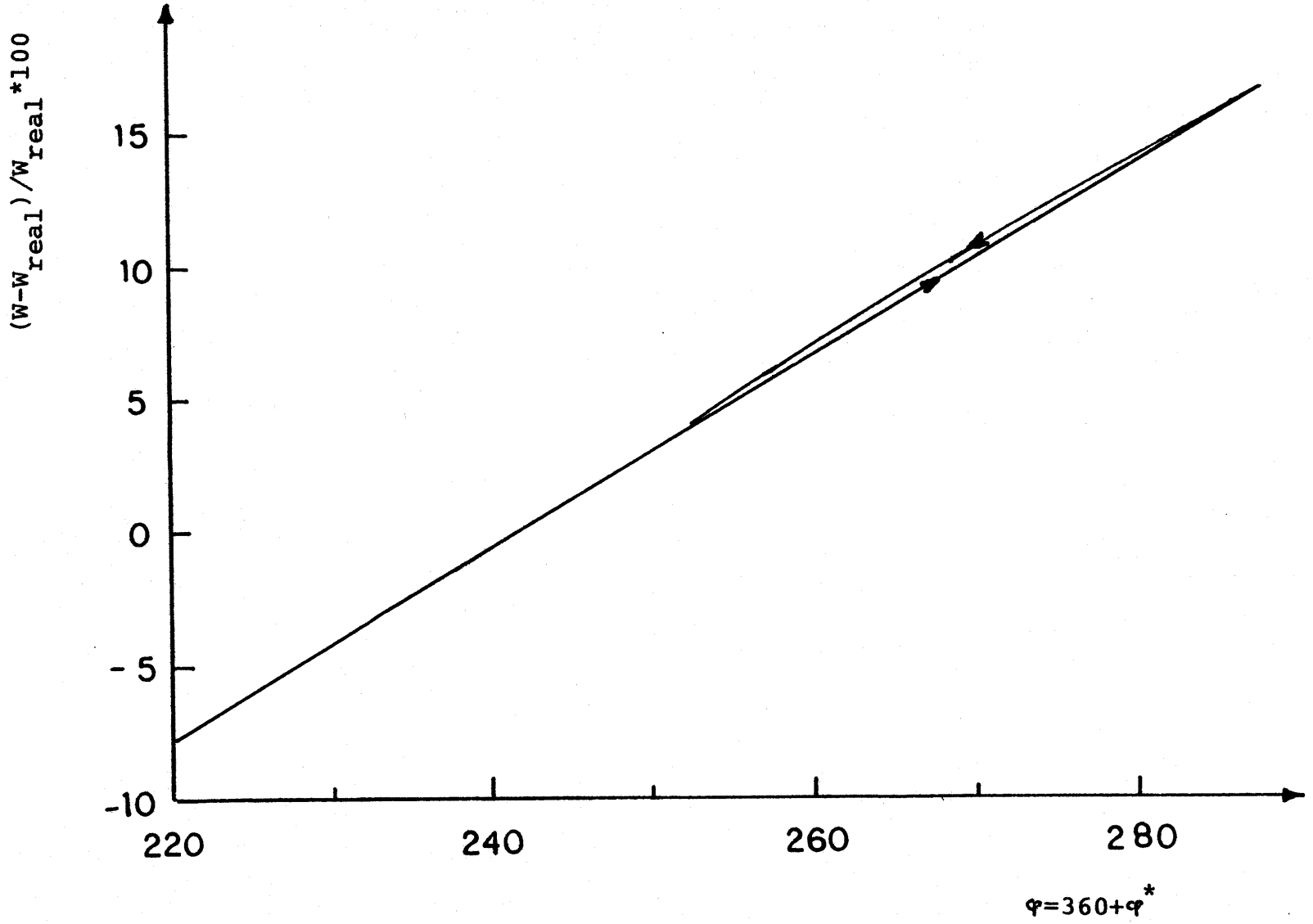

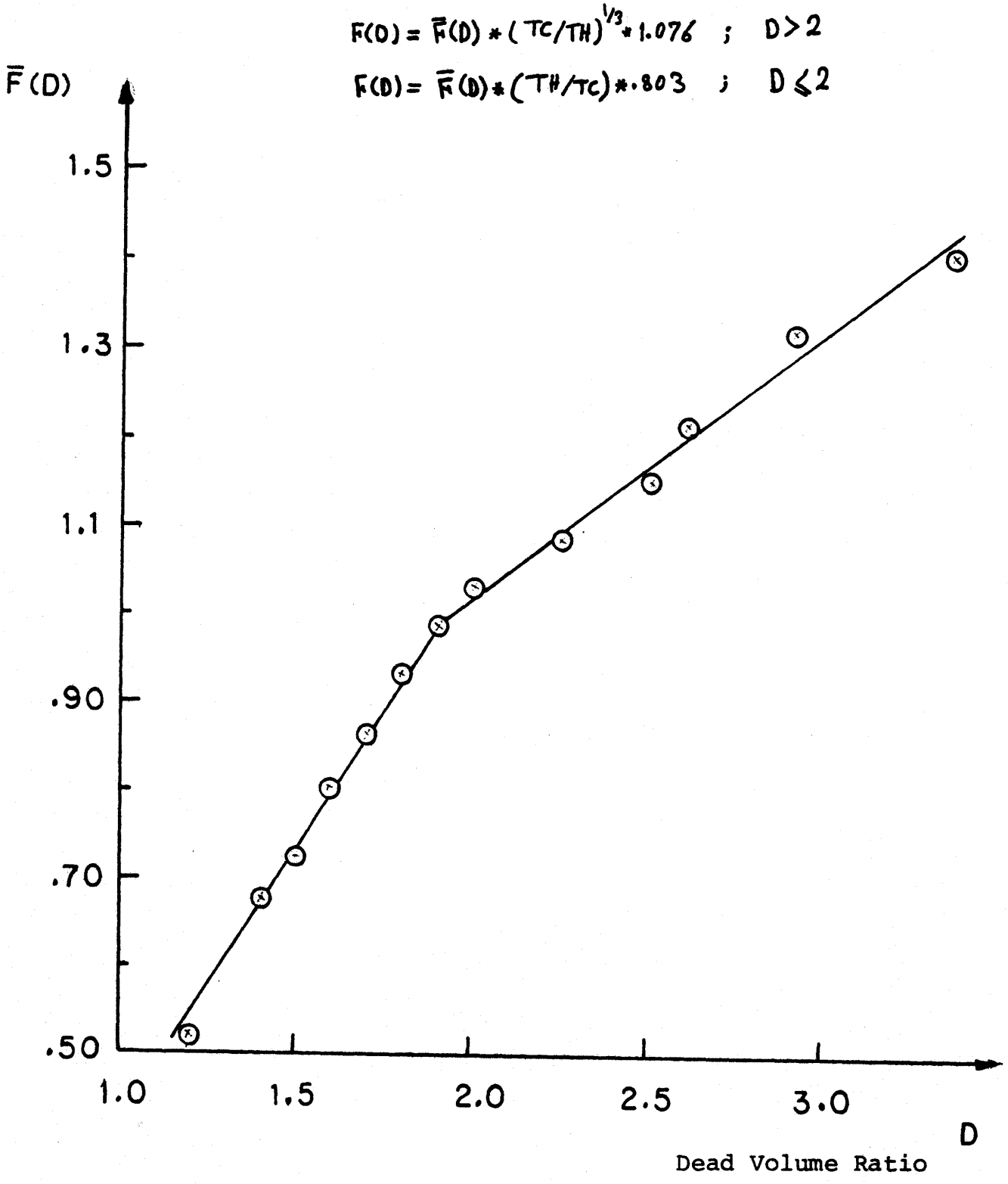

Fig.(35): Dead Volume Correction Factor for Schmidt Equation (TH/TC<1.5), Simplified Model , Equation (3-7A)

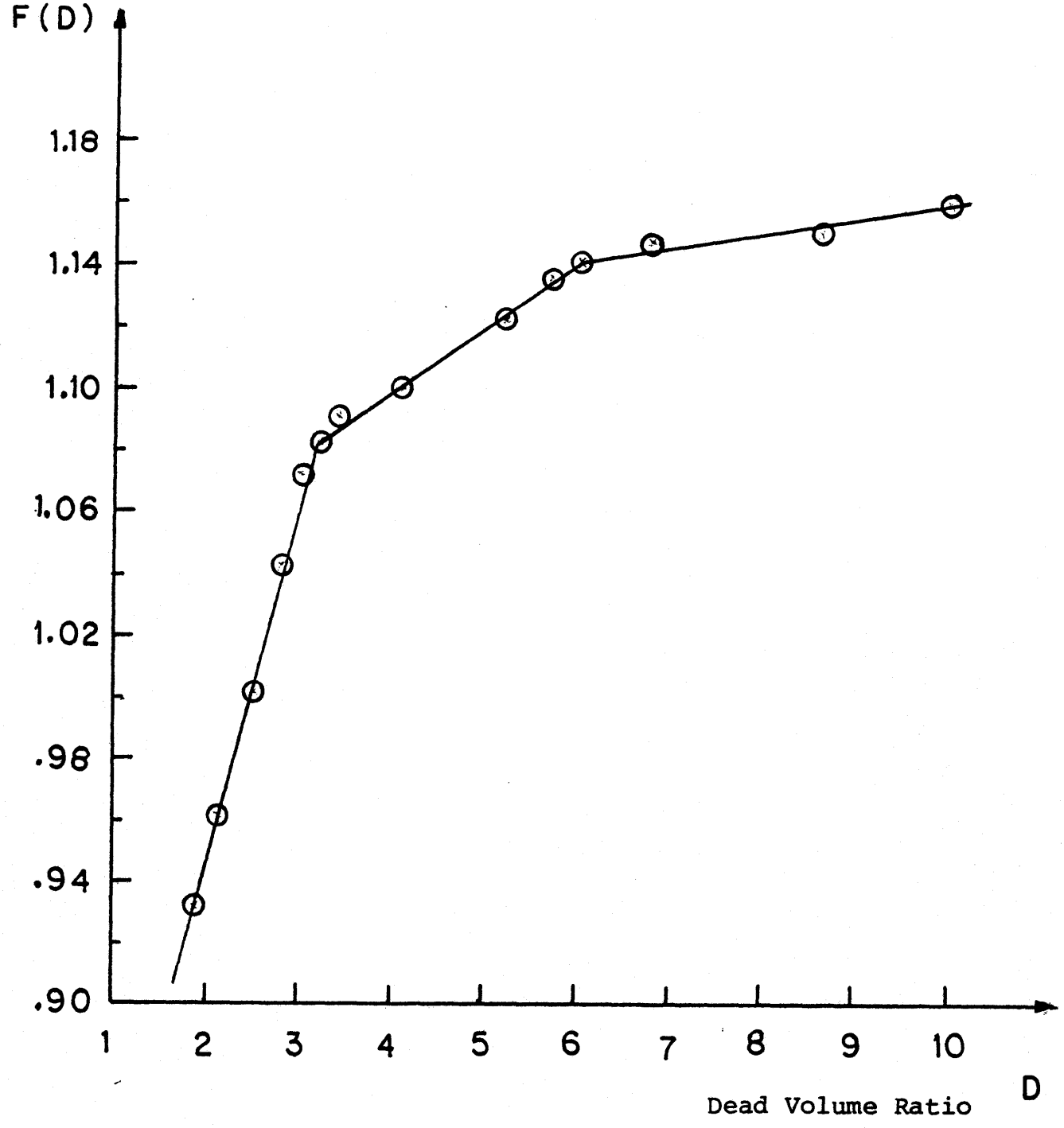

Fig.(36): Dead Volume Correction Factor for Schmidt Equation (TH/TC≥1.5)
Simplified Model , Equation (3-7B)

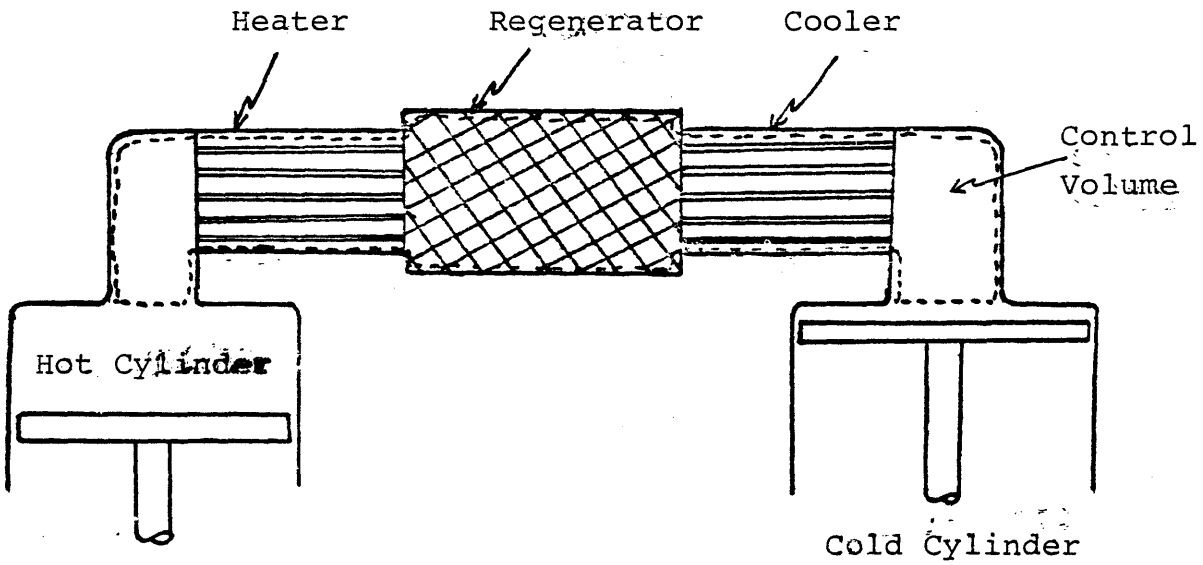

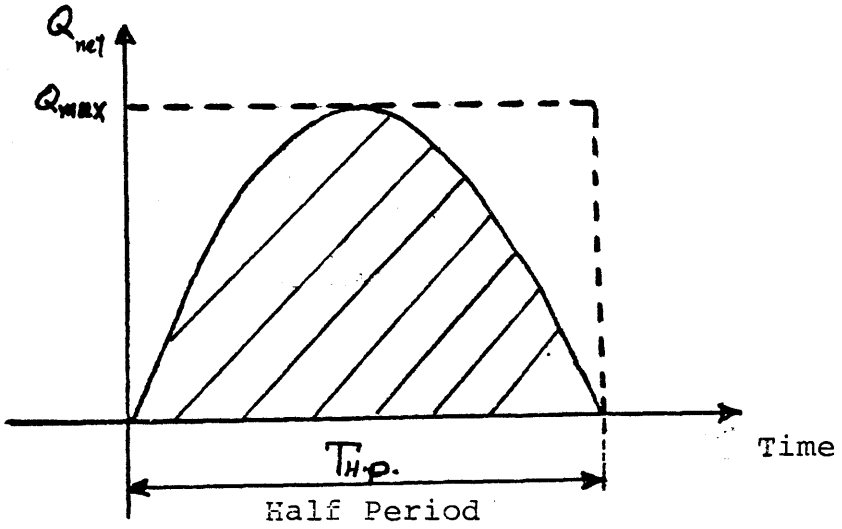

Fig.(37): General Configuration of a Real Stirling Engine

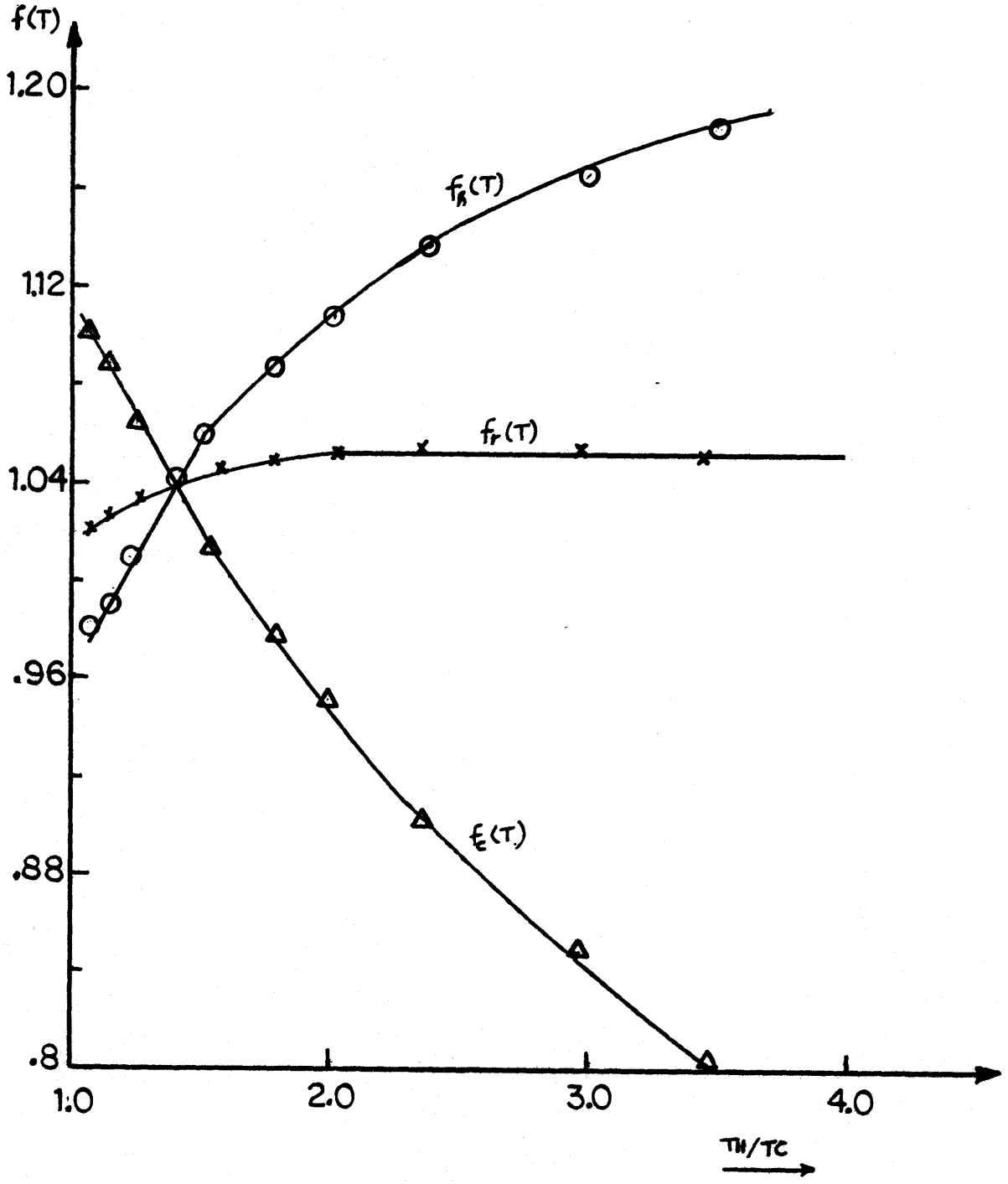

Fig.(38): Temperature Correction Factors for Mass Flow Rates in Heater, Cooler, and Regenerator Simplified Model, Equations (3-21) to (3-23)

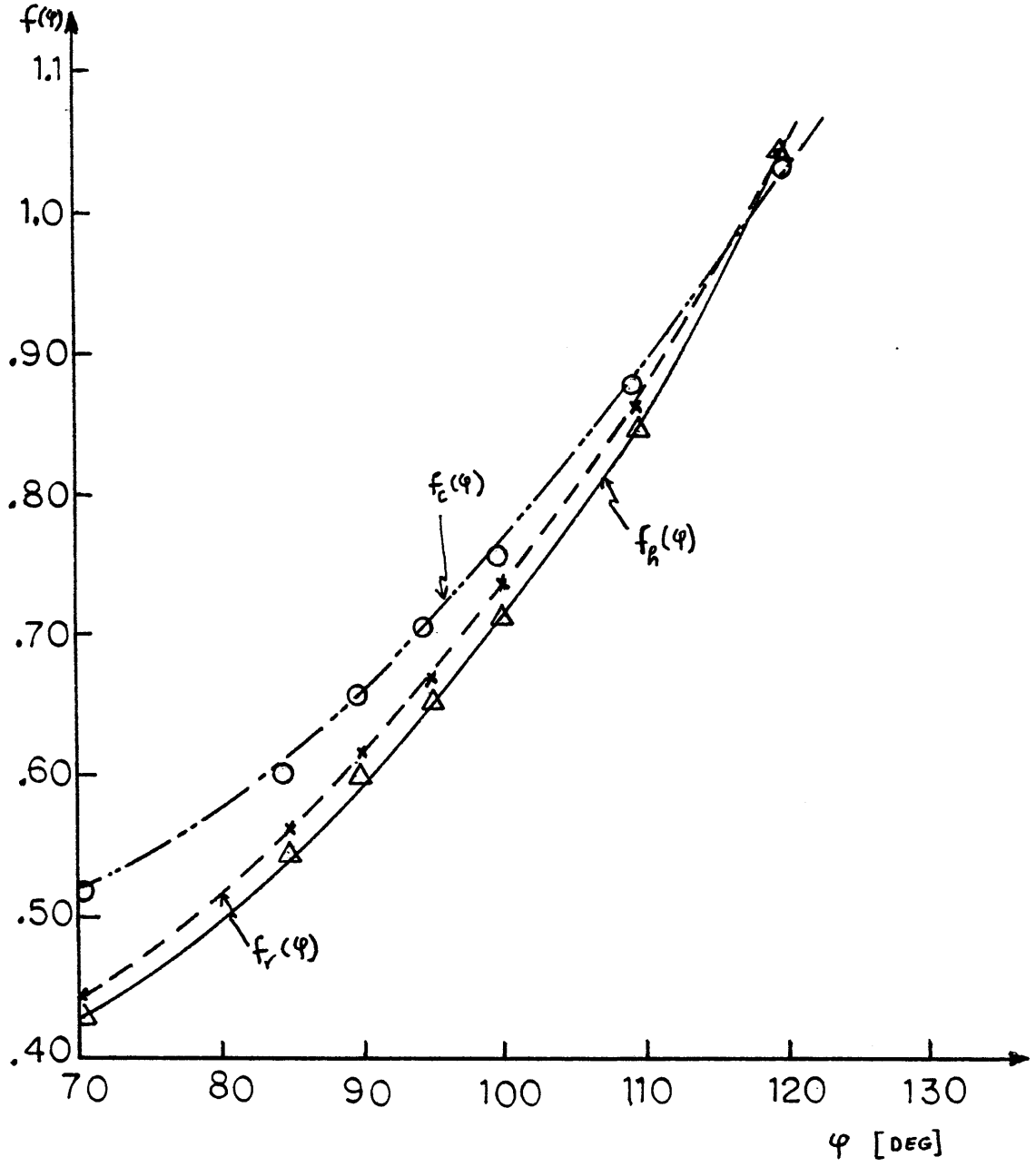

Fig.(39): Phase Angle Correction Factors for Mass Flow Rates in Heater, Cooler, and Regenerator Simplified Model, Equations (3-24) to (3-26)

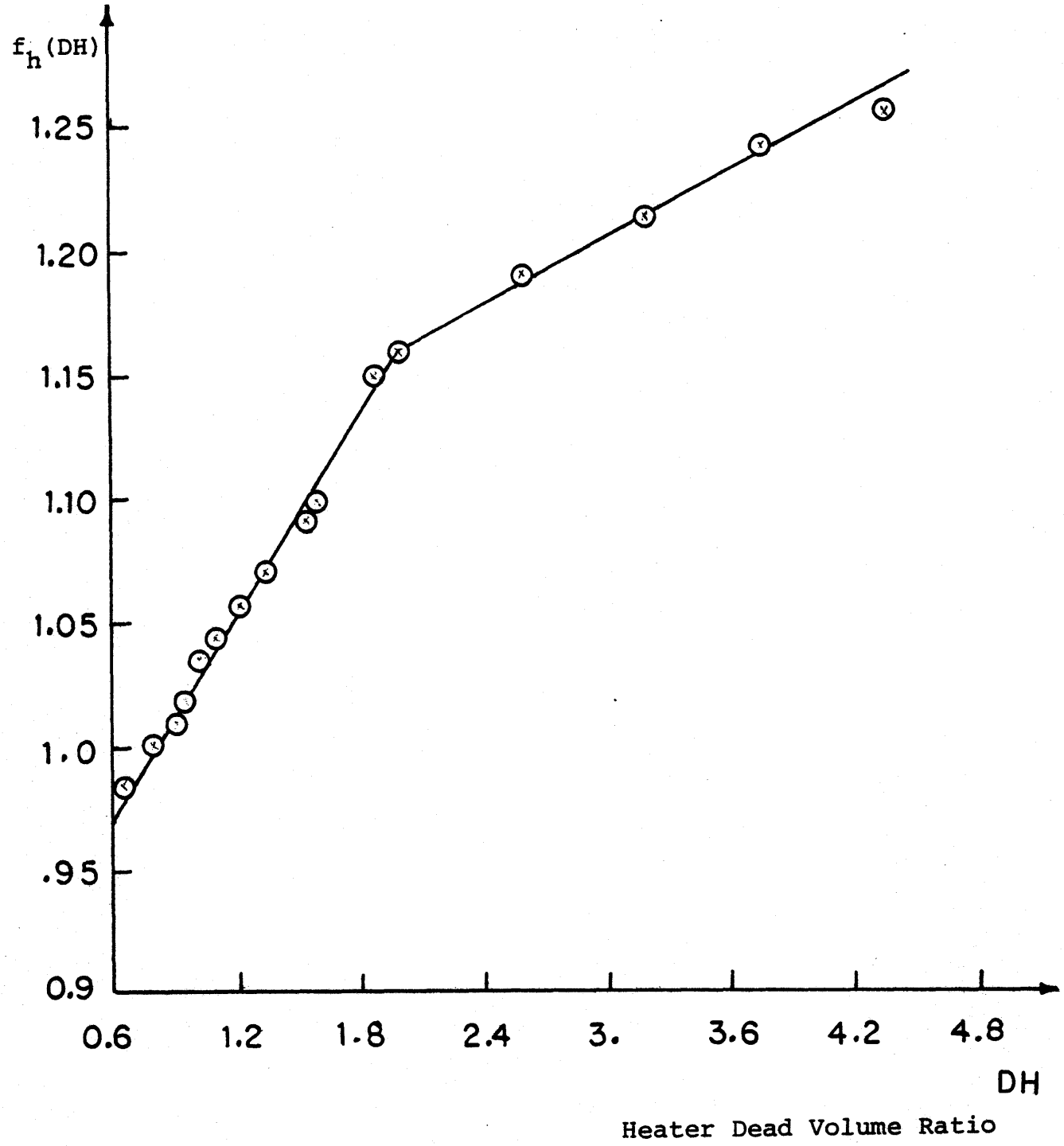

Fig.(40): Dead Volume Correction Factor for Mass Flow Rate in Heater
Simplified Model, Equation (3-27)

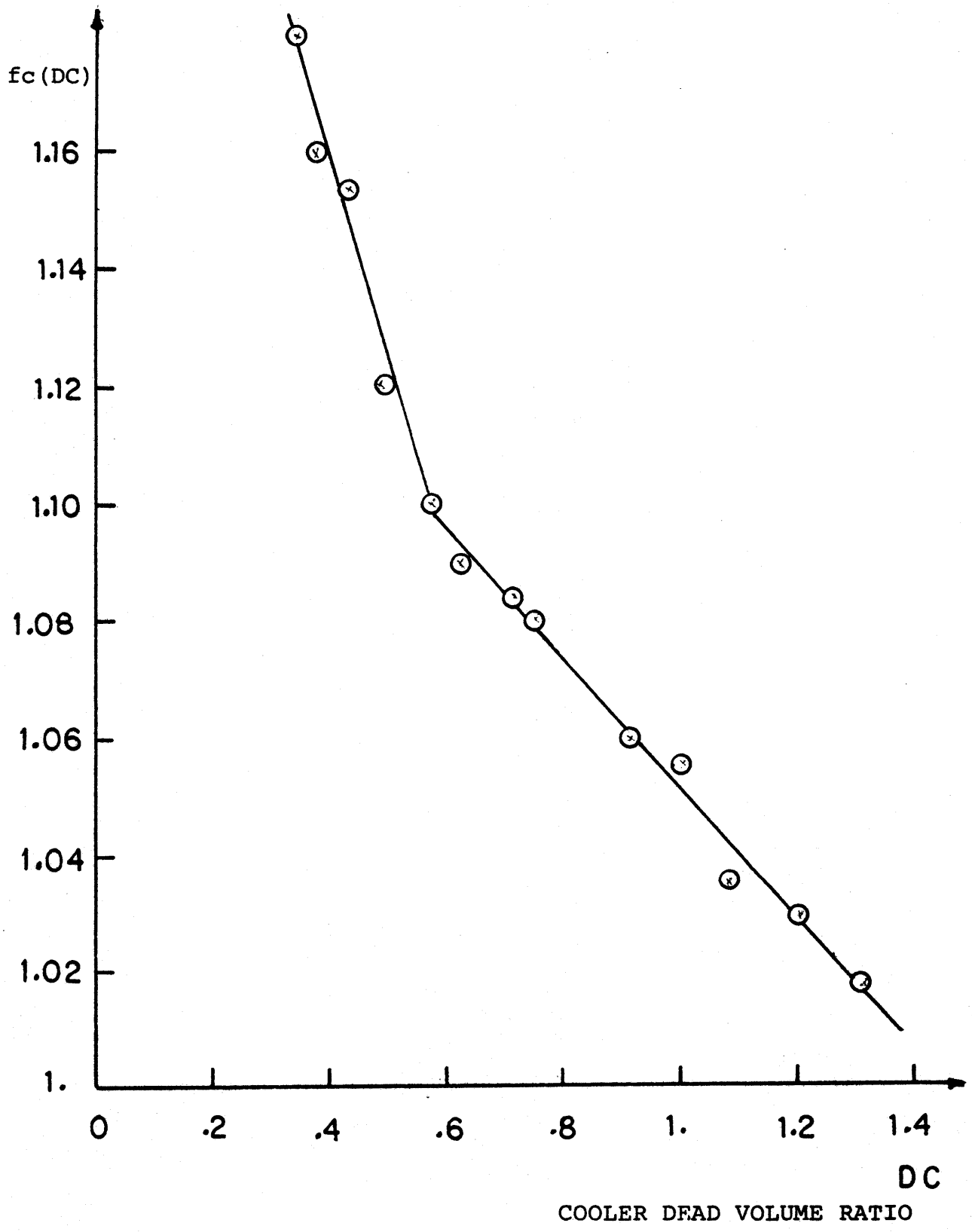

Fig.(41): Dead Volume Correction Factor for Mass Flow Rate in Cooler Simplified Model, Equation (3-28)

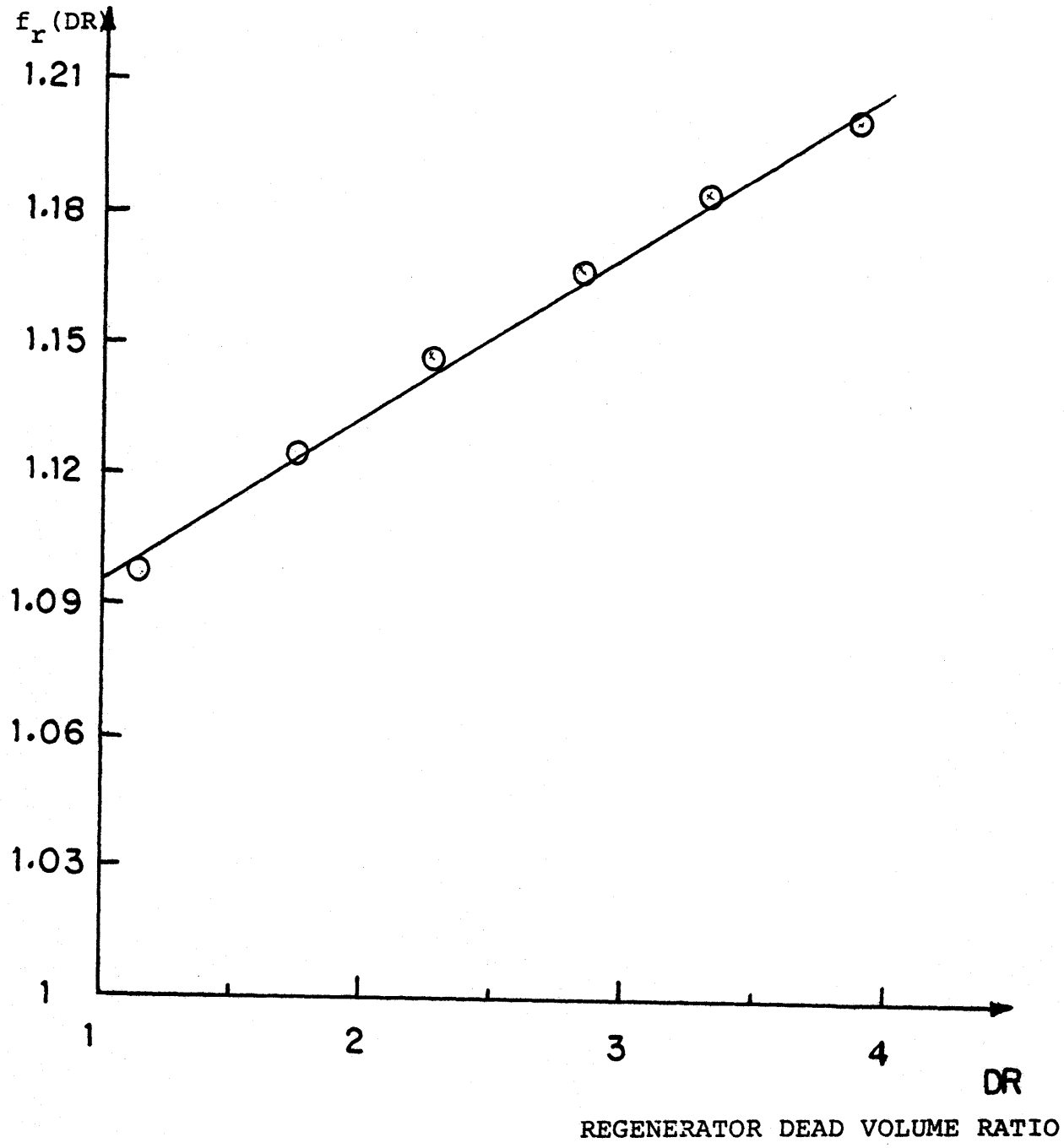

Fig.(42): Dead Volume Correction Factor for Mass Flow Rate in Regenerator Simplified Model , Equation (3-29)

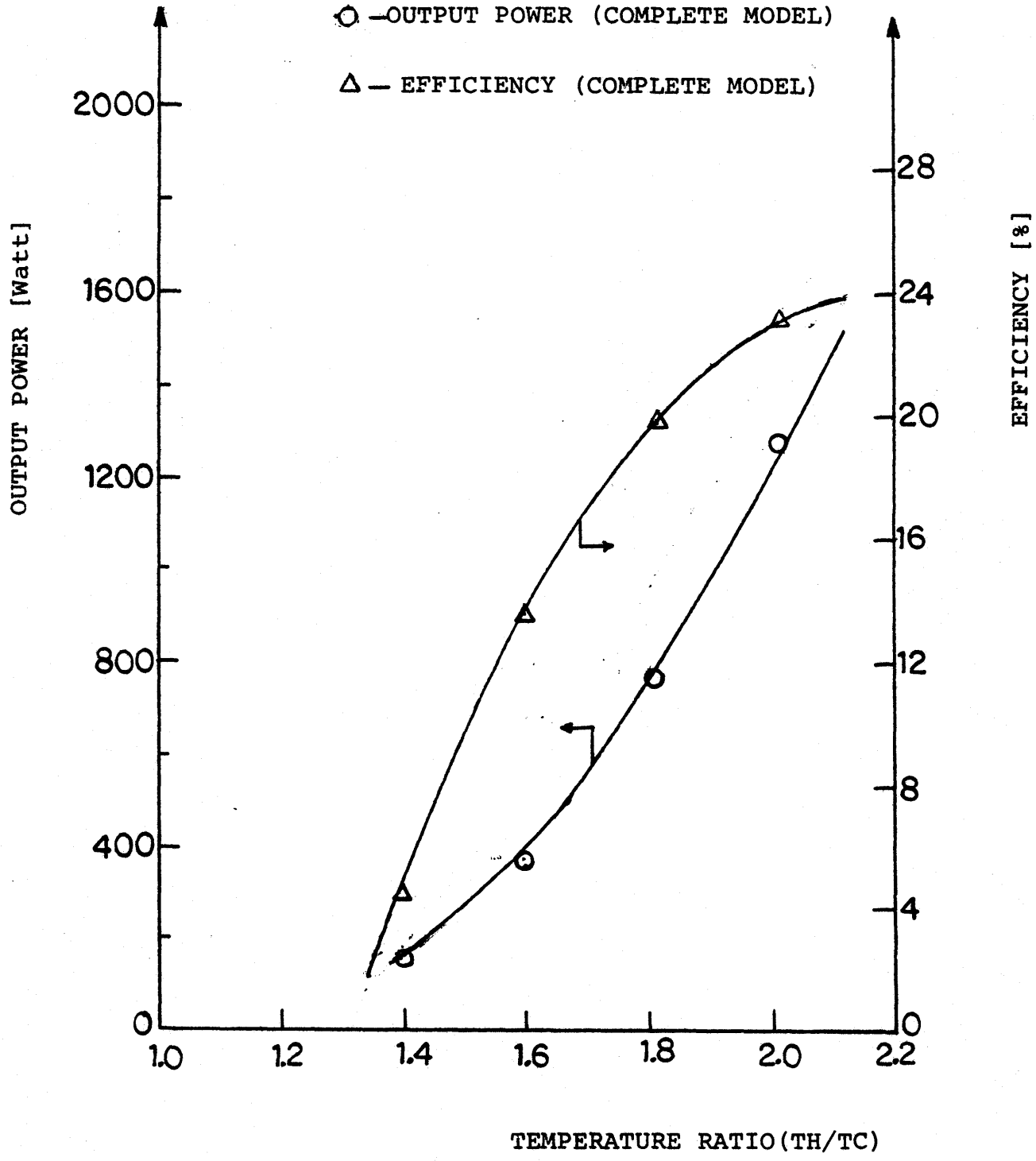

Fig.(43): Comparison of Simplified and Complete Models Predictions (Allison Engine Geometry Has been Used) Table (11)

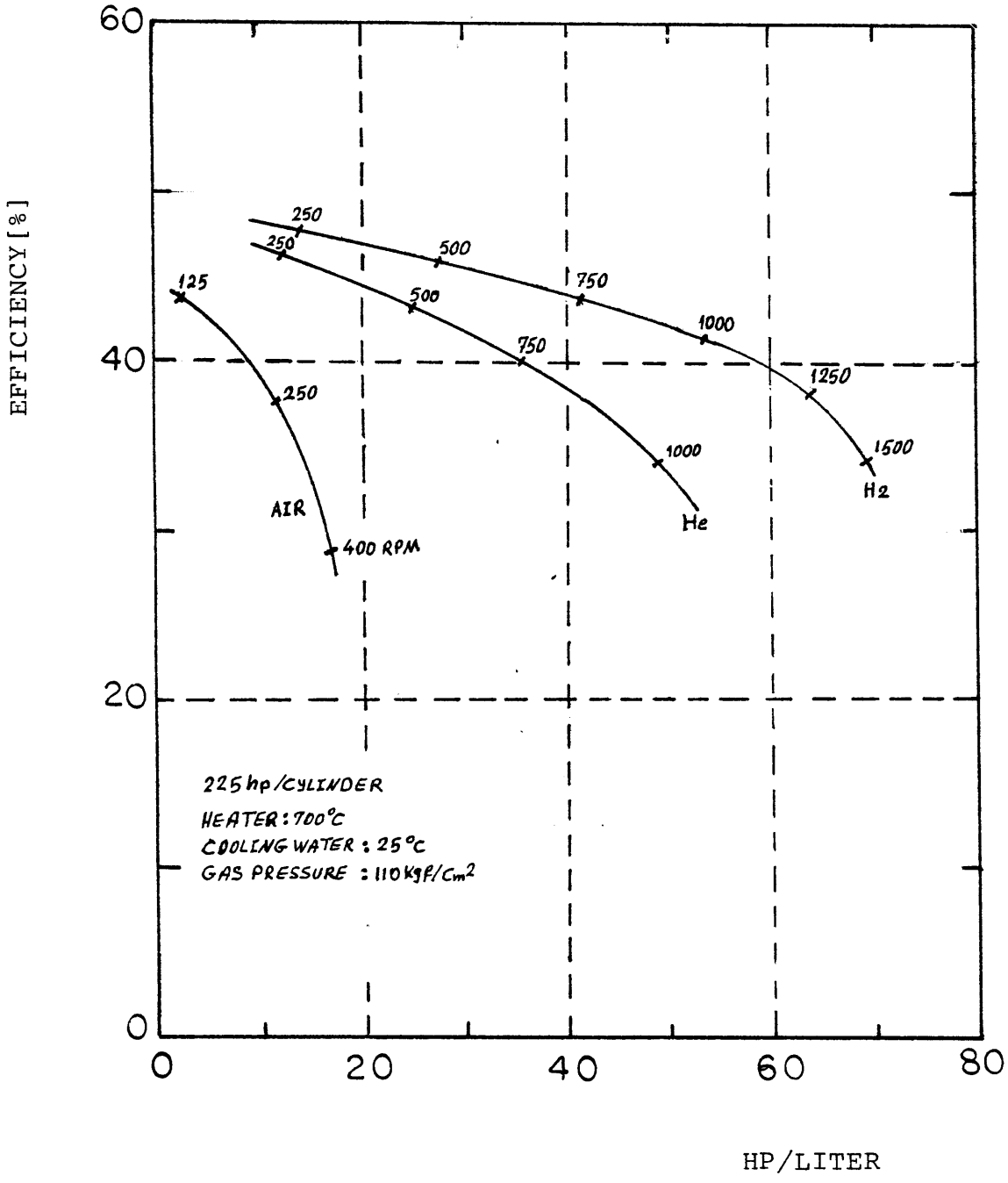

Fig. (44): Comparison of Working Fluids by Philips Laboratories Ref. [15]

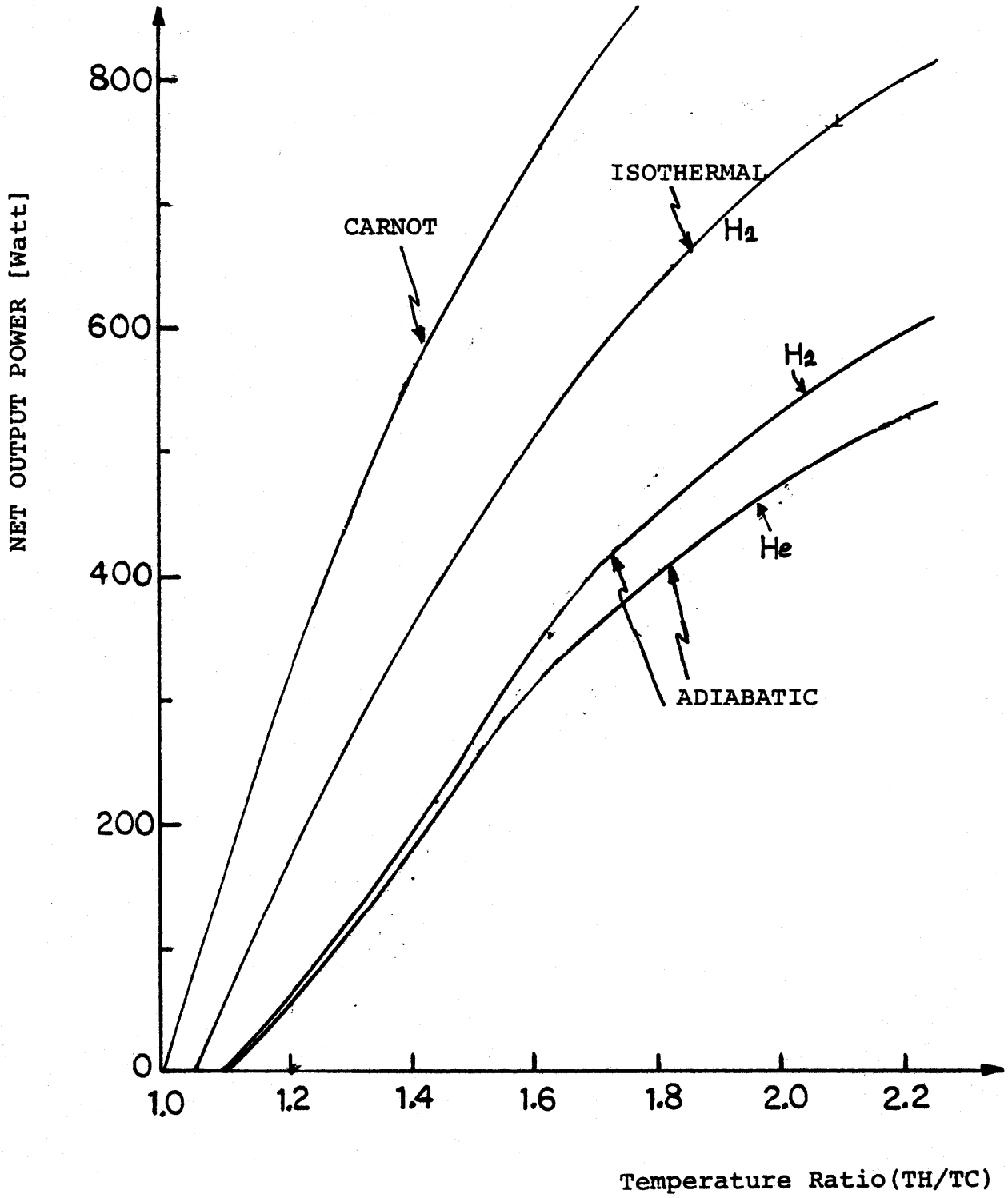

Fig.(45): Comparison of Stirling Engine Output Power with Different Working Fluids and Different Processes, Qin=2000[Watt], Pm=500 Psia
Tables (12),(18)

Note: Different Points Have Different Engine Geometries

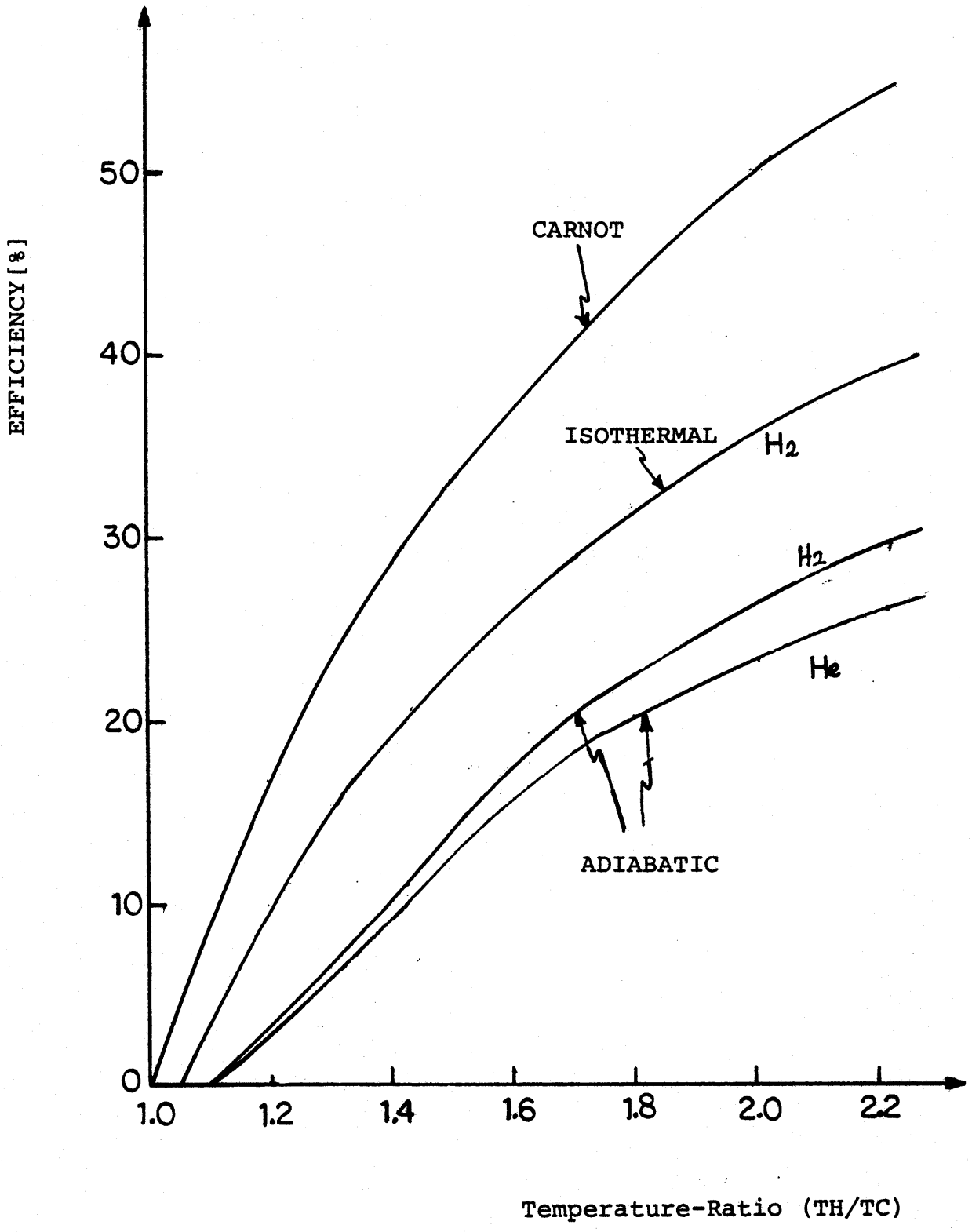

Fig.(46): Comparison of Stirling Engine Efficiency with Different Working Fluids and Different Processes,
Qin=2000[Watt], Pm=500 Psia
Tables (12),(18)

Note: Different Points Have Different Engine Geometries

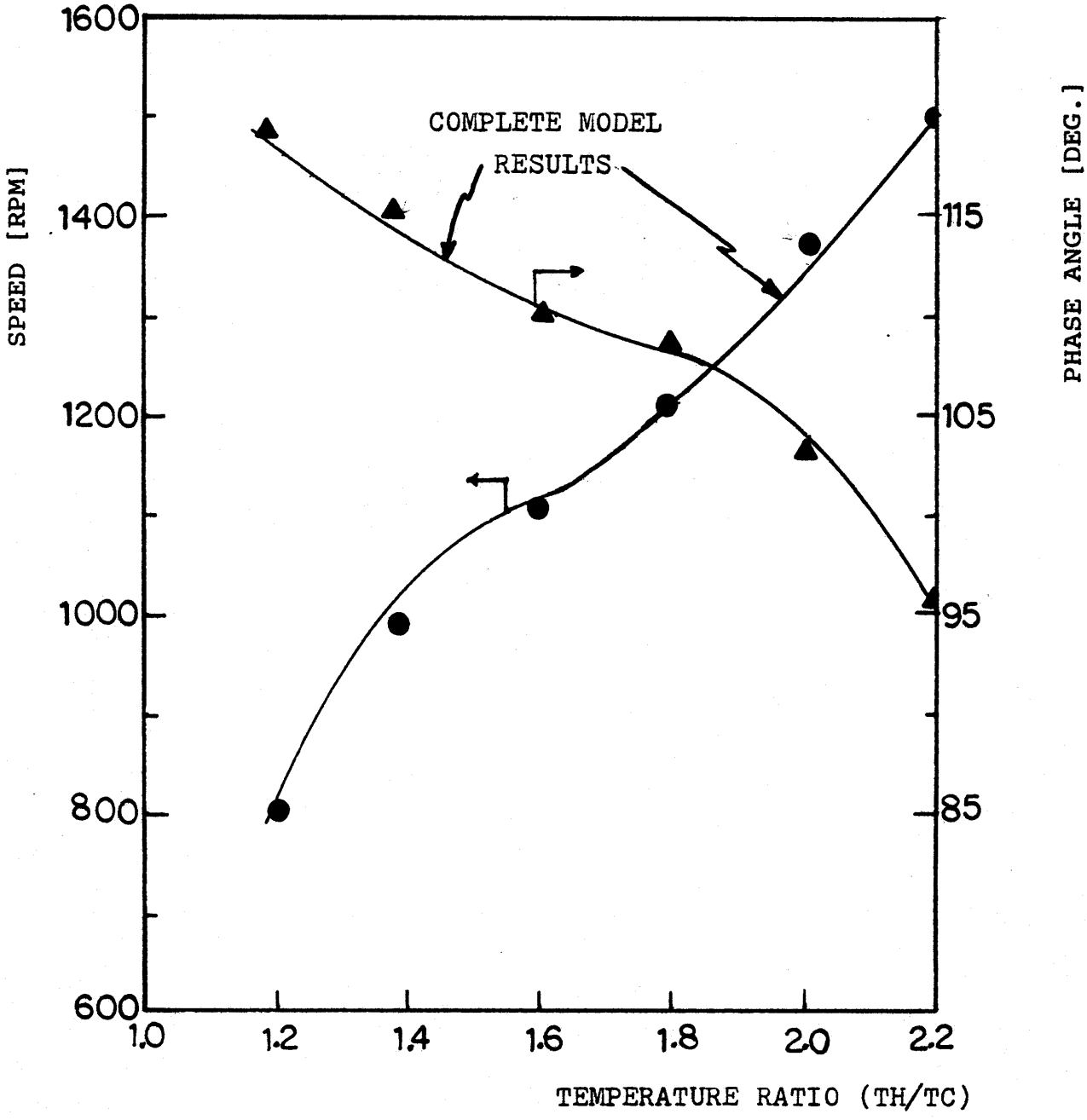

Fig. (47): Variation of Optimum Speed and Phase Angle with Temperature-Ratio
Table (12), Pm=500[Psia], Qin=2000[Watt]
Equations (4-54) & (4-64) (Points)
Complete Model Results (Curves)

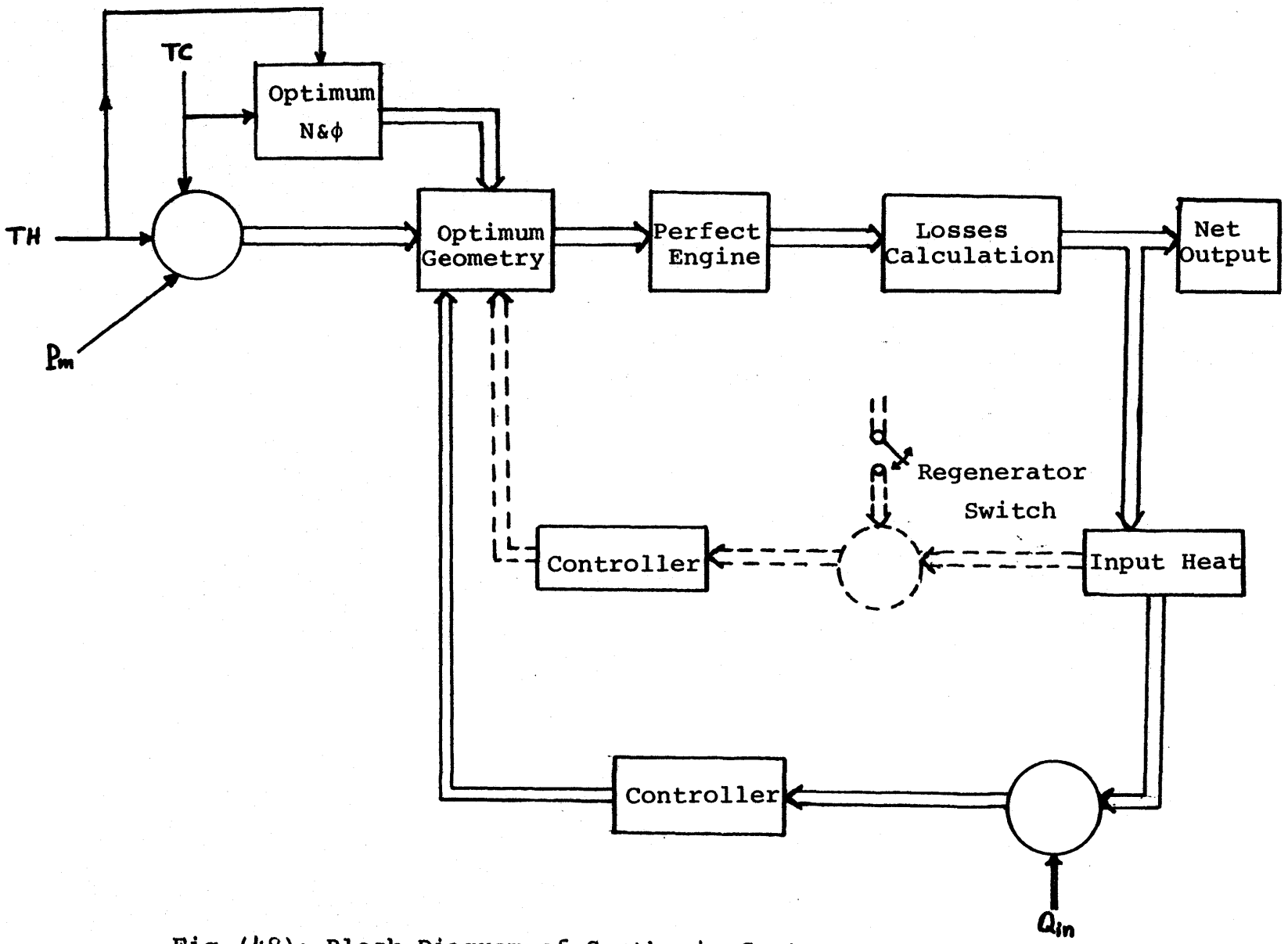

Fig.(48): Block Diagram of Synthesis System

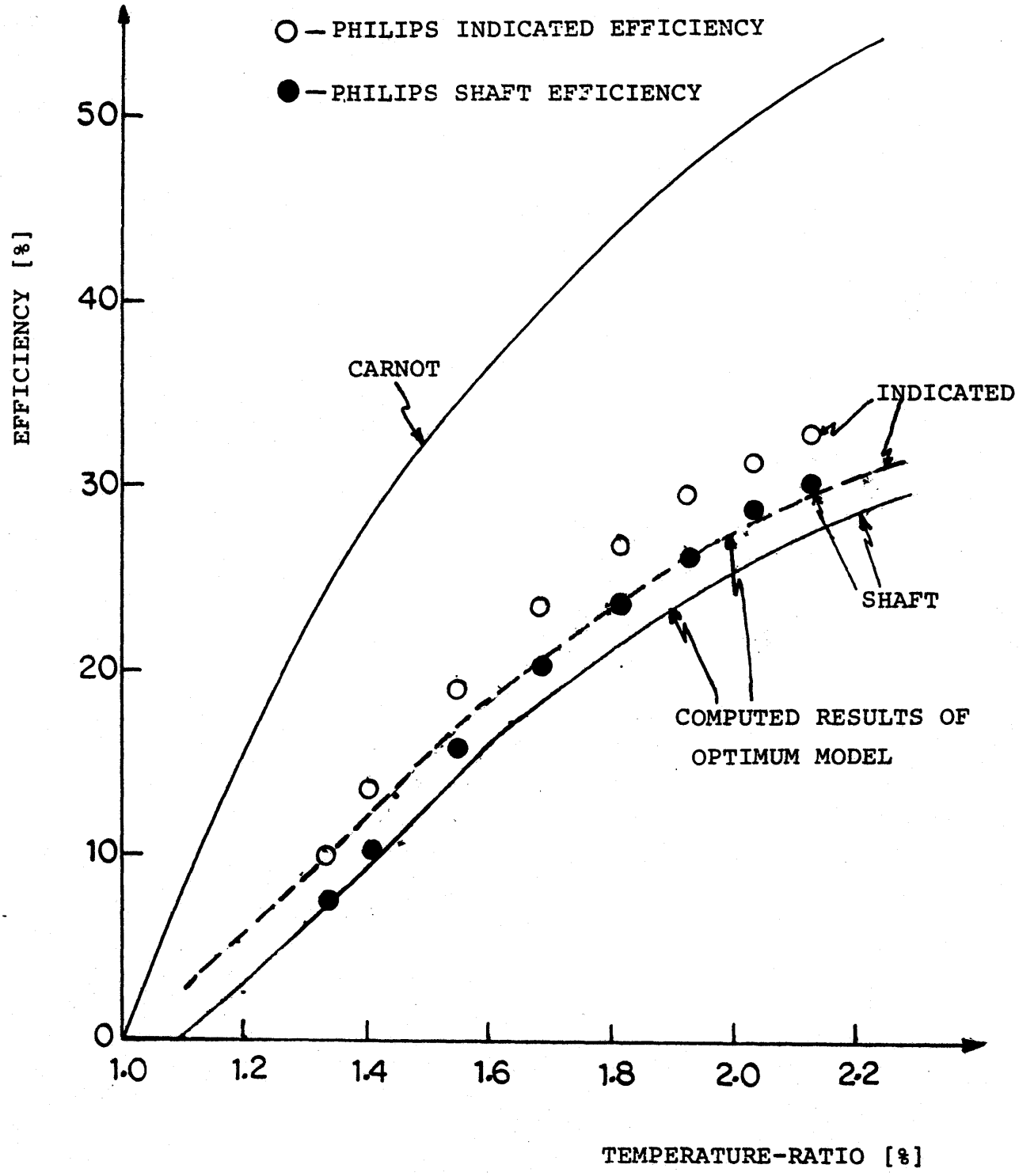

Fig.(49): Comparison of Optimum Model Results and Philips Optimum Design Model Results, Hydrogen as Working Fluid. Ref.[15]
Tables (13A) and (12)

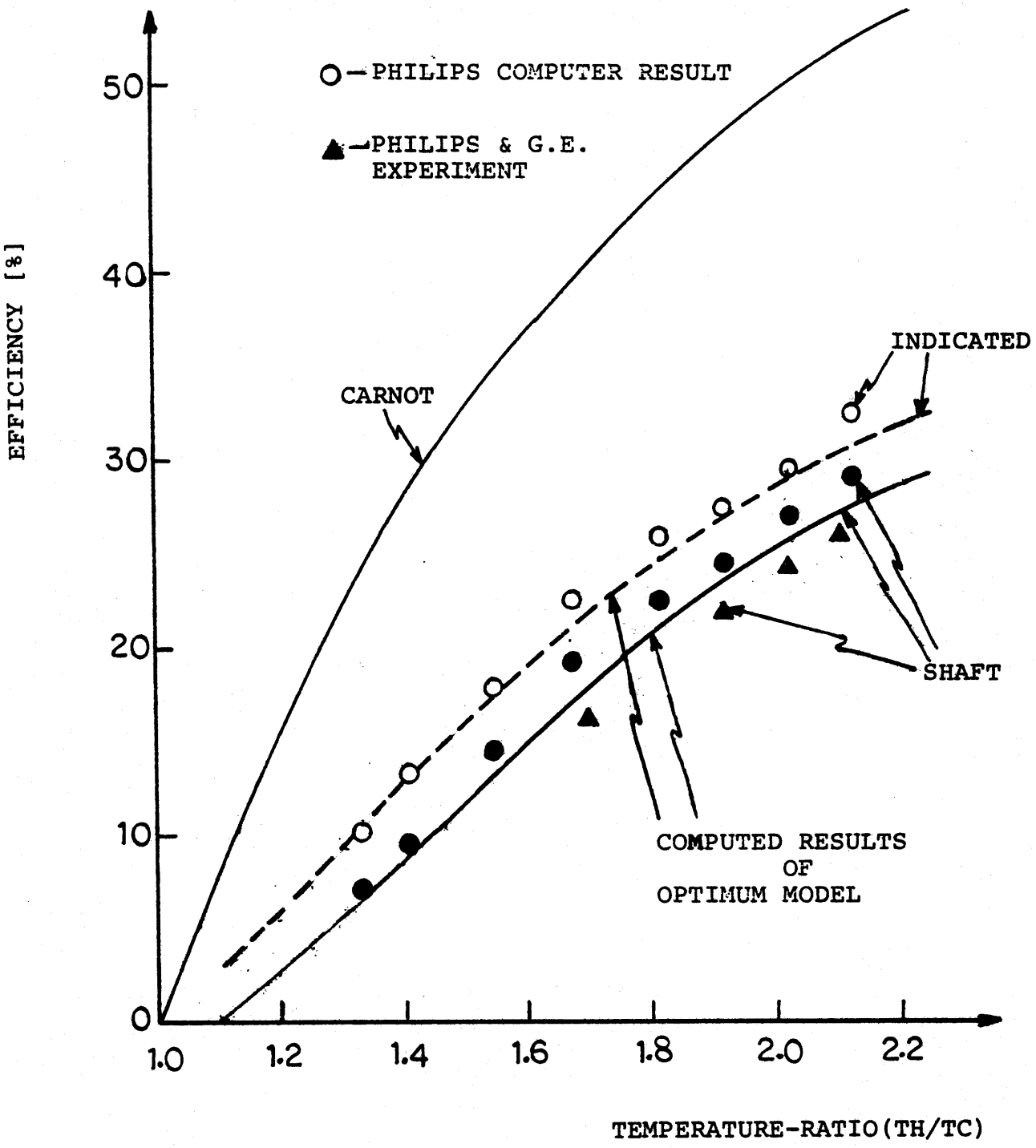

Fig.(50): Comparison of Optimum Model Results, Philips Optimum Design Model Results, and Philips & G.E. Experiment, Hydrogen as Working Fluid
Ref.[11], Tables (13A), (13B), and (12)

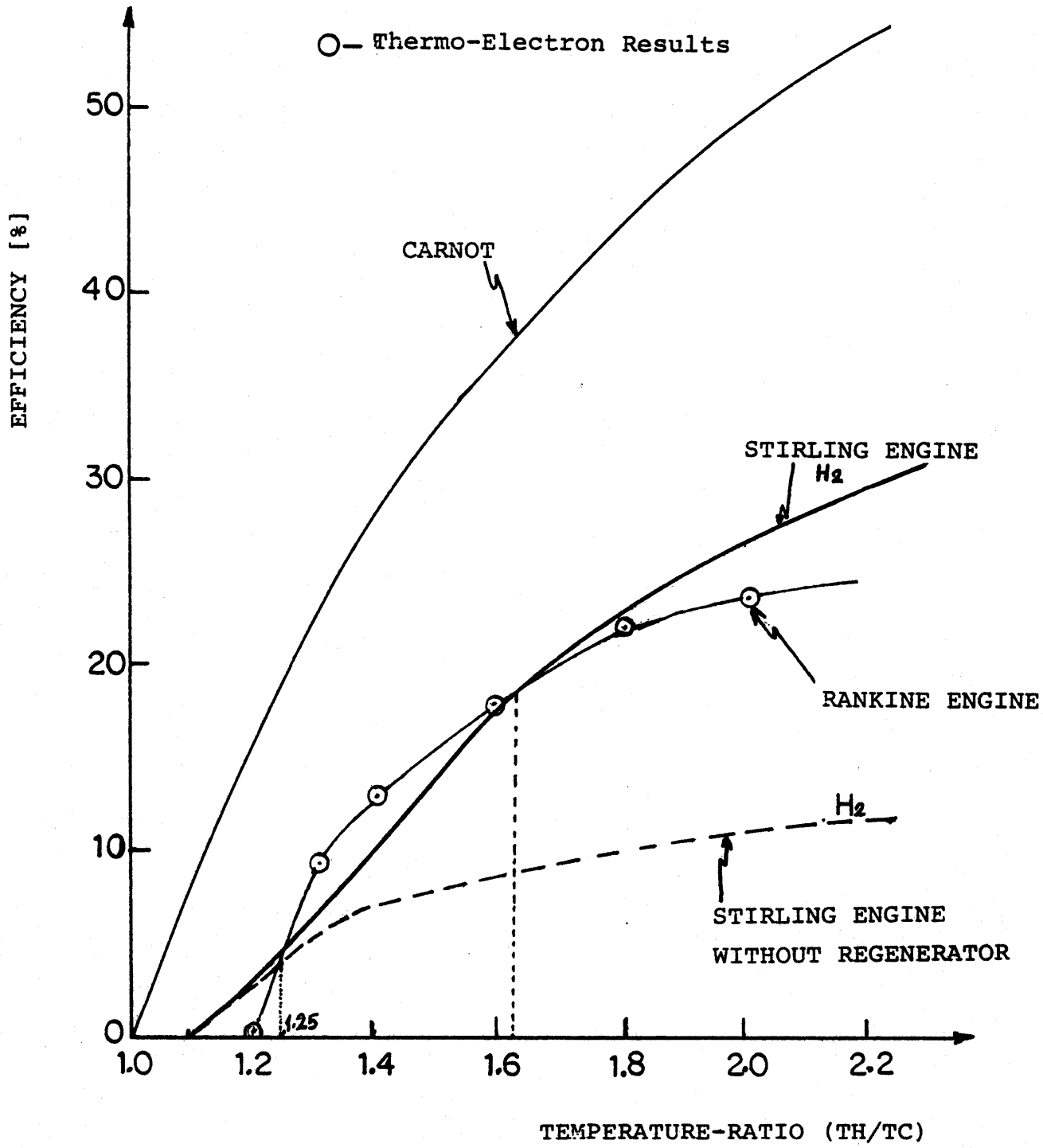

Fig.(51): Comparison of Optimum Designed Stirling Engine Performance and Thermo-Electron Rankine Engine Performance. Ref.[7] Tables (7) and (15)

Note: Different Working Fluids Have Been Used for Rankine Engine Depending on Operating Temperature-Ratio

Qin=4000 Watts Pm=400 Psia

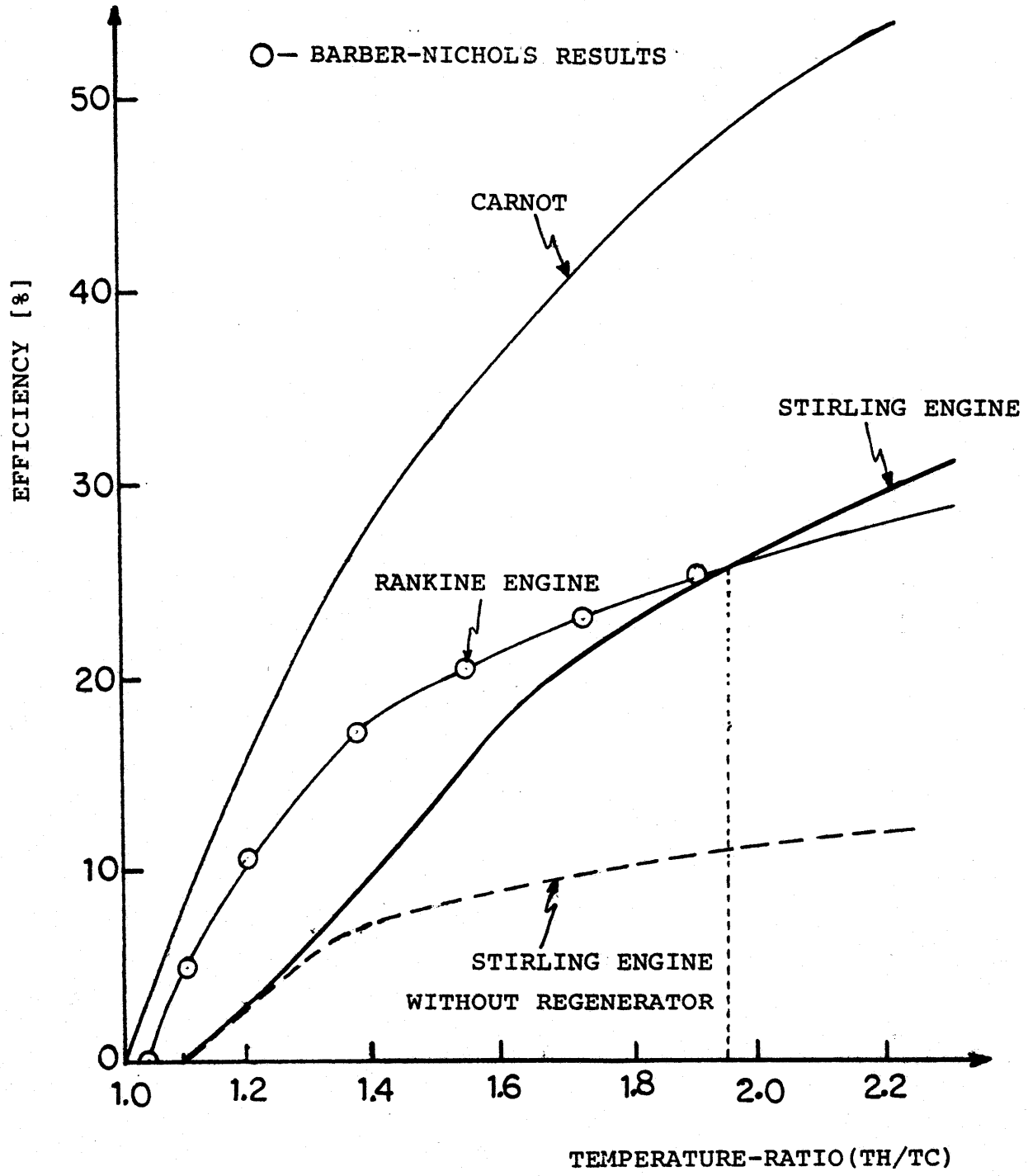

Fig. (52): Comparison of Optimum Designed Stirling Engine Performance and Barber-Nichols Rankine Engine Performance. Ref. [3]
Tables (17), (18)

Note: Different Working Fluids Have Been Used for Rankine Engine Depending on Operating Temperature-Ratio.
Qin=4000 Watts Pm=400 Psia

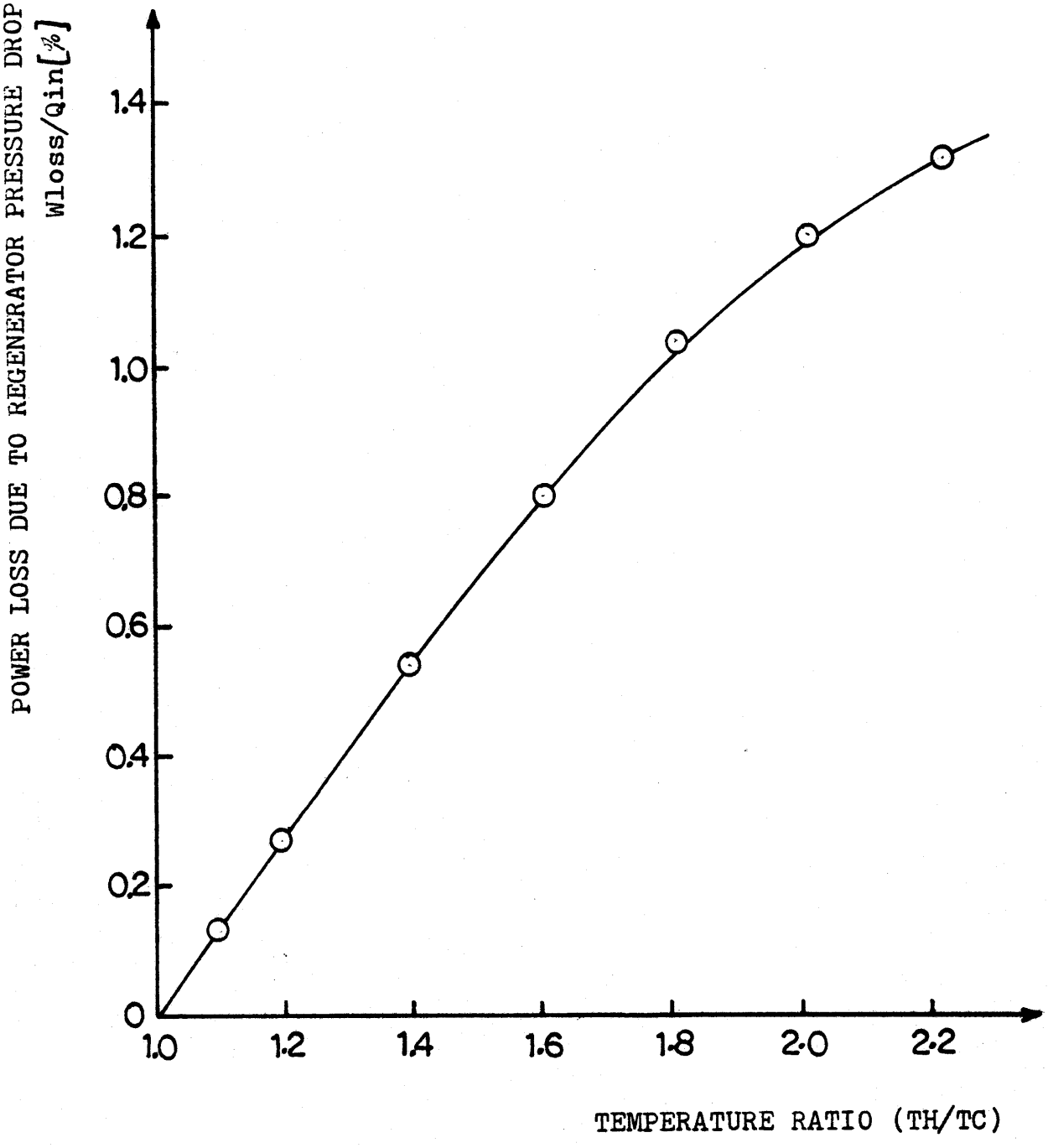

Fig.(53): Stirling Engine Power Loss Due to Regenerator Pressure Drop as Percentage of Input Heat;
Qin=4000 Watts, Pm=400 Psia

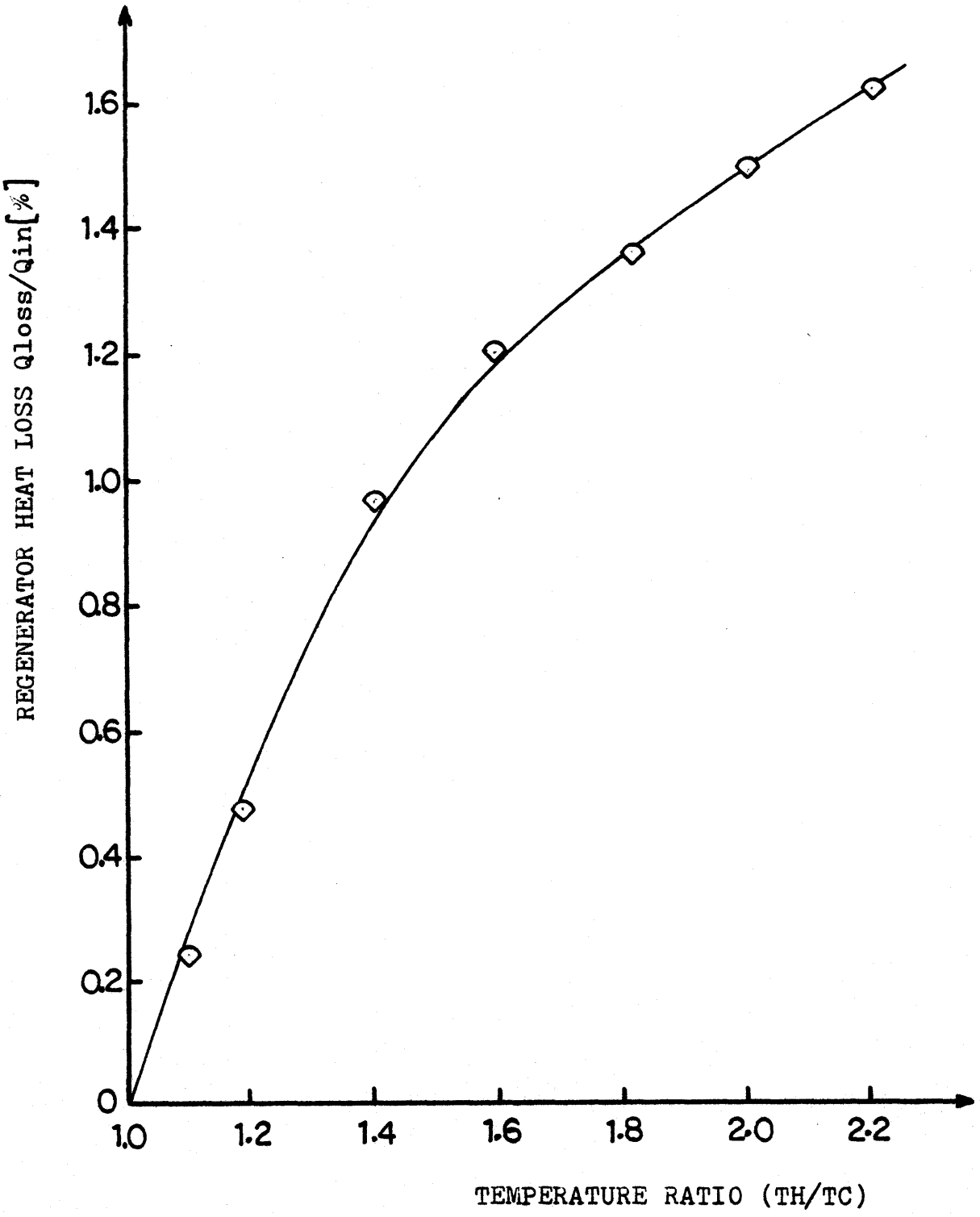

Fig. (54): Stirling Engine Heat Loss Due to Regenerator Imperfection and Axial Conduction as Percentage of Input Heat; Qin=4000 Watts, Pm=400 Psia

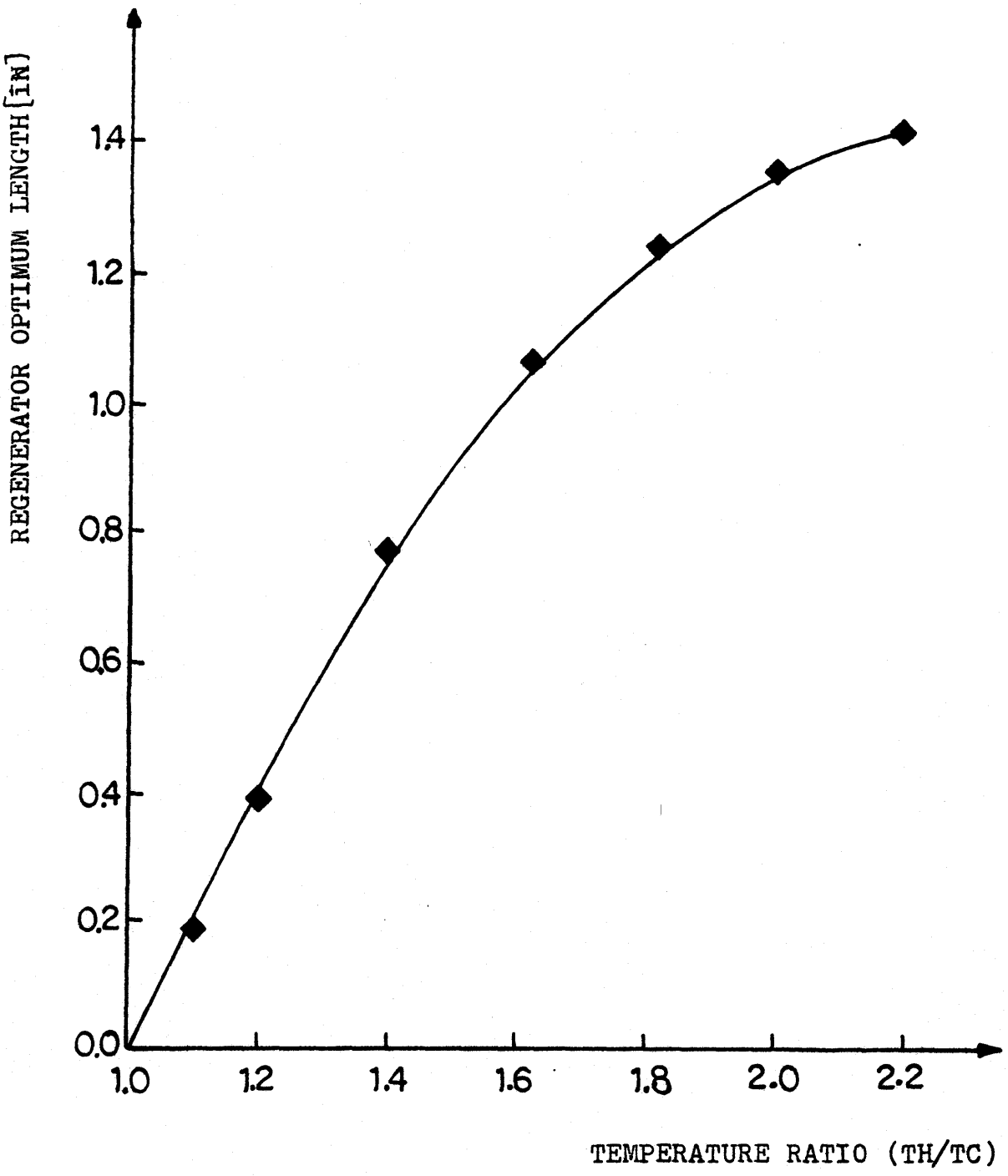

Fig. (55): Variation of Regenerator Optimum Length with Temperature Ratio; Porosity = 70% , Wire Diameter=.0016 in
Qin=4000 Watts , Pm=400 Psia

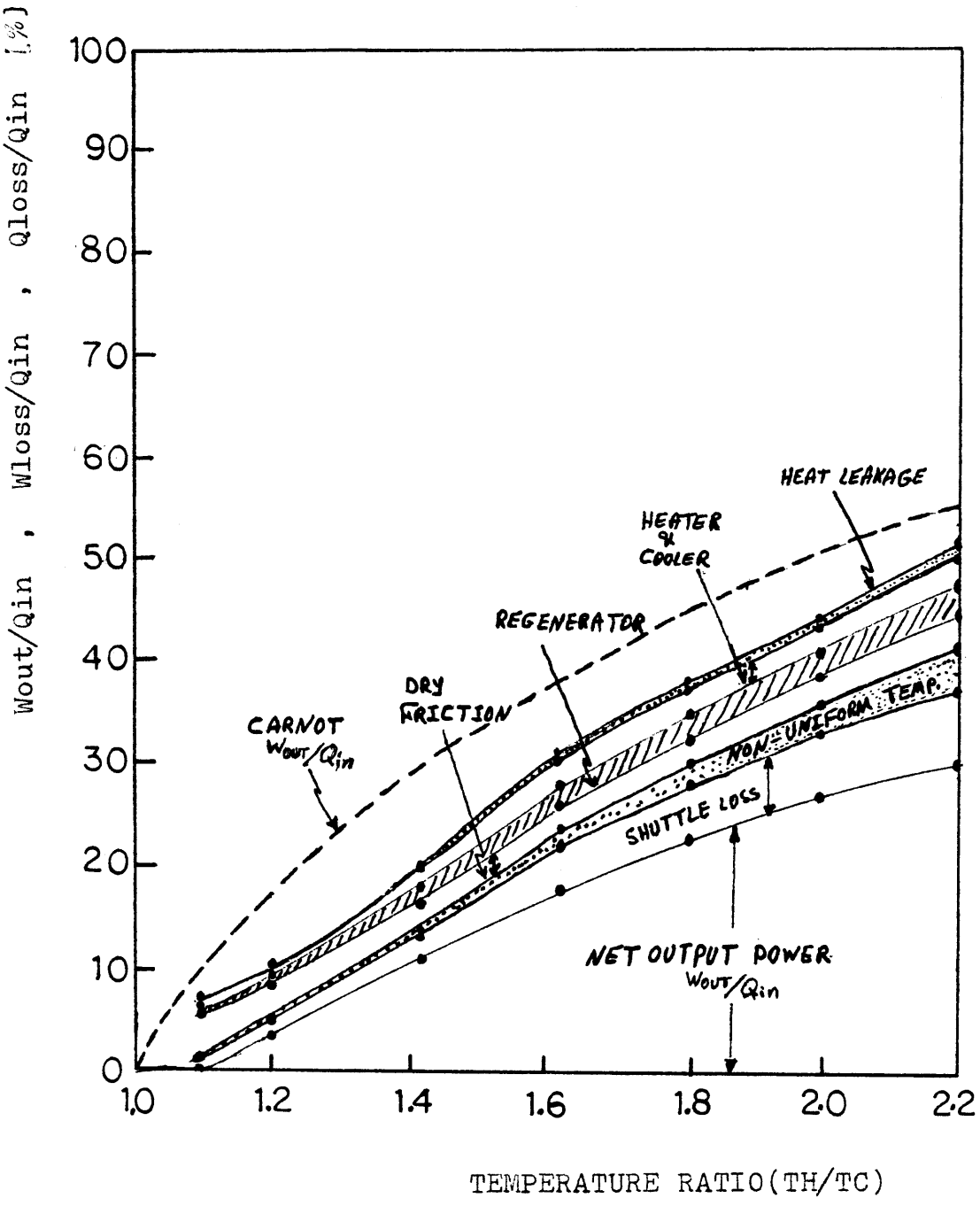

Fig. (56): Variation of Net Output Power, Power losses and Heat Losses with Temperature Ratio as Percentage of Input Heat;
Qin=4000 Watts Pm=400 Psia

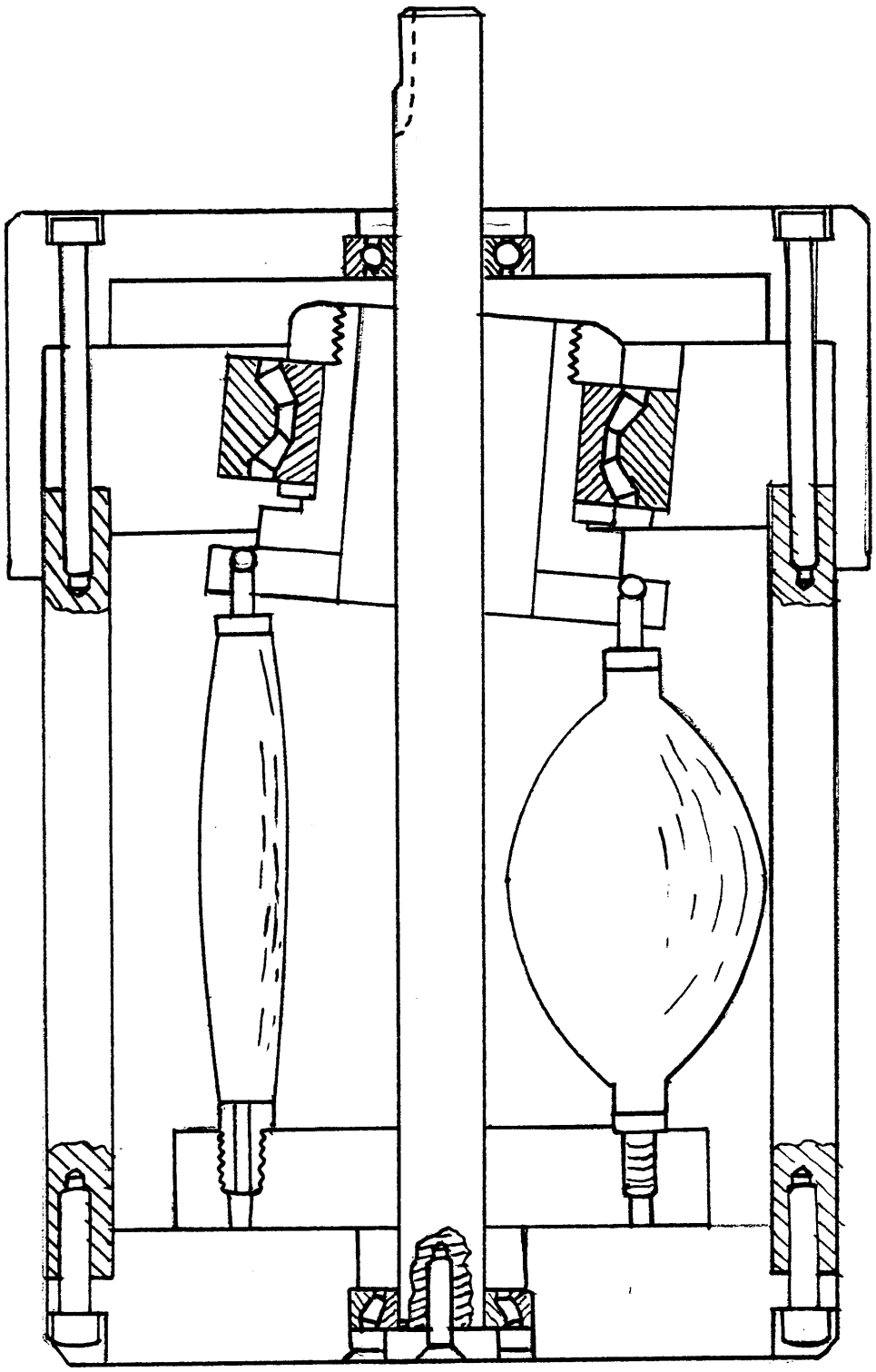

Fig.(57): Tension Actuators Acting Like a Double-Acting Cylinder and Piston, Ref.[32]

REFERENCES

1- W.L. Auxer,"Development of Stirling Engine Powered Heat Activated Heat Pump", General Electric Co., 12th IECEC, Paper 779055, 1977.

2- Robert E. Barber,:Rankine-Cycle Systems for Waste Heat Recovery", Barber-Nichols Engineering Co., Journal of Chemical Engineering, November 25, 1974.

3- Robert E. Barber, "Solar Powered Organic Rankine Cycle Engines-Characteristics and Costs", Barber-Nichols Eng. Co., 11th IECEC, Paper 769200, 1976.

4- Kenneth J. Bell,"Heat Exchangers for the Ocean Thermal Energy Power Plant", Oklahoma State University, Energy Research & Development Administration, Washington D.C. 20454, 1978.

5- G.M.Benson,"Thermal Oscillators, "Erg, Inc., Oakland CA., 12th IECEC, Paper 779247, 1977.

6- F.A. Creswick, "Thermal Design of Stirling-Cycle Machines", Thermal Systems Div., Battelle Memorial Institute, SAE, Paper 949C, 1965

7- Francis. A. DiBella, Thermo-Electron Corp., Personal Conversation, March 1981.

8- Spurgeon E. Eckard,"Test Results for a Rankine Engine Powered Vapor Compression Air-Conditioner for 366 K Heat Source", G.E., 11th IECEC, Paper 769205, 1976.

9- D.W., Kirkly,"A Thermodynamic Analysis of the Stirling Cycle and a Comparison with Experiment", SAE Paper 949B, January 1965.

10- Kanppil Lee, Joseph L. Smith, Jr., Herny B. Faulkner, "Performance Loss due to Transient Heat Transfer in the Cylinder of Stirling Engines", 15the IECEC, Paper 809338, August 1980

11- D. Lehrgeld, A. Sereny, Philips Laboratories; J. Bledsoe, G.E. "Predicted Performance and Testing of a Pre-Prototype Small, Stirling Engine, Generator", 14th IECEC, Paper 799251, August 1979.

12- Gerald P. Lewis, Robert D. Smith, William P. Harkness, Sulfuric Acid Plant Rankine Cycle Waste Heat Recovery", 11th IECEC, Paper 769209 September 1976.

13- W.R. Martini, M.L. Collie, "Stirling Engine Design and Feasibility for Automotive Use", Engergy Technology Review No. 47. 1979.

14- H.M. Meacock, "Refrigeration Processes", Lewes, Sussex, England.

15- A.P.J. Michels, Philips Laboratories, "The Philips Stirling Engine: A Study of Its Efficiency as a Function of Operatinf Temperatures and Workinf Fluids", 11th IECEC, Paper 769258, 1976.

16- D.T. Morgan, J.P. Davis, Thermo-Electron Corp., "High Efficiency Gas Turbine/Organic Rankine Cycle Combined Power Plant", ASME, Paper 74-GT-56, 1974.

17- Ocean Thermal Energy Conversion, Solar Program Assessment: Environmental Factors; Paper ERDA 77-47/8, 1977.

18- Einar B. Qvale, "An Analytical Model of Stirling-Type Engines", Ph.D. Thesis, M.I.T., January 1967.

19- Einar B. Qvale, and J.L. Smith Jr., "A Mathematical Model for Steady Operation of Stirling Type Engines", Transactions of ASME, Journal of Engineering for Power 1968.

20- Einar B. Qvale, and J.L. Smith Jr., "An Approximate Solution for the Thermal Performance of the Stirling Engine Regenerator", ASME Paper 68-WA-Ener-1, 1968.

21- H.L. Rhinehart, C.P. Ketter, "Development Status: Binary Rankine Cycle Waste Heat Recovery Stystem", 12th IECEC, Paper 779175, 1977.

22- Perdro A. Rios, "An Analytical and Experimental Investigation of the Stirling Cycle", D.Sc. Thesis, M.I.T. 1969.

23- Warren M. Rohsenow, Harry Choi,"Heat, Mass, and Momentum Transfer", Prentice-Hall, Inc. 1961.

24- C. Fayette Taylor, Edward S. Taylor," the Internal-Combustion Engine", International Text Book Co., 1966.

25- G. Walker, "Stirling Engines", Oxford Science Publications 1980.

26- R.L. Wiley, G.E., D.Lehrfeld, Philips Laboratories, "Deve-Lopment of a .1KW (e) Isotope Fueled Stirling Cycle Power System", 13th IECEC, Paper 789354, 1978.

27- Edward F. Obert, "Internal Combustion Engines and Air Pollution", Intext Educational Publishers, 3rd Edition, 1973.

28- W.J.D. Annand, "Heat Transfer in the Cylinders of Reciprocating Internal Combustion Engines", Proceedings of Institution of Mechanical Engineers, Volume 177, No. 36, 1963.

29- Woshni, "A Universially Applicable Equation for the Instantaneous Heat Transfer Coefficient in the Internal Combustion Engine", SAE 67093, 1967.

30- R.P. Adair, E. Qvale, "Instantaneous Heat Transfer to the Cylinder Wall in Reciprocating Compressors", Proceedings of 1972 Purdue Compressor Tech. Conference.

31- Henry Paynter,"Advanced System Dynamics and Control", Course Notes, Mechanical Engineering Dept., M.I.T. 1977.

32- Henry M. Paynter,"Tension Actuators", Patent Number 3854383 Dec.17 1974

APPENDIX(A)

Survey of Stirling Engine Technology

The Stirling engine technology began with the early designs which were made by Robert and James Stirling. As with all engineering developments they were beset by limitations of materials. Since that early age, many of the hot-air engines made were small, low-power machines of 100 W to 4 KW. The most notable, large machine was the enormous marine engine built by Ericsson in 1853 having four cylinders 14 ft in diameter with a stroke of 5 ft, running at 9 R.P.M and producing about 220 KW brake power (3000 hp). This low specific power (i.e. power/displacement) was characteristic of all Stirling engines in the last century.

One of the widest uses of early hot-air engines in small sizes was to drive ventilating fans and water pumps. The production of similar machines in substantial quantities was carried on in England to the late 1940s largely for export to tropical countries.

In the 1930's some researchers employed by the Philips company recognized some possibilities in this old engine, provided modern engineering techniques could be applied. Since then, this company has invested millions of dollars and has reached a commanding position in Stirling engine technology. Their developments have lead to smooth, and quiet-running demonstration engines having high efficiency (relative to the Carnot efficiency) which can use many sources of heat. Potentially they might be

used for vehicle propulsion to produce low level of pollution. A great variety of experimental Stirling engines have been built from the same general principles to pump blood, generate electricity, or generate hydraulic power.

Silent electric power is the laboratory application of Stirling engine that has received the earliest attention by Philip [25]. Super-reliable thermo-mechanical generators using a diaphragm Stirling engine and an oscillating electric alternator are used for thermo-electric generators in remote power source applications. It appears possible that certain types of Stirling engines and electric generators will take the place of flame heated or radioisotope heated thermoelectric generators because they will be both cheaper to build and can reach higher efficiencies [13] .

Application of the Stirling engine to motor vehicles has to date received the most attention. On the next section this type of application is discussed in some detail. Stirling engines in reverse cycle, operates as heat pumps, have been used in the cryogenic industry to produce liquified gases and to cool infrared sensors. They have also been tested in systems to replace the electric motor in a common Rankine cycle heat pump for air conditioning. Engine driven heat pumps have the advantage of heating the building with the combined waste heat from the engine and the output of the heat pump. Using systems of this type it appears possible that the primary fuel needed to heat our buildings can be substantially reduced [26] .

Miniature Stirling engines have been developed to power artificial hearts and heart-assist devices. Indeed this engine appears well-suited for this application sicne it is very reliable and can be made efficient in small sizes.

There have been some efforts on the application of Stirling engines for central station electric power. R.J.Meijer[15] calculates that Stirling engines could be made up to a capacity of 3000 hp/cylinder and Stirling engines with 500 hp/cylinder have been checked experimentally [15]. Also, there are efforts to apply Stirling engines to powered wheel chairs which now commonly use lead-acid batteries, control systems and electric motor/belt drives to each large wheel. With a Stirling engine and thermal energy storage comparable performance might be obtained, at substantially reduced bulk and weight.

APPENDIX(B)

Stirling Engine for Automative Application

Philips Laboratory started the design of Stirling engine for automative application. This seemed an interesting area since Stirling engines operate quietly, have low exhaust emissions, and can operate with any fuel or source of heat with high efficiency and rapid response. They are comparable in size and weight with internal combustion engines. Their part-load performance and torque speed characteristic is favorable to vehicular applications they have the promise for long operating life, extended periods between maintenance, and low lubricating oil consumption.

Cost is the principal disadvantage of Stirling engines compared with internal combustion engines. This is due to the need for high strength materials such as cobalt or ceramic components in the hot parts of the engine. Moreover, the heat exchange and control systems are relatively complicated and the cooling system has to handle double the load of an internal combustion engine of comparable power since the exhause heat from the Stirling engine must be kept to a minimum.

Serious interest in Stirling engines for automative applications developed at General Motors in the mid-1960s. Their interest was focused on the Stirling engine for bus applications. A four-cylinder bus engine was designed and built before their program was abruptly terminated in 1970.

After GM, Ford made a contract with Philips for design of

a double-acting Stirling engine with swash-plate drive for passenger cars. A 170 hp four-cylinder engine was developed and installed in a Ford Torino car and a smaller engine for compact passenger was investigated. In these engines tubular gas heaters and gas coolers are used. The coolers are water cooled and heaters may be heated by a flame or a heat pipe. Stacked screens with very fine wire mesh are used for the regenerator. Power control is by adding and removing gas. The engines must be preheated and then cranked to start. One of the important reasons Department of Energy is interested in Stirling engines is that it can have high fuel economy and low pollution and low noise. Ford has not been able to meet emissions standards with the vehicle engine. The results of other tests show that the engine is about 50 lbs over weight objective. The slower start-up and acceleration is attributed to a higher pressure drop through the combustion side of the engine than was anticipated. However, for the program to be successful the big development has to be to lower cost.

Major technical problems encountered and resolved on Philips-Ford program are [13] :

- Swashplate surface galling.
- Drive system noise due to non-concentric crossheads.
- Regenerator end-plate bending.
- Crankcase failure.
- Engine out of balance.
- Piston attachment failure.
- Insufficient exhaust gas recirculation.
- Unstable air/fuel control system.

- Power control contamination.

Problems encountered yet to be resolved on Philips-Ford program are [13] :

- Roll sock seal system failure
- Preheater leakage.
- Preheater binding.
- Fuel burning on preheater core.
- Heater-head temperature distribution.
- Excessive warm-up time.
- Insufficient burner air supply.
- Heater head cracking.
- Power control instability.

United Stirling Company in Sweden is one of the largest research centers on Stirling engine. United Stirling is planning a product line of three engines, all of them are intended to be available as direct flame heated versions as well as heat pipe heated versions. Their production engines are expected to look like Figure (66). They will have two cranks on each of two crankshafts geared to a common drive shaft. The four connecting rods drive the four double-acting pistons through cross heads to take the side thrust. The burner and air preheater is different than the Philips engine. This air preheater is the counter-flow type. This substitution eliminates the machinery needed to rotate the the reversing flow matrix and seals the matrix as it rotates as done in the Ford-Philips design. This burner system can get the engine started rapidly from a cold start. The heater tubes in a Stirling engine must be heated up before the starter motor is

engaged. The burner blower, normally driven by the engine, is driven by a separate electric motor during the heating-up period.

Finally, NASA-Lewis Testing Center has done some work on Stirling engine. Their research is part of the General Motors efforts on GPU-3 engine. Their tests have shown that the brake specific fuel consumption is about the same as that obtained by the Army in their acceptance testing. However, the engine output falls short of that originally obtained by the Army and the difference is suspected to be due to the excessive leakage of gas past the power piston [13].

Although there has been much efforts directed toward the automative application of Stirling engine no commercial vehicle yet exists. This is due to that fact that Stirling engine is not yet economical for this type of application, and most of the researches in this area are now concentrated on investigating different alternatives for materials which can operate at, say, 3000 Psia pressure and 2000 $^{\circ}$R temperature.

APPENDIX(C)

Steady State Analysis of Practical Rankine Engine

In section (2.1.1) a schematic diagram of a practical Rankine engine is shown. Steady state analysis of this engine is done for different temperature-ratios. Followings are the states, shown in figure of section (2.1.1), at different temperatures. Table (1) shows the summary of following results.

Working fluid is R-142b or C2H3F2Cl, which is selected for covering the whole range of temperature-ratio.

a)- TH/TC=1.1

TC=555 R

TH=610 R

State 1:

T=555 R

P=66.11 Psia

H=33.04 Btu/lb

S=.069 Btu/lb R

V=1/67.64 ft^3/lb

State 2:

P=112 Psia

H=33.166 Btu/lb

S=.069 Btu/lb R

State 3:

T=610 R

P=112 Psia

H=125 Btu/lb

S=.226 Btu/lb

State 4:

P=86 Psia

H=122.5 Btu/lb

S=.226 Btu/lb

T=595 R

State 5:

T=610 R

S=.235 Btu/lb

H=127.3 Btu/lb

State 6:

P=66.11 Psia

H=124.5 Btu/lb

S=.235 Btu/lb

$Wout=H_3-H_4+H_5-H_6-H_2+H_1=5.174$ Btu/lb

$Qin=H_3-H_2+H_5-H_4=197$ Btu/lb

Eff.=Wout/Qin=5.35%

b)- TH/TC=1.2

TC=550 R

TH=660 R

State 1:

T=550 R

P=60.99 Psia

H=31.58 Btu/lb

S=.0663 Btu/lb R

$V=1/68.11$ ft^3/lb

State 2:

T=640 R

S=.0663 Btu/lb

P=214.3 Psia

H=32 Btu/lb

State 3:

T=660 R

S=.225 Btu/lb R

H=131 Btu/lb

P=214.3 Psia

State 4:

P=115 Psia

H=124 Btu/lb

T=595 R

State 5:

H=137 Btu/lb

T=660 R

S=.24 Btu/lb R

State 6:

P=60.99 Psia

S=.246 Btu/lb

H=131 Btu/lb

Wout=12.58 Btu/lb

Qin=112 Btu/lb

Eff.=11.23%

c)- TH/TC=1.4

TC=515 R

TH=720 R

State 1:

T=515 R

P=33.23 Psia

H=21.86 Btu/lb

S=.0477 Btu/lb

V=1/71.24 ft^3/lb

State 2:

P=413.8 Psia

H=22.85 Btu/lb

S=.0477 Btu/lb

State 3:

P=413.8 Psia

T=720 R

H=133 Btu/lb

S=.22 Btu/lb

State 4:

P=120 Psia

H=122.5 Btu/lb

T=600 R

State 5:

H=151 Btu/lb

T=720 R

S=.264 Btu/lb R

State 6:

P=33.23 Psia

H=135 Btu/lb

S=.264 Btu/lb R

Wout=25.51 Btu/lb

Qin=138.65 Btu/lb

Eff.=18.4%

d)- TH/TC=1.6

TC=450 R

TH=720 R

State 1:

TC=450 R

P=8.37 Psia

H=6.2 Btu/lb

S=.0146 Btu/lb

State 2:

P=413.8 Psia

H=7.18 Btu/lb

S=.-146 Btu/lb

State 3:

P=413.8 Psia

T=720 R

H=133 Btu/lb

S=.22 Btu/lb

State 4:

P=60 Psia

T=552 R

H=116 Btu/lb

State 5:

P=60 Psia

H=154 Btu/lb

T=720 R

S=.281 Btu/lb R

e)- TH/TC=1.8

TC=400 R

TH=720 R

State 1:

T=400 R

P=2.136 Psia

H=-3.74 Btu/lb

S=-.0093 Btu/lb R

V=1/80.27 ft^3/lb

State 2:

P=413.8 Psia

H=-2.79 Btu/lb

S=-.0093 Btu/lb R

State 3:

P=413.8 Psia

T=720 R

H=133 Btu/lb

S=.22 Btu/lb

State 4:

P=30 Psia

H=109.77 Btu/lb

T=510 R

State 5:

P=30 Psia

T=720 R

H=155 Btu/lb

S=.295 Btu/lb

State 6:

P=2.136 Psia

H=122 Btu/lb

S=.295 Btu/lb

Wout=55.28 Btu/lb

Qin=181.02 Btu/lb

Eff.=30.54%

f)- TH/TC=2.0

TC=380 R

TH=760 R

State 1:

P=1.118 Psia

T=380 R

H=-7.44 Btu/lb

S=-.019 Btu/lb

V=1/81.74 ft^3/lb

State 2:

P=413.8 Psia

H=-6.5 Btu/lb

S=-.019 Btu/lb

State 3:

T=760 R

P=413.8 Psia

H=147.5 Btu/lb

S=.24 Btu/lb R

State 4:

P=21.5 Psia

T=562 R

H=122 Btu/lb

S=.24 Btu/lb R

State 5:

T=760 R

P=21.5 Psia

H=165 Btu/lb

S=.318 Btu/lb

APPENDIX(D)

Ideal Engine Analysis (Schmidt Solution)

In section (2.2.1) the assumptions of the Schmidt's Stirling engine performance derivation are stated. Based on those assumptions the followings can be resulted.

$$Vh=1/2\ VH(1+\cos\omega t) \tag{D-1}$$

$$Vc=1/2\ VC(1+\cos(\omega t-\phi)) \tag{D-2}$$

$$VD=X*VE \quad \text{(Dead Volume)} \tag{D-3}$$

Then the mass of working fluid in different spaces can be written as:

$$Mh=P*Vh/(R*TH) \tag{D-4}$$

$$MC=P*Vc/(R*TC) \tag{D-5}$$

$$MD=P*VD/(R*(TH+TC)/2) \tag{D-6}$$

Since the total mass is constant; then

$$M_T = P\left[\frac{VH*(1+\cos\omega t)}{2*R*TH}\right]+P\left[\frac{1+\cos(\omega t-\varphi)}{2*R*TC}\right]*VC+\frac{2*X*VH*P}{R*(TH+TC)} \tag{D-7}$$

This equation can be summarized by using the following definitions.

$$TAN(\theta)=(VC/VH*SIN\varphi)/[TC/TH+VC/VH*\cos\varphi] \tag{D-8}$$

$$A=\frac{\sqrt{(TC/TH)^2+2*TC*VC*\cos\varphi/(TH*VH)+(VC/VH)^2}}{TC/TH+VC/VH+4*X*TC/(TC+TH)} \tag{D-9}$$

Then the instantaneous pressure can be written as:

$$P=Const./(1+A*\cos(\omega t-\theta)) \tag{D-10}$$

This means that:

$$P_{min}=Const./(1+A) \tag{D-11}$$

$$P_{max}=Const./(1-A) \tag{D-12}$$

$$\text{Pressure Ratio}=P_{max}/P_{min}=(1+A)/(1-A) \tag{D-13}$$

$$P=P_{max}(1-A)/(1+A*COS(\omega t-\theta)) \tag{D-14}$$

$$P_{mean}=1/(2\pi)\int_{o}^{2\pi} P*d(\omega t-\theta) \tag{D-15}$$

$$P_{mean}=P_{max}*\sqrt{(1-A)/(1+A)} \tag{D-16}$$

Expansion and Compression Works:

Because of isothermal expansion process the work and heat transfer are the same:

$$We = \oint P * d V_h \tag{D-17}$$

$$d V_h = -1/2 * VH * SIN(\omega t) * d(\omega t) \tag{D-18}$$

$$We = Q = \oint \frac{-P_{min}(1+A) * VH * SIN(\omega t)}{2 + 2A\cos(\omega t-\theta)} d(\omega t) \tag{D-19}$$

This integration can be carried out analytically, the final result is:

$$We = \pi * P_m * VH * A * SIN(\theta)/(1+\sqrt{1-A^2}) \tag{D-20}$$

By the same procedure, the compression work can be derived as:

$$Wc = \pi * P_m * VC * A * SIN(\varphi-\theta)/(1+\sqrt{1-A^2}) \tag{D-21}$$

$$W_{OUT} = We - Wc = \pi * P_m * A * VH * SIN\theta * (1-TC/TH)/(\sqrt{1-A^2}+1) \tag{D-22}$$

Instantaneous Masses:

Hot space:

$$MH = \frac{P * VH}{R * TH} = \frac{1/2 * VH * Pm * \sqrt{1-A^2} * (1+\cos\omega t)}{R * TH * [1 + A\cos(\omega t - \theta)]} \qquad \text{(D-23)}$$

Cold space:

$$MC = \frac{P * VC}{R * TC} = \frac{1/2 * VC * Pm * \sqrt{1-A^2} * [1+\cos(\omega t - \varphi)]}{R * TC * [1 + A\cos(\omega t - \theta)]} \qquad \text{(D-24)}$$

Dead space:

$$MD = \frac{2 * P * VD}{R * (TH+TC)} = \frac{2X * VH * Pm * \sqrt{1-A^2}}{R * (TC+TH) * [1 + A\cos(\omega t - \theta)]} \qquad \text{(D-25)}$$

Then the total mass in the system is the summation of the above masses.

$$MT = \frac{VH * Pm * \sqrt{1-A^2}}{R * TC * [1+A\cos(\omega t - \theta)]} \left[TC/TH + 2X * TC/(TH+TC) + VC(1+\cos\varphi)/(2 * VH) \right] \qquad \text{(D-26)}$$

Derivation of Optimum Parameters from Schmidt Analysis:

$$W \triangleq \frac{W_{OUT}}{Pm * V_T} = \pi * \frac{1}{1 + VC/VH} * \frac{A}{1 + \sqrt{1-A^2}} * \sin\theta * (1 - TC/TH) \qquad \text{(D-27)}$$

$VC/VH \triangleq V_r$, $TC/TH \triangleq T_r$

$$\Rightarrow A = \frac{\sqrt{T_r^2 + V_r^2 + 2T_r \cdot V_r \cdot \cos\varphi}}{T_r + V_r + 4X/(1 + 1/T_r)} \qquad \text{(D-28)}$$

To see the effect of dead volume on the net output, the derivative of output respect to X(x=VD/VH) is taken:

$$\frac{\partial W}{\partial X} = \frac{\partial W}{\partial A} * \frac{\partial A}{\partial X} \qquad \text{(D-29)}$$

$$\frac{\partial W}{\partial A} = \pi * SIN\theta * \frac{1-T_r}{1+V_r} * \frac{1+\sqrt{1-A^2} + A^2/\sqrt{1-A^2}}{\left[1+\sqrt{1-A^2}\right]^2} \qquad (D\text{-}30)$$

$$\frac{\partial A}{\partial X} = -\frac{4 \cdot A \cdot T_r/(1+T_r)}{T_r + V_r + 4X T_r/(1+T_r)} \qquad (D\text{-}31)$$

$$\frac{\partial W}{\partial X} = \pi\, SIN\theta\, \frac{1-T_r}{1+V_r} * \frac{1}{\sqrt{1-A^2}\left[1+\sqrt{1-A^2}\right]} * \frac{-4A T_r/(1+T_r)}{T_r +} \qquad (D\text{-}32)$$

Since there is no X term in the numerator it means there is no optimum value for dead volumes and as it is increased the output would decrease.

By taking the derivative of output respect to swept-volume ratio (VC/VH), we get:

$$\frac{\partial A}{\partial V_r} = \frac{T_r}{A\left[T_r+V_r+4X T_r/(1+T_r)\right]^2} - \frac{A}{T_r + V_r + 4X T_r/(1+T_r)}$$

$$\frac{\partial W}{\partial V_r} = \pi * \frac{A\,SIN\theta}{1+\sqrt{1-A^2}}(1-T_r) * \frac{-1}{(1+V_r)^2} + \frac{\pi * SIN\theta * (1-T_r)}{(1+V_r)\sqrt{1-A^2}\left[1+\sqrt{1-A^2}\right]} * \frac{\partial A}{\partial V_r} \qquad (D\text{-}33)$$

$$\frac{\partial W}{\partial V_r} = \frac{\pi\, SIN\theta\,(1-T_r)}{(1+V_r)(1+\sqrt{1-A^2})}\left[\frac{-A}{1+V_r} + \frac{V_r}{A\sqrt{1-A^2}\left[T_r+V_r+4X T_r/(1+T_r)\right]^2} - \frac{A}{\sqrt{1-A^2}\left[T_r+V_r+4X T_r/(1+T_r)\right]}\right] \qquad (D\text{-}34)$$

$$\frac{\partial W}{\partial V_r} = 0 \Rightarrow -A^2\sqrt{1-A^2}\left[T_r+V_r+4X\frac{T_r}{1+T_r}\right]^2 + V_r(1+V_r) - A^2(1+V_r)\left[T_r+V_r+4X\frac{T_r}{1+T_r}\right] = 0$$

$$\Rightarrow -(T_r^2+V_r^2+2V_r T_r\cos\varphi)\sqrt{\frac{8T_r X}{1+T_r}\left(T_r+V_r+2X\frac{T_r}{1+T_r}\right) + 2T_r V_r(1-\cos\varphi)} + V_r(1+V_r) *$$

$$* \left[T_r+V_r+4X T_r/(1+T_r)\right] - (1+V_r)(T_r^2+V_r^2+2V_r T_r\cos\varphi) = 0 \qquad (D\text{-}35)$$

Assuming $\cos\phi \approx 0$

$$\Rightarrow (T_r^2+V_r^2)\left[1+V_r+\sqrt{\frac{T_r}{(1+V_r)(1+T_r)}\left[V_r^2(3+2T_r)+10XT_r+3V_r+V_rT_r(8X+2V_r)\right]}\right]=V_r(1+V_r)*$$
$$*\left[T_r+V_r+4XT_r/(1+T_r)\right] \qquad \text{(D-36)}$$

or if A assumed to be constant and first use Vr=1 to calculate A, then the optimum Vr can be calculated from the following quadratic equation:

$$V_r^2\left(1-A^2-A^2\sqrt{1-A^2}\right)-V_r\left(A^2+A^2T_r+4XA^2\frac{T_r}{1+T_r}+2A^2\sqrt{1-A^2}\,T_r+8A^2\sqrt{1-A^2}X\frac{T_r}{1+T_r}-1\right)-$$
$$-A^2*T_r-\frac{4XT_r}{1+T_r}A^2-A^2\sqrt{1-A^2}\,T_r^2-16\left(\frac{AXT_r}{1+T_r}\right)^2\sqrt{1-A^2}-8A^2X\sqrt{1-A^2}*\frac{T_r^2}{1+T_r}=0$$

(D-37)

Finally, to find the optimum phase angle difference ϕ, the derivative of output is taken respect to ϕ:

$$\frac{\partial W}{\partial\varphi}=\Pi*\frac{1-T_r}{1+V_r}*\frac{\partial\left[A/(1+\sqrt{1-A^2})*\sin\theta\right]}{\partial\varphi} \qquad \text{(D-38)}$$

$$\frac{\partial}{\partial\varphi}\left[A/(1+\sqrt{1-A^2})\right]=\frac{-A\,T_r\,V_r}{\sqrt{1-A^2}\left[1+\sqrt{1-A^2}\right]}*\frac{\sin\varphi}{\left[T_r+V_r+4X\frac{T_r}{1+T_r}\right]^2}$$

$$\tan\theta=\frac{V_r\sin\varphi}{T_r+V_r\cos\varphi}$$

$$\Rightarrow \sin\theta=\frac{V_r*\sin\varphi}{\sqrt{T_r^2+V_r^2+2V_rT_r\cos\varphi}}$$

$$\Rightarrow \frac{\partial(\sin\theta)}{\partial\varphi}=\frac{\sin\theta}{\sin\varphi}*\cos\varphi+\frac{V_r\cdot T_r\cdot\sin\varphi*\sin\theta}{T_r^2+V_r^2+2\cdot V_r\cdot T_r\cdot\cos\varphi}$$

(D-39)

$$\frac{\partial W}{\partial\varphi}=\Pi*\frac{1-T_r}{1+V_r}*\left[\frac{A}{1+\sqrt{1-A^2}}\left(\sin\theta\cdot\cot\varphi+\frac{V_r\cdot T_r\cdot\sin\varphi\cdot\sin\theta}{T_r^2+V_r^2+2V_rT_r\cos\varphi}\right)-\frac{A\cdot T_r\cdot V_r*\sin\varphi\cdot\sin\theta}{\sqrt{1-A^2}\left[1+\sqrt{1-A^2}\right]\left[T_r+V_r+4X\frac{T_r}{1+T_r}\right]^2}\right]$$

$$\frac{\partial W}{\partial \varphi} = 0$$

$$\Rightarrow \quad \frac{1}{TAN\varphi} + \frac{V_r \cdot T_r \cdot SIN\varphi}{T_r^2 + V_r^2 + 2V_r T_r \cos\varphi} - \frac{T_r \cdot V_r \cdot SIN\varphi}{\sqrt{1-A^2}\left[T_r + V_r + 4X T_r/(1+T_r)\right]^2} = 0$$

(D-40)

Or

$$COT(\varphi) \cdot \left[T_r^2 + V_r^2 + 4X\frac{T_r}{1+T_r}\right]^2 + \frac{V_r T_r}{A^2} SIN\varphi - \frac{V_r T_r SIN\varphi}{\sqrt{1-A^2}} = 0$$

$$\Rightarrow \quad V_r \cdot T_r\left[\frac{1}{\sqrt{1-A^2}} - \frac{1}{A^2}\right]\cos^2\varphi + \left[T_r^2 + V_r^2 + 4X\frac{T_r}{1+T_r}\right]^2 \cos\varphi + V_r T_r\left[\frac{1}{A^2} - \frac{1}{\sqrt{1-A^2}}\right] = 0$$

(D-41)

This quadratic equation would give the optimum design ϕ based on the schmidt analysis.

APPENDIX(E)

Ideal Engine with Dead Volume

Since the isothermal compression and expansion is still held, then:

$$W_{Exp.} = \int P * dV_E \tag{E-1}$$

$$P = (M * R) / \left[\frac{V_H}{T_H} + \frac{V_D}{T_R} \right] \tag{E-2}$$

Where

VD=1/2(total dead volume)

TR=TH-TC/ln TH/TC

$$W_{Exp.} = \int_{V_{H1}}^{V_{H2}} \frac{M * R}{V_H/T_H + V_D/T_R} * dV_E = M * R * T_H * ln \left[\left(\frac{V_{H2}}{T_H} + \frac{V_D}{T_R} \right) / \left(\frac{V_{H1}}{T_H} + \frac{V_D}{T_R} \right) \right] \tag{E-3}$$

$$W_{Comp.} = \int P * dV_C \tag{E-4}$$

$$P = (M * R) / \left[\frac{V_C}{T_C} + \frac{V_D}{T_R} \right] \tag{E-5}$$

$$W_{Comp.} = \int_{V_{C1}}^{V_{C2}} \frac{M * R}{V_C/T_C + V_D/T_R} dV_C = M * R * T_C * ln \left[\left(\frac{V_{C2}}{T_C} + \frac{V_D}{T_R} \right) / \left(\frac{V_{C1}}{T_C} + \frac{V_D}{T_R} \right) \right]$$

(E-6)

$$W_{OUT} = M * R * T_C \left[\frac{T_H}{T_C} ln \frac{\frac{V_{H2}}{T_H} + \frac{V_D}{T_R}}{\frac{V_{H1}}{T_H} + \frac{V_D}{T_R}} - ln \frac{\frac{V_{C2}}{T_C} + \frac{V_D}{T_R}}{\frac{V_{C1}}{T_C} + \frac{V_D}{T_R}} \right]$$

(E-7)

$$V_{H1} = V_{C1} \quad , V_{H2} = V_{C2} \tag{E-8}$$

$$V_D / V_T = X \tag{E-9}$$

$$V_{H2} / V_{H1} = \bar{A} \tag{E-10}$$

$$V_T = V_D + V_{H1} + V_{C2} = V_D + V_{H2} + V_{C1} \tag{E-11}$$

Or, $$1 = \frac{V_D}{V_T} + \frac{V_{H1}}{V_T} + \frac{V_{C2}}{V_T} = X + \frac{V_{H1}}{V_T} + \frac{\bar{A} \cdot V_{H1}}{V_T} \tag{E-12}$$

$$1 = X + \frac{V_{H1}}{V_T}(1+\bar{A}) \Rightarrow \frac{V_{H1}}{V_T} = \frac{V_{C1}}{V_T} = \frac{1-X}{1+\bar{A}} \tag{E-13}$$

$$\therefore \quad \frac{V_{H2}}{V_T} = \frac{V_{C2}}{V_T} = \frac{1-X}{1+A} * \bar{A} \tag{E-14}$$

$$W_{OUT} = M * R * T_C \left[\frac{T_H}{T_C} \ln \frac{\frac{1-X}{1+\bar{A}} A/T_H + \frac{X}{T_R}}{\frac{1-X}{1+\bar{A}} * \frac{1}{T_H} + \frac{X}{T_R}} - \ln \frac{\frac{1-X}{1+\bar{A}} * \frac{\bar{A}}{T_C} + \frac{X}{T_R}}{\frac{1-X}{1+\bar{A}} * \frac{1}{T_C} + \frac{X}{T_R}} \right] \tag{E-15}$$

If X=0 then, $W_{OUT} = M * R * T_C \left[\frac{T_H}{T_C} \ln \frac{P_1}{P_2} - \ln \frac{P_1}{P_2} \right]$

$\bar{A} = P1/P2 = \frac{V_{H2}}{V_{H1}}$ (Isotherm)

Then,

$$\frac{W_{OUT}}{W_{OUT,Ideal}} = \frac{\frac{T_H}{T_C} \ln \left[\frac{\frac{1-X}{1+\bar{A}} * \frac{\bar{A}}{T_H} + \frac{X}{T_R}}{\frac{1-X}{1+\bar{A}} * \frac{1}{T_H} + X/T_R} \right] - \ln \left[\frac{\frac{1-X}{1+\bar{A}} * \frac{\bar{A}}{T_C} + \frac{X}{T_R}}{\frac{1-X}{1+\bar{A}} * \frac{1}{T_C} + X/T_R} \right]}{(T_H/T_C - 1) \ln \bar{A}} \tag{E-16}$$

$$\frac{T_R}{T_H} = \frac{1 - T_C/T_H}{\ln T_H/T_C} \quad , \frac{T_R}{T_C} = \frac{T_H/T_C - 1}{\ln T_H/T_C}$$

APPENDIX(F)

Stress Analysis for Cylinder Thickness

Consider the following cylinder with Pm to be the mean pressure inside of it and it has radius R and thickness t.

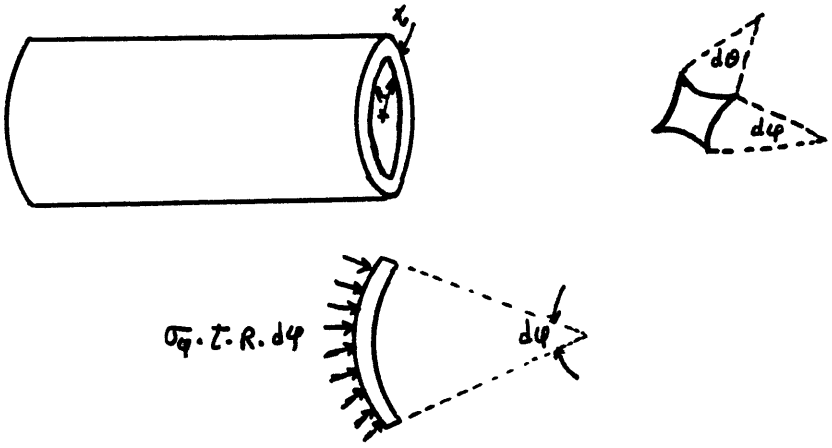

From the stress analysis for a thin cylinder [27] the following equation is resulted:

$$\sigma\phi/R1+\sigma\theta/R2=Pm/t$$

For cylinder:

$$R1=\infty \quad , \quad R2=R$$

Therefore,

$$\sigma\theta=Pm*R/t \quad , \quad \sigma\phi=Pm*R/2t$$

In order to consider the thermal effects too, let the allowable stress be 5000 Psi, then:

$$t=(Pm*R)/5000$$

APPENDIX(G)

In reference [10] the temperature distribution in the radial direction of the cylinder of a Stirling engine has been calculated as:

$$T(t,x) = T_m\left[1 - \frac{k-1}{k} * \frac{P_1}{P_m}\left[1 - e^{(i+1)x/\lambda}\right] * e^{i\omega t}\right]$$

Since temperature is a real quantity, then by using the appropriate phase angles we can write this temperature distribution as:

$$T(t,x) = T_m\left[1 - \frac{k-1}{k} * \frac{P_1}{P_m}\left[1 - e^{-x/\lambda} * SIN(x/\lambda - \varphi_x)\right] * SIN(\omega t - \varphi_p)\right] \qquad (G\text{-}1)$$

Where ϕ_x and ϕ_p are phase differences between temperature and pressure waves with respect to the expansion volume displacement.

In order to calculate the upper bound of the temperature difference between the gas and the cylinder wall we can assume:

$$e^{-x/\lambda} * SIN(x/\lambda - \varphi_x) \approx e^{-x/\lambda} \approx e^{-1}$$

$$\Rightarrow \quad T(t) = T_m\left[1 - \frac{k-1}{k} * \frac{P_1}{P_m}(1 - e^{-1})\right] SIN(\omega t - \varphi_p) \qquad (G\text{-}2)$$

$$\text{or} \quad \frac{\Delta T}{T_m} = \frac{k-1}{k} * \frac{P_1}{P_m} * (1 - e^{-1}) * SIN(\omega t - \varphi_p) \qquad (G\text{-}3)$$

This temperature difference can be used to calculated the corresponding heat transfer, as follows.

$$Q = h * A * \Delta T \qquad (G\text{-}4)$$

The following figure shows a cylinder with sinusoidal volume variation and constant cross-sectional area.

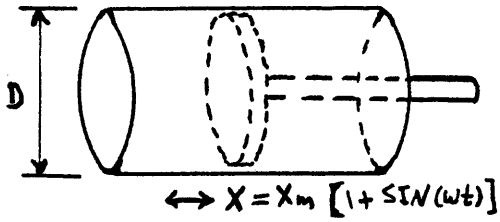

For this cylinder the instantaneous heat transfer area is:

$$A = \pi * D * X = \pi \cdot D \cdot X_m \left(1 + SIN(\omega t)\right) \qquad \text{(G-5)}$$

The heat transfer coefficient (h) is calculated from the following empirical correlations:

$$\frac{h * D}{K_g} = .023\ (Re)^{.8}\ (P_r)^{.4} \qquad \text{(G-6)}$$

Therefore,

$$Q(t) = .023\,(1-\bar{e}')\cdot\pi\cdot K_g \cdot X_m \cdot \frac{k-1}{k}\cdot\frac{P_i}{P_m}\cdot T_m \cdot (1+SIN\omega t)\cdot SIN(\omega t-\varphi_p)\cdot (Re)^{.8}(P_r)^{.4} \qquad \text{(G-7)}$$

The average heat transfer over a cycle would be:

$$Q_{av} = \frac{1}{2\pi}\int_0^{2\pi} Q(t)\cdot d(\omega t)$$

$$Q_{av} = .023(1-\bar{e}')K_g \cdot X_m \cdot T_m \cdot \frac{k-1}{k}\cdot\frac{P_i}{P_m}(Re)^{.8}(P_r)^{.4}\int_0^{\pi}(1+SIN\omega t)\left[SIN(\omega t-\varphi_p)\right]\cdot d(\omega t)$$

$$Q_{av} = \underbrace{.023(1-\bar{e}')\left(2+\frac{\pi}{2}\right)}_{.052}\cdot K_g \cdot T_m \cdot \frac{k-1}{k}\cdot\frac{P_i}{P_m}\cdot (Re)^{.8}(P_r)^{.4}\cdot\cos\varphi_p \qquad \text{(G-8)}$$

Lumped Model Approach

Since each cylinder can be modelled as a combination of thermal capacitances and resistances, then the circuit and bond graph for a cylinder

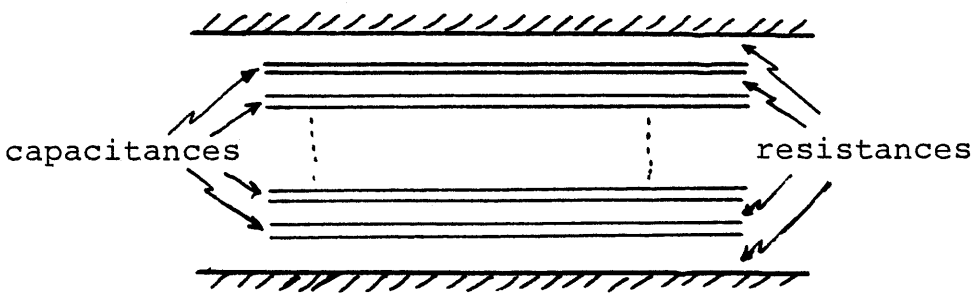

would be:

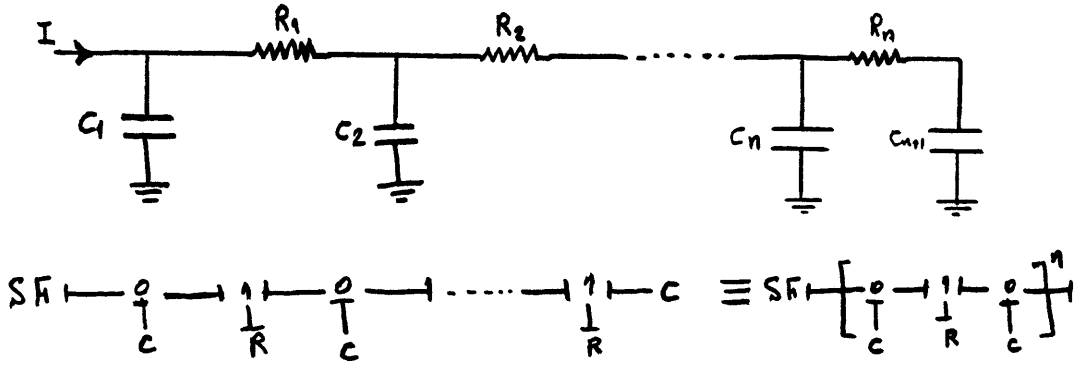

The simplest model would be a two-lump one:

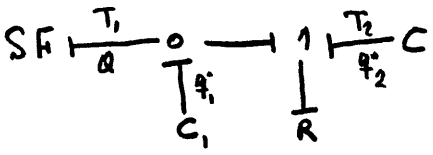

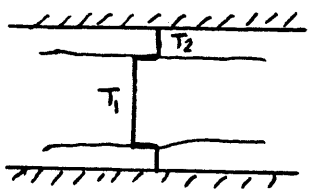

State equation for this system are:

$$\dot{q}_1 = Q - \dot{q}_2 = Q - \frac{1}{R}(T_1 - T_2)$$

$$\dot{q}_2 = \frac{1}{R}\left(\frac{1}{C_1} q_1 - \frac{1}{C_2} q_2\right)$$

In terms of the temperature:

$$T_1/Q = \frac{1+\tau_1 S}{C_t S(1+\tau_0 S)} \qquad \text{(G-9)}$$

$$T_2/Q = \frac{1}{C_t S(1+\tau_0 S)} \qquad \text{(G-10)}$$

Where $t_1=RC_2$, $t=RC_1C_2/(C_1+C_2)$, $C_t=C_1+C_2$, $S\equiv d/dt$

If we assume a one-lump system then its temperature would be the mean temperature of the more detailed system.

$$Q=C_t*S*T_m$$

or

$$\frac{T_1}{T_m} = \frac{1+\tau_1 S}{1+\tau_0 S} \qquad \text{(G-11)}$$

$$\frac{T_2}{T_m} = \frac{1}{1+\tau_0 S} \qquad \text{(G-12)}$$

If we substitude $i\omega$ for S, then $T_1/T_m = \frac{1+\tau_1 j\omega}{1+\tau_0 j\omega}$, this can include the first order approximation to $e^{i\omega t}$; therefore, the equation in reference [10] or equation (2-22) can be easily derived from the above approach. If t_1 and t are selected properly, then the two-lump approximation would be very close to the exact solution.

Calculation of t & t_1

For a two-lump model, the cylinder can be divided to two sections a smaller cylinder and an annular which covers the first one.

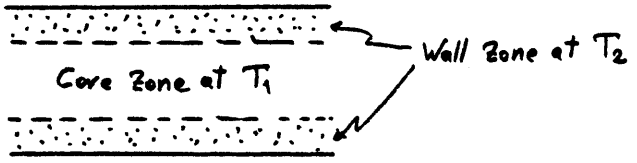

$$t_1 = RC_2 \qquad \text{(G-13)}$$

$$t = RC_1C_2/(C_1+C_2) \qquad \text{(G-14)}$$

C_2 is the thermal capacitance of the annular, C_1 is the thermal capacitance of the internal cylinder, and R is the thermal resistance between them. Since t has the dimension of time and R has dimension [hr R/Btu] then C should have the dimension [Btu/ R]. Since the volume of gas is changing with time then average value which is the volume variation amplitude is used.

$$C_t = m_t * C_V = \frac{P_m}{RT} * \frac{\pi}{4} B^2 * S_{/2} * C_V = \frac{\pi}{8} * \frac{P_m}{T} * \frac{B^2 S}{k-1} \qquad \text{(G-15)}$$

Assume $C_1/C_t = \alpha$, then $C_2/C_t = 1-\alpha$

$$C_1 = \frac{\pi}{8} * \frac{P_m}{T} * \frac{B^2 S}{k-1} * \alpha \qquad \text{(G-16)}$$

$$C_2 = \frac{\pi}{8} * \frac{P_m}{T} * \frac{B^2 S}{k-1} (1-\alpha) \qquad \text{(G-17)}$$

For resistance R, consider the following cross-sectional area of the cylinder:

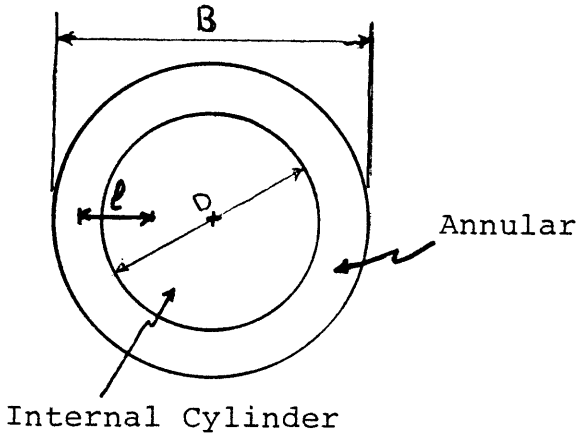

The characteristic length which is going to be used for calculating R would be the summation of one-half of the internal cylinder radius and thickness of a gap which has volume equal to the one-half of annular volume. Heat transfer mechanism between these two sections can be considered as a combination of conduction and convection.

Since each cylinder has a uniform temperature, then coefficient of heat transfer can be assumed to be [23]:

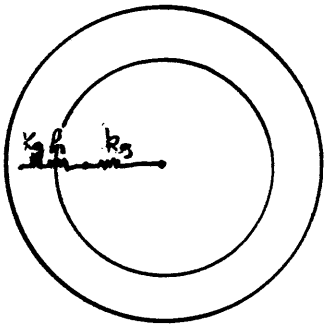

$Nu_R = 3.66 \qquad h = 3.66\ kg/D$ (G-18)

$$R = \frac{\ell}{k_g A} + \frac{1}{h A} = \frac{\ell}{\pi/2 \cdot D \cdot S \cdot k_g} + \frac{1}{\frac{\pi}{2} \cdot 3.66\, S k_g} = \frac{2}{\pi k_g S}\left(\frac{\ell}{D} + \frac{1}{3.66}\right) \quad \text{(G-19)}$$

D is the internal cylinder diameter

$$\frac{\pi}{4} D^2 * \frac{S}{2} = \alpha * \frac{\pi}{4} B^2 * \frac{S}{2}$$

or $$D = \sqrt{\alpha} * B \quad \text{(G-20)}$$

1/2 Gap volume= $\frac{\pi}{8}(1-\alpha) B^2 * \frac{S}{2}$

1/2 Gap volume +Internal cylinder volume= $\frac{\pi}{16}(1-\alpha)B^2 S + \frac{\pi}{8}\alpha B^2 S \equiv \frac{\pi}{8} C^2 S$

$$\Rightarrow \quad C^2 = \frac{1-\alpha}{2} B^2 + \alpha B^2 = \frac{B^2(1+\alpha)}{2}$$

$$C = B\sqrt{(1+\alpha)/2} \quad \text{(G-21)}$$

Therefore:

$$\ell/D = \frac{\ell\sqrt{\alpha}}{B} = \sqrt{\frac{\alpha(1+\alpha)}{8}} - \frac{\alpha}{4} \qquad \text{(G-22)}$$

$$\Rightarrow \quad R = \frac{2}{\pi K_g S}\left(\sqrt{\frac{\alpha(1+\alpha)}{8}} - \frac{\alpha}{4} + \frac{1}{3.66}\right) \qquad \text{(G-23)}$$

$$\tau_1 = R C_2 = R(1-\alpha)C_t = \frac{P_m \cdot B^2(1-\alpha)}{4 T \cdot K_g (k-1)}\left(\sqrt{\frac{\alpha(1+\alpha)}{8}} - \frac{\alpha}{4} + \frac{1}{3.66}\right) \qquad \text{(G-24)}$$

$$\tau_0 = R C_1 C_2 / C_t = R\alpha(1-\alpha)C_t = \frac{P_m \cdot B^2 \cdot \alpha(1-\alpha)}{4 T \cdot K_g (k-1)}\left(\sqrt{\frac{\alpha(1+\alpha)}{8}} - \frac{\alpha}{4} + \frac{1}{3.66}\right) \qquad \text{(G-25)}$$

The only unknown for calculating t_1 & t is α. Since we are considering the radial direction, then it would be resonable to assume $\alpha=0.5$. Based on this value for α, we get:

$$\tau_1 = .056 \cdot P_m \cdot B^2/[T \cdot K_g \cdot (k-1)] \qquad \text{(G-26)}$$

$$\tau_0 = .0284 \cdot P_m \cdot B^2/[T \cdot K_g \cdot (k-1)] \qquad \text{(G-27)}$$

Example:

For hot cylinder with TH=860 R and Pm=500 Psia, B=1.5 in t and t_1 will be:

Assuming helium for working fluid.

TH=860 R

k_g=.118 Btu/hr ft R

$$\tau_0 = \frac{.0284 \cdot 500 \cdot (1.5)^2 \cdot 3600}{860 \cdot .118\,(1.66-1) \times 778} = 2.2 \text{ Sec} \quad \therefore \tau_1 = 4.4 \text{ Sec}$$

APPENDIX(H)

Derivation of State-Equations for Stirling Engine with Perfect Components

Differential equations governing the behavior of a two cylinder Stirling engine with perfect components will be derived with the following assumptions:

a)- The cylinders are adiabatic.

b)- All heat-exchange components are perfect, i.e. no gas-to-wall temperature difference, no axial conduction, and no pressure drop.

c)- The temperature at any point in the heat-exchangers is constant with time.

d)- The temperature is uniform at any crossection perpendicular to the direction of flow.

e)- The gas in the cylinders is perfectly mixed.

f)- The working fluid is an ideal gas.

g)- The mass of the working fluid remains constant throughout the cycle (no leakage).

Assumptions (a) and (b) will allow the first law of thermodynamics to be applied without regard to the heat transfer properties of the gas or any flow considerations.

Assumption (c) allows the mass of working fluid in the heat exchange components to be written as a function of pressure only.

Consider now a cylinder from the engine shown in Fig.(15). The total volume swept by the piston in the cylinder is $2V_A$. The variable V_A will be referred to as the volume variation amplitude.

At time t the volume available to the working gas in the cylinder is V, and the mass contained in this volume is m. The pressure in the cylinder will be denoted by P.

The heat exchanger adjacent to this cylinder exchanges heat with the working fluid at a temperature T^*. Since it has been assumed that there is no gas-to-heat-exchanger-wall temperature difference, then the temperature of the gas entering the cylinder will always be T^*.

The first law of thermodynamics may be written for the control volume consisting of the volume swept by the piston in the cylinder as

$$dE = dQ - P\,dV + h \cdot dm \qquad \text{(H-1)}$$

Where E is the energy of the gas in the control volume, Q is the heat transferred to the gas and h is the specific enthalpy of the gas.

The term dQ in (H-1) is equal to zero for an adiabatic cylinder, and the perfect gas relationship permits writing the other variables in terms of the specific heats C_p and C_v. When gas is moving into the control volume

$$C_v\,dT = -P\,dV + C_p T^* dm \qquad [dm > 0] \qquad \text{(H-2)}$$

and when gas is moving out of the control volume

$$C_v\,dT = -P\,dV + C_p T\,dm \qquad [dm < 0] \qquad \text{(H-3)}$$

With the introduction of the perfect gas relationship (H-2) and (H-3) may be rewritten as

$$dm = \frac{P\,dV}{RT^*} + \frac{1}{k}\frac{V\,dP}{RT^*} \qquad \text{(H-4)}$$

and $$dm = m\left(\frac{dV}{V} + \frac{1}{k}\frac{dp}{p}\right) \quad [dm < 0] \tag{H-5}$$

Where K is the specific heat ratio C_p/C_v and R is the gas constant.

Equations (H-4) and (H-5) are valid for both the hot cylinder, which will be denoted by the subscript h, or the cold cylinder, which will be denoted by the subscript c. Since it has been assumed that the heat-exchange components introduce no pressure drop, then the pressure P will be uniform throughout the system at all times.

The mass in the heat-exchange components or dead space is proportional to the pressure in the system. Therefore, we get the following.

$$m_d = V_d * P * VH/(R * TH) \tag{H-6}$$

The quantity V_d represents the ratio of the mass contained in the dead space to the mass contained in one half the volume displaced by the warm piston at the same pressure and at temperature TH. This mass ratio V_d may be called the reduced dead volume, since it represents the effect of introducing dead space in the system. The amount of working gas which must be moved in an out of the dead space without actually moving through all the heat-exchange components is proportional to V_d for a given pressure ratio. This means that additional work must be transferred in and out of the system in order to pressurize the dead space without actually increasing the net work.

If (H-6) is differentiated, then the change of mass in the dead space is given by:

$$dm_d = V_d * V_H * dP/(R * T_H) \tag{H-7}$$

Based on assumption (g) we get:

$$m_T = m_c + m_d + m_R = \text{Const.} \tag{H-8}$$

or

$$dm_c + dm_d + dm_R = 0 \tag{H-9}$$

Because working gas may be accumulated in the dead space, there are four different possible combinations for the direction in which mass is moving at the interfaces between the cylinders and the adjacent heat exchangers. These possible combinations are:

$$dm_c > 0 \ , \ dm_R > 0 \tag{H-10a}$$

$$dm_c < 0 \ , \ dm_R < 0 \tag{H-10b}$$

$$dm_c < 0 \ , \ dm_R > 0 \tag{H-10c}$$

$$dm_c > 0 \ , \ dm_R < 0 \tag{H-10d}$$

When (H-4), (H-5) and (H-7) are introduced in (H-9) for case (H-10a) the result is

$$\frac{P\,dV_c}{R\,T_C} + \frac{1}{R}\frac{V_c\,dP}{R\,T_C} + V_d\frac{V_R\,dP}{R\,T_H} + \frac{P\,dV_R}{R\,T_H} + \frac{1}{R}\frac{V_R\,dP}{R\,T_H} = 0$$

$$[\,dm_c > 0, \ dm_R > 0\,] \tag{H-11}$$

If the variables

$$P \equiv \frac{P}{P_{max}} \ , \ V_c \equiv \frac{V_c}{V_C} \ , \ V_R \equiv \frac{V_R}{V_H} \ , \ r_{Vt} = \frac{V_C}{V_H}\cdot\frac{T_H}{T_C} \tag{H-12}$$

are introduced, where P_{max} is the maximum pressure during the cycle, then (H-11) may be rewritten as

$$P\left(r_{vt}\, dV_c + dV_R\right) + \left(\frac{1}{k}\, r_{vt}\, V_c + \frac{1}{k}\, V_h + V_d\right) dP = 0$$

$$\left[dm_c > 0\,,\ dm_R > 0\right] \tag{H-13}$$

This leads to the differential equation

$$dP = -kP\, \frac{r_{vt}\, dV_c + dV_R}{r_{vt}\, V_c + V_R + k\, V_d} \qquad \left[dm_c > 0,\ dm_R > 0\right] \tag{H-14}$$

for the dimensionless pressure.

The differential equation for the mass in the cold cylinder is given by (H-4) as

$$dm_c = \frac{P\, dV_c}{R\, T_C} + \frac{1}{k}\, \frac{V_c\, dP}{R\, T_C} \qquad \left[dm_c > 0\right] \tag{H-15}$$

If the dimensionless mass variable

$$M_c \equiv \frac{m_c \cdot R \cdot T_C}{P_{max} \cdot V_C} \tag{H-16}$$

is defined, then (H-15) may be written as

$$dM_c = P \cdot dV_c + \frac{1}{k}\, V_c\, dP \qquad \left[dM_c > 0\right] \tag{H-17}$$

Similarly, the differential equation for the mass in the warm cylinder is given by (H-4) as

$$dm_R = \frac{P\, dV_R}{R\, T_H} + \frac{1}{k}\, \frac{V_R \cdot dP}{R\, T_H} \qquad \left[dm_R > 0\right] \tag{H-18}$$

If the dimensionless mass variable

$$M_R \equiv \frac{m_R \cdot R \cdot T_H}{P_{max} \cdot V_H} \tag{H-19}$$

is defined, then (H-18) may be written as

$$dM_R = P \cdot dV_R + \frac{1}{k}\, V_R \cdot dP \qquad \left[dM_R > 0\right] \tag{H-20}$$

The work W may be found by integrating p dV for the appropriate cylinder, or if a dimensionless work W is defined

$$w_c \equiv \frac{\oint p\, dV_c}{p_{max}\, V_C} = \oint P \cdot d\vec{v}_c \qquad \text{(H-21)}$$

and

$$w_e \equiv \frac{\oint p\, dV_R}{p_{max}\, V_H} = \oint P \cdot d\vec{v}_R \qquad \text{(H-22)}$$

Since (H-9) must be satisfied at all times, the mass changes in the cylinders are related by

$$r_{vc}\, dM_c + dM_R + \vec{v}_d \cdot dP = 0 \qquad \text{(H-23)}$$

When the same procedure is followed for case (H-10b) the differential equation for the pressure becomes

$$dP = -k\, \frac{r_{vc} M_c \frac{d\vec{v}_c}{\vec{v}_c} + M_R \frac{d\vec{v}_R}{\vec{v}_R}}{\frac{r_{vc} M_c}{P} + M_R/\rho + k\vec{v}_d} \qquad [dM_c < 0,\ dM_R < 0] \qquad \text{(H-24)}$$

While the mass changes are given by

$$dM_c = M_c \left(\frac{d\vec{v}_c}{\vec{v}_c} + \frac{1}{k} \frac{dP}{P} \right) \qquad [dM_c < 0] \qquad \text{(H-25)}$$

and

$$dM_R = M_R \left(\frac{d\vec{v}_R}{d\vec{v}_R} + \frac{1}{k} \frac{dP}{P} \right) \qquad [dM_R < 0] \qquad \text{(H-26)}$$

The same procedure may again be followed for cases (H-10c) and (H-10d) to yield the equations

$$dP = -k\, \frac{P\, d\vec{v}_R + r_{vc} M_c \frac{d\vec{v}_c}{\vec{v}_c}}{\vec{v}_R + r_{vc} \frac{M_c}{P} + k\vec{v}_d} \qquad [dM_c < 0,\ dM_R > 0] \qquad \text{(H-27)}$$

and

$$dP = -k\, \frac{r_{vc}\, P\, d\vec{v}_c + M_R \frac{d\vec{v}_R}{\vec{v}_R}}{r_{vc} \cdot \vec{v}_c + \frac{M_R}{P} + k\vec{v}_d} \qquad \text{(H-28)}$$

Equations (H-14), (H-17), and (H-20) through (H-29) describe the behavior of the Stirling cycle with adiabatic cylinders and perfect heat-exchange components. These equations may be integrated numericalyy for an arbitrary set of volume variations. The integration would consist of taking a step with the appropriate pressure differential equation and integrating the mass changes will determine whether the step in the integration is valid or whether a new set of equations must be used. It is necessary, however, to start the integration by assuming a given mass or temperature in the cylinders, and by selecting either (H-1-a), (H-10b), (H-10c) or (H-10d) to start.

The integration has been carried out by the computer program described in Appendix I for two crank-connecting-rod volume variations with no clearance volume. The volume relation is calculated in a separate subroutine which may be changed to an arbitrary set of volume variations. The details of the integration of the equations are given in Appendix I.

The reduced dead volume Vd may be calculated by assuming that all the gas in the cold space is at TC; the gas in the warm space is at TH. The gas in the regenerator is assumed to be at TR.

Equation (H-6) may be rewritten as

$$\tau_d = \tau_{dc} + \tau_{dR} + \tau_{dH} \qquad \text{(H-29)}$$

Where

$$\tau_{dc} = \frac{VDC}{VH} * \frac{TH}{TC} \qquad \text{(H-30)}$$

$$v_{dR} = \frac{V_{DR}}{V_H} \left(\frac{2\,T_H}{T_C + T_H} \right) \qquad \text{(H-31)}$$

and

$$v_{dR} = \frac{V_{DH}}{V_H} \cdot \frac{T_H}{T_H} = \frac{V_{DH}}{V_H} \qquad \text{(H-32)}$$

APPENDIX(I)

Computer Program of Complete Model

The equations for the pressure, mass and work derived in Appendix(H) may be written in discrete form in order to perform a numerical integration of these variables for a complete cycle.

The values of volume, mass and pressure at the beginning of a step are used to calculate the values of the same variabels after one half a step. These values are then used as an average for the calculation of a complete step.

The computer program consists of a main program and five subroutines.

Main Program

The inputs for this program are:

TH: Hot source temperature in (^{o}R)

TC: Cold source temperature in (^{o}R)

ZZC,ZZW: A crank-connecting rod mechanism is assumed. This is the ratio of the connecting rod length to one half the stroke for the cold and warm crankcases respectively.

XNHT: The value of the exponent of the Reynolds number in the heat-transfer correlation for the regenerator matrix.

SHR: Specific-heat ratio K for the working gas.

NFI: A crankshaft revolution is divided up into NDIV

steps. The variable NFI is the number of steps which represent the phase angle between the volumes.

NDIV: The number of divisions into which a crankshaft revolution is divided.

NWR: This is an index which will govern the amount of printout from the program. If it is zero the printout will show only the results for the overall performance. If it is greater than zero it will show values of the variables versus crank angle.

NDS: The number of locations in the dead space for which the pressure-drop and heat-transfer integrals are to be calculated.

VAC: Amplitude of cold cylinder volume variation (in^3)

VAH: Amplitude of hot cylinder volume variation (in^3)

DRR: Diameter of regenerator cross-sectional area (in)

LR: Regenerator length (in)

VDEER: Ends clearance volume of regenerator (in^3)

σ: Regenerator effectiveness

d : Wire or sphere diameter of regenerator filling material (in)

DC: Tube diameter for cooler (in)

LC: Cooler tube length (in)

NC: Number of tubes in cooler

VDC: Ends clearance volume of cooler (in^3)

DH: Tube diameter for heater (in)

LH: Tube length in heater (in)

NH: Number of tubes in heater

VDH: Ends clearance volume of heater (in^3)

N: Engine speed (RPM)

Pm: Mean pressure in the system (Psia)

Qin: Input heat rate (Watts)

R: Gas constant for working fluid (lbf-ft/lbm R)

M: Molecular weight of the working fluid

SW1: Switch for addition or elimination (1 or 0) of mechanical friction loss.

cyL: Indicates wire or sphere (1,0) is used in the regenerator.

The main program starts by reading in the above variables. Since the integration proceeds in steps of equal crank-angle changes, the change DALF is calculated. The integration starts with the crank angle at a value of $3/2\pi$. At this angle the cold cylinder is at top dead center.

Subroutine VOLC and VOLW are called. These subroutines will fill in arrays C, C1, DC, DCI, W, WI, DW, DWI with the values of the volume halfway through a step (C,W), the value of the volume at the beginning of a step (C1, WI), the changes in volume for a step based on the volume derivatives at the beginning of a step (DCI,DWI) and halfway through a step (DC, DW), for the cold and warm volumes respectively. These subroutines are set up for a crank and connecting-rod mechanism, but may be changed for any other relationship.

One set out of the four possible sets of equations is selected depending on the sign of the mass change in the cylinders. The array IND (I, J) describes whether a mass

change is positive (index set equal to 1) or negative (index set equal to 2). The first index refers to the warm mass and the second to the cold mass. The set of equations is then selected by the value of IND (I, J) which may be one through four.

The actual integration is carried out in a DO LOOP. Then volumes and the volume changes equal to the proper values and following line determines which of the four sets of equations are to be used.

When a step is taken, the sign of the mass changes is verified. If there has been a change in sign and the equations which have been used are no longer applicable, then the step will be recalculated by using the new set.

It is possible that due to discretization and truncation errors the value of the mass in a cylinder approach a slightly negative value rather than zero at top dead center. In this case, the value of the mass is set to zero and the calculation continues.

Another possibility is that in searching for the proper set of equations to use, the program will get caught in a loop. In this case an arbitrary set is used to calculate the step. This action is noted on the output.

The integration proceeds until top dead center of the other piston is reached. At this point the mass is set to zero and the integration continues.

At the end of each cycle the initial and final values of the warm mass are compared as well as the initial and

final values of the pressure. When the variation from cycle to cycle is small, then the integration is assumed to have reached an overall steady state.

The changes which have been considered satisfactory are 0.001 for the mass and 0.005 for the pressure. Since both these variables are of the order of one this amounts to about 0.1% and 0.5% change. This point has usually been reached after two cycles.

When the cyclic integration has been completed, then values for the overall variables of the cycle. The maximum and minimum pressures are found to obtain the pressure ratio, and the pressures, works and masses are normalized with the maximum pressure. The maximum mass is found to give the value of M_A. An equivalent phase angle between the cold volume and pressure variations is determined by equating the cold cylinder work to that done by sinusoidal volume and pressure variations of the same amplitude. This value will be useful if it is desired to combine the results with those of the one cylinder model.

The subroutine PDINT evaluates the integrals necessary for the evaluation of pressure-drop and heat-transfer losses. These values are shown on the output as

X/L=X

INTEGRAL= $\oint \frac{1}{P} \left| \frac{\partial M_x}{\partial(\omega t)} \right| \cdot \frac{\partial M_x}{\partial(\omega t)} * \frac{\partial V_c}{\partial(\omega t)} \cdot d(\omega t)$

DMRE= $\frac{1}{2\pi} \oint \left| \frac{\partial M}{\partial(\omega t)} \right| \cdot d(\omega t) = \left| \frac{\partial \bar{M}}{\partial(\omega t)} \right|$

XII= I_{1X}

XI2= I_{2X}

XI3= I_{1X}/I_{2X}

Up to this point the basic output power (difference between the expansion and compression power) can be evaluated. Then power losses are calculated, first by calculating (via two DO LOOP) non-dimensional mass flow rates in each component, then first pressure losses and second the heat transfer losses are calculated. Finally the overall performance is computed. A sample of the output of the program is attached. It shows the input data plus all of the power losses in [Watt], total heat input in heater and heat rejection from cooler, net output power and efficiency, torque, mean effective pressure, and total losses. The same quantities normalized based on the net output power is also presented.

The difference between programs of complete-model and optimum design model is that in optimum case correlations for optimization are given to calculate the optimum geometry. Program needs to have some non-zero, initial,geometrical vales for starting the optimization. The optimum model program has optimum bore-stroke ratio equation which will be solved automatically inside the program.

The first part of the output shows the pressure ratio and phase angle difference between pressure wave and hot volume displacement.

APPENDIX(J)

Derivation of Mass Flow Rate in Heat-Exchangers

Considering Fig.(37) which shows a general configuration of a real Stirling engine. For this engine we have

$$V_R = \tfrac{1}{2} V_H (1 + \sin \omega t) \tag{j-1}$$

$$V_C = \tfrac{1}{2} V_C [1 + \sin(\omega t - \varphi)] \tag{j-2}$$

Since the only flow sources for heatexchangers are the cylinders volume variations, then by considering the control volume of Fig.(37) we get the net volume flow in to be:

$$Q_{net} = Q_C + Q_H = \frac{dV_C}{dt} + \frac{dV_R}{dt} \tag{j-3}$$

$$Q_{net} = \tfrac{1}{2} V_H \cdot \omega \cdot \cos \omega t + \tfrac{1}{2} V_C \cdot \omega \cdot \cos(\omega t - \varphi) \tag{j-4}$$

$$= \tfrac{1}{2} V_C \cdot \omega \left[\frac{V_H}{V_C} \cos \omega t + \cos \omega t \cos \varphi + \sin \omega t \cdot \sin \varphi \right]$$

$$= \tfrac{1}{2} V_C \cdot \omega \left[\left(\frac{V_H}{V_C} + \cos \varphi \right) \cos \omega t + \sin \varphi \cdot \sin \omega t \right]$$

or

$$Q_{net} = \tfrac{1}{2} \cdot V_C \cdot \omega \cdot \sin \varphi \left[\frac{V_H/V_C + \cos \varphi}{\sin \varphi} \cos \omega t + \sin \omega t \right] \tag{j-5}$$

If we define α to be:

$$\tan(\alpha) = \left[V_H/V_C + \cos \varphi \right] / \sin \varphi$$

Then equation (j-5) can be written as:

$$Q_{net} = \tfrac{1}{2} \cdot V_C \cdot \omega \cdot \sin \varphi \left[\frac{\sin \alpha \cdot \cos \omega t + \sin \omega t \cdot \cos \alpha}{\cos \alpha} \right]$$

$$Q_{net} = \frac{V_C \cdot \omega \cdot \sin \varphi}{2 \cos \alpha} \cdot \sin(\omega t + \alpha) \tag{j-6}$$

Since Qnet has sinusoidal form with period $2\pi/\omega$ then it has the following figure:

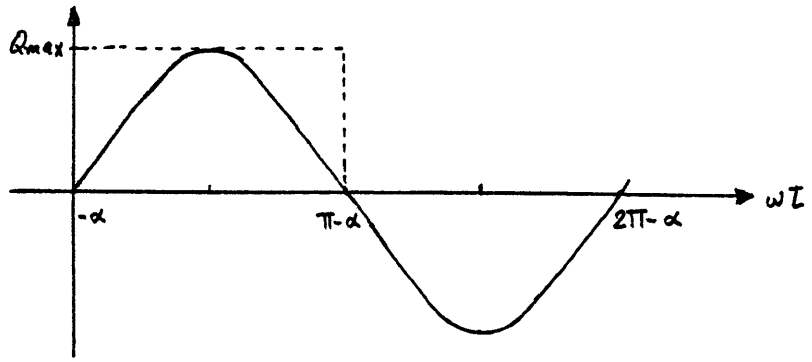

From equation (j-6) we get:

$$Q_{max} = \frac{VC \cdot \omega \cdot SIN\varphi}{2\cos\alpha} \qquad \text{(j-7)}$$

The area under Qnet curve in half of the cycle shows an effective occupied volume during that half cycle.

$$V_{eff} = \int_0^{t_{H.P}} Q_{net} \cdot dt = \frac{Q_{max}}{\omega} \int_{-\alpha}^{\pi-\alpha} SIN(\omega t+\alpha)\, d(\omega t) = \frac{Q_{max}}{\frac{2\pi}{T_p}} \int_{-\alpha}^{\pi-\alpha} SIN(\omega t+\alpha)\, d(\omega t)$$

$$= T_{H.P.} \cdot Q_{max} \cdot \frac{1}{\pi} \left[\cos(\omega t+\alpha)\right]_{-\alpha}^{\pi-\alpha} = T_{H.P.} \cdot Q_{max} \cdot \frac{2}{\pi}$$

$$T_{H.P.} \cdot Q_{max} \cdot \frac{2}{\pi} = V_{eff} \qquad \text{(j-8)}$$

Where T_p is the period and $T_{H.P}$ is half of the period.

Therefore, if we use a correction factor for effective occupied volume we can calculate the volume flow rate to be:

$$Q = \frac{VC \cdot \omega \cdot SIN\varphi}{2\cos\alpha} \cdot F_c$$

Since in the cold end of the system (cooler) the temperature is lower, then by using the ideal gas law we can estimate that maximum pressure should be used for calculating

an average density of gas in heater, minimum pressure should be used for average density in cooler, and the mean pressure should be used for average density of the regenerator. Therefore, we have following pairs of properties for the heat exchangers.

For Heater: $P = P_m (1 + A/\sqrt{1-A^2})$, $T = T_H$ $\Rightarrow$ $\rho_h = \frac{P_m (1 + A/\sqrt{1-A^2})}{R \cdot T_H}$

For Cooler: $P = P_m (1 - A/\sqrt{1-A^2})$, $T = T_C$ $\Rightarrow$ $\rho_c = \frac{P_m (1 - A/\sqrt{1-A^2})}{R \cdot T_C}$

For Regenerator: $P = P_m$, $T = T_R$ $\rho_r = \frac{P_m}{R \cdot T_R}$

Where TR=(TH-TC)/ln(TH/TC)

APPENDIX(K)

Pressure Losses Derivation by Simplified Model

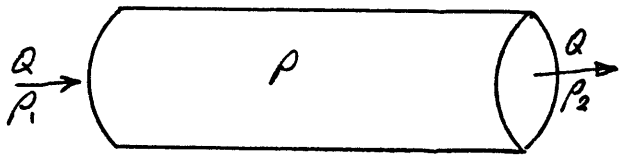

In reference [13] it is shown that for a flow through a component with flow path area AFR, and effective cross-sectional area $A_{eff.}$ the pressure drop would be:

$$\Delta P = \frac{\rho Q^2}{2(AFR)^2}\left[\left(1+\left(\frac{A_{eff}}{AFR}\right)^2\right)\left(\frac{\rho_1}{\rho_2}-1\right) + f\frac{L\cdot\rho_1}{\rho\cdot R_H}\right] \qquad \text{(k-1)}$$

flow acceleration core friction

Where RH=(AFR*L)/AHT, AHT is the total heat transfer area, and f is the friction factor. For the full cycle the acceleration term is negligible because flow rates going to or out of hot and cold spaces are the same. Therefore, the above equation can be written as (assuming $\rho \approx \rho_1$)

$$\Delta P = \frac{1}{2} f \cdot \frac{L}{R_H} \cdot \rho \frac{Q^2}{(AFR)^2} \qquad \text{(k-2)}$$

Equation (3-14) gives the value of Q.

$$\Delta P = \frac{1}{2}\cdot f \cdot \frac{L}{R_H}\cdot \frac{\rho}{(AFR)^2}\cdot\left[\frac{V_c\cdot\omega\cdot SIN\varphi}{2\cos\alpha} + F_c\right]^2 \cdot SIN^2(\omega t+\alpha) \qquad \text{(k-3)}$$

Based on the discussion in Chapter II, the power loss due to the pressure drop is given by:

$$W_{Loss} = \oint \Delta P \, dV_c$$

$$V_c = \bar{V}_c\left[1+SIN(\omega t-\varphi)\right]$$

$$\Rightarrow \quad dV_c = V_c\cdot\omega\cdot\cos(\omega t-\varphi)$$

$$W_{Loss} = \oint \Delta P \cdot dV_c = \frac{2}{T_p} \int_0^{\pi} \frac{1}{\omega} \cdot \Delta P \cdot V_c \cdot \omega \cdot \cos(\omega t - \varphi) \cdot d(\omega t) \qquad \text{(k-4)}$$

Where T_p is the period.

$$W_{Loss} = \frac{f}{2\pi} \cdot \frac{L}{R_H} \cdot \frac{\rho}{(AFR)^2} \cdot \frac{V_c^3 \cdot \omega^3 \cdot \sin^2\varphi}{4\cos^2\alpha} \cdot F_c^2 \cdot \int_0^{\pi} \sin^2(\omega t + \alpha) \cos(\omega t - \varphi) \cdot d(\omega t) \qquad \text{(k-5)}$$

$$\int_0^{\pi} \sin^2(\omega t + \alpha) \cos(\omega t - \varphi) \cdot d(\omega t) = \int_0^{\pi} \tfrac{1}{2} \left[\cos(\omega t - \varphi) - \cos(2\omega t + 2\alpha) \cos(\omega t - \varphi) \right] d(\omega t)$$

$$= \int_0^{\pi} \tfrac{1}{2} \left[\cos(\omega t - \varphi) - \tfrac{1}{2} \cos(3\omega t + 2\alpha - \varphi) - \tfrac{1}{2} \cos(\omega t + 2\alpha + \varphi) \right] \cdot d(\omega t)$$

$$= \tfrac{1}{2} \sin(\omega t - \varphi) - \frac{1}{12} \sin(3\omega t + 2\alpha - \varphi) - \tfrac{1}{4} \sin(\omega t + 2\alpha + \varphi) \Big|_0^{\pi}$$

$$= \sin\varphi + \tfrac{1}{6} \sin(2\alpha - \varphi) + \tfrac{1}{2} \sin(2\alpha + \varphi)$$

Therefore,

$$W_{Loss} = \frac{f}{8\pi} \cdot \frac{L}{R_H} \cdot \frac{\rho}{(AFR)^2} \cdot \frac{V_c^3 \cdot \omega^3 \cdot \sin^2\varphi}{\cos^2\alpha} \cdot F_c^2 \left[\sin\varphi + \tfrac{1}{6} \sin(2\alpha - \varphi) + \tfrac{1}{2} \sin(2\alpha + \varphi) \right] \qquad \text{(k-6)}$$

The only unknown in this equation is f, i.e. friction factor, which is determined as follows.

For Heater:

$$Re_H = \frac{\rho_H V_H D_H}{\mu_H} = \frac{\dot{m}_H \cdot D_H}{AFR_H \cdot \mu_H} \qquad \text{(k-7)}$$

$$Re_H = \frac{4 \dot{m}_H}{\pi D_H N_H \cdot \mu_H} \qquad \text{(k-8)}$$

If ReH<2000

$$f_H = \frac{16}{Re_H} \qquad \text{(k-9)}$$

If ReH>2000

$$f_H = \frac{.0457}{(Re_H)^{.2}} \qquad \text{(k-10)}$$

$\dot{m}H$ is given by equation (3-15).

For Cooler:

$$Re_C = \frac{\rho_C \cdot v_C \cdot D_C}{\mu_C} = \frac{\dot{m}_C \cdot D_C}{AFR_C \cdot \mu_C} \qquad \text{(k-11)}$$

$$Re_C = \frac{4\,\dot{m}_C}{\pi \cdot D_C \cdot N_C \cdot \mu_C} \qquad \text{(k-12)}$$

If ReC<2000

$$f_C = 16/Re_C \qquad \text{(k-13)}$$

If ReC>2000

$$f_C = .0457/(Re_C)^{.2} \qquad \text{(k-14)}$$

$\dot{m}c$ is given by equation (3-16)

For Regenerator:

$$Re_R = \frac{\rho_R v_R \cdot d_R}{\mu_R} = \frac{2\dot{m}_R \cdot d_R}{VDR/L_R \cdot (\mu_H + \mu_C)} \qquad \text{(k-15)}$$

If ReR<60 $f_R = 53.7/(Re_R)^{.93}$ (k-16)

If 60<ReR<1000 $f_R = 5.176/(Re_R).365$ (k-17)

If ReR>1000 $f_R = 1.035/(Re_R)^{.125}$ (k-18)

mR is given by equation (3-17), and VDR is the regenerator dead volume, LR is the regenerator length, and dR is the wire or sphere diameter of the filling materials inside the

regenerator.

Note: For calculation of pressure drop we need to know (L/D) for the regenerator.

$$(L/D)_R = 1/4 * AHT/AFR \qquad \text{(k-19)}$$

Depending on what is inside the regenerator, particle (spheres) or wires, there are two cases.

a)- For Wires:

$$V_{material} = \frac{1-\sigma}{\sigma} * VDR$$

Where VDR is the regenerator dead volume.

An imaginary length for the wires can be determined as:

$$\frac{\pi}{4} * d_w^2 * L_w = V_{material}$$

$$\Rightarrow L_w \equiv 4\, V_{material}/(\pi * d_w^2) = \frac{4}{\pi} * \frac{1-\sigma}{\sigma} * \frac{VDR}{d_w^2} \qquad \text{(k-20)}$$

$$AHT = \pi * d_w * L_w = 4 * \frac{1-\sigma}{\sigma} * \frac{VDR}{d_w}$$

$$AFR = VDR/LR$$

Therefore,

$$(L/D)_R = 1/4 * 4 * \frac{1-\sigma}{\sigma} * \frac{VDR}{d_w} / \left(\frac{VDR}{LR}\right)$$

or

$$(L/D)_R = \frac{1-\sigma}{\sigma} * \frac{LR}{d_w} \qquad \text{(k-21)}$$

This means:

$$DR = \frac{\sigma}{1-\sigma} * d_w \qquad \text{(k-22)}$$

Where σ is the porosity and dW is the wire diameter.

b)- For Sphere Particles:

An imaginary number for the spheres can be determined as:

$$V_{material} = N * \frac{\pi}{6} * d_s^3$$

$$\Rightarrow \quad N = \frac{6\ V_{material}}{\pi\ d_s^3} = \frac{6}{\pi} \cdot \frac{1-\sigma}{\sigma} \cdot \frac{VDR}{d_s^3}$$

$$\Rightarrow \quad AHT = N \cdot \pi\ d_s^2 = 6\ \frac{1-\sigma}{\sigma} \cdot \frac{VDR}{d_s}$$

$$(L/D)_R = 1/4 \cdot 6 \cdot \frac{1-\sigma}{\sigma} \cdot \frac{VDR}{d_s} \Big/ \left(VDR/d_s\right)$$

or $$(L/D)_R = \frac{3}{2} \cdot \frac{1-\sigma}{\sigma} \cdot \frac{L_R}{d_s} \qquad \text{(k-23)}$$

This means:

$$DR = 2/3 \cdot \frac{\sigma}{1-\sigma} \cdot d_s \qquad \text{(k-24)}$$

Where ds is the diameter of the sphere particles.

A Sample of Simplified Model Calculation

For the following temperature-ratio, the optimum design is:

TH=860° R

TC=530° R

VC=2.476*2in^3

VH=2.845*2in^3

Working fluid=helium

Mean pressure=500 Psia

Engine speed=1000 RPM

Phase angle=108

Heater:

LH=9 in

NH=50

DH=.07 in

VHD=1.3 in^3

Cooler:

LC=6.8 in

NC=77

DC=.05 in

VCD=1.22 in^3

Regenerator:

LR=.946 in

DRR=1.5 in

σ=.69

Wire diameter=.0016 in

VRD=1.038 in^3

From equation (3-2):

$$W_{OUT} = \pi N \cdot P_m \cdot A \cdot V_H \cdot \sin\theta \cdot (1 - T_C/T_H) / (1+\sqrt{1-A^2}) * F(T) * F(\varphi) * F(D)$$

$$A = \frac{\sqrt{(T_C/T_H)^2 + 2(T_C/T_H)(V_C/V_H)\cos\varphi + (V_C/V_H)^2}}{T_C/T_H + V_C/V_H + 2 \cdot \frac{T_C}{V_H}\left(\frac{V_{DH}}{T_H} + \frac{V_{DR}}{T_R} + \frac{V_{DC}}{T_C}\right)}$$

$$T_R = (T_H - T_C)/\ln\frac{T_H}{T_C} = 682^\circ R$$

$$V_{DH} = V_{HD} + N_H \cdot \pi \cdot D_H^2 \cdot L_H/4 = 3.032\ in^3$$

$$V_{DC} = V_{CD} + N_C \cdot \pi \cdot D_C^2 \cdot L_C/4 = 2.248\ in^3$$

$$V_{DR} = V_{RD} + \pi \cdot \sigma \cdot D_{RR}^2 \cdot L_R/4 = 2.19\ in^3$$

$$\Rightarrow \quad A = .16$$

$$\tan(\theta) = (V_C/V_H \sin\varphi)/\left[\frac{T_C}{T_H} + \frac{V_C}{V_H}\cos\varphi\right]$$

$$\Rightarrow \theta = 67.2^\circ$$

From equation (3-4):

$F_T(T)=.822$

From equation (3-6):

$F_\varphi(\phi)=.9644$

From equation (3-7B):

$D=(VDH+VDR+VDC)/VC=1.5085$

$F_D(D)=.8924$

Therefore,

Wout=678 Watts = 500 ft-lb/sec

From equation (3-9):

Qin=2390 Watts = 1763 ft-lb/sec

Losses Calculations:

Equation (3-12):

$$TAN\alpha = (VH/VC + COS\varphi)/SIN\varphi \cdot \Rightarrow \alpha = 41.5^\circ$$

$f_{h_T}(T)=1.086$ Eq. (3-21)

$f_{c_T}(T)=1.023$ Eq. (3-22)

$f_{r_T}(T)=1.0417$ Eq. (3-23)

$f_{h_\varphi}(\phi)=.83$ Eq. (3-24)

$f_{c_\varphi}(\phi)=.8605$ Eq. (3-25)

$f_{r_\varphi}(\phi)=.8444$ Eq. (3-26)

$f_{h_D}(DH)=.97$ Eq. (3-27)

$f_{c_D}(DH)=1.142$ Eq. (3-28)

$f_{r_D}(DR)=1.06$ Eq. (3-29)

Therefore,

$F_{ch}=f_{r_T}(T)*f_{r_\varphi}(\phi)*f_{h_D}(DH)=.874$

$f_{cc}=1.005$

fcr=.9324

Mass flow rates:

mH=.039 lbm/s Eq. (3-15)

mC=.062 lbm/s Eq. (3-16)

mR=.49 lbm/s Eq. (3-17)

For Heater:

$$Re_H = \frac{\dot{m}_H \cdot D_H}{AFR_H \cdot \mu_H} = \frac{4\,\dot{m}_H}{\pi D_H \cdot N_H \cdot \mu_H}$$

$$\mu_H = .068 \text{ lbm/ft-s}$$

$$Re_H = \frac{4 \times .039 \times 12 \times 3600}{\pi \times .87 \times 50 \times .068} = 8999$$

$$\Rightarrow f_H = \frac{.0457}{(Re_H)^{.2}} = .0074$$

From equation (3-31):

$$W_{loss\ Heater\text{-}\Delta p} = \frac{8}{\pi^3}(f_H)\cdot\left(\frac{L}{D}\right)_H \times \frac{VC^3 \times \omega^3 \times \rho_m\left(1+A/\sqrt{1-A^2}\right)}{N_H^2 \times D_H^4 \times R \times T_H}(F_{CR})^2 \times \frac{SIN^2\varphi}{\cos^2\alpha}\left[SIN4 + \tfrac{1}{6}SIN(2\alpha-4) + \tfrac{1}{2}SIN(2\alpha+4)\right]$$

Correction factor for units: $1/[(12)^3 * 32.2 * .73756]$

Wloss=6 Watts

For Cooler:

μc=.0475

$$Re_C = \frac{4 \times \dot{m}_C}{\pi (D_C) N_C \cdot \mu_C} = 18\,635$$

$$\Rightarrow f_C = \frac{.0457}{(Re_C)^{.2}} = .0064$$

From equation (3-32)

$W_{loss\ Cooler\text{-}\Delta p}$ = 13.75 Watts

For Regenerator:

ReR=38

fR=1.464

From equation (3-33)

Wloss=148 Watts

Temperature Drop Losses:

Heater-Equation (2-10):

$$W_{Loss} = \frac{We \cdot Wc}{\dot{m}_H \cdot R \cdot T_H} \cdot \frac{k-1}{k} \cdot \frac{1}{e^{2NTUH} - 1}$$

We=1/2(Wout+Qin)=1534 Watts

Wc=1/2(Qin-Wout)=856 Watts

NTUH=4(LH/DH)(.023*ReH$^{-.2}$*Pr$^{-.6}$)=2.35

Wloss=.6 Watts

Cooler-Equation(2-11)

$$W_{Loss} = \frac{Wc^2}{\dot{m}_C \cdot R \cdot T_C} \cdot \frac{k-1}{k} \cdot \frac{1}{e^{2NTUC} - 1}$$

NTUC=2.15

Wloss=.6 Watts

Regenerator Heat Loss:

Equation (3-35):

$$Q_R = \tfrac{1}{3} \cdot \dot{m}_R \cdot C_v \cdot (T_H - T_C) \cdot \frac{2}{NTUV + 2}$$

$$NTUV = 4 \frac{1-\sigma}{\sigma} \frac{L_R}{d_V} \cdot .7413 \, P_r^{-2/3} \cdot (Re_R)^{-.41} \qquad (3\text{-}37)$$

$$Re_R = \frac{2\dot{m} R \cdot d_W}{VDR/L_R * (\mu_H + \mu_C)} = 48$$

NTUV=127.3

QR=66. Watts

Shuttle loss by equation (2-16):

Q_S=86 Watts

Heat leakage by equation (2-19)

Q_L=29 Watts

Transient heat loss in cylinders by equation (2-24)

Q_{TR}=65 Watts

Friction loss by equation (2-33)

Q_{FR}=68 Watts

Pumping loss in negligible because temperatures are not very high.

[equation (2-31)].

Axial conduction loss by equation (2-15).

Q_A=3 Watts

Final Results:

$Wout=Wout_{basic}-(\Delta Ploss)-(\Delta Tlosses)-Q_s-Q_L-Q_{TR}-Q_{FR}$

Wout=270.8 Watts

From complete model we get 262 Watts

$Qin=Qin_{basic}+Q_R+Q_A$=2459 Watts

Complete model:

Qin=2257 Watts

$Efficiency|_{Simplified}$ =270.8/2459=11%

$Efficiency|_{Complete}$ =262/2257=11.6%

APPENDIX (L)

OPTIMIZATION METHOD:

a)- Regenerator Optimization:

As shown in Chapter II, there are three different losses associated with a regenerator: (1) power loss due to the pressure drop; (2) heat transfer loss due to the regenerator imperfection; (3) heat transfer loss due to the axial conduction.

Equation (3-33) expresses the pressure drop power loss as:

$$W_{Loss} = \frac{(PR)}{16\pi} * (L/D)_R * \frac{P_m}{(AFRR)^2} * \frac{Vc^3 * \omega^3 * SIN^2\varphi}{R * TR * \cos^2\alpha} * F_{cr}^2 * \left[SIN\varphi + \tfrac{1}{6} SIN(2\alpha-\varphi) + \tfrac{1}{2} SIN(2\alpha+\varphi)\right]$$

(L-1)

The net output power of a Stirling engine is given by equation (3-2):

$$W_{OUT} = \pi * N * P_m * A * V_H * SIN\theta * \frac{1 - TC/TH}{1+\sqrt{1-A^2}} * F_T(T) * F_\varphi(\varphi) * F_D(D)$$

(L-2)

Therefore the normalized power loss would be:

$$\frac{W_{Loss}}{W_{OUT}} = C_1 * \frac{(PR)}{8\pi} * (L/D)_R * \left(\frac{Vc}{V_H}\right) * \frac{Vc^2 * \omega^2}{R * TR * (AFRR)^2} * \bar{F}_\varphi(\varphi) * \frac{1+\sqrt{1-A^2}}{A(1-TC/TH)} * \frac{1}{F_T(T)} * \frac{1}{F_D(D)}$$

(L-3)

Where:

$$\bar{F}_\varphi(\varphi) = 1/[SIN\theta * F_\varphi(\varphi)]$$

$$C_1 = \frac{SIN^2\varphi}{\cos^2\alpha} * F_{cr}^2 * \left[SIN\varphi + \tfrac{1}{6} SIN(2\alpha-\varphi) + \tfrac{1}{2} SIN(2\alpha+\varphi)\right] \qquad \text{(L-4)}$$

Lets define:

$$\gamma \triangleq \frac{(DR)^3 * P_m * \frac{(1-\sigma)^2}{\sigma}}{\omega * VC * \mu} \qquad \text{(L-5)}$$

$$\beta \triangleq \frac{\sqrt{R*TR} * (DR)^2 (1-\sigma)^2}{\omega * VC * \sigma} \qquad \text{(L-6)}$$

This implies that γ/β^2 is a Reynolds number. In these definitions D_R is the regenerator hydraulic diameter and DRR is the regenerator cross-sectional area diameter.

For a given temperature ratio and mean pressure the regenerator has to have enough thermal capacity to handle the resultant heat transfer. By an averaged energy balance equation (heat transfer), we can get the following relationship LR and DRR, as shown in Appendix (P).

$$LR * (DRR)^2 = 2/3 * \frac{C_p}{(1-\sigma)C_R} * \frac{P_m * VC}{\rho_R * R * TR} \ln T_H/T_C * \frac{SIN\varphi}{\cos\alpha} \qquad \text{(L-7)}$$

Where ρ_R & C_R are density and specific heat of regenerator material. Since in the present optimization method the regenerator porosity (σ) is assumed to be constant, then equation (L-7) indicates that for a given P_m and TH/TC the regenerator dead volume is frozen.

For the regenerator we have:

$$Re_R = \frac{VC * \omega * P_m * \frac{1-\sigma}{\sigma} * DR}{R * TR * \mu * AFRR} * \frac{SIN\varphi}{2\cos\alpha} \qquad \text{(L-8)}$$

$$AFRR = \frac{\pi}{4} (DRR)^2 * \sigma$$

By substituting for DRR in equation (L-8) from equation (L-7) we get:

$$Re_R = \frac{3}{\pi} * \left(\frac{1-\sigma}{\sigma}\right)^2 * \frac{C_R * \rho_R * \omega * DR^2}{C_p \mu} * \left[\ln TH/TC\right]^{-1} * (L/D)_R \quad \text{(L-9)}$$

For most cases the R_{eR} for regenerator is less than 60, then

$$fR = 53.7 / R_{eR}^{.93}$$

Also

$$\frac{Vc^2 * \omega^2}{R * TR * (AFRR)^2} = (Re_R)^2 * \frac{\beta^2}{\gamma^2} * \left(\frac{\sigma}{1-\sigma}\right)^2 * \left(\frac{2\cos\alpha}{\sin\varphi}\right)^2$$

Therefore,

$$fR * \frac{Vc^2 * \omega^2}{R * TR * (AFRR)^2} = 204.8 \left(\frac{3}{\pi}\right)^{1.07} * \left(\frac{1-\sigma}{\sigma}\right)^{.14} * \left(\frac{C_R \rho_R \omega (DR)^2}{C_p \mu}\right)^{1.07} * \frac{(L/D)_R^{1.07} * \beta^2 * \cos\alpha}{\gamma^2 * \sin\varphi * (\ln TH/TC)^{1.07}}$$

Lets define:

$$Z \triangleq \frac{C_R}{C_p} * \frac{\rho_R \omega (DR)^2}{\mu}$$

$$\delta \triangleq TH/TC$$

Then equation (L-3) can be re-written as:

$$\frac{W_{loss}}{W_{OUT}} = C_1 * \frac{53.7}{2\pi} * \left(\frac{3}{\pi}\right)^{1.07} \left(\frac{1-\sigma}{\sigma}\right)^{.14} * Z^{1.07} * (\ln\delta)^{-1.07} * (L/D)_R^{2.07} * \frac{\beta^2}{\gamma^2} * \left(\frac{\cos\alpha}{\sin\varphi}\right)^2 * F_R(\varphi, D, T_r, V_r)$$

(L-10)

Where

$$F_R(\varphi, D, T_r, V_r) = \overline{F}_4(\varphi) * \frac{1}{F_D(\omega)} * \frac{Vc}{VH} * \frac{1+\sqrt{1-A^2}}{A\,(1-TC/TH)\,F_T(T)}$$

(L-11)

Or

$$\frac{W_{LOSS}}{W_{OUT}} = \left[\bar{C}_1 * Z^{1.07} * (\ln\delta)^{-1.07} * \beta^2 * \bar{\gamma}^{-2} * (L/D)_R^{2.07}\right] F_R(\varphi, D, T_r, V_r) \qquad \text{(L-12)}$$

Where:

$$\bar{C}_1 = \frac{53.7}{2\pi}\left(\frac{3}{\pi}\right)^{1.07} * \left(\frac{1-\sigma}{\sigma}\right)^{.14} * F_{cv}^2 * \left[SIN\varphi + \tfrac{1}{6}SIN(2\alpha-\varphi) + \tfrac{1}{2}SIN(2\alpha+\varphi)\right]$$

Since the regenerator dead volume is frozen then F_R in equation (L-12) is independent of $(L/D)_R$.

Heat transfer loss due to the regenerator imperfection is given by equation (3-35):

$$Q_R = \tfrac{1}{3} * \dot{m}_R * C_v * (T_H - T_C) * \frac{2}{NTUV + 2} \qquad \text{(L-13)}$$

Since NTUV$\gg$2, then by substituting for $\dot{m}_R$ we get:

$$Q_R \simeq \tfrac{1}{3} * \frac{P_m * VC * \omega * SIN\varphi * F_{cv}}{2R * (TR) * COS\alpha} * C_v * (T_H - T_C) * \frac{2}{NTUV} \qquad \text{(L-14)}$$

$$NTUV = 2.9652 * (L/D)_R * P_r^{-2/3} * Re_R^{-.41}$$

Therefore, the normalized heat transfer loss would be:

$$\frac{Q_R}{W_{OUT}} = C_2 * \ln\frac{T_H}{T_C} * (L/D)_R^{-1} * P_r^{2/3} * Re_R^{.41} * \frac{VC}{VH} * \frac{(1+\sqrt{1-A^2}) * \bar{F}_\varphi(\varphi)}{A(1-T_C/T_H) F_T(T) F_D(D)} \qquad \text{(L-15)}$$

Where

$$C2 = \frac{SIN\varphi}{COS\alpha} * F_{cv} * \frac{1}{3 * 2.9652 (k-1)}$$

By substituting for ReR from equation (L-9) we get:

$$\frac{Q_R}{W_{OUT}} = \left[\bar{C}_2 * Z^{.41} * (\ln\delta)^{.59} * (L/D)_R^{-.59}\right] * F_R(\varphi, D, T_r, V_r) \qquad \text{(L-16)}$$

Where $\bar{C}_2 = C_2 * Pr^{2/3} * \left(\frac{3}{\pi}\right)^{.41} * \left(\frac{1-\sigma}{\sigma}\right)^{.82}$

Heat transfer loss due to the regenerator axial conduction is given by equation (2-15):

$$Q_C = K_{mg} * (AR) * (TH - TC)/L_R \qquad \text{(L-17)}$$

$$AR = \frac{\pi}{4}(DRR)^2$$

Then the normalized loss would be:

$$\frac{Q_C}{W_{OUT}} = \frac{2K_{mg}}{\mu * R} * \ln\frac{TH}{TC} * \frac{R * TR * \mu * AFRR}{VC * P_m * \omega * DR} * (L/D)_R^{-1} * F_R(\varphi, D, T_r, V_r)$$

Or

$$\frac{Q_C}{W_{OUT}} = \left[\bar{C}_3 * Z^{-1} * (\ln\delta)^2 * (L/D)_R^{-2}\right] * F_R(\varphi, D, T_r, V_r) \qquad \text{(L-18)}$$

Where

$$\bar{C}_3 = \frac{2\pi}{3}\left(\frac{\sigma}{1-\sigma}\right)^2 * P_r * \frac{k}{k-1} * \left[\frac{1+K_m/K_g}{1-K_m/K_g} + \sigma - 1\right] \Big/ \left[\frac{1+K_m/K_g}{1-K_m/K_g} + 1 - \sigma\right] \qquad \text{(L-19)}$$

As discussed in Chapter IV, in order to add these three loss terms W_{loss}, Q_R, and Q_C an efficiency term should be added to Q_R and Q_C because Q_R and Q_C are in the form of an heat transfer rate where as W_{loss} is in form of mechanical power (work transfer).

Therefore, the total power loss due to the regenerator is:

$$\frac{\text{Total } W_{Loss}}{W_{OUT}} = \left\{ \bar{C}_1 * \bar{z}^{1.07} * (\ln\delta)^{-1.07} * \frac{\beta^2}{\gamma^2} * (L/D)_R^{2.07} + \left[\bar{C}_2 \bar{z}^{.41} * (\ln\delta)^{.59} * (L/D)_R^{-.59} + \bar{C}_3 * \bar{z}^{-1} * (\ln\delta)^{2.} * (L/D)_R^{-2.} \right] * \eta \right\} * F_R(\varphi, D, V_r, T_r) \quad \text{(L-20)}$$

For the first round calculation efficiency (η) can be approximated as:

$$\eta = \text{Carnot Efficiency} - 10\% = 0.9 - \frac{T_C}{T_H} = 0.9 - \delta^{-1}$$

Since the regenerator volume is frozen, then F_R (φ, D, T_r, V_r) is independent of $(L/D)_R$, i.e. it has no effect in the following differentiation.

$$\left. \frac{\partial\left(\frac{\text{Total } W_{Loss}}{W_{OUT}}\right)}{\partial (L/D)_R} \right|_{\text{const. Reg. Dead Volume}} = 0$$

$$\Rightarrow \left[2.07 * \bar{z}^{2.07} * \frac{\beta^2}{\gamma^2}\right](L/D)_R^{4.07} - \left[.59 \frac{\bar{C}_2}{\bar{C}_1} \bar{z}^{1.41} (\ln\delta)^{1.66} * \eta\right](L/D)_R^{1.41} - \left[2 \frac{\bar{C}_3}{\bar{C}_1} (\ln\delta)^{3.07} * \eta\right] = 0 \quad \text{(L-21)}$$

Solution to equation (L-21) gives the optimum geometry-ratio for a regenerator.

b)- Cold and Hot Heat-Exchangers Optimization:

There are two forms of power losses for heater and cooler: (1): Power loss due to the pressure drop; (2) Power loss due to the temperature drop.

Equation (3-32) expresses the pressure drop power loss inside the cooler as:

$$W_{Loss} = \frac{8(PC)}{\pi} * (L/D)_C * \frac{V_C^2 * \omega^3 * P_m * (1 - A/\sqrt{1-A^2})}{(N_C)^2 * R * T_C * (D_C)^4} * F_e^2 * \frac{SIN^2\alpha}{\cos\alpha} \left[\sin\varphi + \frac{1}{2}\sin(2x+\varphi) + \frac{1}{2}\sin(2x+\varphi) \right] \quad \text{(L-22)}$$

The normalized form of equation (L-22) with respect to the net output power is:

$$\frac{W_{Loss}}{W_{OUT}} = \frac{(fC)}{\pi} * (L/D)_C * \frac{VC^2 * \omega^2 * C^* * (1-A/\sqrt{1-A^2})(1+\sqrt{1-A^2}) * \bar{F}_R(\varphi) * VC}{(AFRC)^2 R * TC * A * (1-TC/TH) * F_T(T) * F_D(D) * VH} \qquad \text{(L-23)}$$

Where $$C^* = F_{tc}^2 * \frac{SIN^2\varphi}{COS^2\alpha}\left[SIN\varphi + \tfrac{1}{6}SIN(2\alpha-\varphi) + \tfrac{1}{2}SIN(2\alpha+\varphi)\right]$$

Lets define: $$\gamma \triangleq \frac{P_m * (DC)^3}{\omega * VC * \mu_C} \qquad \text{(L-24)}$$

$$\Rightarrow \frac{\gamma}{\beta^2} = \frac{P_m * \omega * VC * DC}{\mu_C * AFRC * R * TC} * NC\left(\frac{\Pi}{4}\right)$$

$$\beta \triangleq \frac{\sqrt{R * TC} * (DC)^2}{\omega * VC} \qquad \text{(L-25)}$$

Where $$AFRC = NC * \frac{\Pi}{4}(DC)^2$$

Or $$\frac{\gamma}{\beta^2} = \frac{\Pi}{2} * NC * \frac{COS\alpha}{SIN^2\varphi} * Rec$$

This means that γ/β^2 forms a Reynolds number.

Since Reynolds number inside the cold heat-exchanger is almost always greater than 2000, then the friction factor can be expressed as:

$$fC = \frac{.0457}{Rec^{.2}} = \left(.0457 * \frac{\Pi}{2} * NC * \frac{SIN\varphi}{COS\alpha}\right)^{-.2} * \gamma^{-.2} * \beta^{.4} \qquad \text{(L-26)}$$

Therefore equation (L-23) can be written as:

$$\frac{W_{Loss}}{W_{OUT}} = \left[E_1 * \bar{\beta}^{-1.6} + \bar{\gamma}^{-2} * (L/D)_c\right] * F_c(\varphi, D, T_r, V_r) \qquad \text{(L-27)}$$

Where:

$$E_1 = \frac{\varepsilon^{3.8} * .0457}{\pi^{2.8} * Nc^{1.8}} \left(\frac{SIN\varphi}{COS\alpha}\right)^{1.8} * \left[SIN\varphi + 1/6\, SIN(2\alpha-\varphi) + 1/2\, SIN(2\alpha+\varphi)\right] * F_{cc}^{1.8} \qquad \text{(L-28)}$$

$$F_c(\varphi, D, T_r, V_r) = \frac{(1-A/\sqrt{1-A^2})(1+\sqrt{1-A^2})}{A\,(1-TC/TH) * F_T(T)} * \frac{V_C}{V_H} * \frac{\bar{F}_\varphi(\varphi)}{F_D(D)} \qquad \text{(L-29)}$$

Since the present optimization method is based on a given input heat (Qin) or net output (Wout), then in either case the heater and the cooler have to have enough heat transfer area to handle the given task. This yields equations for calculation of Nc and NH the number of tubes in cooler and heater. Since it is assumed that both heater and cooler have constant wall temperatures (TH,TC) then the Nusselt number for both of them would be 5.75 for inside the tubes, assuming a slug flow with a mean velocity.

$$Q = h * A * \Delta T$$

$$A = N * \pi * D * L$$

$$h = Kg * 5.75/D$$

$$\Delta T = TR - TC \qquad \text{(cooler)}$$

$$\Delta T = TH - TR \qquad \text{(heater)}$$

For Cooler:

$$QC = 5.75\ Kg * NC * \pi * LC * (TR - TC)$$

or

$$NC = QC/[5.75\pi * Kg * LC * (TR - TC)] \qquad \text{(L-30)}$$

Where Qc is the total heat transferred in cooler which is [(1-Eff.)* Qin] and Kg is the gas thermal conductivity.

For Heater:

$$Q_{in} = 5.75\ K_g * NH * \pi * LH * (TH - TR)$$

or

$$NH = Q_{in} / [5.75\ \pi * K_g * LH * (TH - TR)] \qquad \text{(L-31)}$$

In addition to calculation of NH and NC, equations (L-30) and (L-31) will freeze the cooler and heater dead volumes.

Power loss due to the temperature drop in cooler is given by equation (2-11) as:

$$W_{Loss} = \frac{wc^2}{mc * R * TC} * \frac{k-1}{k} * \frac{1}{e^{2NTUC} - 1} \qquad \text{(L-32)}$$

This can be approximated as:

$$W_{Loss} = \frac{wc^2}{mc * R * TC} * \frac{k-1}{k} * \frac{1}{2NTUC}$$

Where:

$$NTUC = 4 * (L/D)_c * .023 * Re_C^{-.2} * P_r^{-.6}$$

Since we can be approximated by,

$$wc \approx P_m \left(1 - A/\sqrt{1-A^2}\right) * \omega * VC * (TH/TC)$$

Then the normalized power loss would be:

$$\frac{W_{Loss}}{W_{OUT}} = \frac{(1 - A/\sqrt{1-A^2})(1+\sqrt{1-A^2}) * \bar{F}_\varphi(\varphi) * (TH/TC)^2 * (R-1) * P_r^{.6} * (2\cos\alpha)}{A * VH * F_D(D) * F_T(T) * (1 - TC/TH) * k * 4 * (L/D)_c * .023\ Re_C^{-.2} * \sin\varphi} \qquad \text{(L-33)}$$

Or

$$\frac{W_{Loss}}{W_{OUT}} = \left[E_2 * \delta^2 * (L/D)_C^{-1} * \gamma^{.2} * \beta^{-.4}\right] * F_c(D, \varphi, T_r, N_r) \qquad \text{(L-34)}$$

Where: $$E_2 = \frac{2^{.2}}{.046 * (\pi * NC)^{.2}} * \left(\frac{\cos\alpha}{\sin\varphi}\right)^{.8} * \frac{k-1}{k} * P_r^{-.6}$$

$$\delta = TH/TC$$

Therefore, the total power loss due to the cooler would be:

$$\left(\frac{\text{Total } W_{loss}}{W_{out}}\right) = \left[E_1 * \beta^{1.6} * \gamma^{.2} * (L/D)_c + E_2 \delta^2 * \gamma^{.2} * \beta^{.4} * (L/D)_c^{-1}\right] * F_c(\varphi, D, T_r, \nu_r)$$

(L-35)

In equation (L-35) Fc is independent of $(L/D)_c$ because of cooler frozen volume for calculation of NC. Therefore, Fc has no effect in the following differentiation.

$$\left.\frac{\partial\left(\frac{\text{Total } W_{loss}}{W_{out}}\right)}{\partial (L/D)_c}\right|_{\text{Const. Cooler Dead Volume}} = 0$$

$$\Rightarrow \quad (L/D)_c = \sqrt{\frac{E_2}{E_1}} * \delta * \gamma^{.2} * \beta^{.6} \qquad \text{(L 36)}$$

Since heater and cooler are similar, then an equation similar to (L-36) can be written for optimum heater geometry ratio.

$$(L/D)_H = \sqrt{\frac{E_4}{E_3}} * \delta * \gamma_H^{.2} * \beta_H^{.6} \qquad \text{(L-37)}$$

Where:

$$E_4 = E_2 * \left(\frac{NC}{NH}\right)^{.2}$$

$$E_3 = E_1 * \left(\frac{NC}{NH}\right)^{1.8} * \left(\frac{F_{cg}}{F_{cc}}\right)^{1.8}$$

$$\gamma_H = (P_m * DH^3)/(\omega * VC * \mu_H) \qquad \text{(L-38)}$$

$$\beta_H = (\sqrt{R * TH} * DH^2)/(\omega * VC) \qquad \text{(L-39)}$$

-Effect of Ducting and Clearance Volumes:

In order to find the effect of ducting and clearance volumes on optimum aspect ratio we can compare the result of the complete model with equation (4-27). Following are the results of this comparison for some cases:

= 1.6649 , 1.04 , .6243 , .3122 , .104

= -26 , -16 , -6 , -3 , +4

Similar results have been derived for other cases. The simplest correlation which fits very accurately the the above data is:

f( ) = -19.2 * +6

C)- Cylinders Optimization:

As discussed in Chapter IV, three major power losses in cylinders and the output power would determine the optimum volume ratio for cylinders.

Power loss due to the mechanical friction is estimated by:

$$W_{Loss} = \frac{2N}{531}(.002N+1)(V_H+V_C) \qquad \text{(L-40)}$$

$$\frac{W_{Loss}}{W_{OUT}} = \frac{2}{531\pi} * \frac{(.002N+1)(1+V_C/V_H)*\bar{F}_\varphi(\varphi)}{P_m(1-T_C/T_H)*F_T(LT)}*(1+\lambda/\delta+\xi)$$

or

$$\frac{W_{Loss}}{W_{OUT}} = d_1(1+1/\lambda)(1+\lambda/\delta+\xi)/(1-1/\delta) \qquad \text{(L-41)}$$

Where: $\lambda = V_H/V_C$

ξ = Total Dead Volume/V_C

$\delta = T_H/T_C$

Equation (2-16) expresses the shuttle loss as:

$$W_{Loss} = \frac{\pi}{8} * K_g * B * (TH - TC) * S * \frac{S}{\ell L} * (BET)$$

Or

$$\frac{W_{Loss}}{W_{OUT}} = d_2 * Re^{-1} * \delta * (1 + \lambda/\delta + \xi) \qquad \text{(L-42)}$$

Where

$$Re = P_m * \omega * (VC)^2 / [R * TC * \mu C * (Ac)^2]$$

Finally, from equation (2-20) we get the power loss due to the non-uniform temperature distribution inside cylinders as:

$$\frac{W_{Loss}}{W_{OUT}} = d_3 * (\delta^{-.5} * \lambda^{2/3} * Re^{.5} + d_4\ Re^{.5}) \qquad \text{(L-43)}$$

Net Output = Output - Total Power loss

$$\frac{\text{Net Output}}{\text{Wout}} = 1 - \frac{\text{Total Power Loss}}{\text{Wout}}$$

$$\frac{\text{Total } W_{Loss}}{W_{OUT}} = \left[d_1 * (1 + 1/\lambda)\frac{(1 + \lambda/\delta + \xi)}{1 - 1/\delta}\right] + \left[d_2 * Re^{-1} * \delta (1 + \lambda/\delta + \xi)\right] + \left[d_3 * (\delta^{-.5} * \lambda^{2/3} * Re^{.5} + d_4 Re^{.5})\right] \qquad \text{(L-44)}$$

$$\frac{\partial\left(\frac{\text{Net Output}}{W_{OUT}}\right)}{\partial \lambda} = -\frac{\partial\left(\frac{\text{Total } W_{Loss}}{W_{OUT}}\right)}{\partial \lambda} = 0$$

$$\Rightarrow \frac{d_1 (1/\delta - \frac{1+\xi}{\lambda^2})}{1 - 1/\delta} + d_2 * Re^{-1} * \delta (\tfrac{1}{\delta}) + d_3 * \tfrac{2}{3} * \delta^{-.5} * \lambda^{-1/3} * Re^{.5} = 0 \qquad \text{(L-45)}$$

Or

$$-\frac{1}{\delta} - \frac{1+\xi}{\lambda^2} + \bar{d}_1 * Re^{-1} \left(\frac{\delta - 1}{\delta}\right) + \bar{d}_2 (\delta - 1)\, \delta^{-1.5} * \lambda^{-1/3} * Re^{.5} = 0 \qquad \text{(L-46)}$$

For simplicity and because of the fact that $\lambda \approx 1$, then we combine $\lambda^{-1/3}$ and $\bar{d}_2$ as a new constant then we get the following equation:

$$\lambda = \sqrt{d_3 * \delta(1+\xi) / \left[1 + d_1(\delta-1)Re^{-1} + d_2(\delta-1)\bar{\delta}^{-.5} * Re^{.5}\right]} \qquad \text{(L-47)}$$

Figures (L-1) through (L-6) show how the optimum geometries of different components vary with the non-dimensional numbers, such as Mach number and Reynolds number.

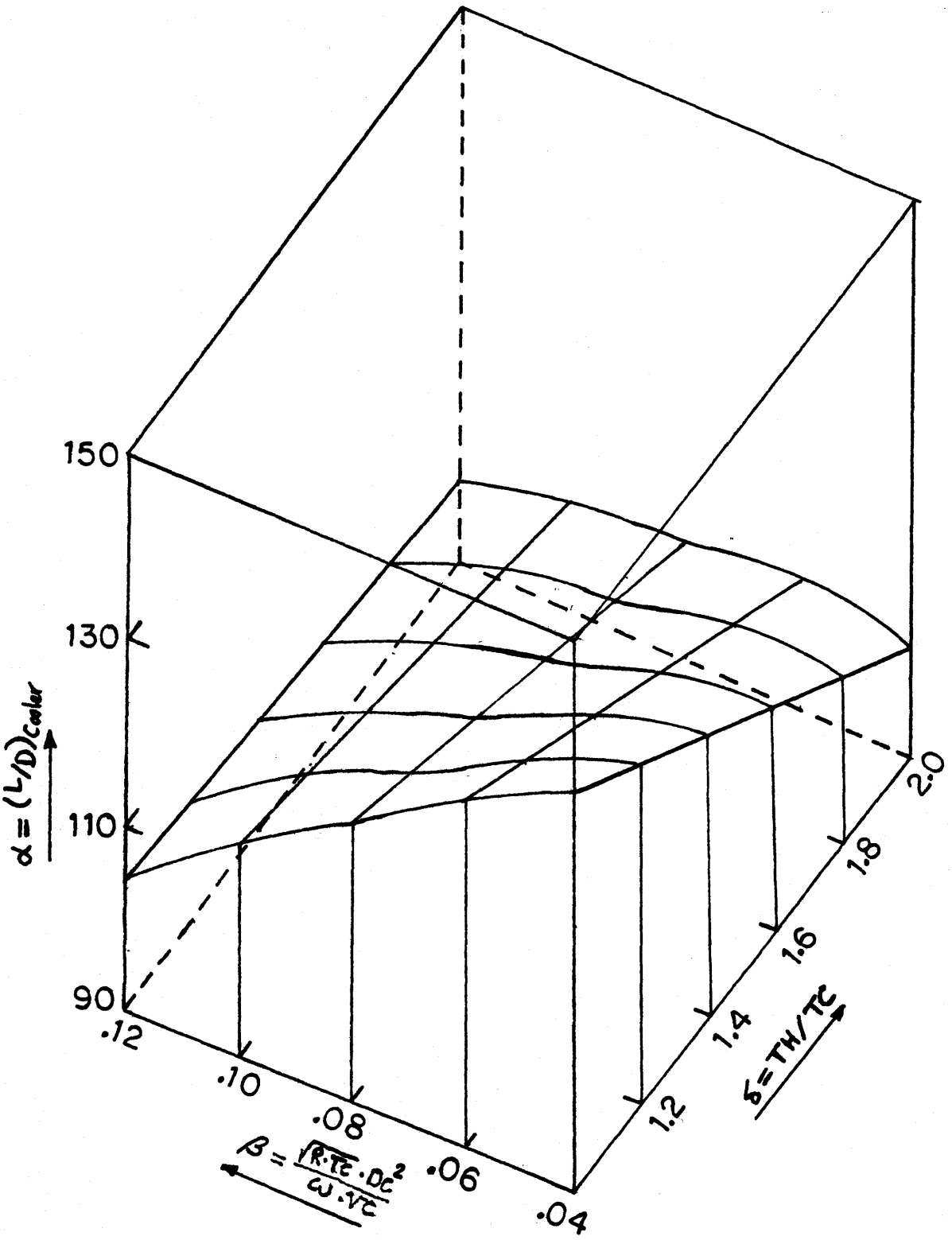

Fig.(L1): Optimum Cooler Aspect Ratio as a Function of Mach Number and Temperature Ratio (ξ=.4, γ=300) Equation (4-24)

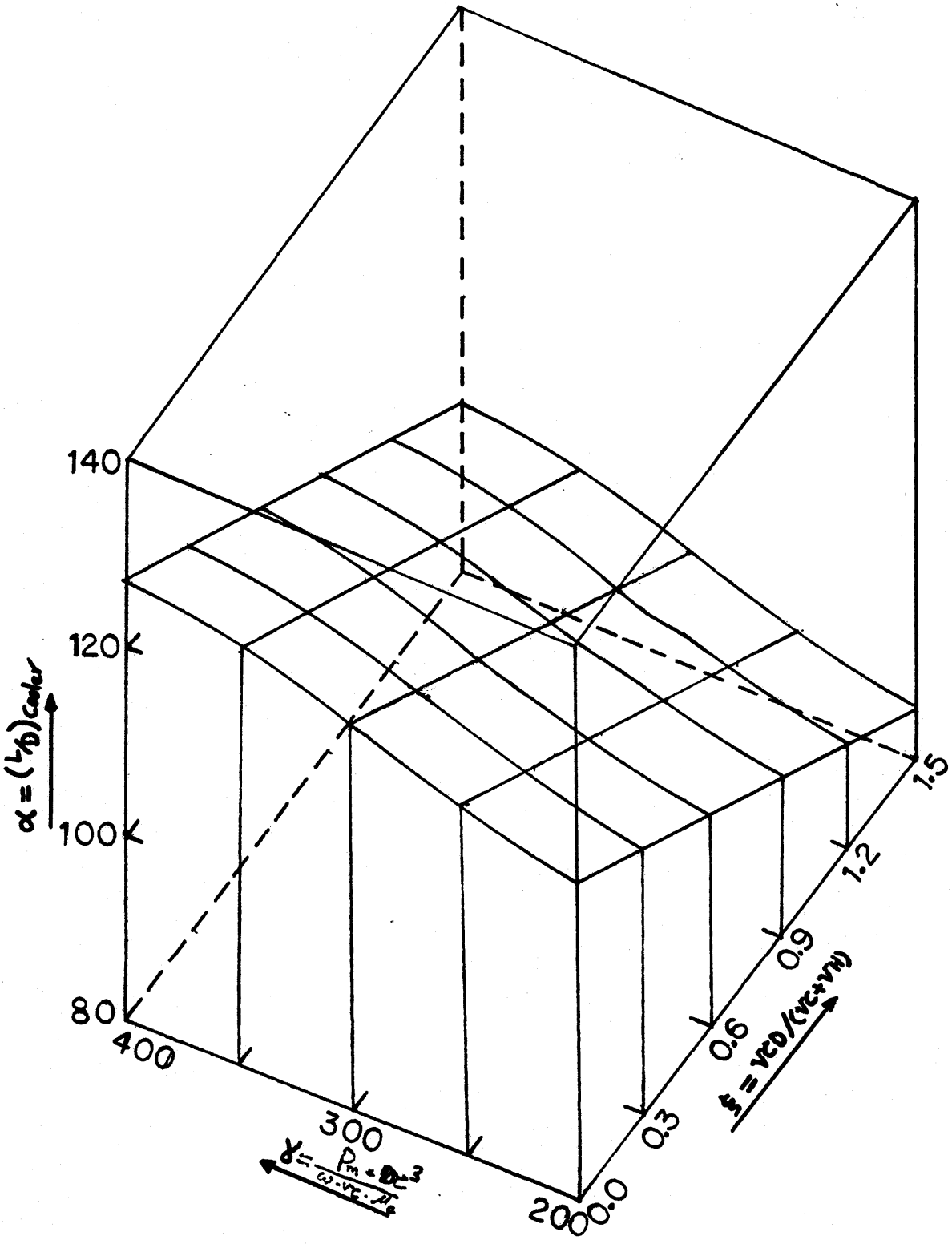

Fig.(L2): Optimum Cooler Aspect Ratio as a Function of Cooler Dead Volume and Reynolds to Mach Number Ratio (β-.08, δ=1.4 Equation (4-24)

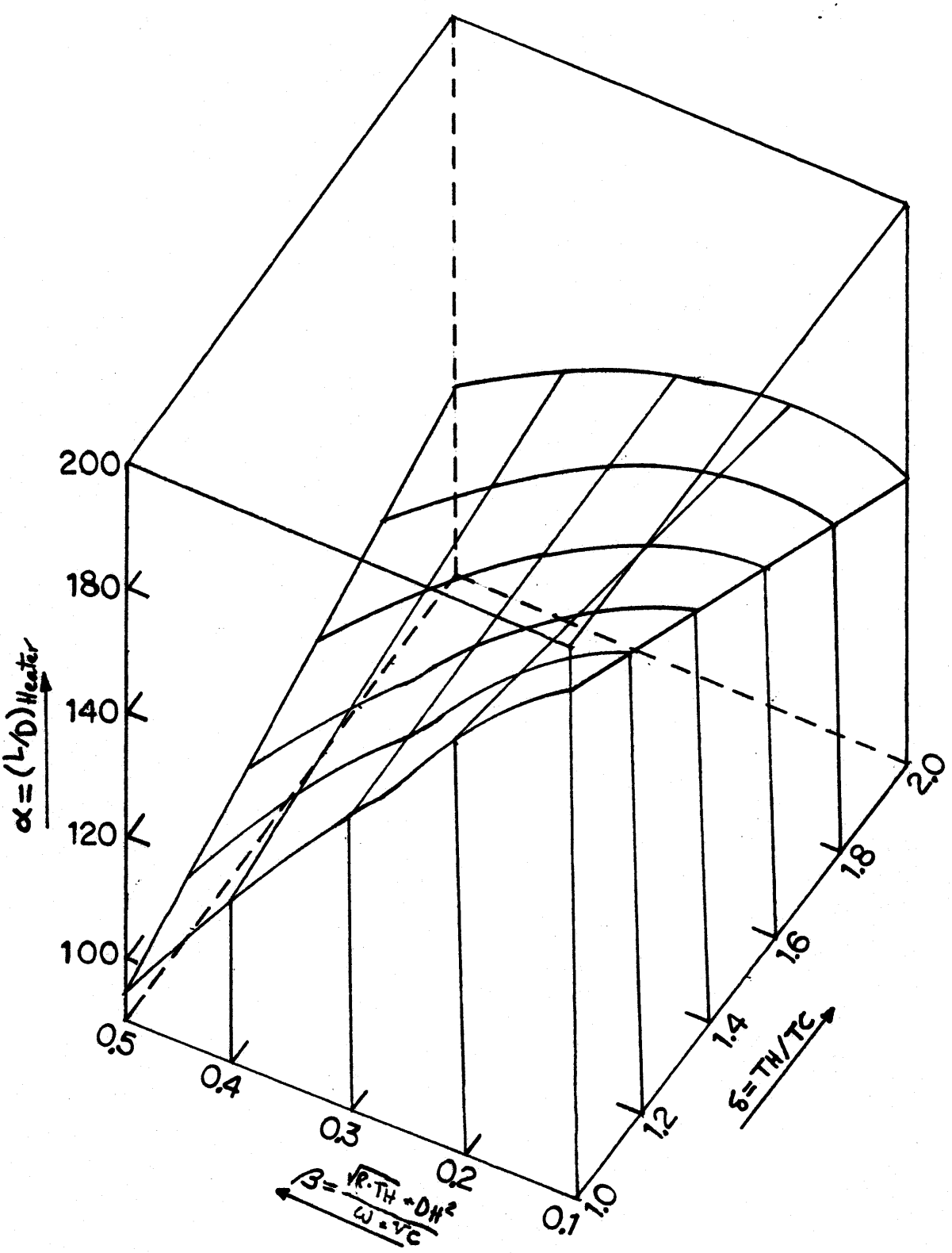

Fig.(L3): Optimum Heater Aspect Ratio as a Function of Mach Number and Temperature Ratio (ξ=.4, γ=800) Equation (4-37)

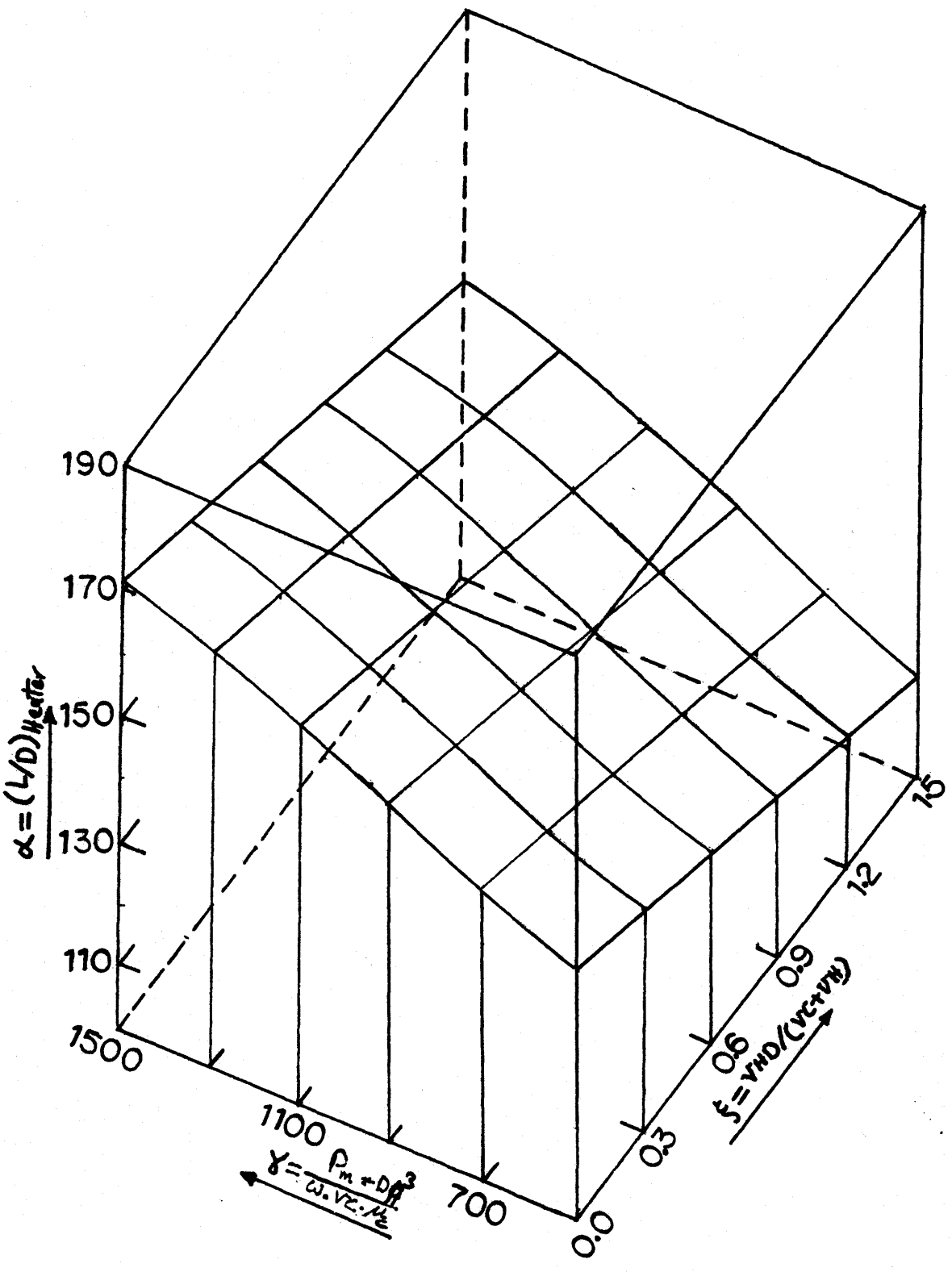

Fig.(L4): Optimum Heater Aspect Ratio as a Function of Heater Dead Volume and Reynolds to Mach Number Ratio (β=.25, δ=1.4) Equation (4-37)

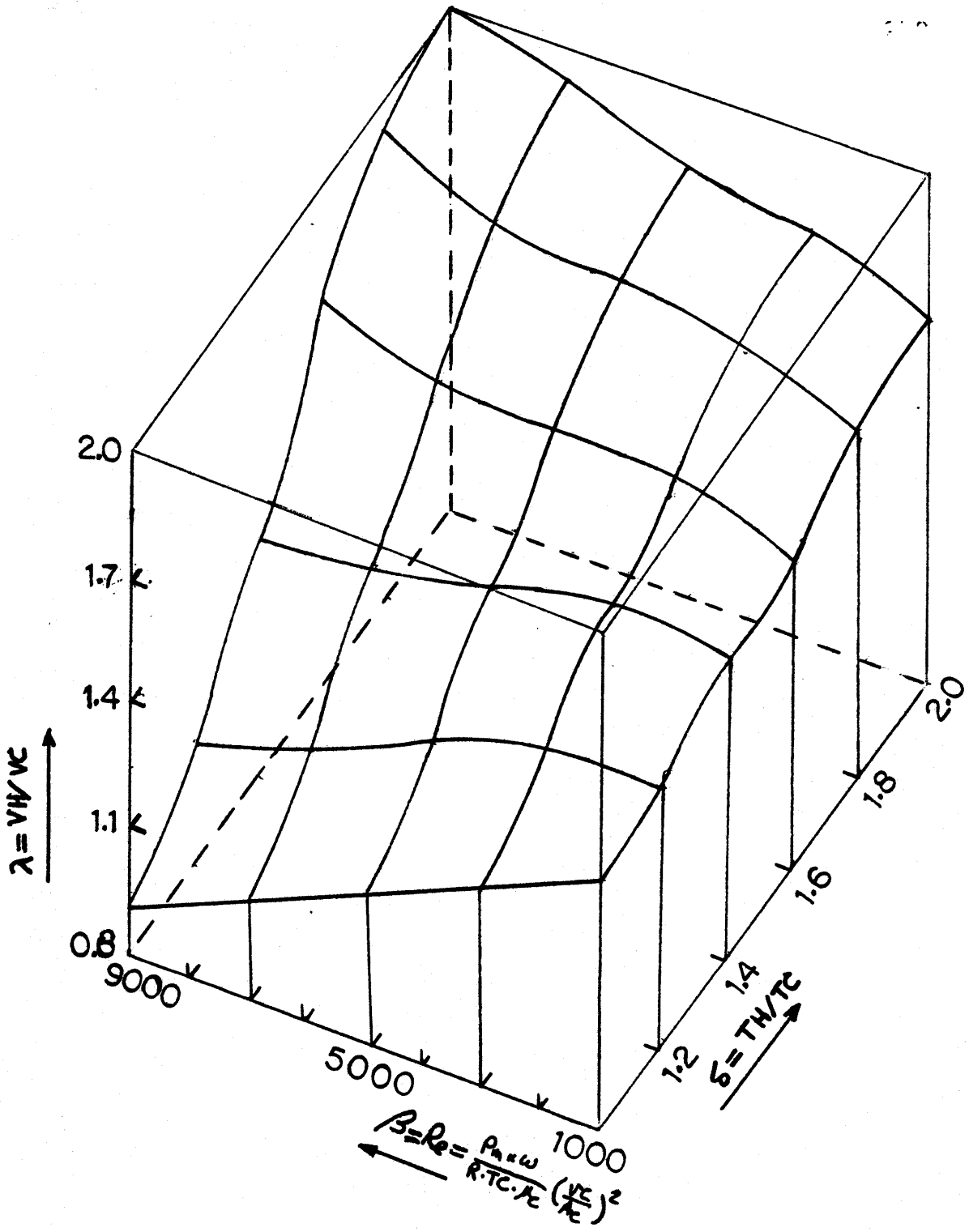

Fig.(L5): Optimum Swept-Volume Ratio as a Function of Reynolds Number and Temperature Ratio (ξ=3.5)
Equation (4-47)

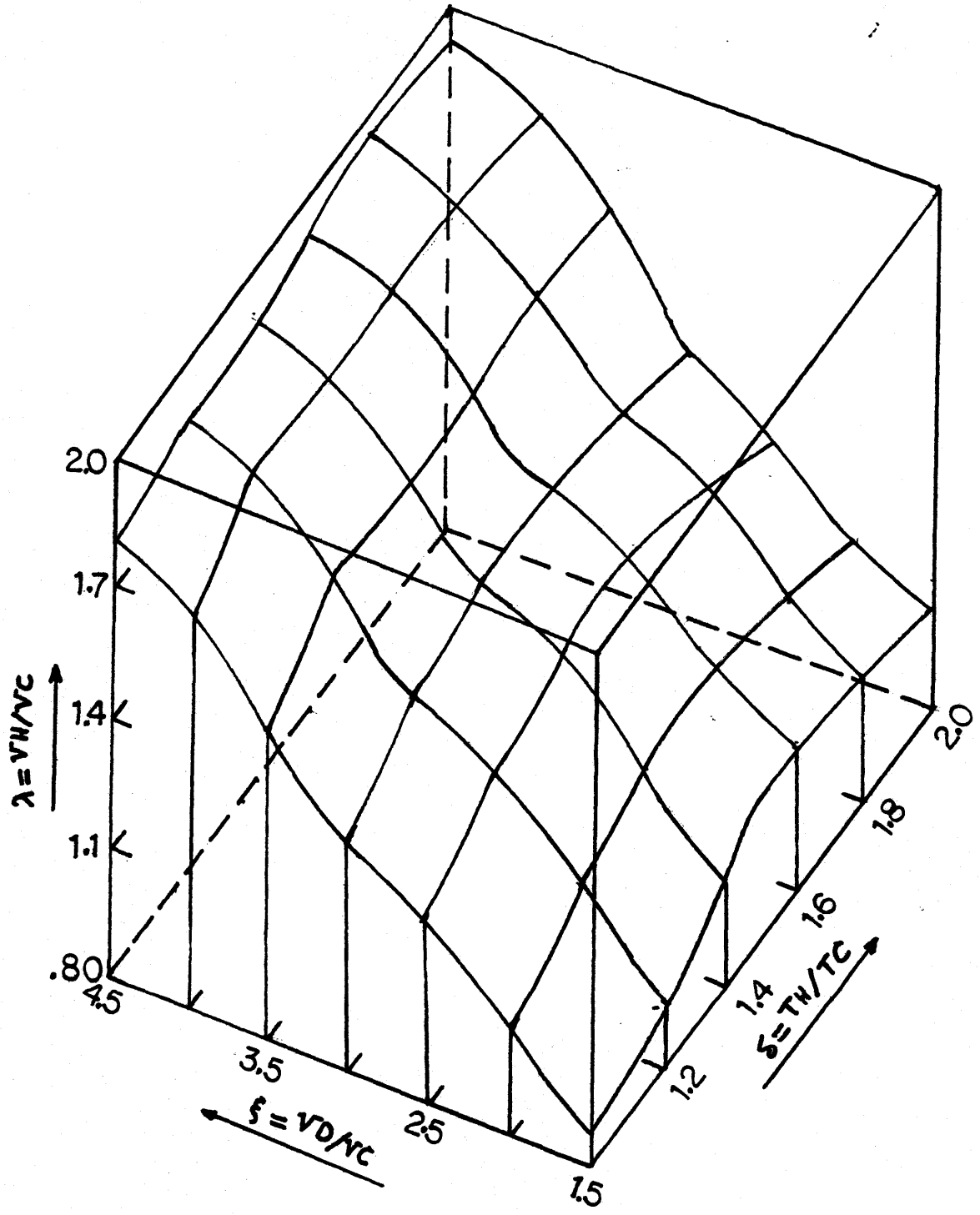

Fig.(L6): Optimum Swept-Volume Ratio as a Function of Dead Volume and Temperature Ratio (β=5000) Equation (4-47)

APPENDIX(M)

Derivation of Optimum Phase Angle & Speed:

a)- Optimum Phase Angle

In order to find the optimum phase angle we need to differentiate the net output with respect to ϕ.

Wout=Basic Wout-Total Losses

$$\frac{\partial V_{OUT}}{\partial \varphi} = \frac{\partial W}{\partial \varphi} - \frac{\partial (Total\ Loss)}{\partial \varphi} \qquad (M\text{-}1)$$

Appendix(D) has the derivative of basic power with respect to phase angle.

$$\frac{\partial W}{\partial \varphi} = \pi \frac{1-T_r}{1+V_r}\left[\frac{A}{1+\sqrt{1-A^2}}\left(SIN\theta \cdot COT\varphi + \frac{V_r \cdot T_r \cdot SIN\varphi \cdot SIN\theta}{T_r^2+V_r^2+2V_r T_r COS\varphi}\right)\right] - \frac{A \cdot T_r \cdot V_r \cdot SIN\varphi \cdot SIN\theta}{\sqrt{1-A^2}\left[1+\sqrt{1-A^2}\right]\left[T_r+V_r+4X \cdot T_r/(1+T_r)\right]^2} \qquad (M\text{-}2)$$

In this equation everything except the phase angle terms would be consider constant because differentiation is respect to ϕ.

$$\frac{\partial W}{\partial \varphi} = K_1\, SIN\theta \cdot COT\varphi + K_2\, SIN\varphi \cdot SIN\theta = SIN\theta\,(K_1 \cdot COT\varphi + K_2\, SIN\varphi) \qquad (M\text{-}3)$$

Losses can be determined from Chapter III, simplified model.

ΔP-loss in Heater:

$$W_{Loss} = K_3 \cdot \left(\frac{SIN\varphi}{COS\alpha}\right)^{1.8}\left[SIN\varphi + \tfrac{1}{6} SIN(2\alpha-\varphi) + \tfrac{1}{2} SIN(2\alpha+\varphi)\right] \qquad (M\text{-}4)$$

ΔP-loss in Cooler:

$$W_{Loss} = K_4 \cdot \left(\frac{SIN\varphi}{COS\alpha}\right)^{1.8}\left[SIN\varphi + \tfrac{1}{6} SIN(2\alpha-\varphi) + \tfrac{1}{2} SIN(2\alpha+\varphi)\right] \qquad (M\text{-}5)$$

Note that 1.8 of $(SIN\phi/COS\alpha)^{1.8}$ is the combination of friction

factor and $(SIN\phi/COS\alpha)^2$ terms.

ΔP-loss in Regenerator:

$$W_{Loss} = K_5 * \left(\frac{SIN\varphi}{COS\alpha}\right)^{1.07} \left[SIN\varphi + 1/6\, SIN(2\alpha-\varphi) + 1/2\, SIN(2\alpha+\varphi)\right] \qquad (M-6)$$

Power loss due to the non-uniform temperature distribution inside the cylinders can be summarized as:

$$W_{Loss} = K_6 (COS\varphi + K_7\, SIN\varphi) \qquad (M-7)$$

The only other losses which have effects on the net output power and include the phase angle are temperature drops in heat and cooler. However, they are insignificant comparing with non-uniform temperature loss.

In the above equations:

$$K_1 = \pi * A * (1-T_r) / [(1+V_r)(1+\sqrt{1-A^2})] \qquad (M-8)$$

$$K_2 = \frac{\pi * V_r * T_r * (1-T_r)}{(1+V_r)(T_r^2 + V_r^2 + 2V_r T_r\, COS\varphi)} - \frac{A \cdot T_r \cdot V_r}{(\sqrt{1-A^2}+1-A^2)\left(T_r + V_r + 4XT_r/(1+T_r)\right)^2} \qquad (M-9)$$

$$K_3 = \frac{8}{\pi^{2.8}} * \left(\frac{L}{D}\right)_H * \frac{.0457}{2^{.2}} * \frac{VC^{2.8} \cdot \omega^{2.8} \cdot P_m^{.8} \left(1 + A/\sqrt{1-A^2}\right)^{.8} F_{CR}^{1.8}}{N_H^{1.8} * D_H^{3.8} * R^{.8} * T_H^{.8}} \qquad (M-10)$$

$$K_4 = \frac{8}{\pi^{2.8}} \left(L/D\right)_C * \frac{.0457}{2^{.2}} * \frac{VC^{2.8}\, \omega^{2.8} \cdot P_m^{.8} \left(1 - A/\sqrt{1-A^2}\right)^{.8} F_{CC}^{1.8}}{NC^{1.8} \cdot DC^{3.8} * R^{.8} * TC^{.8}} \qquad (M-11)$$

$$K_5 = \frac{53.7 * 2^{.93}}{4\pi} * \frac{1-\sigma}{\sigma} * \frac{P_m^{.07}}{(R \cdot TR)^{.07}} * \left(\frac{\mu_C + \mu_H}{2 d_W}\right)^{.93} * (VC \cdot \omega)^{2.07} * \left(\frac{F_{CR} \cdot LR}{VDR}\right)^{1.07} \qquad (M-12)$$

$$K_6 = \frac{30}{\pi} \sqrt{\left(\frac{R-1}{R}\right)^2} * N * \frac{P_1}{P_m \sqrt{P_m}} * \frac{\left(TC/TH \sqrt{K_g \cdot TH} * Fe \cdot A_e + \sqrt{K_c \cdot TC} * F_C \cdot A_C\right)}{VC\left(1 + \lambda\, TC/TH + V^2\right)} * (SIN\varphi_p + COS\varphi_p) \qquad (M-13)$$

$$K_7 = \frac{SIN\varphi_p - COS\varphi_p}{SIN\varphi_p + COS\varphi_p} \qquad (M-14)$$

Since

$$TAN(\alpha) = \frac{1/V_r + COS\varphi}{SIN\varphi}$$

and

$$TAN(\theta) = \frac{V_r\ SIN\varphi}{T_r + V_r\ COS\varphi}$$

Then:

$$COS\alpha = \frac{SIN\varphi}{\sqrt{SIN^2\varphi + (\frac{1}{V_r} + COS\varphi)^2}}$$

$$\Rightarrow \quad \frac{SIN\varphi}{COS\alpha} = \sqrt{1 + \frac{1}{V_r^2} + \frac{2}{V_r} COS\varphi} \qquad (M-15)$$

and

$$SIN\theta = \frac{V_r \cdot SIN\varphi}{\sqrt{T_r^2 + V_r^2 + 2V_r T_r COS\varphi}} \qquad (M-16)$$

ϕ_p is the phase angle difference between pressure wave and expansion volume displacement and it is measured by peak to peak of pressure [22].

$$SIN\phi_p = \frac{2}{\pi} * \frac{RP}{RP-1} * \frac{1}{N} * \frac{W_C}{P_{max} * VC} \qquad (M-17)$$

RP is the pressure ratio and with the proper correction factor, 1.04 obtained by trial and error from complete model, is given:

$$RP = \frac{1+A}{1-A} * 1.04 \qquad (M-18)$$

$$W_C = \pi \cdot N \cdot P_m * VC * A * SIN(\varphi - \theta) / (1 + \sqrt{1-A^2}) \qquad (M-19)$$

$$SIN\phi_p = 2A \frac{1.04(1+A)}{.04 + 2.04A} * \sqrt{\frac{1-A}{1+A}} * SIN(\varphi - \theta) / (1 + \sqrt{1-A^2}) \qquad (M-20)$$

If we define M as:

$$M \equiv \frac{SIN\varphi}{COS\alpha} = \sqrt{1+\frac{1}{V_r^2}+\frac{2}{V_r}COS\varphi} \qquad (M\text{-}21)$$

Then the total loss is:

$$Total\ Loss = \left[(K_3+K_4)M^{1.8}+K_5M^{1.07}\right]\left[SIN\varphi+\tfrac{1}{6}SIN(2\alpha-\varphi)+\tfrac{1}{2}SIN(2\alpha+\varphi)\right]+K_6(COS\varphi+K_7SIN\varphi) \qquad (M\text{-}22)$$

$$\frac{\partial(Total\ Loss)}{\partial\varphi} = \left[(K_3+K_4)M^{1.8}+K_5M^{1.07}\right]\left[COS\varphi-\tfrac{1}{6}COS(2\alpha-\varphi)+\tfrac{1}{2}COS(2\alpha+\varphi)\right]+\left[1.8(K_3+K_4)M^{.8}+\right.$$
$$\left.+1.07K_5M^{.07}\right]\frac{\partial M}{\partial\varphi}*\left[SIN\varphi+\tfrac{1}{6}SIN(2\alpha-\varphi)+\tfrac{1}{2}SIN(2\alpha+\varphi)\right]-K_6(SIN\varphi-K_7COS\varphi)$$

$$\frac{\partial M}{\partial\varphi} = \frac{SIN\varphi}{V_r\sqrt{1+\frac{1}{V_r^2}+\frac{2}{V_r}COS\varphi}} = \frac{SIN\varphi}{V_r*M}$$

Since in most cases $2\alpha+\phi\simeq 180$ and $2\alpha-\phi\simeq 0$, then we can write:

$$\frac{\partial(Total\ Loss)}{\partial\varphi} = \left[(K_3+K_4)M^{1.8}+K_5M^{1.07}\right](COS\varphi-1/6)+\frac{SIN\varphi}{V_r\cdot M}\left[1.8(K_3+K_4)M^{.8}+1.07K_5M^{.07}\right]*$$
$$*(SIN\varphi)-K_6(SIN\varphi-K_7COS\varphi) \qquad (M\text{-}23)$$

Therefore,

$$\frac{\partial W_{OUT}}{\partial\varphi} = \frac{\partial W}{\partial\varphi}-\frac{\partial(Total\ Loss)}{\partial\varphi} = 0$$

$$\Rightarrow \quad SIN\theta(K_1COT\varphi+K_2SIN\varphi)-(COS\varphi-1/6)\left[(K_3+K_4)M^{1.8}+K_5M^{1.07}\right]-\frac{SIN^2\varphi}{V_r\cdot M}*$$
$$*\left[1.8(K_3+K_4)M^{.8}+1.07K_5M^{.07}\right]+K_6(SIN\varphi-K_7COS\varphi)=0 \qquad (M\text{-}24)$$

Since ϕ is close to 90, $COS\phi\simeq 0$, and M is not strongly depend on ϕ then for simplicity we assume M is not a variable term.

$$\frac{\partial W_{OUT}}{\partial \varphi} = SIN\theta\,(K_1 \cot\varphi + K_2 SIN\varphi) - (\cos\varphi - 1/6)K_8 - SIN^2\varphi * K_9 + K_6(SIN\varphi - K_7\cos\varphi) = 0$$

Where $K_8 = (K_3+K_4)M^{1.8} + K_9 M^{1.07}$

$$K_9 = \frac{1}{V_r}\left[1.8\,(K_3+K_4)\bar{M}^{.2} + 1.07\,K_5\,\bar{M}^{.93}\right]$$

$$SIN\theta = \frac{V_r\,SIN\varphi}{\sqrt{T_r^2+V_r^2+2V_rT_r\cos\varphi}} \approx K_{10}\,SIN\varphi$$

$$K_{10} = V_r \Big/ \sqrt{T_r^2+V_r^2+2V_rT_r\cos\varphi}$$

Therefore,

$$K_{10}K_1\cos\varphi + K_2K_{10}SIN^2\varphi - K_8\cos\varphi + 1/6\,K_8 - K_9SIN^2\varphi + K_6SIN\varphi - K_6K_7\cos\varphi = 0 \quad \text{(M-25)}$$

Since $SIN^2\varphi = 1 - \cos^2\varphi$

$$\Rightarrow (K_9 - K_2K_{10})\cos^2\varphi - (K_8 - K_1K_{10} + K_6K_7)\cos\varphi + 1/6\,K_8 + K_2K_{10} - K_9 + K_6SIN\varphi = 0 \quad \text{(M-26)}$$

In order to make this equation analytically solvable, it is assumed that $SIN\phi \simeq .93$

$$(K_9 - K_2K_{10})\cos^2\varphi - (K_8 - K_1K_{10} + K_6K_7)\cos\varphi + 1/6\,K_8 + K_2K_{10} - K_9 + .93K_6 = 0 \quad \text{(M-27)}$$

Example:

We want to calculate the optimum ϕ for the previous case in Appendix(K), i.e. for TH=860° R, TC=530° R. The specifications of the engine are given in Appendix(K).

A=.16 , Tr=.6163 , Vr=.87

$$K_1 = \frac{\pi * A * (1-T_r)}{(1+V_r)\left(1+\sqrt{1-A^2}\right)} = .0519$$

K2=.3770

In order to calculate K3, k4, and k5, it is easier to divide each of the correspondingpower losses by their phase angle terms.

$$K_3 = W_{Loss} \Big/ \left\{ \left(\frac{SIN\varphi}{\cos\alpha} \right)^{1.8} * \left[SIN\varphi + \tfrac{1}{6} SIN(2\alpha - \varphi) + \tfrac{1}{2} SIN(2\alpha + \varphi) \right] \right\}$$

ϕ=108 , α=41.5 , Wloss=6

K_3=4.97

K_4=11.4

k_5=146

For K_6 and K_7 we use the power loss due to the non-uniform temperature.

$$W_{Loss} = C * \left[(SIN\phi_p + \cos\phi_p)\left(\frac{\sqrt{H}}{\sqrt{2}} + \cos\varphi\right) + SIN\varphi * (SIN\phi_p - \cos\phi_p) \right]$$

Since $\phi_p = 17^\circ$, Then:

$$C = \frac{65}{1.0537 - .621} = 150.237$$

$$K_6 = C * (SIN\phi_p + \cos\phi_p) = 188.46$$

$$K_7 = \frac{TAN\phi_p - 1}{TAN\phi_p + 1} = -.532$$

$$M = \sqrt{1 + \frac{1}{V_r^2} + \frac{2}{V_r}\cos\varphi} = 1.269$$

$$K_8 = (K_3 + K_4) M^{1.8} + K_5 M^{1.07} = 213.5$$

$$K_9 = \frac{1}{V_r}\left[1.8\,(K_3 + K_4) M^{-.2} + 1.07\, K_5 M^{-.93} \right] = 176.12$$

$$K_{10} = V_r \Big/ \sqrt{V_r^2 + T_r^2 + 2V_r T_r \cos\varphi} = .97$$

Then by substituting these in the equation:

$$(K_9 - K_2 K_{10})\cos^2\varphi - (K_8 - K_1 K_{10} + K_6 K_7)\cos\varphi + \tfrac{1}{6} K_8 + K_2 K_{10} - K_9 + .93 K_6 = 0$$

$$\Rightarrow \cos\varphi = -.292$$

$$\varphi_{opt} = 107^\circ$$

By iteration and trial and error of complete model ϕ_{opt}=110 then we can see how well the above equation predict the optimum ϕ.

b)- Optimum Speed Derivation

Since the trade-off, for determination of speed, is between output power and different losses, then we have to consider those losses which are speed dependent.

$$W_{OUT} = \pi \cdot N \cdot P_m \cdot A \cdot V_H \cdot \sin\theta \cdot (1 - T_C/T_H) / (1 + \sqrt{1 - A^2}) \cdot F(T) \cdot F(\varphi) \cdot F(D)$$

$$\Rightarrow W_{OUT} = K_1 \cdot \omega$$

Power loss due to the pressure drop:

Heater:

$$W_{Loss} = \frac{8}{\pi^3} \cdot f_H \cdot (L/D)_H \cdot \frac{V_C^3 \cdot \omega^3 \cdot P_m (1 + A/\sqrt{1-A^2})}{N_H^2 \cdot D_H^4 \cdot R \cdot T_H} \cdot F_{CR}^2 \cdot \frac{\sin^2\varphi}{\cos^2\alpha} \left[\sin\varphi + \tfrac{1}{6}\sin(2\alpha - \varphi) + \tfrac{1}{2}\sin(2\alpha + \varphi)\right]$$

(M-28)

Where

$$f_H = \frac{.0457}{Re_H^{.2}} \simeq \frac{.0457 \pi^{.2} \cdot D_H^{.2} \cdot N_H^{.2} \cdot \mu_H^{.2}}{4^{.2} \cdot \dot{m}_H^{.2}}$$

$$\dot{m}_H = \frac{P_m}{2 \cdot R \cdot T_H} (1 + A/\sqrt{1-A^2}) \cdot F_{CR} \cdot V_C \cdot \omega \cdot \frac{\sin\varphi}{\cos\alpha}$$

$$\Rightarrow W_{Loss} = .0129 (L/D)_H \frac{\mu_H^{.2} V_C^{2.8} F_{CR}^{1.8} P_m^{.8} (1 + A/\sqrt{1-A^2})^{.8} \sin^{1.8}\varphi}{N_H^{1.8} \cdot D_H^{3.8} \cdot R^{.2} \cdot T_H^{.2} \cdot \cos^{1.8}\alpha} \left[\sin\varphi + \tfrac{1}{6}\sin(2\alpha - \varphi) + \tfrac{1}{2}\sin(2\alpha + \varphi)\right] \cdot \omega^{2.8}$$

(M-29)

By the same procedure we get the following for cooler:

$$W_{Loss} = .0129\,(L/D)_C \cdot \frac{M_c^{.2} \cdot V_c^{2.8} \cdot F_{cc}^{1.8} \cdot P_m^{.8} \cdot (1 + A/\sqrt{1-A^2})^{.8} \cdot SIN^{1.8}\varphi}{N_C^{1.8} \cdot D_C^{3.8} \cdot R^{.2} \cdot T_C^{.2} \cdot COS^{1.8}\alpha} \left[SIN\varphi + \tfrac{1}{6} SIN(2\alpha - \varphi) + \tfrac{1}{2} SIN(2\alpha + \varphi)\right] \cdot \omega^{2.8}$$

(M-30)

Regenerator:

$$W_{Loss} = \frac{f_R}{16\pi} \cdot \frac{L_R}{R_H} \cdot \frac{P_m}{(V_{DR}/L_R)^2} \cdot \frac{V_c^2 \cdot \omega^3 \cdot SIN^2\varphi}{COS^2\alpha \cdot R \cdot T_R} F_{cr}^2 \cdot \left[SIN\varphi + \tfrac{1}{6} SIN(2\alpha - \varphi) + \tfrac{1}{2} SIN(2\alpha + \varphi)\right]$$

(M-31)

Where

$$f_R = \frac{53.7}{(Re_R)^{.93}} = \frac{53.7\,(V_{DR}/L_R)^{.93}\left(\frac{\mu_C + \mu_H}{2}\right)^{.93}}{(\dot{m}_R)^{.93} \cdot (d_w)^{.93}}$$

$$\dot{m}_R = P_m \cdot V_C \cdot \omega \cdot SIN\varphi / (2 \cdot R \cdot T_R \cdot COS\alpha) \cdot F_{cr}$$

$$W_{Loss} = \frac{53.7}{4\pi}\left(\frac{\mu_C + \mu_H}{d}\right)^{.93} \cdot \frac{L_R}{d_w} \cdot \frac{1-\sigma}{\sigma} \cdot \left(\frac{P_m}{R\,T_R}\right)^{.07} \cdot \frac{SIN^{1.07}\varphi \cdot F_{cr}^{1.07} \cdot V_c^{2.07}}{\left(\frac{V_{DR}}{L_R}\right)^{1.07} COS^{1.07}\alpha} \left[SIN\varphi + \tfrac{1}{6} SIN(2\alpha - \varphi) + \tfrac{1}{2} SIN(2\alpha + \varphi)\right] \omega^{2.07}$$

(M-32)

Therefore, pressure drop power losses can be written as:

Heater:

$$W_{Loss} = K_2 \cdot \omega^{2.8}$$

(M-33)

Cooler:

$$W_{Loss} = K_3 \cdot \omega^{2.8}$$

(M-34)

Regenerator:

$$W_{Loss} = K_4 \cdot \omega^{2.07}$$

(M-35)

For Power loss due to the temperature drops in heat and cooler we have following equations from Chapter II:

$$W_{Loss} = \frac{W_R \cdot W_C \cdot (k-1)}{\dot{m}_H \cdot R \cdot T_H \cdot k} \cdot \frac{1}{e^{2\pi T_H R} - 1}$$

$$W_{Loss} = \frac{W_C^2 \cdot (k-1)}{\dot{m}_C \cdot R \cdot T_C \cdot k} \cdot \frac{1}{e^{2\pi T_C R} - 1}$$

These equations can be approximated as:

$$W_{Loss} = K_5 \cdot \omega \qquad \text{(M-36)}$$

$$W_{Loss} = K_6 \cdot \omega \qquad \text{(M-37)}$$

The other losses which affect the output power and are speed dependent are:

1)- Power loss due to the non-uniform temperature, which can be rewritten as (see equation (2-20)).

$$W_{Loss} = K_7 \cdot \omega^{.5} \qquad \text{(M-38)}$$

2)- Friction Loss:

$$W_{Loss} = K_8 (.002\omega^2 + \omega) \qquad \text{(M-39)}$$

Therefore, the net output can be written as

$$\text{Net Output} = K_1\omega - (K_2+K_3)\omega^{2.8} - K_4\omega^{2.07} - (K_5+K_6)\omega - K_7\omega^{.5} - K_8(.002\omega^2+\omega) \qquad \text{(M-40)}$$

In order to find the optimum ω, the above equation should be differentiated with respect to ω.

$$\frac{\partial(\text{Net Output})}{\partial\omega} = K_1 - 2.8(K_2+K_3)\omega^{1.8} - 2.07K_4\omega^{1.07} - (K_5+K_6) - .5K_7\omega^{-.5} - .004K_8\omega - K_8$$

$$\frac{\partial(\text{Net output})}{\partial\omega} = 0$$

$$\Rightarrow \quad 2.8(K_2+K_3)\omega^{1.8} + (2.07K_4\omega^{.07} + .004K_8)\omega + K_5 + K_6 + K_8 - K_1 + .5K_7\omega^{-.5} = 0 \qquad \text{(M-41)}$$

Following example shows how this equation can be used.

Example: The designed engine of Appendix(K) is used to determine its optimum speed.

$N = 1000$ RPM

$$K_1 = \frac{W_{OUT}}{\omega} = \frac{678}{1000} = .678$$

$$K_2 = \frac{W_{Loss,Heater}}{\omega^{2.8}} = \frac{6}{(1000)^{2.8}} = 2.39 \times 10^{-8}$$

$$K_3 = \frac{W_{Loss,Cooler}}{\omega^{2.8}} = \frac{13.75}{(1000)^{2.8}} = 5.474 \times 10^{-8}$$

$$K_4 = \frac{W_{Loss,Reg.}}{\omega^{2.07}} = 9.126 \times 10^{-5}$$

$$K_5 = \frac{W_{Loss,Heater}}{\omega} = 6 \times 10^{-4}$$

$$K_6 = \frac{W_{Loss,Cooler}}{\omega} = 6 \times 10^{-4}$$

$$K_7 = \frac{W_{Loss,Non-Temp.}}{\omega^{.5}} = 2.0555$$

$$K_8 = \frac{W_{Loss,Friction}}{.002\omega^2 + \omega} = .0227$$

By substituting the above K's into the equation for optimum speed by some trial and error we get:

ω_{opt}=1120 RPM

For the same engine by using the complete model we get ω_{opt}=1080 RPM

APPENDIX(N)

Optimum Bore/Stroke Ratio:

Since equation (2-23) and (2-24) are easier to work with, for non-uniform temperature loss, then they have been used for this derivation. Equation (2-24) shows the power loss in radial direction.

$$\overleftrightarrow{W_{Loss}} = .052\,(Re)^{.8}\,(Pr)^{.4} \cdot \frac{k-1}{R} \cdot \frac{P_i}{P_m} \cdot K_g \cdot T_m \cdot X_m \cdot \cos\varphi_p \qquad (3\text{-}24)$$

We can cerive a similar equation for axial direction as follows.

$$Q = h \cdot A \cdot \Delta T \qquad (N\text{-}1)$$

h the heat transfer coefficient is given by equation (2-21), ΔT is given by (2-22).

$$A=\pi/4*B^2$$

Where B is the bore.

$$Q = \frac{\Pi}{4} \cdot .023\,(Re)^{.8}\,(Pr)^{.4} \cdot B \cdot \frac{k-1}{k} \cdot T_m \cdot \frac{P_i}{P_m} \cdot (1-\bar{e}^{1}) \sin(\omega t-\varphi_p) \qquad (N\text{-}2)$$

This equation can be integrated over a cycle to find the average power loss in the axial direction. The results of integration follows.

$$\updownarrow W_{Loss} = \frac{1}{\pi}\oint Q \cdot dt = \frac{1}{2\pi}\int_0^{2\pi} Q \cdot d(\omega t)$$

$$\updownarrow W_{Loss} = .00727\,(Re)^{.8}\,(Pr)^{.4} \cdot B \cdot \frac{k-1}{R} \cdot T_m \cdot \frac{P_i}{P_m} \cdot \cos\varphi_p \qquad (N\text{-}3)$$

For a given volume of cylinder we can write followings.

$$V = \frac{\pi}{4} B^2 \times S \qquad \beta = B/S \quad \Rightarrow \quad B = \sqrt[3]{\frac{4V}{\pi}}\,\beta^{1/3} \qquad \text{(N-4)}$$

$$S = \sqrt[3]{\frac{4V}{\pi}}\,\beta^{-2/3} \qquad \text{(N-5)}$$

Therefore, losses in both directions can be written as:

$$Re = \frac{\rho \omega B^2}{\mu} \quad , \quad X_m = \tfrac{1}{2} S$$

$$W_{\leftrightarrow_{Loss}} = .052 \left(\frac{\rho\omega}{\mu}\right)^{.8} (Pr)^{.4} \times \frac{k-1}{k} \times \frac{P_1}{P_m} \times K_g \times T_m \times \cos\varphi_p \times \sqrt[3]{\frac{4V}{\pi}}\,\beta^{-2/3} \times \left[\sqrt[3]{\frac{4V}{\pi}}\,\beta^{1/3}\right]^{1.6}$$

$$W_{\leftrightarrow_{Loss}} = .026 \left(\frac{\rho\omega}{\mu}\right)^{.8} (Pr)^{.4} \frac{k-1}{k} \times \frac{P_1}{P_m} \times K_g \times T_m \times \cos\varphi_p \times \left(\frac{4V}{\pi}\right)^{2.6/3} \beta^{-.4/3} \equiv K_1 \times \beta^{-.4/3}$$

(N-6)

$$W_{\updownarrow_{Loss}} = .00727 \left(\frac{\rho\omega}{\mu}\right)^{.8} (Pr)^{.4} \times \frac{k-1}{k} \times \frac{P_1}{P_m} \times K_g \times T_m \times \cos\varphi_p \left(\frac{4V}{\pi}\right)^{2.6/3} \times \beta^{2.6/3} \equiv K_2 \times \beta^{2.6/3}$$

(N-7)

If we wanted to consider only this loss for determination of Bore/Stroke ratio then we get:

$$\partial\left(W_{\leftrightarrow_{Loss}} + W_{\updownarrow_{Loss}}\right)/\partial\beta = 0$$

$$-.026 \times \frac{.4}{3}\,\beta^{-3.4/3} + .00727 \times \frac{2.6}{3}\,\beta^{-.4/3} = 0 \qquad \text{(N-8)}$$

$$\Rightarrow \beta = .55$$

Since the shuttle loss is very significant, then we have to consider that too. Equation (2-16) gives this loss.

$$W_{Loss} = \frac{\pi}{8} \times K_g \times S \times (T_H - T_C) \times \frac{B}{\ell} \times \frac{S}{L} \times (BET) \qquad \text{(2-16)}$$

$$\Rightarrow \quad W_{Loss} = \frac{\pi}{8} \times \frac{K_g}{\ell L} \times (T_H - T_C) \times (BET) \times \sqrt[3]{\frac{4V}{\pi}}\,\beta^{1/3} \times \sqrt[3]{\frac{16V^2}{\pi^2}}\,\beta^{4/3}$$

$$W_{Loss} = \frac{\pi}{8} \times \frac{K_g}{\ell L} \times (T_H - T_C) \times (BET) \times \frac{4V}{\pi} \times \beta^{-1} \equiv K_3 \beta^{-1} \qquad \text{(N-9)}$$

$$\text{Total Loss} = K_1 \beta^{-.4/3} + K_2 \beta^{2.6/3} + K_3 \beta^{-1} \qquad \text{(N-10)}$$

$$\frac{\partial(\text{Total loss})}{\partial \beta} = 0 \Rightarrow -.4 K_1 \beta^{-3.4/3} + 2.6 K_2 \beta^{-.4/3} - 3 K_3 \beta^{-2} = 0$$

or

$$.4 K_1 - 2.6 K_2 \beta + 3 K_3 \beta^{-2.6} = 0 \qquad \text{(N-11)}$$

Where

$$K_1 = .026 \left(\frac{\rho\omega}{\mu}\right)^{.8} (Pr)^{.4} \times \frac{k-1}{k} \times \frac{\rho_1}{\rho_m} \times K_g \times T_m \times \cos\varphi_p \left(\frac{4V}{\pi}\right)^{2.6/3} \qquad \text{(N-12)}$$

$$K_2 = .28 K_1 \qquad \text{(N-13)}$$

$$K_3 = \frac{\pi}{8} \times \frac{K_g}{\ell L} \times (T_H - T_C) \times (BET) \times \frac{4V}{\pi} \qquad \text{(N-14)}$$

Example:

For the engine in Appendix(K) we want to calculate the optimum bore/stroke ratio.

N=1000 RPM

P=500 Psia

μ=.068 lbm/hr ft

$$\frac{\rho\omega}{\mu} = \frac{500 \times \frac{1000\pi}{30} \times 3600}{386.85 \times 860 \times .068} = 8345 \left[\frac{1}{in^2}\right]$$

Pl/Pm≃.1

Kg=.118 Btu/hr ft

Q_p=17

V=2.845 in^3

l=.005 in

L=1.5 in (assumed)

From equation (4-73) through (4-75) the K's have been calculated:

K_1=107.3

K_2=30

K_3=162.3

By these coefficients equation (4-72) gives the optimum bore, stroke ratio to be 1.8.

APPENDIX(P)

Regenerator Heat Transfer Area Derivation:

Consider the following figure.

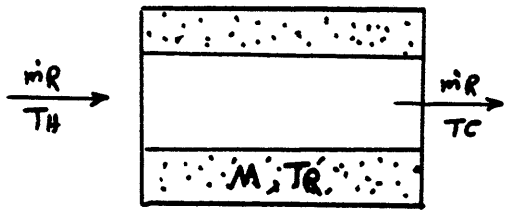

When the working fluid flows through the regenerator with mass flow rate mR and temperature TH, it will releases heat to the regenerator material and brings its temperature from TC to a nominal regenerator temperature TR. Therefore, by assuming no heat leakage, the amount of heat released by the working fluid should be equal to the heat gained by the regenerator material.

$$\dot{m}_R \cdot c_p (T_H - T_C) \cdot t_p = M \cdot C_R \cdot (T_R - T_C) \qquad \text{(P-1)}$$

Where t_p is the average passing time for the working fluid through the regenerator, and M is the regenerator filling material mass with specific heat CR.

Mass of the regenerator material can be written in terms of the density and its volume.

$$M = \rho \cdot V = \rho \cdot (1-\sigma) \cdot V_R = \rho \cdot (1-\sigma) \cdot \frac{\pi}{4} \cdot D_R^2 \cdot L_R \qquad \text{(P-2)}$$

t_p is usually one third of the half period, therefore,

$$t_p = \frac{1}{3} \cdot \frac{\pi}{\omega} = \frac{\pi}{3\omega} \qquad \text{(P-3)}$$

mR is given by equation (3-17) and for simplicity we assume

$F_{cr}=1.$

$$\Rightarrow \dot{m}_R = P_m \cdot V_C \cdot \omega \cdot SIN\varphi / (2 \cdot R \cdot TR \cdot COS\alpha)$$

Therefore, from the above equations we get:

$$\frac{P_m \cdot V_C}{2 R \cdot TR} \times \frac{\Pi}{3} \times \frac{SIN\varphi}{COS\alpha} \cdot C_p (TH - TC) = \rho (1-\sigma) \cdot \frac{\Pi}{4} \cdot DR R^2 \cdot L_R \cdot C_R \cdot (TR - TC) \quad \text{(P-4)}$$

or

$$L_R \cdot DR R^2 = 2/3 \cdot \frac{P_m V_C}{\rho \cdot R \cdot TR} * \frac{C_p}{(1-\sigma) C_R} * \frac{SIN\varphi}{COS\alpha} * \frac{TH - TC}{TR - TC} \quad \text{(P-5)}$$

Where ρ and C_R are density and specific heat of the regenerator material.

APPENDIX(Q)

Computer Program of Optimum Model

```
      0DIMENSION XDMC(720),XDMW(720),IND(2,2),PR(720),XMCX(720),XMWX(720)
      1     ,TEC(720),TEW(720),XMT(720)
           DIMENSION AX(10),AXINT(10),ADMRE(10),AXI2(10)
          1,AXI3(10)
      0DIMENSION W(720),C(720),WI(720),CI(720),DW(720),DC(720),DWI(720),
      1    DCI(720),DPR(720)
       DIMENSION SIFI(720),COFI(720),SALF(720),CALF(720)
           DIMENSION XC(6),XINTC(6),DMREC(6),XI3C(6),XI2C(6)
           DIMENSION TTW(20)
           REAL MIUC,MIUW,LC,LR,LW,M,N,LV,NC,NW
C NDIV = MULTIPLE OF 4
           READ(91,5)TH,DELV
5          FORMAT(F6.1,F5.2)
           FACTC=1.
           FACTH=1.
           SAR=DELV
           TW=TH
           READ(92,901)ZZC,ZZW,XNHT,SHR,NFI,NDIV,NWR,NDS,TC
901        FORMAT(2F4.1,F7.4,F6.4,I3,3I3,F6.1)
           READ(93,902)VAC,VAH,DRR,RC,DH,LR,LC,LH,NC,NH,DO,VWD,VCD,VDEER
902        FORMAT(2F6.3,3F5.3,3F5.2,2F5.1,F7.5,3F7.3)
           AFI=(360.-NFI)*3.1415/180
           READ(94,903)N,PM,QIN,SW1
903        FORMAT(2F6.1,F10.2,F3.1)
           READ(95,904)R,SIG,M,CYL,SW3
904        FORMAT(F6.2,F5.3,F6.2,2F3.1)
           RW=DH
           NW=NH
           VAW=VAH
           GL=.005
           IF(M.EQ.4.)PRW=.711
           IF(M.EQ.4.)PRC=.711
           SH=SHR
           OMG=N*3.1415/30
           AC=5.8584*(VAC**.66667)
           WOUT=QIN*(1-TC/TW-.20)
           IF(WOUT.LT.100.) WOUT=100.
           IF(SW3.EQ.1.) WOUT=QIN
           BS=1.
           IF(M.EQ.2.)PRC=6.54139*TC/100000+.6881
           IF(M.EQ.2.)PRW=6.54139*TW/100000+.6881
           NCC=1
           VCDO=VCD
           VWDO=VWD
           IF(SIG.EQ.1)GOTO 1751
           VAC=WOUT*6*10.516/(OMG*PM*(1-TC/TW)*SIN(AFI))
1751       NUM=1
           WH=WOUT/(1-TC/TW)*1.5
           AWC=WOUT*TC/TW/(1-TC/TW)*1.5
           AVM=VAC
```

```
20000     MM=1
          SHW=SHW+1.
          NAH=1
          PUSH=1.
          OMG=3.1415*N/30
          TR=(TW-TC)/ALOG(TW/TC)
          IF(M.EQ.2.)GOTO 1635
          MIUC=(196.14+.464*(TC/1.8-293)-.093*PM*.00689)/1000000*241.9076
          MIUW=(196.14+.464*(TW/1.8-293)-.093*PM*.00689)/1000000*241.9076
          GOTO 1636
1635      MIUC=(88.73+.2*(TC/1.8-293)+.118*PM*.00689)/1000000*241.9076
          MIUW=(88.73+.2*(TW/1.8-293)+.118*PM*.00689)/1000000*241.9076
1636      NMM=1
          AKC=(1.7704*TC+521)/17300
          AKH=(1.7704*TW+521)/17300
          IF(M.EQ.2.)AKC=(.0194444*TC+8.)/173
          IF(M.EQ.2.)AKH=(.0194444*TW+8.)/173
1740      NW=WH*3.563/(AKH*LW*(TW-TR))*1.1*ZAP
          NC=AWC*3.563/(AKC*LC*(TR-TC))*1.1*ZAP
          IF(NW.LT.10) NW=10.
          IF(NC.LT.10) NC=10.
30000     NC=NC*FACTC
          NW=NW*FACTH
C           OPTIMUM COOLER
1728      BC=((R*TC)**.5)*RC*RC/(OMG*VAC)*34.047
          GC=PM*(RC**3)*83462.4/(OMG*VAC*MIUC)
          A=1.535*(NC**.8)
          DLC=TW/TC
          IF(SIG.EQ.1.)VCD=VCD0+.5*(VDEER+3.1415*DRR*DRR*LR/4)
          IF(MM.GE.2)GOTO 1700
          ZC=VCD/(2*VAC)
          GOTO 1702
1700      ZC=VCD/(VAC+VAW)
1702      LC=RC*(DLC*A*(GC**.2)*(BC**.6)+192-59.2*DLC+.0275*GC
         1-688.3*BC-19.2*ZC)
          AFRC=NC*3.1415*RC*RC/4
C
C         OPTIMUM HEATER
C
          BH=((R*TW)**.5)*RW*RW/(OMG*VAC)*34.047
          GH=PM*(RW**3)*83462.4/(OMG*VAC*MIUW)
          DLH=TW/TC
          B=1.535*(NW**.8)
          IF(SIG.EQ.1.)VWD=VWD0+.5*(VDEER+3.1415*DRR*DRR*LR/4)
          IF(MM.GE.2)GOTO 1703
          ZH=VWD/(2*VAC)
          GOTO 1704
1703      ZH=VWD/(VAC+VAW)
1704      LW=RW*(DLH*B*(GH**.2)*(BH**.6)+244-75.7*DLH+GH/100-356*BH-
         116*ZH)
          AFRW=NW*3.1415*RW*RW/4
          NMM=NMM+1
          IF(NMM.LE.3)GOTO 1740
```

```
C
C          OPTIMUM REGENERATOR
C
          IF(SIG.EQ.1.)GOTO 1749
          VEF=AFRW*LW+AFRC*LC+VDEER+VWD+VCD+3.1415/4*DRR*DRR*LR
C            FOR METAL C=.11 BTU/LB/R , RHO=488 LB/FT3
          CAL=(VAW/VAC+COS(AFI))/SQRT(1+(VAW/VAC)**2+2*VAW/VAC*COS(AFI))
          DRR=(288/3*PM*VAC/(488*TR)*SHR/(SHR-1)*SIN(AFI)/(1-SIG)/.11
         1*(TW-TC)/(TR-TC)/(CAL*778*LR))**.5
          AL=ATAN((VAW/VAC+COS(AFI))/SIN(AFI))
          A=47.6*SIN(AFI)/(CAL)/(SIN(AFI)+1/6*
         1SIN(2*AL-AFI)+.5*SIN(2*AL+AFI))
          DEL=TH/TC
          DR=SIG*DO/(1-SIG)
          Z=.11*778*(SHR-1)/(R*SHR)*OMG*DR*DR*488/
         1((MIUC+MIUW)/2)*3600/144
          GA=(DR**3)*PM*83462.4/(OMG*VAC*(MIUC+MIUW))
          BET=((R*TR)**.5)*DR*DR*((1-SIG)**2)*68.094
         1/(SIG*OMG*VAC)
          IF(EFF.EQ.0.0) EFF=0.9-1/DEL
          AREG=(.285*A*((ALOG(DEL))**1.66)*EFF*GA*
         1GA/(BET*BET*(Z**.66)))**2.66
          ZET=(VDR+VDEER)/(VAW+VAC)
          FZ=80*ZET-20.
          ARN=AREG+FZ
          LR=ARN*DO*SIG/(1-SIG)
1749      VDDR=SIG*(3.1415*DRR*DRR*LR/4)
          AFRR=VDDR/LR
C
C            OPTIMUM CYLINDERS
C
          BCY=PM*OMG*VAC*VAC/(R*TC*MIUC*AC*AC)*3600*.047548
          DLCY=TW/TC
          ZCY=(AFRC*LC+VCD+TC/TW*(AFRW*LW+VWD)+VDDR*TC/TR)/VAC
          FZCY=.357*ZCY-.78
          FDL=.548*DLCY-.54
          FBY=.525-8.8*BCY/100000
          AAA=.11*(ZCY+1)*DLCY/(1+3400*(DLCY-1)/BCY-.02*(DLCY-1)*((BCY
         1/DLCY)**.5))
          VAW=VAC*(AAA**.5+FZCY+FBY+FDL)
          WRITE(6,1743)VAW,BCY,DLCY,ZCY
          IF(SIG.EQ.1)GOTO 1730
          IF(NCC.NE.1)GOTO 1730
          DELA=(TC/TW)**2+2*TC*VAC/(TW*VAW)*COS(AFI)+(VAC/VAW)**2
          DELB=TC/TW+VAC/VAW+2*TC/VAW*((AFRW*LW+VWD)/TW+(VDDR+VDEER)/TR
         1+(AFRC*LC+VCD)/TC)
```

```
      DEL=(DELA**.5)/DELB
      TET=ATAN(VAC*SIN(AFI)/(VAW*(TC/TW+VAC/VAW*COS(AFI))))
      VAC=WOUT*(1+(1-DEL*DEL)**.5)*1.409*3/(OMG*PM*DEL*SIN(TET)*
     1(1-TC/TW))/1.5*AZ
      IF(VAC.LT.0.9) VAC=0.9
      NCC=NCC+1
      GOTO 30000
1730  VAW=VAW
      IF(ABS(VAW/AVM-1).LT.0.05)GOTO 1725
      AVM=VAW
      MM=MM+1
      GOTO 1728
1743  FORMAT(////////////,10X,'REAL VAW=',F10.5,//,5X,'BCY=',F10.5
     1,//,5X,'DLCY=',F10.5,//,5X,'ZCY=',F10.5)
1725  WRITE(6,1726)VAC,VAW,LW,LR,LC,NW,NC,DRR
1726  FORMAT(1H1,///,15X,'OPTIMUM DESIGN RESULTS',///,5X,'VAC=',
     1F10.5,//,5X,'VAW=',F10.5,//,5X,'LH=',F10.5,//,5X,'LR=',F10.5
     1,//,5X,'LC=',F10.5,//,5X,'NW=',F10.5,//,5X,'NC=',F10.5,//,
     15X,'DRR=',F10.5)
      IF(SIG.EQ.1)GOTO 5000
      IF(SIG.EQ.1)GOTO 5000
      IF(CYL.EQ.1.)GOTO 4000
      DR=SIG*D0/(1-SIG)
      GOTO 5000
4000  DR=2*SIG*D0/(3*(1-SIG))
5000  VDC=(LC*AFRC*TW)/(VAW*TC)
      VDEC=VCD*TW/(VAW*TC)
      VDEW=VWD/VAW
      VDW=AFRW*LW/VAW
      VDER=VDEER*2*TW/(VAW*(TW+TC))
      VDR=VDDR*2*TW/(VAW*(TW+TC))
      RVT=VAC*TW/(VAW*TC)
      VD=VDC+VDEC+VDER+VDR+VDW+VDEW
      NNN=NDIV
      XND=NDIV
      NDIV1 = NDIV + 1
      DALF = 6.2831853/XND
      NT = NDIV/4+2
      NE = NT - 1
      ALF = 4.7123889
      NF = NDIV/4
      CALL       VOLC(DALF,NF,C,CI,DC,DCI,ZZC,NDIV,SIFI,COFI,SALF,CALF)
  100 FI = DALF*NFI
      SFI = SIN(FI)
      CFI = COS(FI)
      IND(1,1) = 1
     0CALL       VOLW(W,WI,DW,DWI,CFI,SFI,ZZW,NDIV,SIFI,COFI,SALF,CALF,
     1       DALF)
      IND(1,2) =3
      IND(2,1) =4
      IND(2,2) =2
      NN = 1
      XMC = 0.
      P = 1.
```

```
      XMW = 1.-CFI
      XMWS = 0.
      PS = 1.
      NO = 4
      WW = 0.
      WC = 0.
      NITE = 1
      NST = 1
      NFIN = NFI
      NLOP = 0
  404 DO 102 I=NST,NFIN
      VW = W(I)
      VC = C(I)
      VWI = WI(I)
      VCI = CI(I)
      DVW = DW(I)
      DVC = DC(I)
      DVWI = DWI(I)
      DVCI = DCI(I)
      GO TO (201,202,203,204),NO
  601 NLOP = NLOP+1
      IF(NLOP-6) 201,201,605
  201 DP = -SHR*P*(RVT*DVCI+DVWI)/(RVT*VCI+VWI+SHR*VD)*DALF
      S = P+DP/2.
      DP = -SHR*S*(RVT*DVC+DVW)/(RVT*VC+VW+SHR*VD)*DALF
      DMW = S*DVW*DALF+VW*DP/SHR
      DMC = -(DMW+VD*DP)/RVT
      IF(DMW)302,301,301
  301 K = 1
      GO TO 303
  302 K = 2
  303 IF(DMC) 304,305,305
  305 L = 1
      GO TO 306
  304 L = 2
  306 NO = IND(K,L)
      GO TO (400,602,603,604),NO
  602 NLOP = NLOP+1
      IF(NLOP-6) 202,202,605
  202 IF(XMC) 803,801,801
  803 XMC = 0.0
  801 IF(XMW) 805,802,802
  805 XMW = 0.0
 8020DP = -SHR*(XMC*RVT*DVCI/VCI+XMW*DVWI/VWI)/
     1     (XMC*RVT/P+XMW/P+SHR*VD)*DALF
      DMC = XMC*(DVCI*DALF/VCI+DP/SHR/P)
      DMW = -RVT*DMC-VD*DP
      S = P+DP/2.
      SMC = XMC+DMC/2.
      SMW = XMW+DMW/2.
     0DP = -SHR*(SMC*RVT*DVC/VC+SMW*DVW/VW)/
     1     (SMC*RVT/S+SMW/S+SHR*VD)*DALF
```

```
      DMC = SMC*(DVC*DALF/VC+DP/SHR/S)
      DMW = -RVT*DMC-VD*DP
      IF(DMW)312,312,307
  312 K = 2
      GO TO 308
  307 K = 1
  308 IF(DMC) 309,309,310
  309 L = 2
      GO TO 311
  310 L = 1
  311 NO = IND(K,L)
      GO TO (601,400,603,604),NO
  603 NLOP = NLOP+1
      IF(NLOP-6) 203,203,605
  203 IF(XMC) 704,703,703
  704 XMC = 0.
 7030DP = -SHR*(P*DVWI+XMC*RVT*DVCI/VCI)/(VWI+XMC*RVT
     1      /P+SHR*VD)*DALF
      DMC = XMC*(DVCI*DALF/VCI+DP/SHR/P)
      DMW = -RVT*DMC-VD*DP
      S = P+DP/2.
      SMC = XMC+DMC/2.
      SMW = XMW+DMW/2.
     0DP = -SHR*(S*DVW+SMC*RVT*DVC/VC)/(VW+SMC*RVT
     1      /S+SHR*VD)*DALF
      DMC = SMC*(DVC*DALF/VC+DP/SHR/S)
      DMW = -RVT*DMC-VD*DP
      IF(DMW) 313,314,314
  314 K = 1
      GO TO 315
  313 K = 2
  315 IF (DMC) 316,316,317
  316 L = 2
      GO TO 318
  317 L = 1
  318 NO = IND(K,L)
      GO TO (601,602,400,604),NO
  604 NLOP = NLOP+1
      IF(NLOP-6) 204,204,605
  204 IF(XMW) 705,702,702
  705 XMW = 0.
 7020DP = -SHR*(P*RVT*DVCI+XMW*DVWI/VWI)/(RVT*VCI
     1        +XMW/P+SHR*VD)*DALF
      DMW = XMW*(DVWI*DALF/VWI+DP/SHR/P)
      DMC = -(DMW+VD*DP)/RVT
      S = P+DP/2.
      SMC = XMC+DMC/2.
      SMW = XMW+DMW/2.
     0DP = -SHR*(S*RVT*DVC+SMW*DVW/VW)/(RVT*VC
     1        +SMW/S+SHR*VD)*DALF
      DMW = SMW*(DVW*DALF/VW+DP/SHR/S)
      DMC = -(DMW+VD*DP)/RVT
      IF(DMW) 319,319,320
  319 K = 2
      GO TO 321
  320 K = 1
```

```
321 IF(DMC) 322,323,323
323 L = 1
    GO TO 324
322 L = 2
324 NO = IND(K,L)
    GO TO(601,602,603,400),NO
605 WRITE(6,17) NITE,I,NO
    WRITE(6,45) I,NO,DP,DMC,DMW,P,XMC,XMW
400 P = P+DP
    XMC = XMC+DMC
    XMW = XMW+DMW
    PW = P-DP/2.
    WC = WC+PW*DVC*DALF
    WW = WW+PW*DVW*DALF
    PR(I) = P
    DPR(I) = DP
    XMCX(I) = XMC
    XMWX(I) = XMW
    XDMC(I) = DMC
    XDMW(I) = DMW
    NLOP = 0
102 CONTINUE
    GO TO (401,402),NN
401 NST = NFI+1
    NFIN = NDIV
    XMW = 0.
    NN = 2
    NO = 3
    GO TO 404
402 TEST = SQRT((XMWS-XMW)**2)
    TEST1 = SQRT((PS-P)**2)
    IF(NITE-15) 471,471,406
471 IF(TEST-.001)473,473,405
473 IF(TEST1-.005) 406,406,405
405 NN = 1
    XMC = 0.
    PS = P
    XMWS = XMW
    WW = 0.
    WC = 0.
    NST = 1
    NFIN = NFI
    NITE = NITE+1
    NO = 4
    GO TO 404
406 PMAX = XLARGE(PR,NDIV)
    PMIN = SMALL(PR,NDIV)
    WC = WC/PMAX
    WW = WW/PMAX
    RP = PMAX/PMIN
    FI = FI*180./3.141593
    WRITE(6,11) SHR,RVT,FI,VD,NDIV
    WRITE(6,12) WC,WW,RP
    WRITE(6,13) NITE
```

```
      CMMAX = XLARGE(XMCX,NDIV)
      WMMAX = XLARGE(XMWX,NDIV)
      CMMAX = CMMAX/PMAX
      WMMAX = WMMAX/PMAX
      WRITE(6,19) WMMAX,CMMAX
      ARG = 2.*RP/(RP-1.)*WC/3.1416
      IF(1.-ARG**2) 1607,1608,1608
1608     FIPV=ASIN(ARG)
      WRITE(6,18) FIPV
      XNDS = NDS
      X = 0.
      DX = 1./XNDS
      WRITE(6,21)
      NIN = NDS + 1
      COR = PMAX**(XNHT-2.)*DALF**(XNHT-1.)
      DO 854 I=1,NIN
      CALL PDINT(X,XDMW,XDMC,RVT,DC,NDIV,DMRE,PR,XINT,DPR,XI1,XI2,XNHT)
      XINT = XINT/DALF/PMAX
         AXINT(I)=XINT
      DMRE = DMRE/PMAX/6.2832
         ADMRE(I)=DMRE
      XI1 = XI1*COR/(1.5708*DMRE)**(1.-XNHT)
      XI2 = XI2*COR/(1.5708*DMRE)**(2.-XNHT)
         AXI2(I)=XI2
      XI3 = XI1/XI2
         AXI3(I)=XI3
         AX(I)=X
      WRITE(6,22) X,XINT,DMRE,XI1,XI2,XI3
      X = X+DX
  854 CONTINUE
 1607 IF(NWR) 1509,606,1509
 1509 DO 509 I=1,NDIV
      PR(I) = PR(I)/PMAX
      XMCX(I) = XMCX(I)/PMAX
  509 XMWX(I) = XMWX(I)/PMAX
      WI(NDIV1) = WI(1)
      CI(NDIV1) = CI(I)
      DO 1001 I=1,NDIV
      IF(XMCX(I)) 1003,1003,1002
 1002 TEC(I) = PR(I)*CI(I+1)/XMCX(I)
      GO TO 1006
 1003 TEC(I) = 0.
 1006 IF(XMWX(I)) 1004,1004,1005
 1005 TEW(I) = PR(I)*WI(I+1)/XMWX(I)
      GO TO 1001
 1004 TEW(I) = 0.
 1001 CONTINUE
      TEW(NDIV1) = TEW(1)
      TEC(NDIV1) = TEC(1)
      PR(NDIV1) = PR(1)
      XMCX(NDIV1) = XMCX(1)
      XMWX(NDIV1) = XMWX(1)
```

```
      TWDM = 0.
      TCDM = 0.
      DO 573 I=1,NDIV
      DMW = XMWX(I+1)-XMWX(I)
      IF(DMW) 574,575,575
  574 TMPW = (TEW(I)+TEW(I+1))/2.
      TWDM = TWDM+(TMPW-1.)*DMW
  575 DMC = XMCX(I+1)-XMCX(I)
      IF(DMC) 576,573,573
  576 TMPC = (TEC(I)+TEC(I+1))/2.
      TCDM = TCDM+(TMPC-1.)*DMC
  573 CONTINUE
      TWDM = TWDM*SHR/(SHR-1.)
      TCDM = TCDM*SHR/(SHR-1.)
      DO 1021 I=1,NDIV
 1021 XMT(I) = XMCX(I)*RVT+XMWX(I)+PR(I)*VD
      WRITE(6,51) TWDM,TCDM
      WRITE(6,14) PR(NDIV),(PR(I),I=1,NDIV)
      WRITE(6,15) XMCX(NDIV),(XMCX(I),I=1,NDIV)
      WRITE(6,16) XMWX(NDIV),(XMWX(I),I=1,NDIV)
      WRITE(6,1010) TEC(NDIV),(TEC(I),I=1,NDIV)
      WRITE(6,1011) TEW(NDIV),(TEW(I),I=1,NDIV)
      WRITE(6,1022) (XMT(I),I=1,NDIV)
606      NDIV=0
      IF(NDIV) 511,511,100
511      GO TO 10000
   110FORMAT (22H1SPECIFIC HEAT RATIO =F8.3,10X,18H (VC/VW)*(TW/TC) =F8.
     13//17X,5H FI =F8.3,22X,5H VD =F8.3//11X,11H DIVISION =I8//)
   120FORMAT (10X,12H COLD WORK =F8.3//10X,12H WARM WORK =F8.3//5X,
     117H PRESSURE RATIO =F8.3///)
   13 FORMAT (10X,I10,11H ITERATIONS )
   14 FORMAT (24H1ARRAYS START AT MC = 0.///12H PRESSURE   /(10F10.4))
   15 FORMAT (12H1COLD MASS  /(10F10.4))
   16 FORMAT (12H1WARM MASS  /(10F10.4))
   17 FORMAT (5H0LOOP 3I10)
   18 FORMAT (20H P-V  ANGLE IN RAD = F10.4//)
   19 FORMAT(16H MAX WARM MASS = F10.4, 16H MAX COLD MASS = F10.4//)
   21 FORMAT (/// 23H PRESSURE DROP INTEGRAL)
   220FORMAT (6H X/L = F6.2,11H INTEGRAL = E12.4,7H DMRE = E12.4,
     1 6H XI1 = E12.4, 6H XI2 = E12.4,6H XI3 = E12.4/)
   45 FORMAT (2I10,10X,6E10.3)
   510FORMAT (16H INTEGRAL (H*DM)  /9H WARM END  F10.4,10X,9H COLD END
     1      F10.4,1H1)
 1010 FORMAT(12H1COLD TEMP  /(10F10.4))
 1011 FORMAT(12H1WARM TEMP  /(10F10.4))
 1022 FORMAT (11H1TOTAL MASS/(10F10.4))
10000    HR=SHR
         IF(SHR.LT.1.4.AND.M.EQ.2.)HR=1.4
         IF(SHR.LT.1.4.AND.M.EQ.4.)HR=1.66
         NDIV=NNN
         PMIN=2*PM/(1+RP)
         PMAX=RP*PMIN
         IF(SIG.EQ.1)DR=DRR
```

```
      WDW=N*PMAX*VAW*WW/720.
      WDC=N*PMAX*VAC*WC/720.
      WNET=WDW+WDC
      OMG=N*3.1415/30
      OMGN=OMG*((2.54648*VAW)**.333)/((HR*16.1*R*(TW+TC))**.5)
      WDWN=WDW/((PMAX-PMIN)*VAW*OMG)*6.
      WDCN=WDC/((PMAX-PMIN)*VAW*OMG)*6.
      IF(M.EQ.2.)GOTO 7001
      IF(M.EQ.4.)GOTO 7002
      MIUC=(181.94+.536*(TC/1.8-293)+1.22*(PM*.00689))/1000000*241.91
      MIUW=(181.94+.536*(TW/1.8-293)+1.22*(PM*.00689))/1000000*241.91
      GOTO 8000
7001  MIUC=(88.73+.2*(TC/1.8-293)+.118*PM*.00689)/1000000*241.907568
      MIUW=(88.73+.2*(TW/1.8-293)+.118*PM*.00689)/1000000*241.907568
      GOTO 8000
7002  MIUC=(196.14+.464*(TC/1.8-293)-.093*PM*.00689)/1000000*241.9076
      MIUW=(196.14+.464*(TW/1.8-293)-.093*PM*.00689)/1000000*241.9076
8000  XC(1)=VDEC/VD
      XC(2)=(VDEC+VDC)/VD
      XC(3)=(VDEC+VDC+.5*VDER)/VD
      XC(4)=1-(VDEW+VDW+.5*VDER)/VD
      XC(5)=1-(VDEW+VDW)/VD
      XC(6)=1-VDEW/VD
      DO 7100 I=1,6
      DO 7200 J=1,NIN
      K=NIN
      IF(XC(I)-AX(J)) 7044,7022,7200
7022  XC(I)=AX(J)
      XINTC(I)=AXINT(J)
      DMREC(I)=ADMRE(J)
      XI2C(I)=AXI2(J)
      XI3C(I)=AXI3(J)
      GO TO 7100
7044  XINTC(I)=(AXINT(J)-AXINT(J-1))*(XC(I)-AX(J-1))
     1/(AX(J)-AX(J-1))+AXINT(J-1)
      DMREC(I)=ADMRE(J-1)-(ADMRE(J-1)-ADMRE(J))*(XC(I)-
     1AX(J-1))/(AX(J)-AX(J-1))
      XI2C(I)=(AXI2(J)-AXI2(J-1))*(XC(I)-AX(J-1))
     1/(AX(J)-AX(J-1))+AXI2(J-1)
      XI3C(I)=(AXI3(J)-AXI3(J-1))*(XC(I)-AX(J-1)
     1)/(AX(J)-AX(J-1))+AXI3(J-1)
      GO TO 7100
7200  CONTINUE
7100  CONTINUE
      XINTCC=(AXINT(1)+XINTC(1))/2
      DMRECC=(ADMRE(1)+DMREC(1))/2
      XI2CC=(AXI2(1)+XI2C(1))/2
      XI3CC=(AXI3(1)+XI3C(1))/2
      XINTCL=(XINTC(1)+XINTC(2))/2
      DMRECL=(DMREC(1)+DMREC(2))/2
      XI2CL=(XI2C(1)+XI2C(2))/2
      XI3CL=(XI3C(1)+XI3C(2))/2
      XINTCR=(XINTC(2)+XINTC(3))/2
```

```
      DMRECR=(DMREC(2)+DMREC(3))/2
      XI2CR=(XI2C(2)+XI2C(3))/2
      XI3CR=(XI3C(2)+XI3C(3))/2
      XINTMR=(XINTC(3)+XINTC(4))/2
      DMREMR=(DMREC(3)+DMREC(4))/2
      XI2MR=(XI2C(3)+XI2C(4))/2
      XI3MR=(XI3C(3)+XI3C(4))/2
      XINTWR=(XINTC(4)+XINTC(5))/2
      DMREWR=(DMREC(4)+DMREC(5))/2
      XI2WR=(XI2C(4)+XI2C(5))/2
      XI3WR=(XI3C(4)+XI3C(5))/2
      XINTHT=(XINTC(5)+XINTC(6))/2
      DMREHT=(DMREC(5)+DMREC(6))/2
      XI2HT=(XI2C(5)+XI2C(6))/2
      XI3HT=(XI3C(5)+XI3C(6))/2
      XINTHC=(XINTC(6)+AXINT(K))/2
      DMREHC=(DMREC(6)+ADMRE(K))/2
      XI2HC=(XI2C(6)+AXI2(K))/2
      XI3HC=(XI3C(6)+AXI3(K))/2
C        PRESSURE DROP LOSSES
C        COOLER
      AL=LC+VCD/AFRC/2
      REAVC=DMRECL*PMAX*VAC*OMG*RC*3600/(R*TC*AFRC*
     1MIUC)
      IF(REAVC.LE.2000) GO TO 708
      AP1=-1.34-0.2*ALOG10(REAVC)
      FC=10.**(AP1)
      GO TO 710
708   FC=16/REAVC
710   QCP=(OMG**3)*PMAX*(VAC**3)*(AL/RC)*XINTCL*FC
     1/(TC*AFRC*AFRC*R*699212.9672*.73756)
C        HEATER
      BL=LW+VWD/(2*AFRW)
      REAVW=DMREHT*PMAX*VAC*OMG*RW*3600/(R*TC*AFRW*
     1MIUW)
      IF(REAVW.LE.2000) GO TO 711
      AP2=-1.34-.2*ALOG10(REAVW)
      FW=10.**(AP2)
      GO TO 713
711   FW=16/REAVW
713   QWP=(OMG**3)*PMAX*(VAC**3)*(BL/RW)*XINTHT*FW
     1/(TC*AFRW*AFRW*R*699212.9672*.73756)*TW/TC
C        REGENERATOR COLD END
      RECR=DMRECR*PMAX*VAC*OMG*DR*3600/(R*TC*AFRR*
     1MIUC)
      LV=LR+VDEER*2/(3.1415*DRR*DRR)
      IF(RECR.LE.60.)GOTO 714
      IF(RECR.GT.60.AND.RECR.LE.1000)GOTO 715
      AR3=.015-.125*ALOG10(RECR)
      FCR=10.**(AR3)
      GO TO 716
714   AR1=1.73-.93*ALOG10(RECR)
```

```
      FCR=10.**(AR1)
      GO TO 716
715   AR2=.714-.365*ALOG10(RECR)
      FCR=10.**(AR2)
716   QCRP=(OMG**3)*PMAX*(VAC**3)*(LV/DR)*XINTCR*FCR
     1/(TC*AFRR*AFRR*R*699212.9672*.73756)
C        REGENERATOR HOT END
      REWR=RECR*(MIUC/MIUW)*(DMREWR/DMRECR)
      IF(REWR.LE.60.)GOTO 717
      IF(REWR.GT.60.AND.REWR.LE.1000)GOTO 718
      AR4=.015-.125*ALOG10(REWR)
      FWR=10.**(AR4)
      GO TO 719
717   AR5=1.73-.93*ALOG10(REWR)
      FWR=10.**(AR5)
      GO TO 719
718   AR6=.714-.365*ALOG10(REWR)
      FWR=10.**(AR6)
719   QWRP=QCRP*(XINTWR/XINTCR)*(FWR/FCR)*(TW/TC)
C        MIDDLE OF REGENERATOR
      REAM=RECR*(MIUC/(MIUW+MIUC)*2)*(DMREMR/DMRECR)
      IF(REAM.LE.60.)GOTO 720
      IF(REAM.GT.60.AND.REAM.LE.1000)GOTO 721
      AR7=.015-.125*ALOG10(REAM)
      FMR=10.**(AR7)
      GO TO 722
720   AR8=1.73-.93*ALOG10(REAM)
      FMR=10.**(AR8)
      GO TO 722
721   AR9=.714-.365*ALOG10(REAM)
      FMR=10.**(AR9)
722   QMRP=QCRP*(XINTMR/XINTCR)*(FMR/FCR)*(TW+TC)
     1/(2*TC)
      WRITE(6,10006)REAVC,REAVW,RECR,REWR,REAM,FC,FW,FCR,FWR,FMR
10006 FORMAT(//,5X,5F13.5,5F7.3)
C        TOTAL ENERGY DROP IN REGENERATOR
      QRP=(QCRP+QWRP+4*QMRP)/6
C        HEAT TRANSFER LOSSES
C        COOLER
      VDR=VDDR+VDEER
      ANUC=.023*(REAVC**.8)*(PRC**.4)
      ANTUC=4*LC*ANUC/(RC*REAVC*PRC)
      AMAC=1.5708*DMRECL
      AC=EXP(2*ANTUC)-1
      COOLOSS=WDC*WC*(HR-1)/(HR*AC*2*AMAC*.73756)
C        HEATER
      ANUW=.023*(REAVW**.8)*(PRW**.4)
      ANTUW=4*LW*ANUW/(RW*REAVW*PRW)
      AMAW=1.5708*DMREHT
      AW=EXP(2*ANTUW)-1.
      HEATLOSS=WDW*WW*(HR-1)/(HR*AW*2*AMAW*.73756)
C        REGENERATOR
C        COLD END
      IF(SIG.EQ.1.)GOTO 24000
```

```
      REC=1.5708*RECR
      STC=1.1*SIG/(REC**.405)/(PRC**.667)
      ANTUCR=4*LR/DR*STC
C        HOT END
      REH=1.5708*REWR
      STW=1.1*SIG/((REH**.405)*(PRW**.667))
      ANTUWR=4*LR/DR*STW
      AMR=(DMRECR+DMREMR/2)/(DMREWR+DMREMR/2)
      ANPH=.63662*VDR*(HR-1)/(VAC*HR*(DMRECR+DMREMR
     1/2)*(TW/TC-1))
      ALANDR=(1+ANPH*(XI3CR+XI3WR*AMR)/2)/(ANTUCR/
     1XI2CR+ANTUWR*AMR/XI2WR)
      IF(SIG-1)25000,24000,25000
24000 ALANDR=1.
25000 RHEATLOSS=ALANDR*HR/(HR-1)*(TW-TC)/TC*PMAX*VAC
     1*OMG*DMRECR/(24*M*.73756)
      DLPC=8*FC*LC*((PMAX*VAC*N*DMRECL/(RC*RC*NC))**2)/(28980*RC*PM
     1*R*TC)
      DLPH=8*FW*LW*((PMAX*VAC*N*DMREHT/(RW*RW*NW))**2)/(28980*RW*PM*
     1R*TC)*TW/TC
      DLPR=8*FMR*LR*((PMAX*VAC*N*DMREMR/(SIG*DRR*DRR))**2)/(28980*DR*
     1PM*R*TC)*TR/TC
      WRITE(6,26000)ALANDR,DLPC,DLPH,DLPR

26000 FORMAT(///,10X,'LANDA=',F10.6,///
     1,5X,'PRESSURE DROP IN COOLER [PSI]=',F8.3,//,5X,'PRESSURE DROP
     1 IN HEATER [PSI]=',F8.3,//,5X,'PRESSURE DROP IN REG. [PSI]=',
     1F8.2)
C        SHUTTLE HEAT TRANSFER
C       ASSUMING CONSTANT:DENSITY=488 LB/FT3 , C=.11 BTU/LB.R
C       FOR AKG,AKM THE UNITS ARE WATT/CM.K
      AKG=(1.7704*TR+521)/1000000
      IF(M.EQ.2.)AKG=(.0194444*TR+8)/10000
      AKM=.01111*((TR/1.8)**.45425)
      ALP=AKM/.928664
1624  BS=BS
      B=(8*VAW*BS/3.1415)**.3333
      S=(8*VAW/(3.1415*BS*BS))**.3333
      AL1=AKM/AKG*((OMG*GL*GL/(2*ALP))**.5)*5
      BET1=(2*AL1*AL1-AL1)/(2*AL1*AL1-1.)
      SHUTLOSS=AKG*S*(TW-TC)*B/(2*GL)*BET1*.554142
C        REGENERATOR AXIAL CONDUCTION
      AMM=(1+AKM/AKG)/(1-AKM/AKG)
      VDR=VDDR
      AKMG=AKG*(AMM+SIG-1.)/(AMM+1.-SIG)
      AXILOSS=AKMG*DRR*DRR*(TW-TC)/LR*1.108284075
C        DRY FRICTION LOSS
      FRLOSS=N*(.002*N+1)*(VAW+VAC)/265.5*SW1
C        SPRING GAS LOSSES
      AE=(8.*VAW*VAW*3.1415/BS)**.3333
      PA=(PM**.5)*(RP-1)/(2*(RP**.5))
      AKL=(1.7704*TC+521)/1000000
```

```
      IF(M.EQ.2.)AKL=(.0194444*TC+8)/10000
      AC=(8.*VAC*VAC*3.1415/BS)**.3333
      ALANDA=VAW/VAC
      VETA=(AFRC*LC+VCD+TC/TW*(AFRW*LW+VWD)+VDDR*TC/TR)/VAC
      AKW=(1.7704*TW+521)/1000000
      IF(M.EQ.2.)AKW=(.0194444*TW+8)/10000
      FE=3.84*PM*N*((2*VAW)**.6667)/(100000*TW*MIUW)+2.22
      FC=2.1*PM*N*((2*VAC)**.6667)/(100000*TC*MIUC)+2.95
      SGL=.35381*((OMG*(((SHR-1)/SHR)**3))**.5)*PA/(1+ALANDA
     1*TC/TW+VETA)*(TC/TW*((AKW*TW)**.5)*FE*AE+((AKL*TC)**.5)
     1*FC*AC)*((COS(FIPV)-SIN(FIPV))*(ALANDA+COS(AFI))-(SIN(AFI))
     1*(SIN(FIPV)+COS(FIPV)))
      TIC=PM*((VAW/3.1415)**.3333)/5000
      ARI=B/2
      ARO=TIC+ARI
      AB=12/(1089.54*S*AKG)+ALOG(ARO/ARI)*12/(3.1415*S*10)+
     1144/(21.99*S*ARO)*2
      QLEAK=(TW-TC)/AB*778/(3600*.73756)
      GK=AKW/.0173
      QP=2*OMG/(3*3.1415)*(300/778*OMG*B/(2*GK))**.6*((12*(PMAX-PMIN)
     1*GL/TR)**1.6)*GL*(TW-TC)*S*HR/(144*.73756*(HR-1))
C          FINAL RESULTS
C          TCP=TOTAL COOL CYLINDER SHAFT POWER [WATTS]
C          THP=TOTAL HOT CYLINDER SHAFT POWER [WATTS]
C          THC=TOTAL HEAT FLOW IN COOLER [WATTS]
C          THH=TOTAL HEAT FLOW IN HEATER [WATTS]
C          SGL=SPRING GAS LOSS [WATTS]
      TCP=WDC/.73756-QCP-QWP-QRP-COOLOSS-HEATLOSS
      THC=TCP-RHEATLOSS-SHUTLOSS-AXILOSS-SGL
      THH=WDW/.73756+RHEATLOSS+AXILOSS
C          BORE-STROKE OPTIMIZATION
      AK=(1.7704*TW+521)/17300
      AKK1=.026*((PM*OMG*3600/(R*TW*MIUW))**.8)*(PRW**.4)*(SHR-1)/
     1SHR*PA/PM*AK*TW*COS(FIPV)*((4*VAW/3.1415)**.9)
      IF(M.EQ.2.)AK=(.0194444*TW+8)/173
      AKK2=.28*AKK1
      AKK3=3.1415/8*AK/(S*GL)*(TW-TC)*(BET1)*4*VAW/3.1415*778/12/3600
      RLG=.4*AKK1*(BS**2.6)+3*AKK3
      RIG=2.6*AKK2*(BS**3.6)
      IF(ABS(RIG-RGL)-10)1610,1611,1612
1610  BS=BS+.05
      IF(BS.GT.2.5)GOTO 1611
      GOTO 1624
1611  WRITE(6,1626)BS
      GOTO 1625
1612  BS=BS-.05
      IF(BS.LT.0.8)GOTO 1611
      GOTO 1624
1626  FORMAT(////,10X,'OPTIMUM BORE-STROKE RATIO=',F5.2)
1625  IF(NAH.GT.3)GOTO 28000
      NAH=NAH+1
      WH=ABS(THH)
      AWC=ABS(THC)
```

```
      WRITE(6,1741)WH,AWC
1741  FORMAT(/////,5X,'WH=',F10.5,//,5X,'WC=',F10.5)
      SHR=SH
      GOTO 1740
28000 IF(SIG.NE.1.)GOTO 27000
      NUM=NUM+1
      IF(NUM.NE.2)GOTO 27000
      FACTC=FACTC*THC/(THC+RHEATLOSS)
      FACTH=FACTH*THH/(THH-RHEATLOSS)
      SHR=SH
      GO TO 30000
27000 THP=WDW/.73756-QLEAK-QP
      OUTPUT=THP+THC+RHEATLOSS+AXILOSS-FRLOSS
      DLV=2*VAW+VAC*(1+COS(AFI))
      BMEP=OUTPUT*.73756*12/(DLV*OMG)
      PANOR=BMEP*OMG*DLV/(12*.73756)
      THPN=THP/PANOR
      TCPN=TCP/PANOR
      WRITE(6,1726)VAC,VAW,LW,LR,LC,NW,NC,DRR
      THCN=THC/PANOR
      WCC=WDC/.73756
      WRITE(6,10011)PMAX,PMIN,TC,TW,N,SIZE,WCC
10011 FORMAT(1H1,//,10X,'MAX. PRESSURE [PSIA]=',F7.2,//,10X
     1,'MIN. PRESSURE [PSIA]=',F7.2,//,10X,'COLD TEMP.[R]='
     1,F6.1,//,10X,'HOT TEMP.[R]=',F6.1,//,10X,'SPEED[RPM]=',F6.1
     1,//,10X,'SIZE=',F6.3,//,10X,'COMPRESSION WORK=',F14.5)
      IF(SIG.NE.1.)GOTO 7013
      WRITE(6,10010)FACTC,FACTH
10010 FORMAT(///,20X,'ALL OF THE FOLLOWING QUANTITIES ARE IN WATTS',
     1/////,5X,'FACTOR FOR CHANGING COOLER=',F7.3,//,5X,'FACTOR FOR
     1 CHANGING HEATER=',F7.3)
7013  THHN=THH/PANOR
      QCPN=QCP/PANOR
      QWPN=QWP/PANOR
      QRPN=QRP/PANOR
      QM=QP/PANOR
      COOLOSN=COOLOSS/PANOR
      HEATLOSN=HEATLOSS/PANOR
      RHEATLOSN=RHEATLOSS/PANOR
      SHTOSN=SHUTLOSS/PANOR
      AXILOSN=AXILOSS/PANOR
      FRLOSN=FRLOSS/PANOR
      SGLN=SGL/PANOR
      OUTPUTN=OUTPUT/PANOR
      TOR=OUTPUT/OMG*.73756
      TORN=TOR/((PMAX-PMIN)*2*VAW)*12
      BMEPN=BMEP/(PMAX-PMIN)
      EFFN=100*OUTPUT/(THH*(1.-TC/TW))
      TOTLOSS=QCP+QWP+QRP+COOLOSS+HEATLOSS+RHEATLOSS+SHUTLOSS+AXILOSS
     1+FRLOSS+SGL+QLEAK+QP
      IF(SIG.EQ.1.) TOTLOSS=TOTLOSS-RHEATLOSS
```

```
      TOTLOSN=TOTLOSS/PANOR
      EFF=OUTPUT/THH*100
      QL=QLEAK
      QN=QLEAK/PANOR
      WRITE(6,90)QCP,QWP,QRP,COOLOSS,HEATLOSS,RHEATLOSS,SHUTLOSS,QL
     1,QP
     1,SGL,AXILOSS,FRLOSS,TCP,THP,THC,THH,OUTPUT,EFF,TOR,BMEP,
     1TOTLOSS
90    FORMAT(//,25X,'PRESSURE LOSSES:',//,5X,'COOLER=',F10.5,/
     1,5X,'HEATER=',F10.5,/,5X,'REGENERATOR=',F10.5,//,25X,'
     1HEAT TRANSFER LOSSES:',/,5X,'COOLER=',F10.5,/,5X,'HEATER
     1=',F10.5,/,5X,'REGENERATOR=',F13.5,/,5X,'SHUTTLE LOSS=',
     1F10.5,/,5X,'HEAT LEAKAGE=',F10.5,/5X,'PUMPING LOSS=',
     1F10.5,/,5X,'SPRING GAS LOSS=',F10.5,/,5X,'AXIAL LOSS=',F10.5,
     1/,5X,'COULUMB FRICTION LOSS=',F10.5,//,5X,'TOTAL COOL CYLINDER
     1 POWER=',F12.5,/,5X,'TOTAL HOT CYLINDER POWER=',F12.5,/,5X,
     1'TOTAL HEAT FLOW IN COOLER=',F14.5,/,5X,'TOTAL HEAT FLOW IN
     1 HEATER=',F12.5,//,10X,'NET OUTPUT POWER=',F12.5,/,10X,'EFFIC
     1IENCY=',F8.4,'%',///,10X,'TORQUE [LB-FT]=',F12.5,//,10X,'BMEP
     1 §PSIA†=',F12.5,//,10X,'TOTAL LOSS=',F12.5)
      IF(ABS(QIN-THH).LE.50.)GOTO 1738
      IF(QIN-THH)1627,1738,1628
1627  VAC=VAC-SAR
      IF(VAC.LE.0.7.OR.SHW.GT.(VAX/SAR))GOTO 1738
      SHR=SH
      GOTO 20000
1628  VAC=VAC+SAR
      IF(VAC.GT.VAX.OR.SHW.GT.(VAX/SAR))GOTO 1738
      SHR=SH
      GOTO 20000
1738  WRITE(6,10013)PANORN,WDWN,WDCN
10013 FORMAT(////,20X,'THE NONDIMENSIONAL OUTPUTS IN PERCENTAGE',////
     1,10X,'NORMALIZE QUANTITY:',//,10X,'PM*VC*N [WATTS]=',F11.3,
     1////,10X,'WARM WORK=',F10.5,///,10X,'COLD WORK=',F10.5)
      WRITE(6,90)QCPN,QWPN,QRPN,COOLOSN,HEATLOSN,RHEATLOSN,SHTOSN,QN,
     1QM,
     1SGLN,AXILOSN,FRLOSSN,TCPN,THPN,THCN,THHN,OUTPUTN,EFFN,TORN,
     1BMEPN,TOTLOSN
      STOP
      END
```

```
      SUBROUTINE PDINT (X,DMW,DMC,RVT,DVC,NDIV,DM,PR,XINT,
     1       DPR,XI1,XI2,XNHT)
      DIMENSION DMW(720),DMC(720),DVC(720),PR(720),DPR(720)
      DM = 0.
      XINT = 0.
      XI1 = 0.
      EX1 = 1.-XNHT
      XI2 = 0.
      EX2 = 2.-XNHT
      DO 101 I=1,NDIV
      DMX = DMC(I)-X*(DMW(I)/RVT+DMC(I))
      Y = ABS(DMX)
      DM = DM+Y
      A = DPR(I)*Y**EX1
      IF(DMX) 201,202,202
  201 A = -A
  202 XI1 = XI1+A
      XI2 = XI2+Y**EX2
  101 XINT  =  XINT+Y*DMX/PR(I)*DVC(I)
      XNDIV = NDIV
      RETURN
      END
```

```
      SUBROUTINE VOLW(W,WI,DW,DWI,CFI,SFI,ZZW,NDIV,SIFI,COFI,SALF,CALF,
     1       DALF)
      DIMENSION SIFI(720),COFI(720),SALF(720),CALF(720)
      DIMENSION W(720),WI(720),DW(720),DWI(720)
      SIFIP = SIFI(1)*CFI-COFI(1)*SFI
      DO 101 I=1,NDIV
  201 SALF1 = SIFI(I+1)*CFI-COFI(I+1)*SFI
      SALFP = (SIFIP+SALF1)/2.
      CALFP = (SALF1-SIFIP)/DALF
      CRW = SQRT(ZZW**2-CALFP**2)
      W(I)=1.+SALFP-CRW+ZZW
      WI(I)=1.+SIFIP-CRW +ZZW
      DW(I)=CALFP*(1.-SALFP/CRW)
      DWI(I)=CALFP*(1.-SIFIP/CRW)
  101 SIFIP = SALF1
      RETURN
      END
```

```
      SUBROUTINE VOLC(DALF,NF,C,CI,DC,DCI,ZZC,NDIV,SIFI,COFI,SALF,CALF)
      DIMENSION C(720),CI(720),DC(720),DCI(720)
      DIMENSION SIFI(720),COFI(720),SALF(720),CALF(720)
      ALF = 4.7123889
      NDIV1 = NDIV+1
      DO 852 I=2,NF
      ALF = ALF + DALF
      COFI(I) = COS(ALF)
  852 SALF(I) = SIN(ALF)
      SALF(1) = -1.
      COFI(1) = 0.
      NFF = NF+1
      SALF(NFF) = 0.
      COFI(NFF) = 1.0
      NS = NFF+1
      NL = NFF+NF
      J = NF
      DO 853 I=NS,NL
      SALF(I) = -SALF(J)
      COFI(I) = COFI(J)
  853 J = J-1
      NS = NL+1
      J = NL-1
      DO854 I=NS,NDIV
      SALF(I) = SALF(J)
      COFI(I) = -COFI(J)
  854 J = J-1
      SALF(NDIV1) = SALF(1)
      COFI(NDIV1) = COFI(1)
      DO 855 I=1,NDIV
  855 CALF(I) = (SALF(I+1)-SALF(I))/DALF
      CALF(NDIV1) = CALF(1)
      DO 851 I=1,NDIV
      SIFI(I) = SALF(I)
  851 SALF(I) = (SALF(I)+SALF(I+1))/2.
      COFI(NDIV1) = COFI(1)
      SIFI(NDIV1) = SIFI(1)
      N = NF*4
      DO 302 I = 1,N
  201 CRC = SQRT(ZZC**2-CALF(I)**2)
      C(I)=1.+SALF(I)-CRC+ZZC
      CI(I)=1.+SIFI(I)-CRC+ZZC
      DC(I)=CALF(I)*(1.-SALF(I)/CRC)
  302 DCI(I)=CALF(I)*(1.-SIFI(I)/CRC)
      RETURN
      END
```

```
      FUNCTION SMALL(X,NDIV)
      DIMENSION X(720)
      SMALL = X(1)
      DO 507 I=2,NDIV
      IF(SMALL-X(I)) 507,507,508
  508 SMALL = X(I)
  507 CONTINUE
      RETURN
      END
```

```
      FUNCTION XLARGE(X,NDIV)
      DIMENSION X(720)
      XLARGE = X(1)
      DO 505 I=2,NDIV
      IF(XLARGE-X(I)) 506,505,505
  506 XLARGE = X(I)
  505 CONTINUE
      RETURN
      END
```

1 Sample of the Output:

OPTIMUM DESIGN RESULTS

VAC= 1.98000 [in^3]

VAW= 2.19500 [in^3]

LH= 8.00000 [in]

LR= 0.90000 [in]

LC= 5.60000 [in]

NW= 76.00000

NC= 90.00000

DRR= 1.98000 [in]

1SPECIFIC HEAT RATIO = 1.659 (VC/VW)*(TW/TC) = 1.634

FI = 252.000 VD = 4.628

DIVISION = 360

COLD WORK = -0.415

WARM WORK = 0.581

PRESSURE RATIO = 1.669

2 ITERATIONS

MAX WARM MASS = 1.6278 MAX COLD MASS = 1.3421

P-V ANGLE IN RAD = -0.7199

MAX. PRESSURE [PSIA]= 625.29

MIN. PRESSURE [PSIA]= 374.71

COLD TEMP.[R]= 530.0

HOT TEMP.[R]= 960.0

SPEED[RPM]=1200.0

PHASE ANGLE=108

PRESSURE LOSSES [Watts]

COOLER= 16.36585
HEATER= 3.20996
REGENERATOR= 17.91938

HEAT TRANSFER LOSSES [Watts]

COOLER= 0.82483
HEATER= 1.06657
REGENERATOR= 10.09036
SHUTTLE LOSS= 100.97824
HEAT LEAKAGE= 7.72464
SPRING GAS LOSS= 32.42121
AXIAL LOSS= 7.00228
COULUMB FRICTION LOSS= 64.15820

TOTAL COOL CYLINDER POWER= -1200.55603
TOTAL HOT CYLINDER POWER= 1793.96497
TOTAL HEAT FLOW IN COOLER= -1351.04822
TOTAL HEAT FLOW IN HEATER= 1818.78223

NET OUTPUT POWER= 395.85120
EFFICIENCY= 21.7646%

TORQUE [LB-FT]= 2.32344

BMEP §PSIA†= 4.84198

TOTAL LOSS= 261.76154